IAEA-TECDOC-946

Acoustic signal processing for the detection of sodium boiling or sodium–water reaction in LMFRs

Final report of a co-ordinated research programme 1990–1995

INTERNATIONAL ATOMIC ENERGY AGENCY IAEA

The IAEA does not normally maintain stocks of reports in this series. However, microfiche copies of these reports can be obtained from

INIS Clearinghouse
International Atomic Energy Agency
Wagramerstrasse 5
P.O. Box 100
A-1400 Vienna, Austria

Orders should be accompanied by prepayment of Austrian Schillings 100,– in the form of a cheque or in the form of IAEA microfiche service coupons which may be ordered separately from the INIS Clearinghouse.

The originating Section of this publication in the IAEA was:

Nuclear Power Technology Development Section
International Atomic Energy Agency
Wagramerstrasse 5
P.O. Box 100
A-1400 Vienna, Austria

ACOUSTIC SIGNAL PROCESSING FOR THE DETECTION OF SODIUM BOILING OR SODIUM–WATER REACTION IN LMFRs

IAEA, VIENNA, 1997
IAEA-TECDOC-946
ISSN 1011–4289

Printed by the IAEA in Austria
May 1997

FOREWORD

This report is a summary of the work performed under a co-ordinated research programme entitled Acoustic Signal Processing for the Detection of Sodium Boiling or Sodium-Water Reaction in Liquid Metal Cooled Fast Reactors (LMFRs). The programme was organized by the IAEA and carried out from 1990 to 1995. It was the continuation of an earlier research co-ordination programme entitled Signal Processing Techniques for Sodium Boiling Noise Detection, which was carried out from 1984 to 1989.

Local blockages in the fuel assemblies or other coolant disturbances in a primary circuit could lead to boiling of sodium coolant. In the secondary circuit, on the other hand, leaks in the steam generator units could result in sodium-water reactions taking place. Sodium boiling and sodium-water reaction are events that could be precursors of serious conditions in the reactor, core melting in the primary circuit, and multiple tube rupture in the secondary. Both require rapid detection if the reactor is to be adequately protected, and in both cases, acoustic detection would appear to be the only satisfactory means of achieving the necessary speed. Detection of sodium boiling or sodium-water reaction acoustically depends on first recognizing the specific sound of the event against all other noises, and on distinguishing it against the prevailing background.

The problem of achieving this in the case of sodium boiling was first addressed at a Specialists Meeting organized by the International Working Group on Fast Reactors (IWGFR) of the International Atomic Energy Agency at Chester, United Kingdom in 1981. Various methods were reported for the detection of sodium boiling, but it was not possible to make a comparison of the methods because the signal condition in each experiment varied so widely. Accordingly, it was recommended by participants that a benchmark test should be carried out to evaluate and compare signal processing methods. Organization of a co-ordinated research programme (CRP) was accordingly recommended by the IWGFR.

The results of the CRP on Signal Processing Techniques for Sodium Boiling Noise Detection were reported in 1989. It was noted that whilst many techniques had been demonstrated to be capable of detecting sodium boiling in the presence of substantial background noise, the benchmark tests had not fully tested the capabilities of these techniques. At the same time, the problem of acoustic detection of sodium-water reaction was also demanding the attention of reactor designers. Accordingly, an extension to the CRP, now on the expanded topic of Acoustic Signal Processing for the Detection of Sodium Boiling or Sodium-Water Reaction in Liquid Metal Fast Reactors (LMFRs), was agreed in 1989. Australia, France, Germany, India, Japan, the Russian Federation and the United Kingdom participated in the CRP. In the years 1994 and 1995, the Netherlands also joined the CRP. This publication provides the main conclusions and achievements of this CRP and includes a selection of papers of the final Research Co-ordination Meeting.

The IAEA would like to express its thanks to all those who took part in the programme and particularly the European Fast Reactor R&D organizations, AEA Technology (UK) and the Institute of Physics and Power Engineering (Russian Federation) for providing experimental data. Special thanks go to J. McKnight (AEA Technology, UK), Om Pal Singh and R. Prabhakar (Indira Gandhi Centre for Atomic Research, India), V. Yughay (Institute of Physics and Power Engineering, Obninsk, Russian Federation) for assisting in the preparation of this publication. The IAEA officer responsible for this work is A. Rinejski of the Division of Nuclear Power and the Fuel Cycle.

EDITORIAL NOTE

In preparing this publication for press, staff of the IAEA have made up the pages from the original manuscripts as submitted by the authors. The views expressed do not necessarily reflect those of the governments of the nominating Member States or of the nominating organizations.

Throughout the text names of Member States are retained as they were when the text was compiled.

The use of particular designations of countries or territories does not imply any judgement by the publisher, the IAEA, as to the legal status of such countries or territories, of their authorities and institutions or of the delimitation of their boundaries.

The mention of names of specific companies or products (whether or not indicated as registered) does not imply any intention to infringe proprietary rights, nor should it be construed as an endorsement or recommendation on the part of the IAEA.

The authors are responsible for having obtained the necessary permission for the IAEA to reproduce, translate or use material from sources already protected by copyrights.

CONTENTS

SUMMARY OF THE CO-ORDINATED RESEARCH PROGRAMME

1. INTRODUCTION

1.1. History of the programme

In 1981, a Specialists Meeting, initiated by the International Working Group on Fast Reactors (IWGFR) of the International Atomic Energy Agency, was held at Chester, United Kingdom. The meeting reviewed, among other topics, the various methods of signal processing for use in the detection of the acoustic noise produced by boiling in sodium. As a result of the recommendations of this meeting, a CRP was established to carry out a benchmark exercise to compare the signal processing methods under development in the various participating countries. The report on this first stage of the CRP was published in 1989 [1]. It was concluded that several varied methods for the detection of sodium boiling signals in the presence of background had been demonstrated successfully; however it was recognized that this benchmark exercise had not been able to fully test the capabilities of the analysis methods due to unfavourable signal to noise ratio. The report also concluded that consideration should be given to continuing the work for the specialized topic of sodium-water reaction detection in fast reactor steam generator units (SGUs). Accordingly, a consultants meeting was held at IAEA headquarters in Vienna from 5-7 April 1989 to draw up proposals for a second stage as an extension of the Co-ordinated Research Programme and the objectives were defined.

The first part of the extended CRP concentrated on a more stringent test of boiling noise detection, at the same time imposing a more rigorous definition of signal to noise ratio for the tests. The benchmark tapes were based as before, on an admixture of signals from an out-of-pile experiment at Kernforschungszentrum Karlsruhe, Germany. The results demonstrated conclusively that most methods were capable of detecting boiling reliably enough for a reactor trip system.

The remainder of the extended CRP tested systems for detection of sodium-water reaction. For this, sodium-water reaction sounds from experiments performed at Obninsk, Russian Federation, were combined with background sounds from steam generator units of the Prototype Fast Reactor (PFR) at Dounreay, United Kingdom. In these tests, signals were successfully detected even when the signal to noise ratio was -22 dB, a performance significantly better than what is likely to be demanded by reactor operators in the future.

Some limitations were evident, however. For example, it was also demonstrated that signals from other sources, such as leak noise from the UK PFR, and background from the Superphenix 1 reactor in France, could modify the quantified conclusions. The dependence by most techniques on some form of learning process, implying that the wanted signals could be predefined, was also clear. The participants, therefore, had recommended that the CRP be further extended to include the detection of acoustic noise signals in mixed files prepared from the background noise of steam generator units of PFR and leak signals generated on ASB loop, Bensberg, Germany with different leak rates of 1.8 g/s and 3.8 g/s. The signal to noise ratio in these data ranged from -8 dB to -24 dB. In addition, multichannel leak data from the above experiments were also analyzed to examine the advantage of multichannel analysis over single channel analysis and to test/develop the methods of discovering the position of the leak. The analysis confirmed that the techniques developed by different countries could convincingly detect leak signals in data with signal to noise ratio down to -16 dB with very good reliability. Analysis methods can also detect leak signals even down to -24 dB, but with less reliability. Regarding location of the leak, the beam forming method has been found successful.

1.2. Objectives of the extended CRP

The consultants meeting referred to above noted that the benchmark tapes so far had not caused any great difficulties in detection, and consequently the first objective agreed was to provide more stringent data with respect to boiling noise detection.

The second objective was to provide similar sets of data to enable extension of the work to include acoustic leak detection in steam generator units. Before formulating the detailed programme, the consultants reviewed the situation with the intention of identifying any specific features of ALD which would place different requirements on the signal processing from those of acoustic boiling noise detection. It was agreed that in general the adaptive methods which had been developed for ABND should be applicable to ALD but the training sets of data used for ABND were to be replaced by training sets for ALD. There appeared, however, to be two areas which could place different requirements on the data processing.

The first point raised was that the time response required for ALD was faster than that required in the ABND study; not more than 3 seconds were specified by Russian specialists. It was therefore thought advisable to test the capability of the algorithms to achieve rapid response. This involved in practice both the use of a short data sample (approx. 2 s max.) and also fast computation. It would not be necessary to achieve fast on-line computation in the test but only to demonstrate that, given the appropriate computing facilities, the algorithm could be calculated quickly.

The second point was that it seemed likely that the nature of the signal from a leak would be a function of the leak properties. It was therefore decided that it should be necessary to compare signals from leaks of different sources. Data for this was offered by Russian specialists for a leak in the range of 0.1 to 1 g/s. The UK delegate offered to supply some data for a leak above 1 g/s.

In addition to the principal work area of signal analysis and data processing discussed above, it was also intended that the extended CRP would cover two additional topics.

The first additional topic was computerized decision making based on the use of expert systems. This task would consider how various inputs can be combined to produce a more reliable decision. The output from the various analysis techniques tested in the analysis work could be used as inputs. While these are not statistically independent, as truly separate variables might be, they accurately represented the computational problem of a multiparameter input and would allow the benefits of using diverse parameters to be assessed.

The second additional topic was to examine what requirements a plant operator or licensing authority might place on the design of such a sophisticated detection system for application to a power plant.

The consultants originally envisaged two benchmark tapes being issued and analyzed over a three year period. The first one was to be on ABND trial, a more stringent version of the boiling noise data mixed with background noise; the second one on ALD trial; being a similar mix using sodium-water reaction sounds and actual steam generator background data. However at the first Research Co-ordination Meeting it was realized that as the nature of ALD sounds is significantly different from those of boiling, a familiarization tape should also be distributed containing samples of typical leak and background sounds to enable the delegates

to qualify the signals. This involved an additional RCM, which was hosted by the UK. Based on the success of this study, it was decided to test the techniques on data with Signal to Noise Ratio down to -22 dB. On the prospects of getting multichannel data from ASB loop and from end-of-life experiments performed on PFR SGU in the UK, it was decided to study the advantages of multichannel analysis over single channel analysis, the dependence of the detection technique on leak rates and applicability of different ALD methods on real field data including the identification of different types of injection like argon, hydrogen and water/steam and of the location of the leak by multichannel analysis.

Input data which were sent to the participants contained the descriptions of the test tapes. The participants of course did not know the actual signal/noise ratio and time of occurrence of the simulated event in each record. This additional information was provided to the delegates at the time of discussions during the RCMs. Some necessary details of the test data are described briefly in the respective sections.

A major difficulty experienced by some participants had been the differing tape standards used by the different countries for analog magnetic tapes. As a consequence, it had been necessary in some instances to copy the tapes locally, and this had given reason to doubt some of the calibrations. For the third tape, both one inch and half inch standards were prepared and distributed by the UK, using equipment that had been calibrated and set up by the recorder manufacturers immediately prior to the recordings. Digital tapes were distributed for 1994 and 1995 data.

2. ACOUSTIC BOILING NOISE DETECTION (ABND)

2.1. Re-calibration of boiling noise data

In the preparation of the first tape, difficulties were found in interpretation of the signal to noise ratios as defined for the first stage of the CRP and as reported in [1]. The reason was that for the first stage, data had been recorded directly from the KNS 1 loop experiments as separate boiling and background signals, and then mixed in proportion. A signal to noise ratio of 0 dB meant that both sources of signal were unchanged. In fact, for a mix reported as 0 dB, the boiling signal RMS value was 9 dB higher than the RMS value of the background. In addition, the acoustic data for boiling and background had been recorded on different magnetic head stack, with significantly different upper frequency characteristics. Overall, above 60 kHz the background signal was attenuated by as much as 12 dB when compared to the boiling signal as illustrated in Figure 1.

It was decided that for the second stage of the CRP, a signal to noise ratio should be defined according to the definition:

$$\text{Signal/Noise Ratio (dB)} = 10\ \text{Log}_{10}\ (\text{Signal Power/Noise Power})$$

and that both signal and noise data should be subjected to the same spectral response characteristics during mixing. Thus, a S/N ratio of 0 dB means that the powers of the signal and background are identical.

Table 1 indicates the differences between data as defined for both stages of the CRP. It is argued that the revised specification would be of greater value when using the data to synthesize an instrumental characteristic for a future plant. Indeed, for the acoustic leak detection part of the CRP, it would be the only way to combine the data, since signal and background information were selected from a variety of sources world-wide.

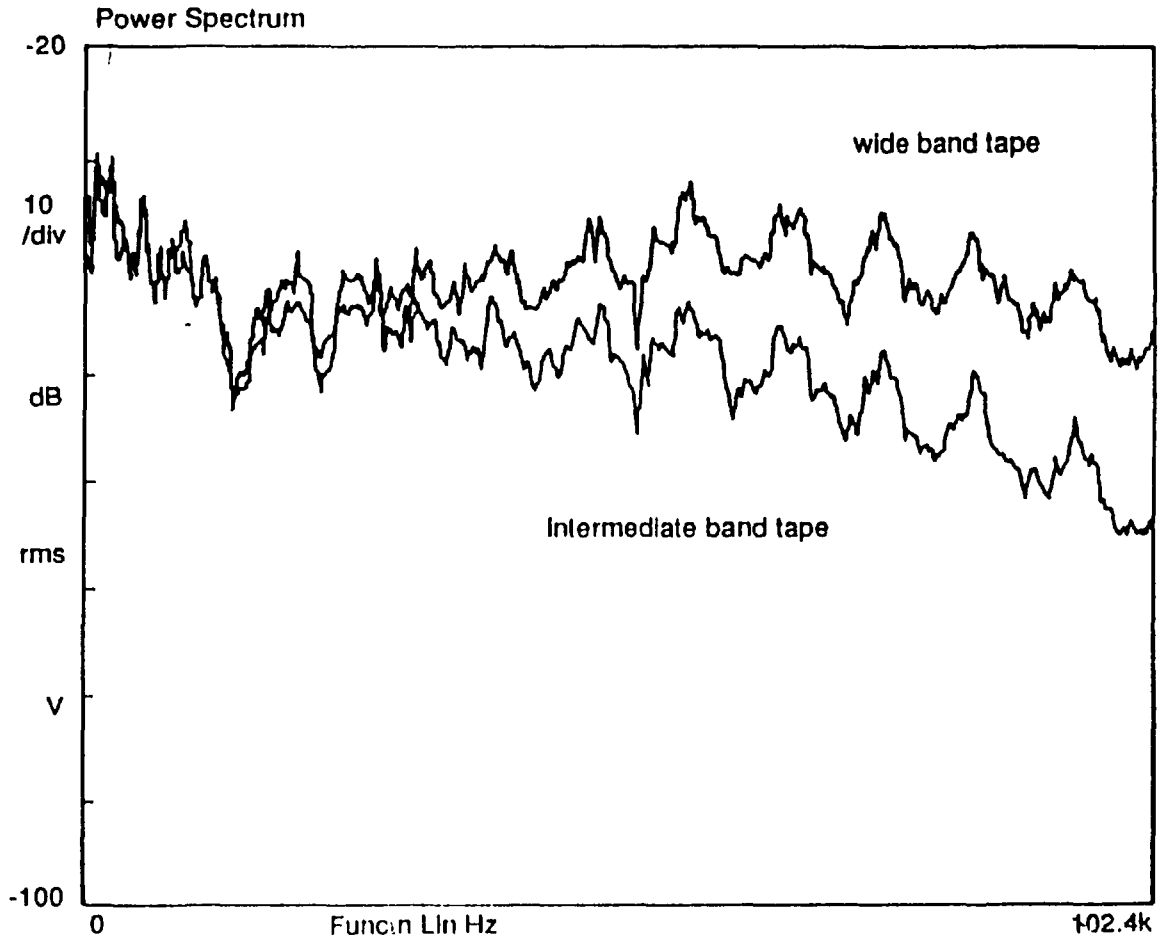

FIG. 1. Comparison of background noise from wide-band tape and intermediate band tape

Table 1 also shows the peak signal ratios for the different signals as used for the first tape. Of particular interest is the fact that for a S/N value of -12 dB, the signal peak was just equal to peak background level. This means that for S/N ratios of greater than -12 dB, plain threshold detection methods could be an option.

2.2. Boiling noise test data

The test data were prepared at Risley Laboratory, Warrington, UK from the acoustic noise signals of boiling experiment performed on the KNS 1 loop at KfK, Germany. The test data consisted of background flow noise of the loop and seven records containing background noise mixed with a 2 to 3 s burst of boiling noise signals. The S/N in the records ranged from -3 dB to -21 dB in -3 dB steps. The objective of the analysis was to find the records containing boiling noise, the start time and duration of the burst of boiling and the probabilities of spurious (Ps) and missing (Pm) the boiling detection.

2.3. Analysis of boiling noise data

Australia, India, Japan and the UK had applied the detection procedures described in the first stage report [1] to the new tape.

TABLE 1. COMPARISON OF SIGNAL TO NOISE RATIOS AS DEFINED IN BOTH STAGES OF THE CO-ORDINATED RESEARCH PROGRAMME

Signal to Noise ratios, in dB		
As defined for second stage	As defined for first stage	Peak signal above 60 KHz
-3	-15	+9
-6	-18	+6
-9	-21	+3
-12	-24	0
-15	-27	-3
-18	-30	-6
-21	-32	-9

2.3.1. Australian analysis

The results from the Australian team were not reported until the second RCM in September 1991. Some difficulties had been found with the tape received, and it was suspected that it may have been contaminated during despatch. As a consequence, analysis had been confined to just three records. An analytical approach described as "conditional expectation strategy" was used. In this, it is assumed that very little a priori information regarding useable boiling noise characteristics will be available at the time an event is to be detected. Conversely, it may be assumed that "normal" operating conditions would be guaranteed for a sufficient time before an anomalous event for a learning process. The principle is, in fact, to look for the unexpected, and for this, an expectation function is defined [2]. The mean square of this function is taken as a suitable feature for the detection of boiling. An alternative approach is the method of differentiation. It is argued that as flow noise and boiling noise have differing spectral characteristics (f^{-4} and f^{-2} respectively), then a differential process can be used to emphasize boiling noise. For determination of the probability of spurious trip and missed events, the probability density functions were calculated on the known background and boiling signals. The results of the analysis are summarized in Table 2.

2.3.2. Indian analysis

The records were analyzed by four different methods. The first involved evaluating different kinds of statistical descriptors. Features like mean, root mean square value, variance, standard deviation, skewness and kurtosis were all evaluated. Each feature was calculated by averaging 2048 points over 7.987 ms. Only variance, as an isolated feature, was found to be significantly sensitive to boiling noise.

The second method of analysis was to employ pulse counting. Pulses were counted if they exceeded a threshold of (mean value) + {(I-1) * 0.25 +1} * S.D., where S.D. is the standard deviation of the mean value, and I represents a "window" number, which was varied from 1 to 13.

TABLE 2. SUMMARY OF TAPE 1 RESULTS FROM AUSTRALIAN TEAM

File	S/N ratio	Averaging Time (ms)	Ps	Pm
		Conditional Expectation Strategy		
3	-3 dB	5	0.0191	0.135
		15	0.0134	0.0144
		50	0.0	0.0
		150	0.0	0.0
5	-9 dB	150	0.00129	0.00345
		300	0.0	0.0
6	-6 dB	5	0.0601	0.116
		15	0.00798	0.0556
		50	0.0	0.0
		150	0.0	0.0
		Differencing Technique		
6	-6 dB	5	0.0584	0.122
		15	0.0228	0.0466
		50	0.000064	0.001419
		150	0.0	0.0

The third and fourth methods were to calculate the determinant and trace of co-variance matrix constructed from the auto power spectral density (APSD) of the data. The entire frequency range in which the APSD shows sensitivity to boiling is divided into several segmented areas under the APSD curve and then the co-variance matrix of these areas is calculated. The determinant and trace of the co-variance matrix are used as features. These two features have been found to be extremely sensitive to the boiling noise [4].

The adaptive learning network (ALN) technique was applied on the new boiling data with a modified approach. In this new approach, the two generation network was trained using background data and an assumed boiling data which was derived from the background data itself. The RMS value, number of pulses above a threshold and skewness were the network input features. Boiling pulses were detected down to -12 dB signal to noise ratio. The no/No criterion was further applied to reduce spurious trip rate to the target level of 0.1 per year. This new approach enables the application of ALN technique to a plant where boiling signal can not be generated for training the network [5].

The results of the analyses are summarized in Tables 3 and 4. They show clearly that the boiling signals to a S/N ratio of -12 dB can be accurately detected, and determinant and trace show better sensitivity to the boiling noise. At a later RCM, additional evidence was presented showing that signals down to -21 dB could be detected, necessarily with lower reliability figures.

2.3.3. Japanese analysis

The method used for analysis in Japan is a non-linear analog system, as shown in the schematic diagram of Fig. 2. The original signal is first passed through a band-pass filter

TABLE 3 DETECTED TIMINGS OF BOILING SIGNALS, INDIAN ANALYSIS OF TAPE 1

		Time and duration of boiling signal											
		Actual		Variance		Pulse count		Determinant		Trace		ALN	
Record	S/N	Onset	Dura-tion	Onset	Dura-tion	Onset	Dura-tion	Onset	Dura-tion	Onset	Dura-rion	Onset	Dura-rion
		(s)	(s)	(s)	(s)	(s)	(s)	(s)	(s)	(s)	(s)	(s)	(s)
1													
2													
3	-3	8 90	2 35	9 30	2 50	9 06	2 34	9 08	2 69	9 01	2 50		
4	-	-	-	-	-	-	-	-	-	-	-		
5	-9	18 35	3 05	18 93	2 66	18 93	2 63	18 61	2 97	18 84	2 71		
6	-6	14 20	2 90	14 40	2 84	14 40	2 84	14 39	2 94	14 33	2 96	14 25	2 79
7	-15	7 40	1 90	-	-	-	-	-	-	-		-	-
8	-12	21 05	2 30	21 18	2 42	21 31	2 39	21 21	2 34	21 25	2 28	21 25	2 24
9	-18	11 85	2 05	-	-	-	-	-	-	-	-	-	
10	-	-	-	-	-	-	-	-	-	-	-	-	
11	-21	3 90	2 20	-	-	-	-	-	-	-	-	-	

Note Onset times are from start of record

TABLE 4 DETECTION RELIABILITY OF BOILING SIGNALS, INDIAN ANALYSIS OF TAPE 1

		Probabilities of Spurious trip and Missed events							
		Variance		Pulse count		Determinant		Trace	
Record No	S/N ratio	Ps	Pm	Ps	Pm	Ps	Pm	Ps	Pm
1									
2									
3	-3	0 06	0 17	0 23	0 19	0	0	0	0
4	-	-	-	-	-	-	-		
5	-9	0 10	0 22	0 15	0 26	0 027	0 038	0 065	0 008
6	-6	0 04	0 10	0 04	0 13	0	0	0	0
7	-15	-	-	-	-	-	-	-	-
8	-12	0 42	0 30	0 30	0 46	0 272	0 218	0 345	0 185
9	-18		-	-	-	-	-		
10	-	-	-	-	-	-	-	-	
11	-21	-	-	-		-	-	-	

having lower and upper limits of f_{c1} and f_{c2}, and is then squared. The squared signal is again filtered with a high-pass filter with cut-off f_{c3}, and again squared. The resultant signal is then integrated over a time interval DT to obtain what is described as the "feature signal". The sample mean value M and standard deviation D of the feature signal are calculated over a selected time interval T to determine a threshold value L = M + F*D, where F is an adjustable factor. The frequencies for the analysis are chosen following an examination of the PSD for the signals. It was noted, as shown in Fig. 3, that the PSDs for all signals were similar, and so could not be used in themselves for discrimination of background noise.

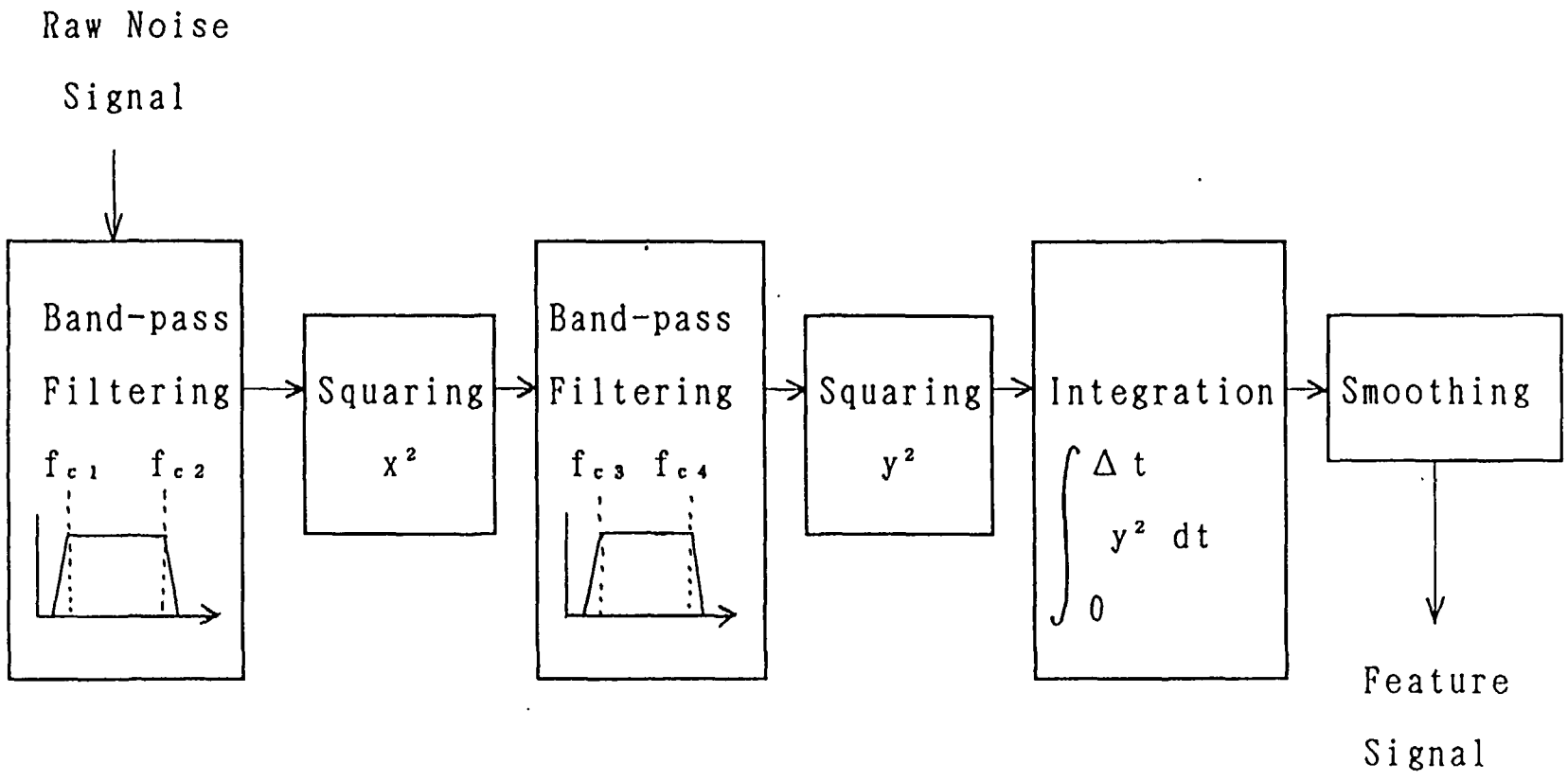

FIG. 2. Schematic diagram of the twice-squared signal processing method

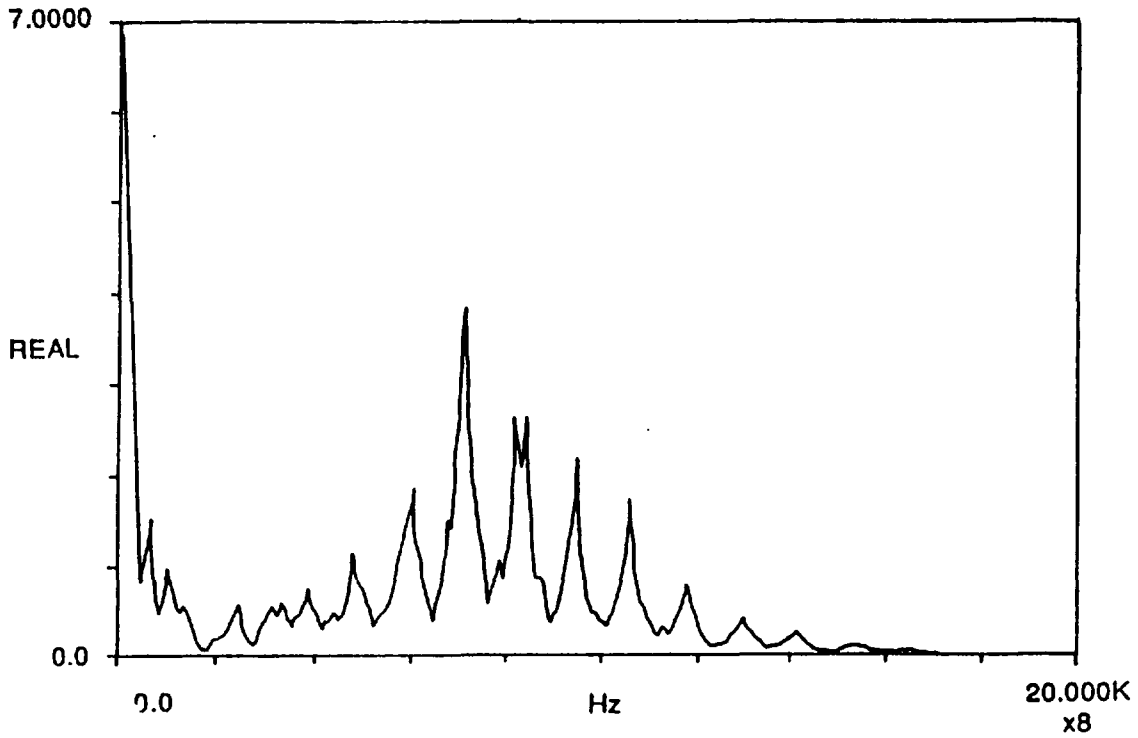

FIG. 3. PSD function for all records (first tape, boiling data)

The value of L was chosen after examination of the feature signal. Once chosen, the probability density functions (PDF) can then be determined to calculate the probability of spurious trip, Ps, and the probability of missing the boiling detection, Pm. Figure 4 shows these procedures for the case of a S/N of -12 dB. It is immediately clear that the PDFs of background and boiling signal do not overlap, which explains the conclusion that for this case and higher S/N ratios, the values of Ps and Pm are zero. For worse S/N ratios, it is not possible to isolate the feature signal from background conclusively with an analog threshold value, and so reliable detection is not claimed, although a visual examination enables the boiling burst to be detected. Table 5 summarizes the results. It demonstrates clearly that all cases of boiling were accurately detected, even in those cases where the detection was not claimed reliable.

TABLE 5. DETECTION OF BOILING SIGNALS, JAPANESE ANALYSIS OF TAPE 1

Record No.	S/N ratio	Start time	Measured time	Ps	Pm
1	-	-	-	-	-
2	-	-	-	-	-
3	-3	14:26:46.85	14:26:46	0	0
4	-	-	-	-	-
5	-9	14:32:12.90	14:32:14	0	0
6	-6	4:39:14.00	14:39:14	0	0
7	-15	14:42:45.90	14:42:47	-	-
8	-12	14:45:14.95	14:45:15	0	0
9	-18	14:48:22.55	14:50:56	-	-
10			-	-	-
11	-21	14:52:50.45	14:53:14	-	-

2.3.4. UK analysis

Although the test tape had been prepared in the UK, none the less it was subjected to pattern recognition analysis using the standard procedure used in the Risley Laboratories of AEA Technology. It had been shown in the first stage of the CRP [1] that, since boiling signals are impulsive, best results were obtained by choosing narrow time windows which contained boiling pulses rather than assuming that all of the signal in the boiling regime was characteristic of boiling. This required capturing only events above a predetermined threshold, for example, at six times the standard deviation. However, for this analysis, where peak boiling signal amplitudes were close to peak background, it was decided not to prejudge the result and to attempt a "worst case analysis" by using all of the signal during boiling. Samples were digitized in records of 1000 samples each. The total record length was 5 milliseconds. It has been noted that the boiling pulse rate was about 100 pps, and so roughly half the records during the training phase would not contain any boiling pulses. Consequently, it was not surprising that the pattern recognition method did not isolate the boiling regime completely from background. Figures 5 and 6 show the scatter plot and probability distribution for the two analytical features peak and rms values at the -6 dB S/N level. A more detailed 20 feature analysis for the same data gave much the same result. A similar analysis for the -9 dB level showed somewhat worse discrimination.

The method of applying pattern recognition analysis to a trip system would be to rely on a pulse counting technique accumulating to trip. Thus, assuming that the threshold level has been set as in Fig. 6, the probability of classifying a background pulse as boiling is 4.65×10^{-2} and the probability of classifying a boiling pulse as background is 0.194. Since the mean rate of boiling pulses was 100 pps, the method of statistical analysis previously described [1] gave an estimated failure rate of less than 10^{-6}, and a spurious trip rate of less than once in 2 years. This was an encouraging result in view of the "worst case" assumption made regarding the boiling signal.

For the -9 dB signal to noise ratio test data, although boiling was clearly identifiable, reliable detection with a low spurious trip rate was not judged possible. Consequently it was concluded that for S/N ratios of this level, or worse, pattern recognition methods seemed unlikely to give the required discrimination, although subjectively the boiling at the -12 dB level had been detected. It should be noted, however, that with the large number of samples involved (200 in 1 second) this data would be an excellent input for the n_o/N_o technique devised by the Indian team [1]. This factor had not been taken into consideration at the time of analysis.

2.4. Appraisal of boiling detection results

The original questions asked about boiling noise detection at the Research Co-ordination Meeting held at Vienna in October 1987, were the following:

1. Can the performance of the signal processing system be set so that the spurious trip rate is less than 10^{-1} per year?
2. If such a trip rate can be achieved, what is
   - i. the minimum averaging time that would be required,
   - ii. the probability of missing a boiling event, and
   - iii. the level of discrimination between the boiling and non-boiling phases in the signal.

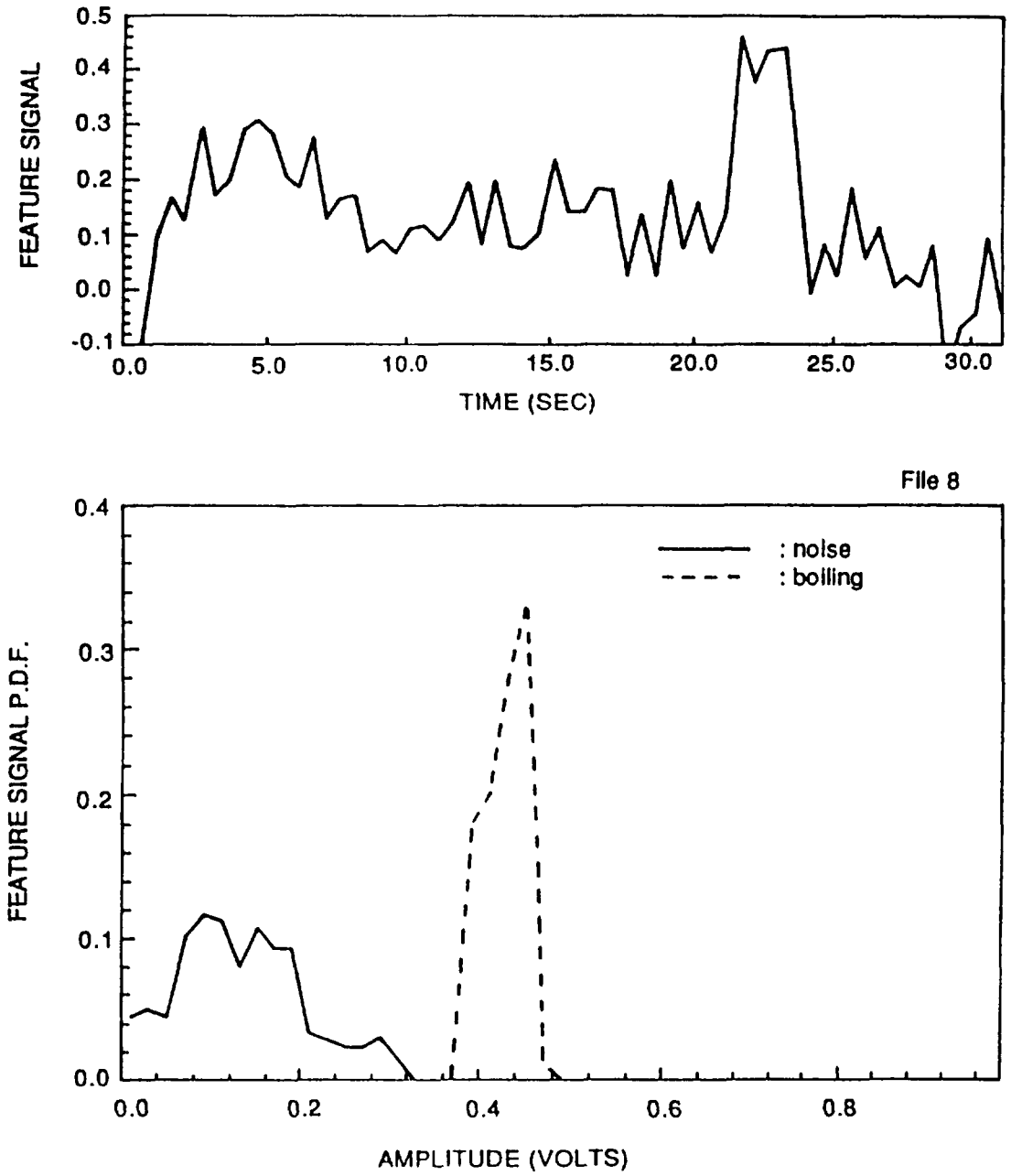

FIG. 4. Feature signal and PDFs for record No. 8, (first tape, boiling data)

Since these questions were asked, the results of a feasibility study into the applicability of acoustic boiling noise detection to the safety case of European Fast Reactor (EFR) have been published [6]. They show (Fig. 7) that for satisfactory detection of local boiling within a fuel subassembly, signal and background acoustic levels are likely to be within the same order of magnitude. Thus, the requirement for detection sensitivity for a trip instrument could be the ability to detect boiling with a S/N ratio of -10 dB or so.

The results reported here represent the conclusion of the work on boiling noise detection, having tested the techniques to a higher degree than previously reported. The three countries who successfully tested the final boiling noise tape all had difficulty in measuring signals for S/N ratios of worse than -12 dB. It is significant, when examining Table 1, that this level is that at which the peak impulse boiling signals are the same level as background.

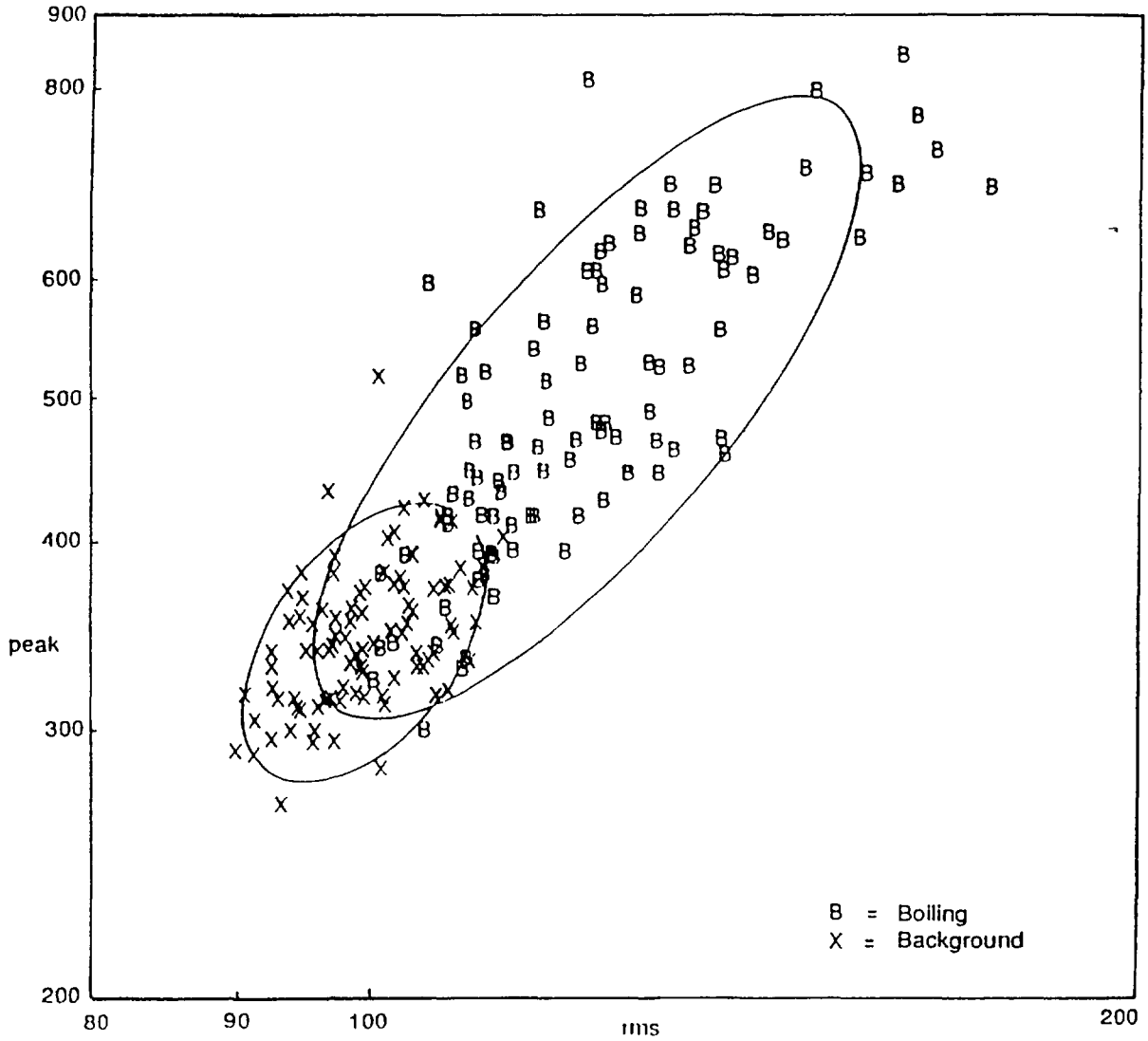

FIG. 5. Scatter plot for two features, peak and RMS, of background and boiling (Record 7, S/N ratio = -6 dB)

It is not surprising, therefore, that the Japanese analog system, which relies on stretching the threshold margins, succeeded down to this level, but could not find a reliable threshold below it. In this, all workers were effectively finding that at the -12 dB level, the discrimination between signal and background was effectively zero.

Another difficulty that should be mentioned is that the desired criterion for the spurious trip rate is for a Ps value of the order of 10^{-8}, probably below the resolution of the individual values reported. Clearly, any approach to this value can only be judged on statistical grounds. In fact, only from the Japanese work could there be confidence that the spurious trip rate could be low enough on a single reading to meet the criterion at this level, although there was promise in the Australian work of similarly low "zero" values. Both the UK and Indian teams were finding spurious trip rates that seem at first to be too high.

To understand this, it has first to be recognized that the Japanese method includes an integration time constant of typically 0.5 s, whilst the Australian methods also produced low

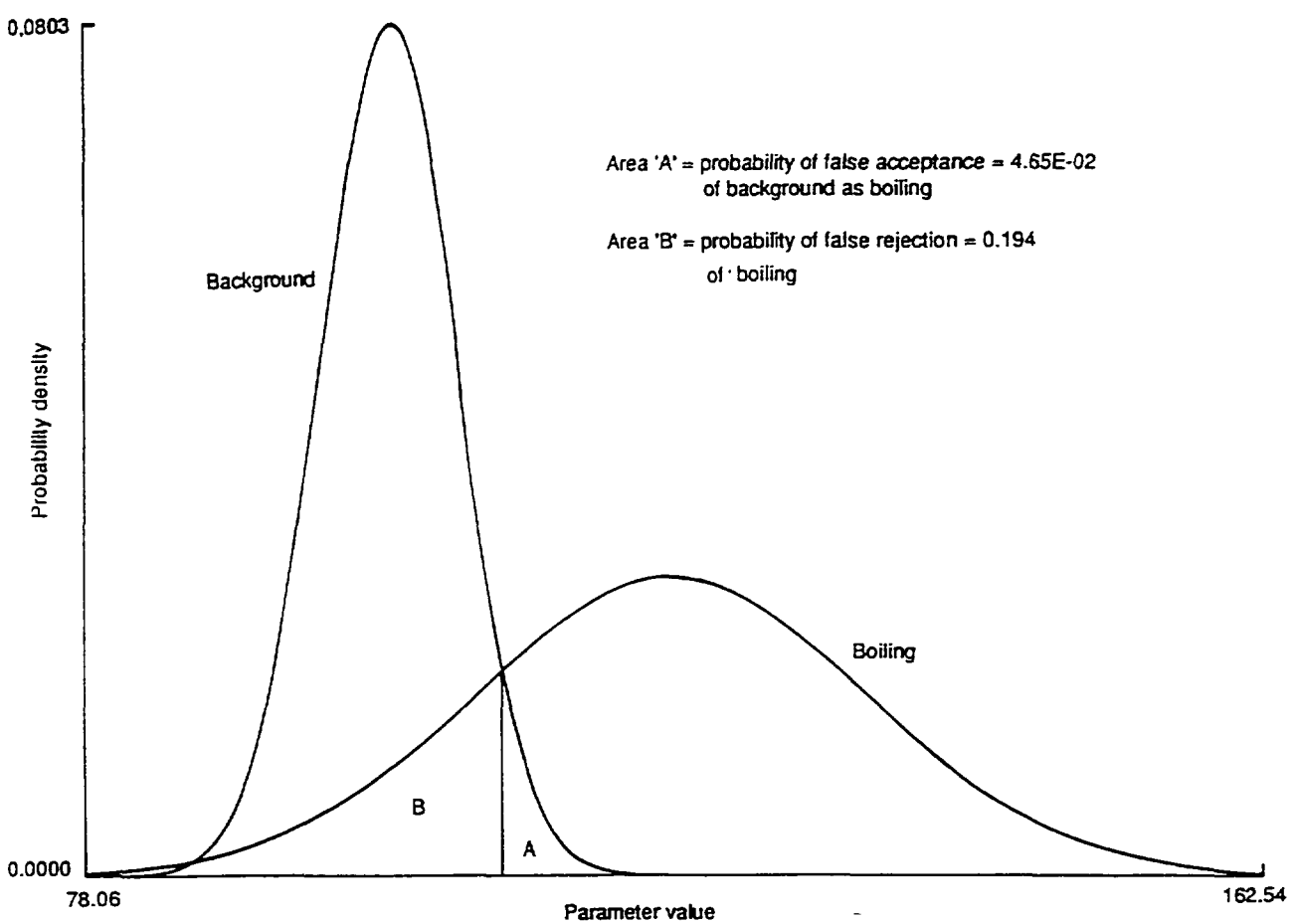

FIG. 6. Probability distributions for RMS feature, background and boiling (Record 7, S/N ratio = -6dB)

probabilities for the higher averaging times. On the other hand the other methods involve rapid digital analysis with time slices of only 5-7 ms. Without some additional processing, the latter methods are not exploiting all the information available in the second or so available before a reactor would be required to trip. This was well recognized by the Indian team who addressed the problem in the second RCM of the first phase, in December 1986 [1], when they introduced the n_o/N_o criterion. Briefly, to reduce the probability of spurious or missing the boiling event, the decision should not be based on a single event, but on N_o estimates evaluated at a time, and by checking whether n_o estimates show the boiling above the preset level. The estimates show that for the most pessimistic result from Table 4, a Ps value of 0.42 for the variance method when at a S/N value of -12 dB, a spurious trip rate of less than 1 in two years can be achieved by requiring 42 in 50 samples to show the event. The Indian team observed that one can always find a n_o/N_o value for a given P_s or P_m to meet the target criterion, and with sample rates of 100-200 per second , the target times can also be met.

Thus, the conclusion of the acoustic boiling noise detection phase can be summarized as follows:

1. Reliable detection with low spurious trip rates (less than 0.1 per year) can be achieved for signal to noise levels of -12 dB. This represents a peak boiling impulse level equal to background. This meets the requirements of the protection system of a large fast reactor like the EFR.

2. Signals with a poorer signal to noise ratio could not be detected with sufficient confidence.

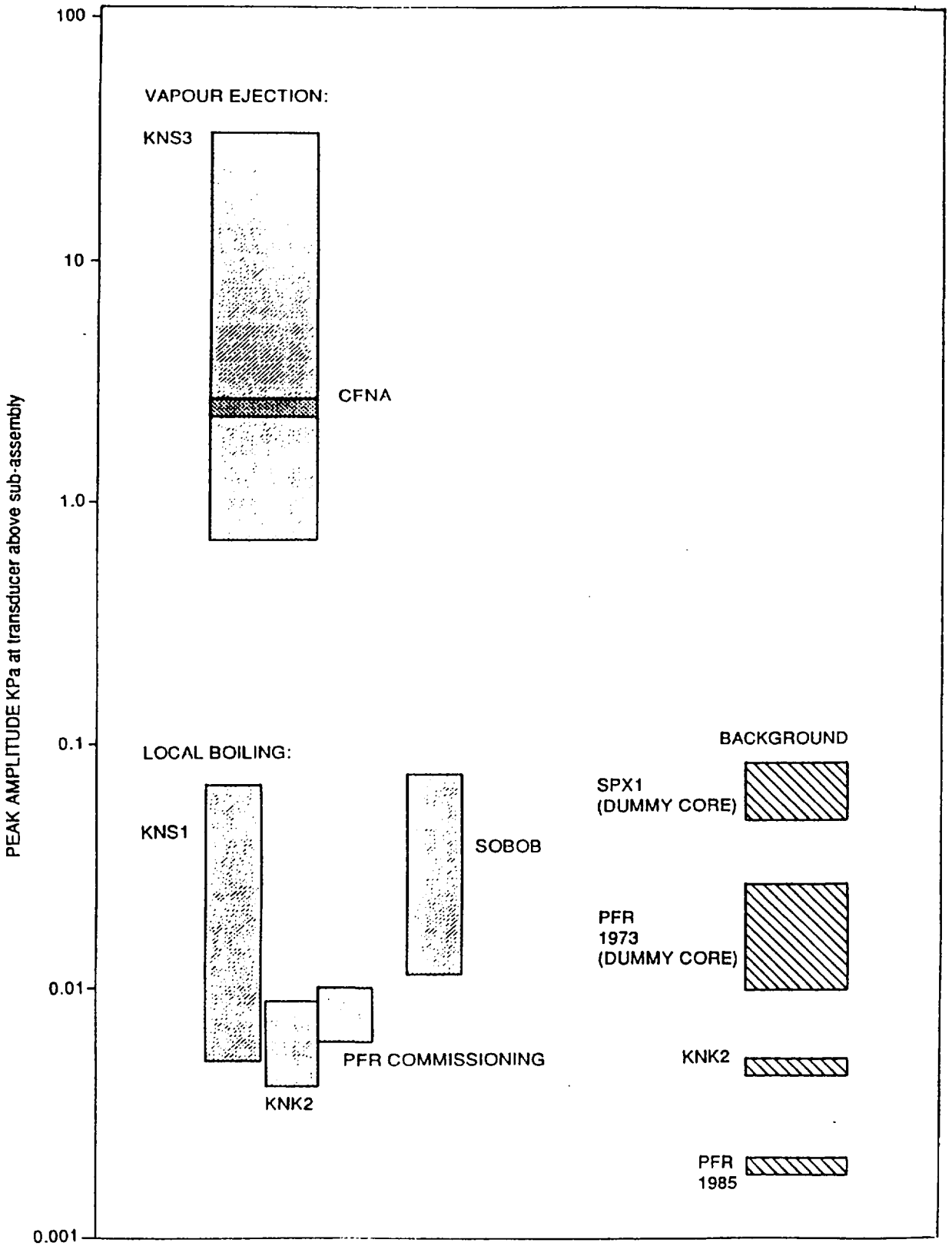

FIG. 7. Comparison of sodium boiling signal amplitudes and reactor background noise from various sources

3. ACOUSTIC LEAK DETECTION OF SODIUM/WATER REACTION

3.1. Assessment of sensitivity required for plant operation

The UK delegate provided details concerning the assessment made by the UK for detection of sodium-water reaction in the European fast reactor project. Design details of possible leak detection instrumentation have been published [6-8].

Passive leak detection listens to the noise produced by leak of water/steam into sodium in the steam generator. This can be the noise due to the velocity of the steam jet (which can increase if it impinges on a target) and noise from the sodium/water reaction itself including hydrogen bubbles or, under severe leak conditions, noise from the boiling of the sodium. Further sources of noise would include the movement of the hydrogen bubbles through grids. Hydrogen bubbles also have a markedly detectable effect in the absorption of certain background frequencies.

The following five factors have to be studied to deduce detection performance: (1) the nature of the sound from actual sodium-water reaction, (2) the manner in which the sound propagates through the SGU to the detector, (3) the nature of the SGU background noise, (4) the performance of data analysis routines, especially when the background is high, and (5) techniques for sound source location, not only to assist the operators in case of a leak, but also to provide discrimination against extraneous noises.

Concerning the sound from actual leaks, water/steam leaks were studied in facilities at both Dounreay and Bensberg. In a number of these tests acoustic transducers were placed close to the leak to provide data on the strength of the acoustic signal generated. For the assessment, data obtained from the Small Water Leak Rig and Super Noah facilities at Dounreay have been used. The details of the experiment have been reported elsewhere [9].

Transmission characteristics have been determined on PFR steam generators, and water model facilities at Risley have been used to assess the effect of the SGU construction on the transmission of sound [10]. There is no doubt that the geometry of the tube bundle itself has a dominant effect, and to assist the modelling work a theoretical study has also been undertaken [11].

The collected data can be used to estimate the possible sensitivity of a leak detection system using steam generators of similar noise performance to PFR. Figure 8 shows the method. Horizontal bounds mark the extremes of noise experienced in PFR. With an allowance for transmission losses, these represent the levels against which the leak must be detected. The sloping bounds indicate the range of actual sound output from leaks as a function of leak rate. The range reflects the fact that not all leaks, as measured, give the same amount of sound. With a simple threshold type of detection, the actual sensitivity will lie somewhere within the enclosed rectangle. For a noisy unit (PFR Reheater No. 2) the sensitivity is in the range 34-67 g/s, whilst for the quieter Superheater No 3, the range is 0.55-13 g/s. It is clear that with the latter, a sensitivity of a few g/s would be no great problem.

At present, it seems likely that a detection sensitivity of 1 g/s would be required for EFR which typically represents a large fast reactor. From the foregoing, only for the quieter unit, and for a favourably noisy leak, could this be done with simple detection. Extrapolation of the bounds on the figure indicates that for certain detection, a signal to noise ratio of -17

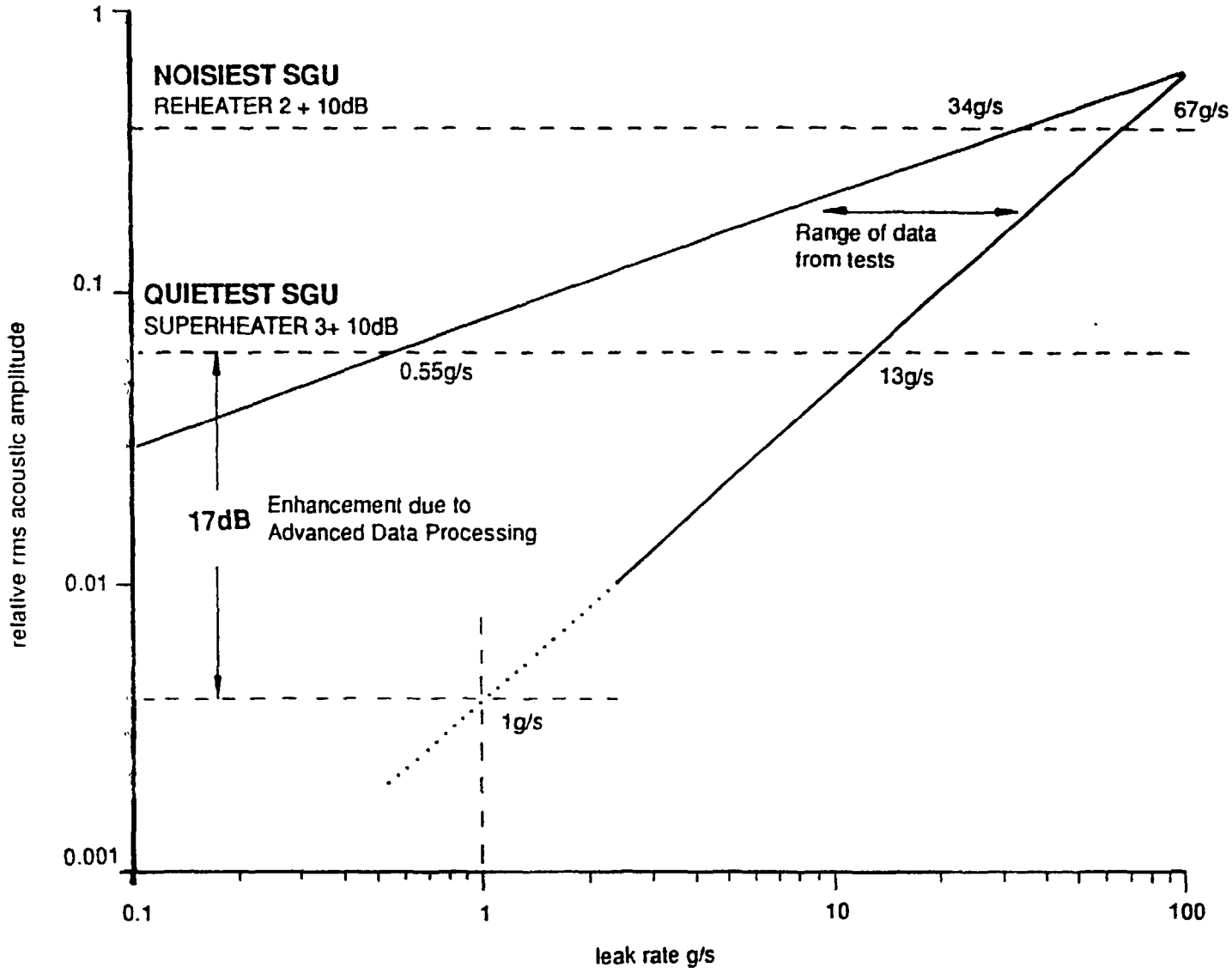

FIG. 8. Estimated sensitivity for acoustic detection of sodium/water leaks

dB may exist, demanding that the techniques being developed by the CRP meet this target.

3.2. Signal strengths

The Australian delegate has supplied a theoretical study of the hydrodynamic sources of sound to be expected when steam leaks into the sodium of a LMFR steam generator. The model is based on a submerged jet of steam that expands over an axial distance at a constant (sonic) velocity, then spreads producing an instability in the steam/sodium interface. Using simplifying assumptions, the study shows that for a one gram per second leak through a one mm dia orifice, the following parameters apply:

Source	Radiation power (mW)	Probable frequency
Jet Noise	18	600 kHz
Bubble Noise	750	low
Droplet Noise	400	100 to 1000 kHz

3.3. Leak noise test data

The tapes included separate examples of leak noise (from Germany, the Russian Federation and the UK) and steam generator background noise from PFR and SPX1. The five sets of data supplied are summarized below:

(i) The first set of data (second tape) was prepared for familiarization with leak noise. Along with samples of pure leak noise and background noise data from SGUs of PFR, two sets of synthesized data were prepared mixing the Russian leak (leak rate 0.05 g/s) data with PFR background noise with S/N of -1.7 and -6.7 dB. The data were prepared in the UK.

(ii) The second set of data (third tape) was also prepared by the UK. It contained along with pure leak and background noise five records of data synthesized by mixing Russian leak noise and PFR background noise with S/N ranging from -8 dB to -22 dB. Another data record contained synthesized data with S/N of -15 dB prepared from UK leak noise data (leak rate 1 g/s) and SPX1 SGU background noise data. The data with such a low S/N (-22 dB) was the special feature of this set and data from SPX1 background and UK leak provided diversity in data.

Figures 9-12 show the spectral characteristics of the signals used in the preparation of this tape.

(iii) The third set of data (fourth tape) was prepared by mixing leak noise of ASB loop, Bensberg, Germany with PFR SGU background noise. Similar measuring equipment was used in both the experiments. The S/N ratio in 4 records ranged from -8 dB to -20 dB. The special feature of this set was that two sets of synthesized data were prepared, one with a leak rate of 1.8 g/s and the other with 3.8 g/s. It was to be checked whether the analysis methods were to be changed for different leak rates. The data were prepared by France and Japan.

(iv) The fourth set of data (fifth tape) contained multichannel data, i.e., 4 channel leak noise data (3.8 g/s leak) from ASB loop and 5 sets of mixed data prepared for each channel by mixing with PFR background noise measured on four wave guides and the S/N ranging from -6 dB to -24 dB. Similar measuring equipment was used in both the

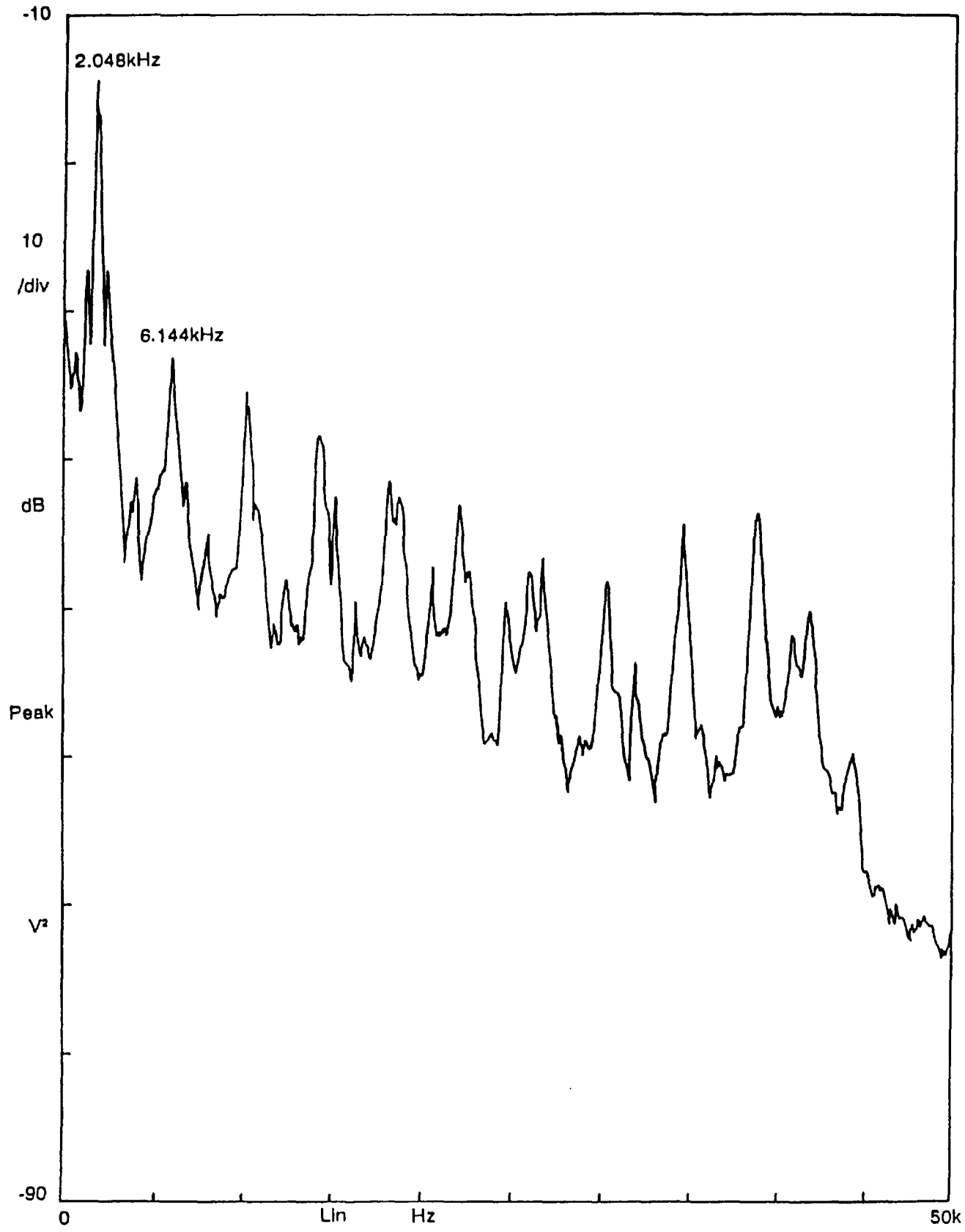

FIG. 9. Spectrum of PFR SGU background noise (Record 2, third tape)

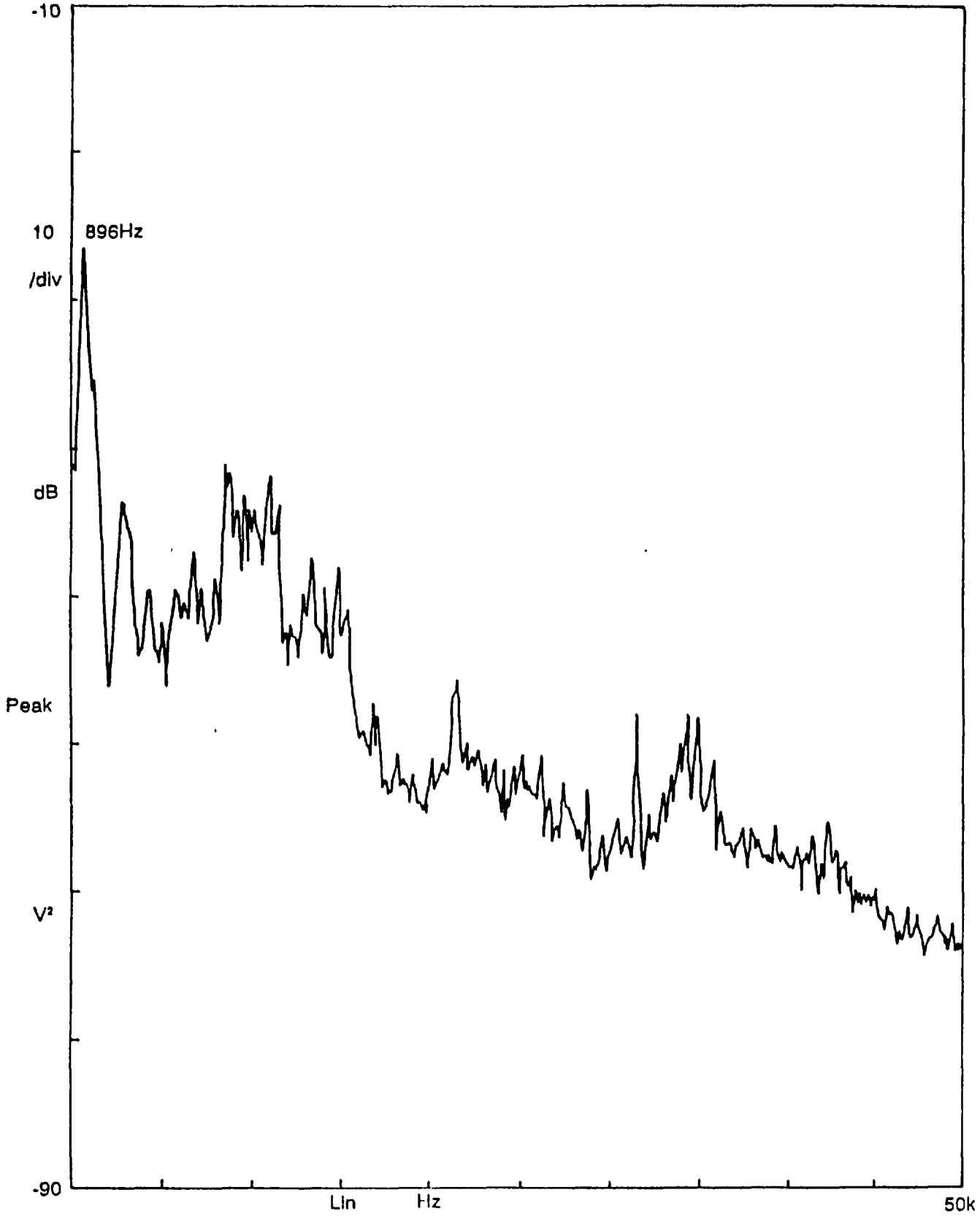

FIG. 10. Spectrum of Russian water/sodium leak noise (Record 3, third tape)

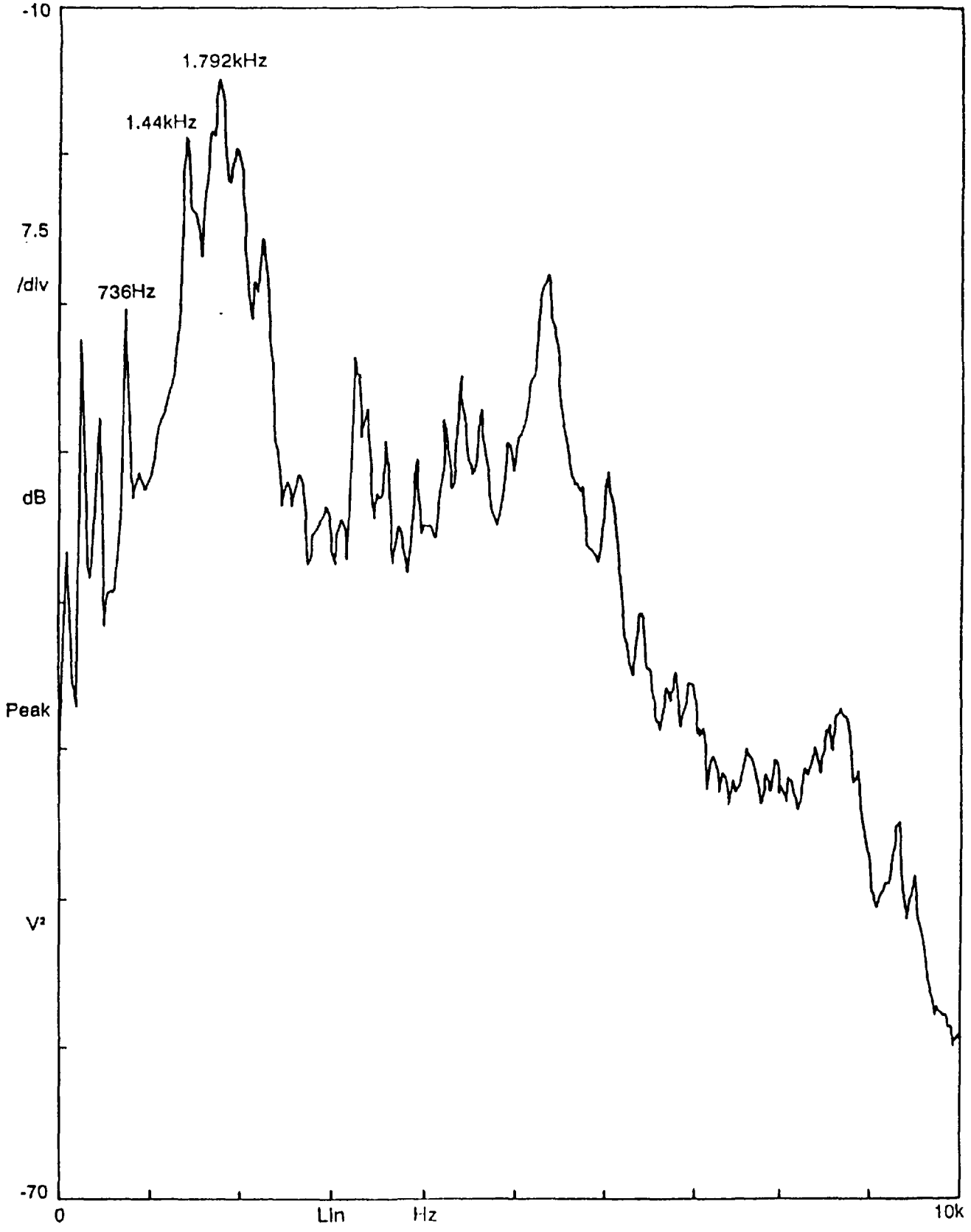

FIG. 11. Spectrum of SPX1 background noise (Record 10, third tape)

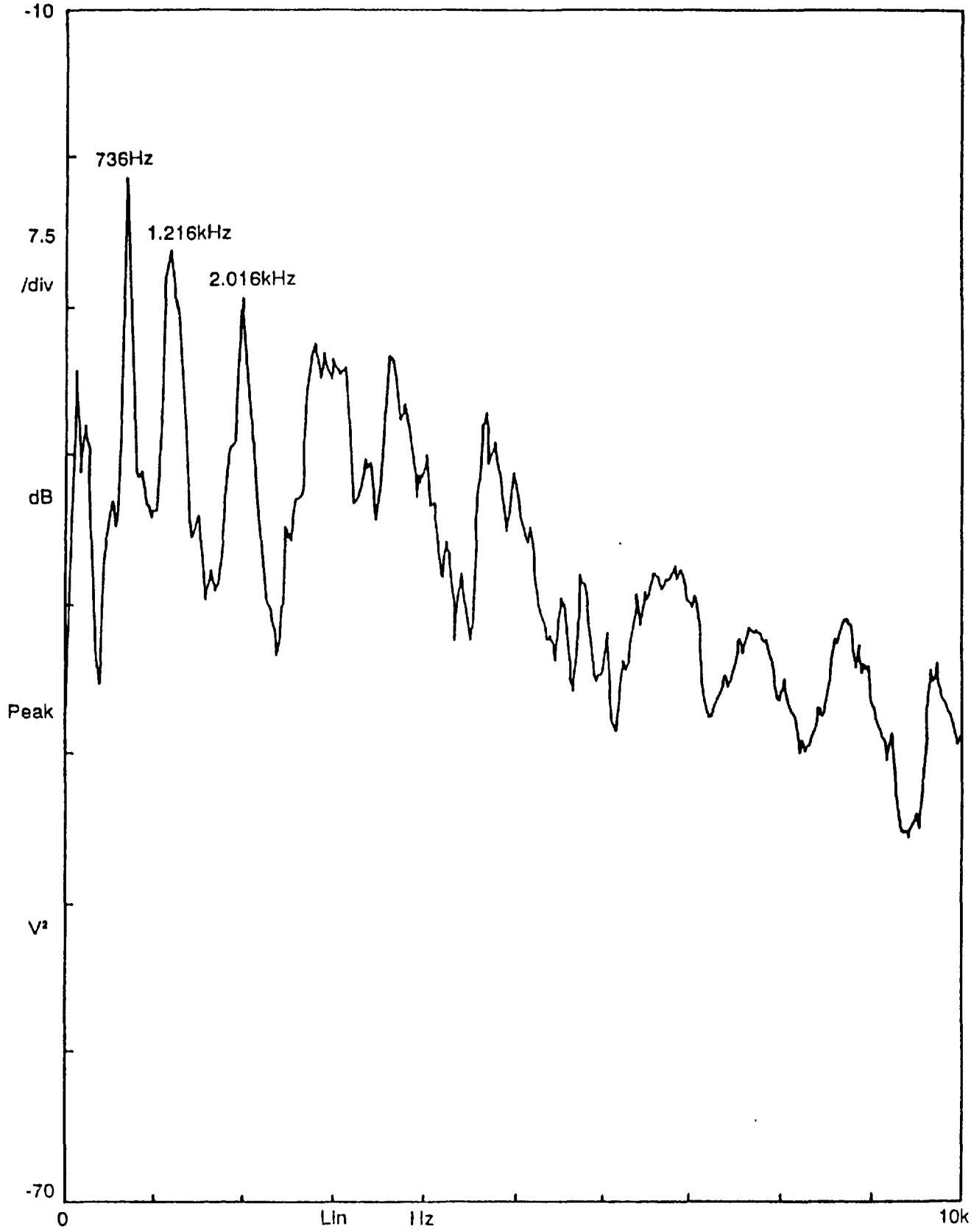

FIG. 12. Spectrum of UK water/sodium leak noise (Record 9, third tape)

experiments. The special features of this set of data were to bring out the advantage of multichannel analysis over single channel analysis and to find the location of the leak. The test data were prepared by France.

(v) The fifth set of data (sixth tape) was prepared by the UK using the data from background noise measurements on PFR SGUs and from the end-of-life acoustics leak experiments carried out on PFR evaporator-3. In these experiments, argon, hydrogen and water/steam injections were carried out and acoustic noise was measured at different locations. This was the first data in which both background and leak noise signals were obtained from the same unit. The data also contained signals from different injection medium.

The participants were asked to: (1) determine the start time and duration of the leak signal in those records consisting of a mix of leak noise with background; (2) estimate the detection margin above the background noise; (3) comment on the realistic decision time to initiate a trip signal; (4) where appropriate (tape 3, which contained data from different sources), comment on how the analysis method may be influenced by different SGU background noise and leak characteristics; (5) estimate the location of leak in multichannel ASB loop data, and (6) identify the injection medium, transmission characteristics to different channels and location of leak on the fifth set of data from PFR end-of-life ALD experiments.

3.4. Analysis of leak noise data

3.4.1. Leak noise familiarization

Along with samples of pure leak noise and background noise, only two mixes of leak noise with background were offered, using the Russian leak data with PFR background data, with signal to noise ratios of -1.7 and -6.7 dB, and it was not expected to give much difficulty in analysis. The results were presented at an IAEA RCM held at Chester, UK from 25-27 September, 1991. Three complete analyses were performed on the tape, by the Indian, Japanese and UK teams, and a summary of their findings is given in Table 6. The Australian team found that their conditional expectation procedure showed no improvement on the variance technique, whilst their differencing method was not appropriate to SGU leak detection because of spectral similarity between signal and noise in the upper frequency region.

The Indian team analyzed the data using conventional features like variance, probability density function and auto power spectral density and the newly defined features like determinant and trace. In addition, a new ratio called PSD ratio (ratio of APSDs of leak noise to the background noise) was also defined to identify the frequencies sensitive to the anomaly noise signals. Thus the determinant and trace were calculated from the co-variance matrix constructed for several frequencies identified by the PSD-ratio method. This further improved the sensitivity of determinant and trace to the anomaly noise. A new feature, called the added PSD ratio was also defined and studied with different thresholds, and has been found to be a sensitive feature for detecting leak noise buried in the background noise of the steam generator. The added PSD ratio is basically the sum of the PSD ratios at discrete frequencies at which leak noise is predominantly high over the background noise. Table 6 summarizes the results of the analysis by the Indian team.

TABLE 6. SUMMARY OF ANALYSIS FOR SECOND TAPE (ALD-FIRST DATA SET)

	Record 5				Record 6			
Feature	Onset (s)	Duration (s)	Margin (dB)	Decision Time (s)	Onset (s)	Duration (s)	Margin (dB)	Decision Time (s)
UK Analysis								
1KHz band			10				10	
11KHz band			15				15	
Japanese Analysis								
measured	22:03	9	3	0.5	25.17	10	3	0.5
actual time (Note 1)	22:02	9.91			25:17	9.91		
Indian Analysis								
Visual	43.2				43.2			
Variance	38.92 ±0.01	9.96	34	0	43.92	7.98	6.28	0
PSD-Ratio	38.92 ±0.01	9.60	70	1.0	41.11	9.99	69	1.0
Deter-minant	38.07 0.51	10.82	811	1.1	41.21	10.91	627	1.1
Trace	38.19 ±0.51	10.70	75	1.1	41.35	10.84	64	1.1
ALN	42.58	8.14	-	0.4	43.7	9.65	-	0.4
Actual Time (Note 2)	39.04	9.91			41.63		9.91	

Notes: 1. Time in minutes and seconds, absolute; 2. Time in seconds from start of record

Preliminary inspection of the tape by the Japanese team suggested that signal components in the range 8-18 kHz should be used. The signal processing method they used is essentially the same as that used for detection of sodium boiling. The raw signal is first filtered by a band-pass filter with cut-off frequencies fc_1 and fc_2 and then squared. The squared signal is again filtered by a band-pass filter with cut-off frequencies fc_3 and fc_4 and then squared. The twice-squared signal is integrated over a specified time interval DT to obtain the feature signal. The sample mean value M and the standard deviation D of the feature signal for the background noise are calculated to determine the threshold level $L = M + FxD$, where F is the adjustable margin for leak detection.

The start time and the duration of the leak noise are determined as the time when the feature signal exceeds level L and remains above it, respectively. The minimum decision time is determined by the integration time dT. Table 6 shows that no difficulty was experienced in detecting and timing the signal bursts.

Analysis by the UK showed (Fig. 13) that most of the energy was in the region below about 15 kHz, and in particular two bands centred around 1kHz and 11 kHz. The 1 kHz signal was shown to result largely from individual impulsive events which were assumed to be hydrogen bubble resonances, corresponding to bubble diameters of the order of a few millimetres. A comparison of the spectra between the leak noise and background (Fig. 14) suggested that these frequency bands could be used for leak noise discrimination, and the results in Table 6 confirm this assumption with margins of 10 and 15 dB being achieved.

The reason for the presence of the strong lower frequency band was discussed; the Indian team attributed it to resonances in the Russian facility that had generated the sounds, but the Russian team themselves attributed it to bubble resonances [12]. This is also the opinion of the UK team, who have had previous experience of working with bubbles and recognize the narrow band resonance characteristics of them in these signals. Figure 15 is an analysis of bubble sizes against resonant frequency using the theories of Nishi and Minnaert.

3.4.2. Signal to noise ratio down to -22 dB

Whilst the tape again contained examples of various noise sources, five of the records were leak/background noise mixes similar to those in the second tape, that is, Russian leak noise mixed with PFR background, but with S/N ratios ranging from -8 dB to -22 dB. One

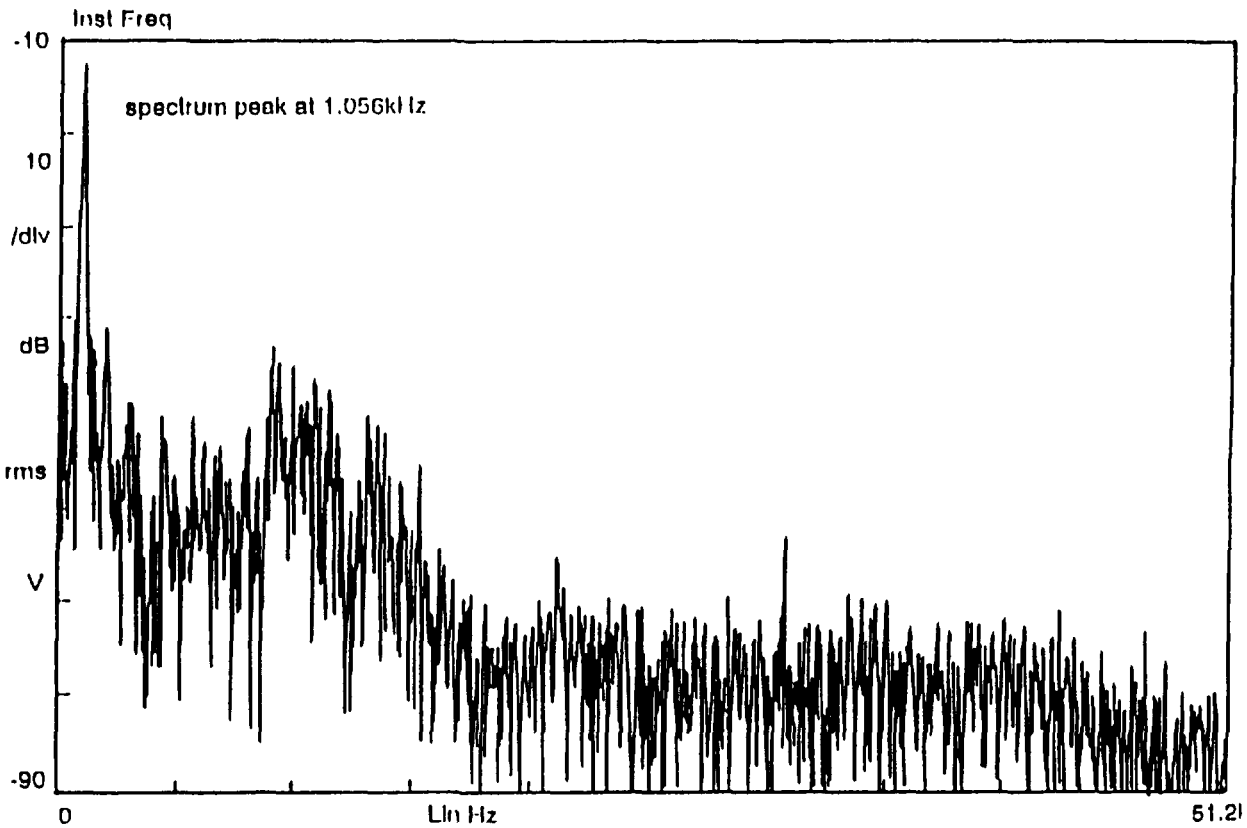

FIG. 13. Spectrum of Russian leak noise, (Record 4, second tape)

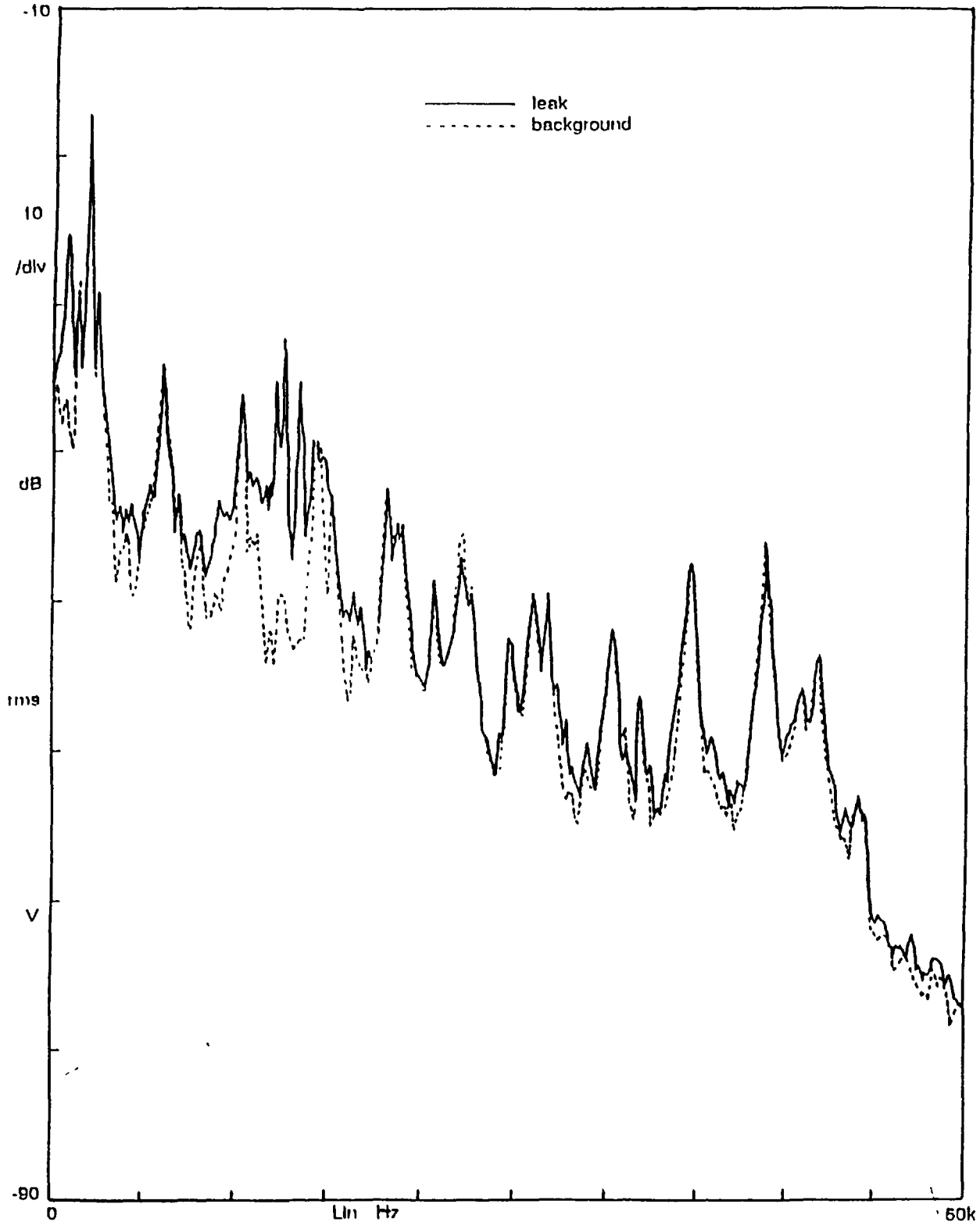

FIG. 14. Comparison of leak and background spectra, (Record 6, second tape, S/N ratio = -6.7 dB)

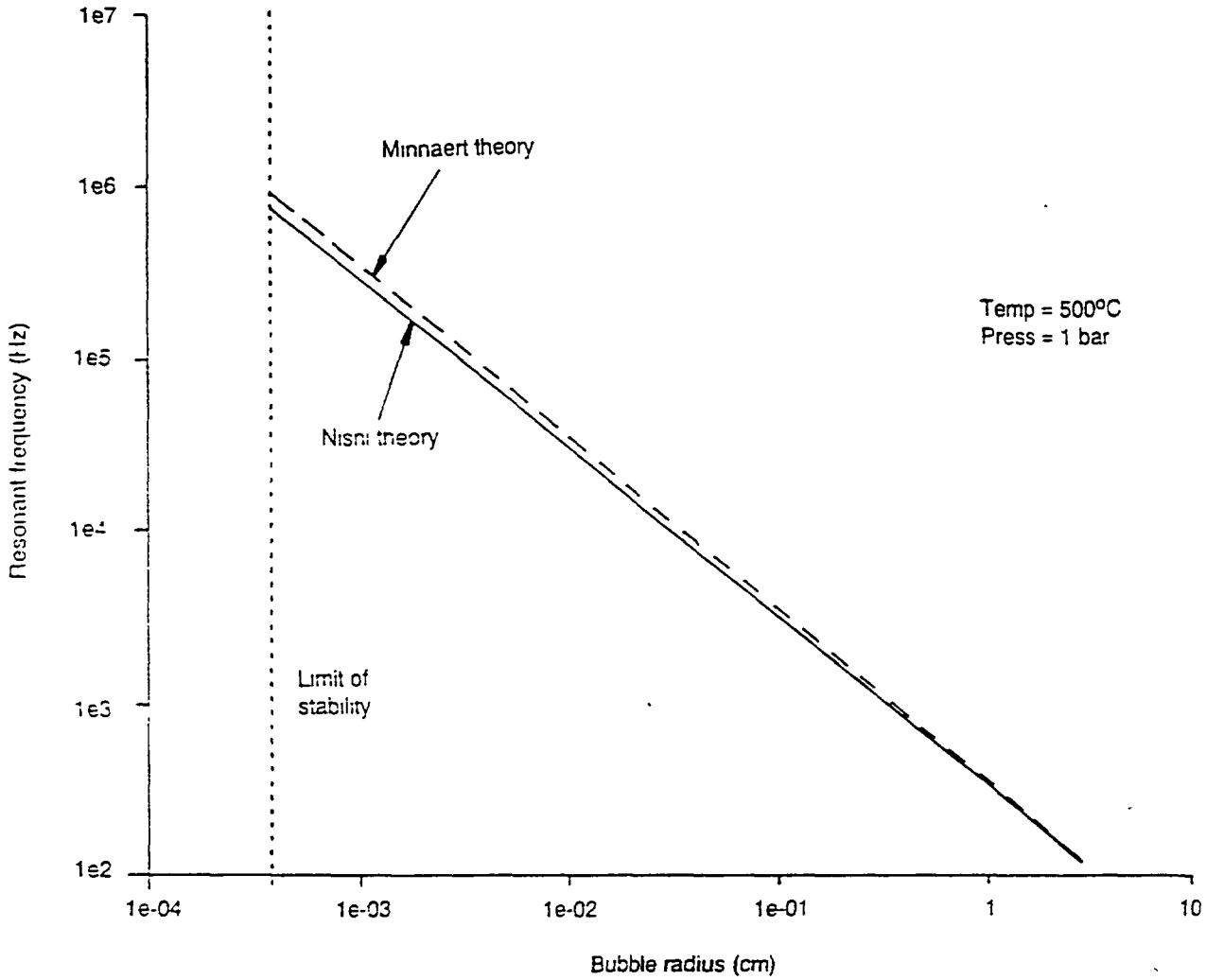

FIG. 15. Resonant sizes of hydrogen bubbles in sodium

record (number 11) consisted of quite a different mix, being UK leak noise data combined with background data from the French SPX1 reactor. The tapes were analyzed by six participants, namely Australia, France, India, Japan, the Russian Federation and the UK. The results reported to an RCM held in Vienna from 17-19 November 1992 have been combined into Tables 7 and 8.

(i) Australian analysis

Two strategies were considered by the Australian team. The first was to employ narrow band-pass filtering, with the pass-band being chosen after analyzing the independent leak and background data provided on the tape. It would be expected that the first technique would be superior, but would suffer from the lack of generality to many other applications. In fact, narrow band analysis around a centre frequency of 1 kHz gave very good results. However, it was decided to attempt to use a signal processing strategy which made no a-priori assumption about the likely spectral composition associated with a leak.

A suitable strategy appeared to be the use of wavelet filters [13] in which a set of contiguous band pass filters cover the entire signal bandwidth such that each higher frequency filter has double the bandwidth of its lower frequency neighbour. Wavelet filters satisfy the Heisenberg inequality for time/frequency resolution and in principle two very close bursts of signals can always be separated by going up to higher frequencies in order to increase the time resolution. Wavelet analysis works well if the signal to be analyzed consists of high frequency components of short duration plus low frequency components of long duration. It was also noted that the output of the wavelet filters would be a suitable input to a neural network.

(ii) French analysis

It was reported that a prototype leak detection system had been designed by Electricité de France, and the benchmark data had been examined in the light of the characteristics of this device. Two band pass filters are used, one broad band covering 200-1000 Hz and the other, narrow band covering 700-900 Hz. The benchmark test gave good discrimination over these bands, and with the narrow band filter successful discrimination down to an S/N ratio of -20 dB was achieved. However, it is understood that the equipment is really intended for longer signal duration than actually given by the tests.

(iii) Indian analysis

The data were subjected to an exhaustive analysis by a range of techniques which have given considerable insight into understanding the problem of detecting leaks. Some techniques did not work very well. Pulse counting was tried over a range of thresholds, but failed conspicuously despite the technique having worked so well in the past with either higher S/N ratios or more favourable data (such as the boiling noise tests). The K factor feature (ratio of the variance of RMS values to the square of the mean of RMS values), was also tested, but gave little encouragement. PSD-SUM analysis was also investigated. The PSD-SUM is the sum of PSD values in selected frequency regions. In most cases PSD-SUM gave good discrimination, but not on the two worse S/N ratios (-20 and -22 dB). Ideally, the number of frequency values must be optimized; best results being obtained with 128 frequency values.

The Indian team also investigated adaptive learning networks (ALN), which showed good results when applied to the earlier data (second tape, with S/N ratios of -1.7 dB and -6.7 dB) but were now less successful with the more difficult records. In view of the input to the ALN being pulse counting, K factor and RMS, all of which did not show discrimination individually, perhaps this conclusion is not surprising. Features were estimated for data over the entire frequency bandwidth.

The most powerful methods, however, were those based on the co-variant matrix, both the determinant and trace features being successful in detecting the leak signals in all cases, and with the widest margins reported. Examples and demonstrations of the analysis were provided as software on PC to the delegates at the third RCM in November 1992.

(iv) Japanese analysis

Analysis used the method of twice-squaring with band-pass filtering described previously. For the main analysis, the frequency band was restricted to 8-18 kHz for the incoming data, whilst after squaring the frequency band 12-36 kHz was chosen. Leak sounds were identified correctly in all cases down to -22 dB S/N ratio, although the detection margin was quite small in the latter cases. For record 11, it was necessary to choose different cut-off

frequencies. For the input filter a range of 2.4-13.6 kHz was chosen, having noted a lower frequency PSD function for the UK leak noise, but avoiding a particularly strong peak at about 2 kHz in the SPX1 background data. The detection margin for this latter record was noticeably lower than for the corresponding S/N ratio of the other records.

(v) Russian analysis

The Russian team was the only participant to apply adaptive filtering combined with a neural network (see Figs 16, 17). Adaptive filtering has some advantages over optimal filtering in that they can adjust their own parameters automatically and thus require no knowledge of the signal or noise characteristics. Thirty-two processing units provided PSD coefficients to the bottom layer of a neural network. The neural network itself (Figure 18) was a modified version of the usual perception with separate input layers for low and high frequencies. This network has less connection than for the conventional case, and hence learns faster.

The Russian team had no difficulty in detecting a leak in all the test records. However, the detection margin is not a factor which was readily extracted from the data. It can be considered as a radius of a fixed point attractor corresponding to the background noise pattern, but at the time of the RCM, the Russian team had only empirical data concerning this. An example and demonstration of the analysis was provided as software to the delegates at the 1992 RCM.

(vi) UK analysis

The bulk of the UK analysis was made by those who were not employed in the preparation of the test tapes. As done by the French team, frequency band-pass filters were employed. One broad filter covered from 0.5-1.3 kHz, the upper limit being determined to reduce the effects of wave guide resonance at about 2 kHz. A number of narrow bands, 64

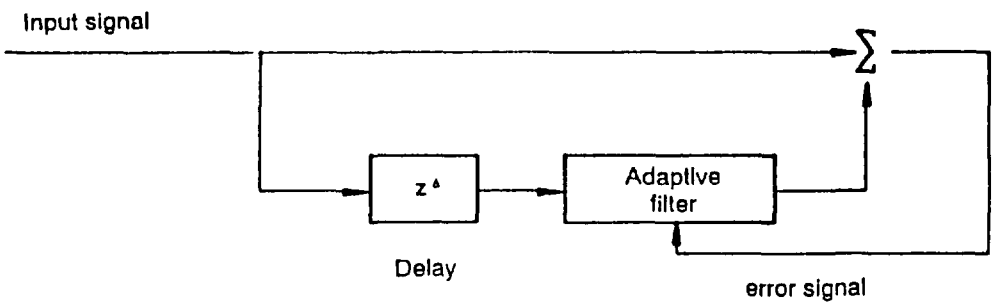

FIG. 16. Schematic diagram of adaptive filter

FIG. 17. Diagram of Russian signal processing technique

Hz wide were computed from 576 Hz-1.28 kHz, and one, centred on 1.02 kHz was chosen for the analysis. This was argued as justifiable, because of the strong resonance apparent in the signal, and attributed to bubbles in the range 6-8 mm. In all cases the leak noise could be detected visually on an oscilloscope. However, for this analysis detection thresholds were chosen in advance in order to ensure a low spurious trip rate. The background data were used to determine a suitable detection threshold 6 standard deviations above the mean. With this criterion, detection was still possible for all test records down to -22 dB with the 64 Hz bandwidth, and down to -20 dB with the wider 800 Hz band.

The above analysis assumes a fundamentally random distribution of the background signal. However, a more likely cause of spurious trip would be the presence of random acoustic "spikes" in the background signal itself. Such an event occurs towards the end of record 2. The cause is unknown, but causes a very clear threshold crossing in both wide and narrow frequency bands. The UK team seemed to be the only one to note that the background signal actually contained signals that could be mistaken for a leak event. One reason could be the reliance on shorter decision times in their analysis. The possibility of spurious background signals, however, leads to the concept of cluster analysis, and this is discussed in detail in a later section.

3.4.3. ASB loop leak noise data

The third set of data (fourth test tape) was analyzed by Australia, India, Japan and Russia. India, Japan and Russia applied the techniques used in analyzing previous sets of data and detected the leak signals with reasonable reliability up to -16 dB S/N test data. The presence of leak noise in test data with S/N of -20 dB was also indicated.

Australian analysis indicated that wavelet transform analysis is unsuitable for this data. A spectral distance measure was used with good effect on 3.8 g/s leak data series while narrow band filter (500 Hz) produced fair results on both data series of 1.8 g/s and 3.8 g/s leak rates. Indian analysis attempted to improve the sensitivity of Determinant and Trace features by evaluating them through diagnolisation of covariance matrix. Russian participant reported two filtering techniques for background noise removal and leak noise amplification. It was noted that techniques developed by the participants were equally sensitive to both the leak rates (1.8 g/s and 3.8 g/s) and that while the techniques could detect earlier leak noise in data with S/N of -22 dB, this time, the detection was possible up to -16 dB only. This is mainly because in previous records, Russian leak noise showed distinct higher power in frequency range near 1 kHz while the ASB loop leak noise spectra showed overlap with PFR background noise spectrum. The results from analysis of this set of data were reported in IAEA RCM held in Vienna fom 9-10 December 1993 and some of the results are summarized in Table 9.

3.4.4. Multichannel leak noise data

The data were analyzed by Australia, France, India, Japan, the Russian Federation and The Netherlands and the results were presented (except by Australia who subsequently submitted their report) in the IAEA RCM held at Kalpakkam, India from November 1-3 1994. The sensor locations in the ASB loop are shown in Fig. 19. The spectra of leak signals from ASB loop and background noise from PFR SGU are compared in Fig. 20.

TABLE 7 COMPARISON OF DETECTION MARGINS IN dB, AS MEASURED BY THE PARTICIPANTS (THIRD TAPE - ALD SECOND SET OF DATA)

Record No	S/N ratio dB	Japan dB	Australia dB	India det dB	India trace dB	France wide dB	France narrow dB	U K wide dB	U K narrow dB
Russian Leak/PFR Background									
4	-8	3 0	20 8	895	78 4	6	8 7	17	27
5	-20	<3 0	3 6	131	5 4	-	1 3	3	3
6	-22	<3 0	2 1	87 9	3 2	-	-	-	2
7	-16	3 0	6 4	229	7 8	1 9	2 7	3	9
8	-12	3 0	13 9	617	31 2	3 5	5 6	10	16
UK Leak/SPX1 Background									
11	-15	<3 0	-	425	18 5	-	-	-	2

Abbreviations

det	=	determinant technique	narrow	=	narrow band analysis
trace	=	trace technique	wide	=	wide band analysis

TABLE 8 COMPARISON OF LEAK TIMINGS MEASURED BY THE PARTICIPANTS (THIRD TAPE-ALD SECOND SET OF DATA)

Record	Time	Russia	Japan	Australia	India det	India trace	France	U K wide	U K narrow
Russian Leak/PFR Background									
4	abs 11 57 2		11 50					11 57 2	11 57 3
	st 20 1	20 8		20 6	19 46	19 62	20		
	dur 5 2	3			5 9	5 9			
5	abs 22 40 4		22 47					22 41 8	22 40 6
	st 15 2	15 6		15 3	14 72	15 01			
	dur 5 6	5			6 7	5 6			
6	abs 32 37		32 38						32 37
	st 22 2	23 5		23 3	22 3	22 6			
	dur 5 4	5 4			5 9	5 4			
7	abs 40 31 1		40 35					40 31 2	40 32 2
	st 17 8	18 6		18 1	18 0	17 83	17		
	dur 5 0	4			5 19	5 18			
8	abs 51 25 7		51 29					51 25 8	51 25 8
	st 23 4	26 2		23 6	23 28	22 98	23 2		
	dur 5 2	5			5 36	5 82			
UK Leak/SPX1 Background									
11	abs 1 17 47 8		1 17 50						1 17 49 3
	st 24 0	30 3		25 0	23 41	23 41			
	dur 5 7	3 3			8 18	8 18			

Abbreviations

abs	= absolute time of start of leak	det	= determinant technique
st	= time from start of tape record, seconds	trace	= trace technique
dur	= duration of leak signal, seconds	narrow	= narrow band analysis
		wide	= wide band analysis

TABLE 9. COMPARISON OF RESULTS (FOURTH TAPE)

Record No	S/N dB	Country	Onset of Leak (s)	Duration of Leak (s)
3	-20	Japan	-	-
		India	9.8	4.3
		Russia	12.54	0.57
		Actual	10.0	5.0
4	-12	Japan	15.0	4.0
		India	15.4	4.3
		Russia	15.5	3.38
		Actual	15.5	4.5
5	-24	Japan	-	-
		India	-	-
		Russia	12.51	2.51
		Actual	12.5	5.5
6	-16	Japan	-	-
		India	18.40	5.3
		Russia	19.81	1.34
		Actual	19.4	4.8
9	-12	Japan	13.5	3.5
		India	11.8	5.3
		Russia	-	-
		Actual	12.01	5.5
10	-24	Japan	-	-
		India	-	-
		Russia	-	-
		Actual	17.5	5.1
11	-20	Japan	16.5	0.5
		India	-	-
		Russia	-	-
		Actual	16.0	4.7
12	-16	Japan	16.0	1.0
		India	14.4	-
		Russia	-	-
		Actual	13.8	5.3

(i) Australian analysis

Australian analysis dealt with three different autoregressive modelling approaches, i.e. the mean square of prediction error, distance in parameter space and likelihood ratio tests. Of the three methods, the distance in parameter space has been found to be the most suitable, being able to detect leaks down to S/N of -24 dB. Spectral analysis of the data revealed differences in signal characteristics between sensors suggesting that signal characteristics could

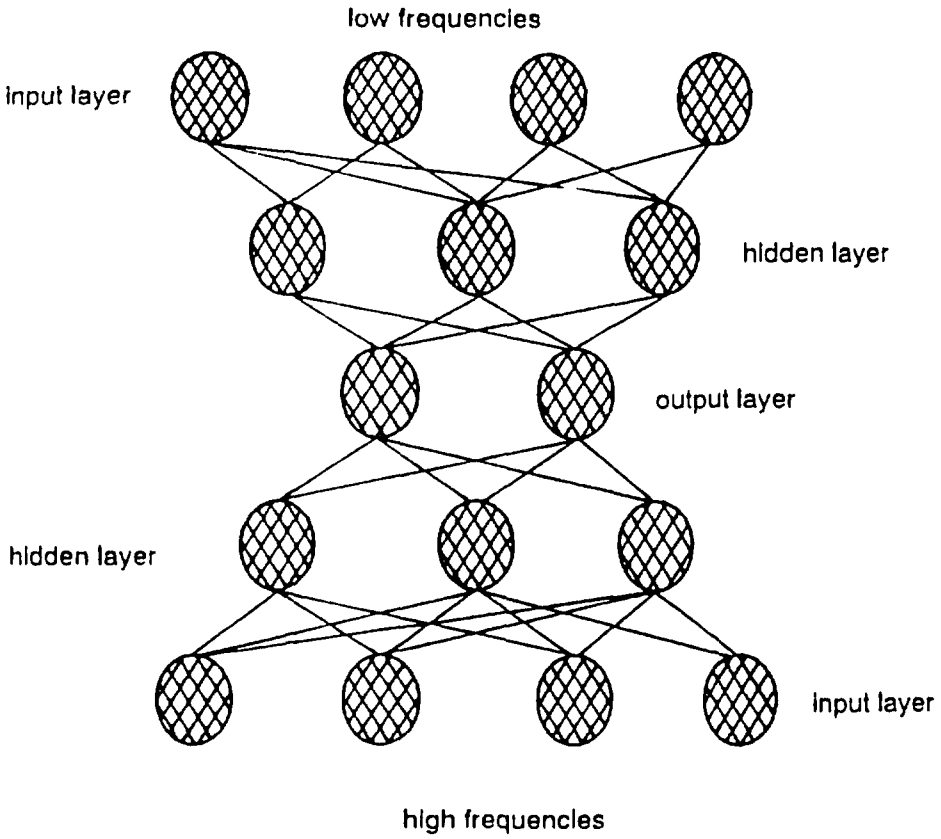

FIG. 18. Architecture of Neural network used by Russian team

be dependent on sensor location. Correlation analysis of the multisensor data showed difficulty in locating the leak. The analysis suggested that the media comprising the acoustic path is most likely dispersive, with multiple paths for acoustic transmission of leak noise and that the acoustic noise source may itself be distributed and not localized.

(ii) French analysis

The French analysis identified the useful frequency range as 200-1000 Hz and used the time domain beam forming technique to find the leak location. This method permitted location of the leak even for a S/N of -24 dB with a precision of 30% of the diameter of the vessel. Figure 21* shows the results from the beam forming technique on data with a S/N of -24 dB. The start and duration of leak signals in the mixed regions were also roughly determined using the same technique. It was pointed out that the success of the method of beam forming depends on the correct knowledge of the velocity of sound in sodium and acoustic wave propagation in wave guides that are mounted with the sensors and in the structure of the vessel.

---

* For Figure 21, see Figure 8 of the paper on Sodium/Water Reaction Detection Confirmation and Location with Time Domain Beam Former, by C. Cornu (page 131).

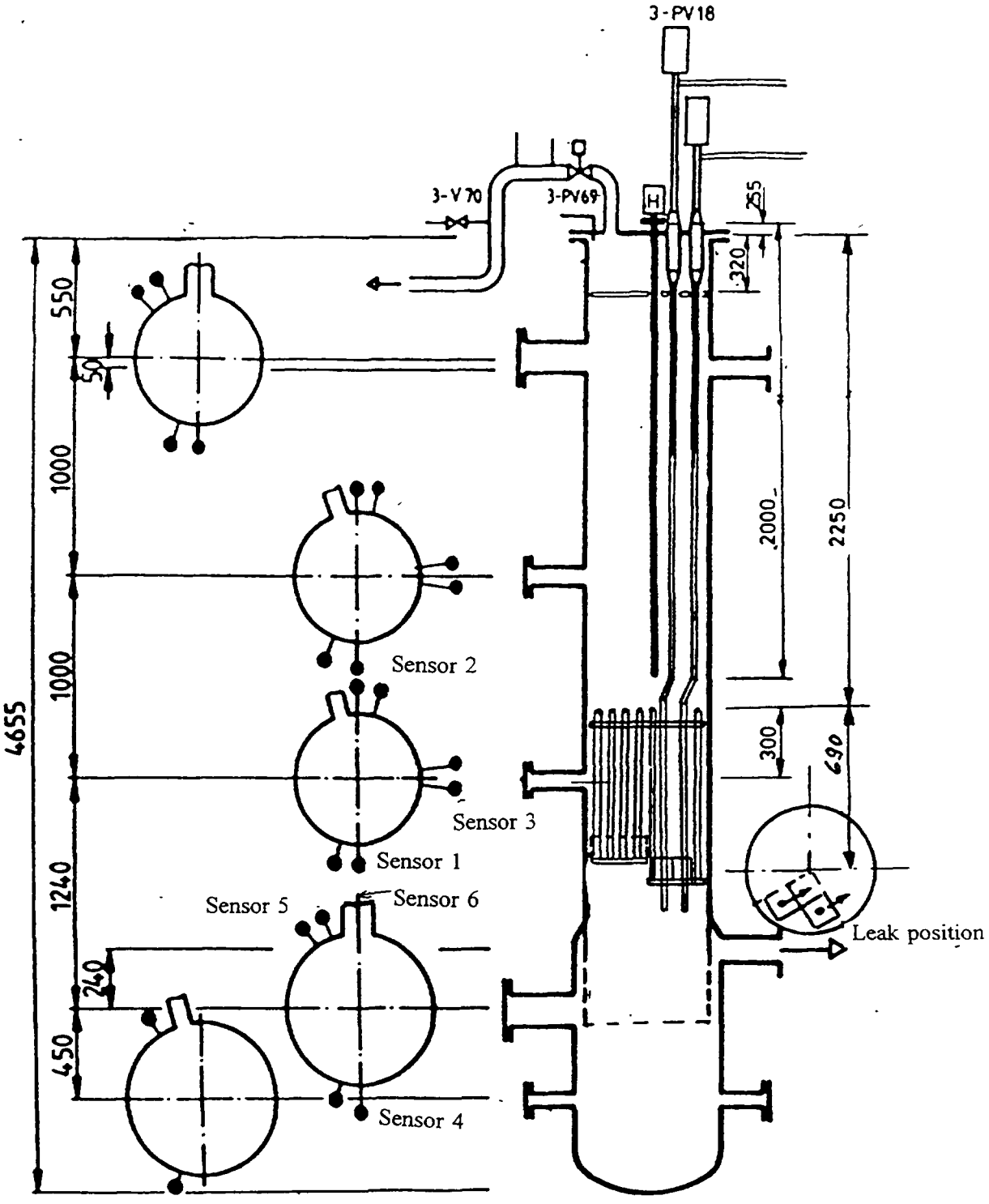

FIG. 19. Sensor location in ASB loop

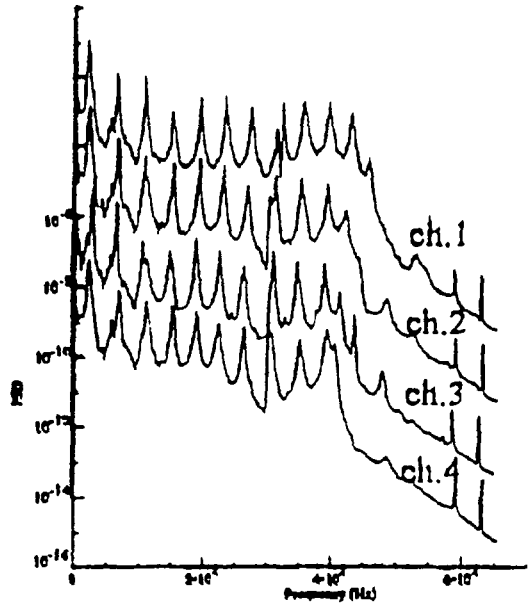

(a) Background Signals
(bkgd_1,..,bkgd_4)

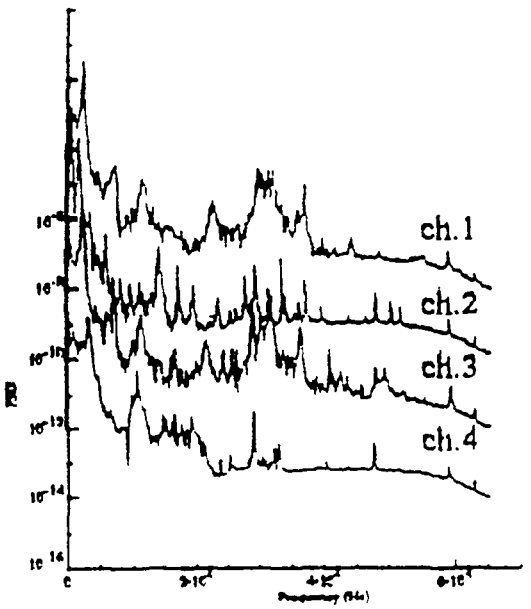

(b) Leak Signals
(leak_1,..,leak_-4)

FIG. 20. PSDs of background and leak signals (Fifth tape)

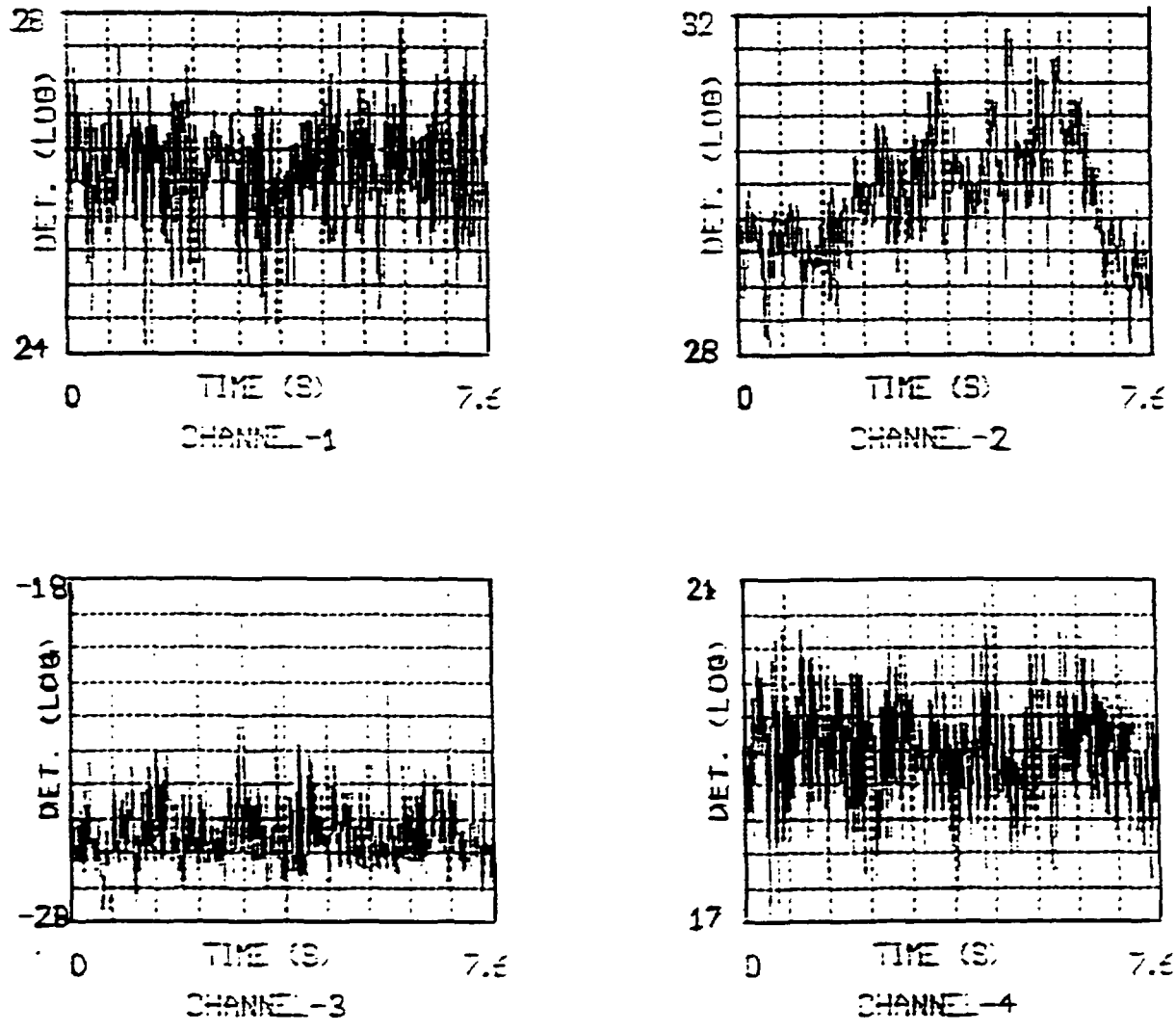

FIG. 22. Fifth tape, set -4, determinant

(iii) Indian analysis

Indian analysis, using PSD-SUM, determinant and trace indicated that the detection was best for channel 2 followed by channel 3, 4 and 5. The detection of leak noise was possible even for the case of -24 dB with channel 2 using Determinant as shown in Fig. 22. The Determinant and Trace features detected the leak signals with better detection margins. The PSD-SUM feature detected the leak signals in data of S/N up to -16 dB. Attempts to locate the leak by the cross correlation techniques using unfiltered data were not successful. Sinusoidal profiles were observed in the cross correlations and are attributed to the presence of a strong sinusoidal component in the data around 1 kHz. CPSD phase plots also did not indicate any positive results.

(iv) Japanese analysis

The analysis from Japan applied the background signal whitening filter built by Univariate Autoregressive (UAR). It was concluded that the signal processing using this method can detect reliably the leak signals with S/N down to -20 dB. As an example, the results for channel 3 are shown in Fig. 23. Application of the twice squaring technique,

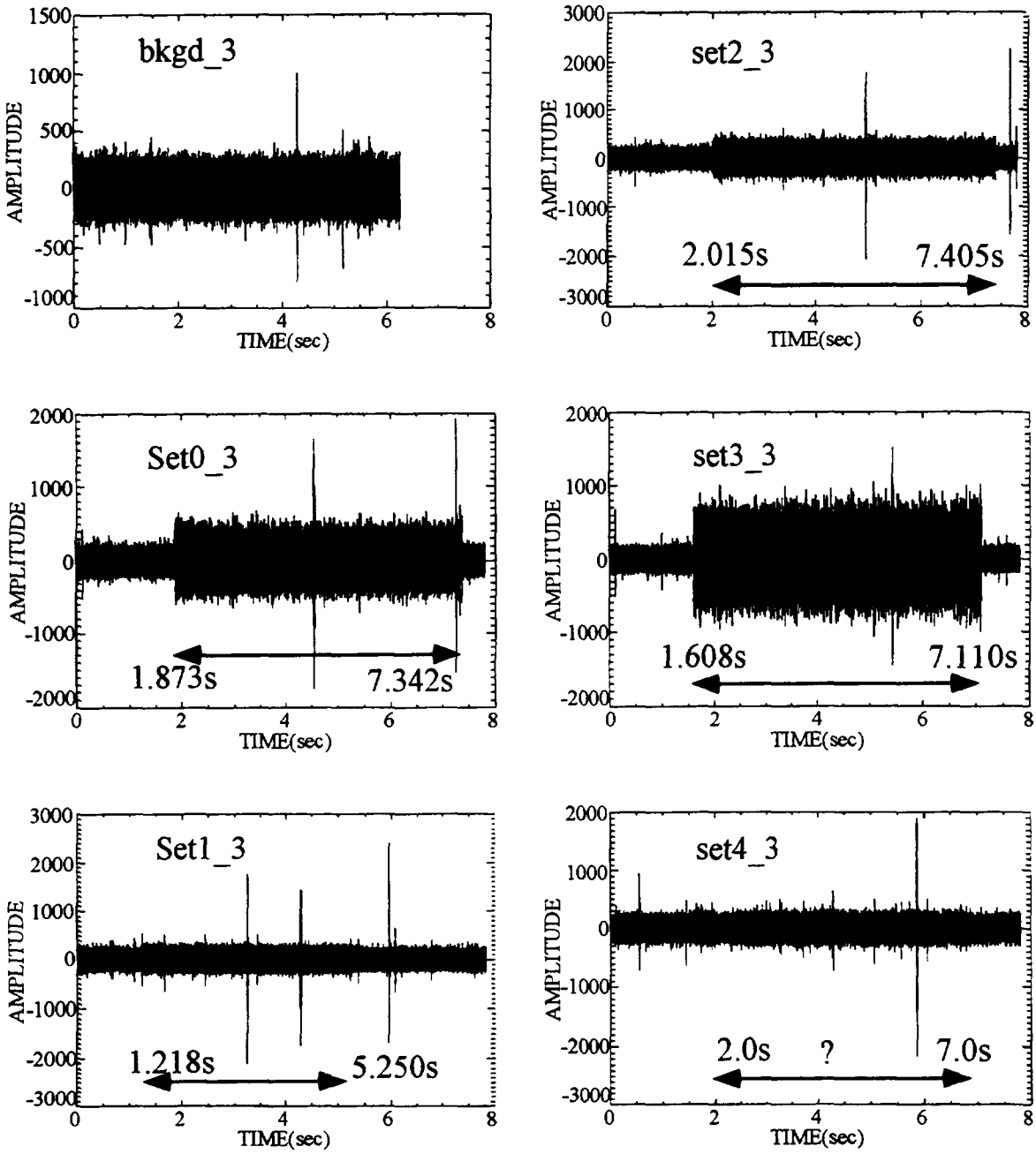

FIG. 23. Filtering results of background signal and five test signals for channel '3' using UAR whitening filter (Start time and duration are indicated by <——>) (Fifth tape)

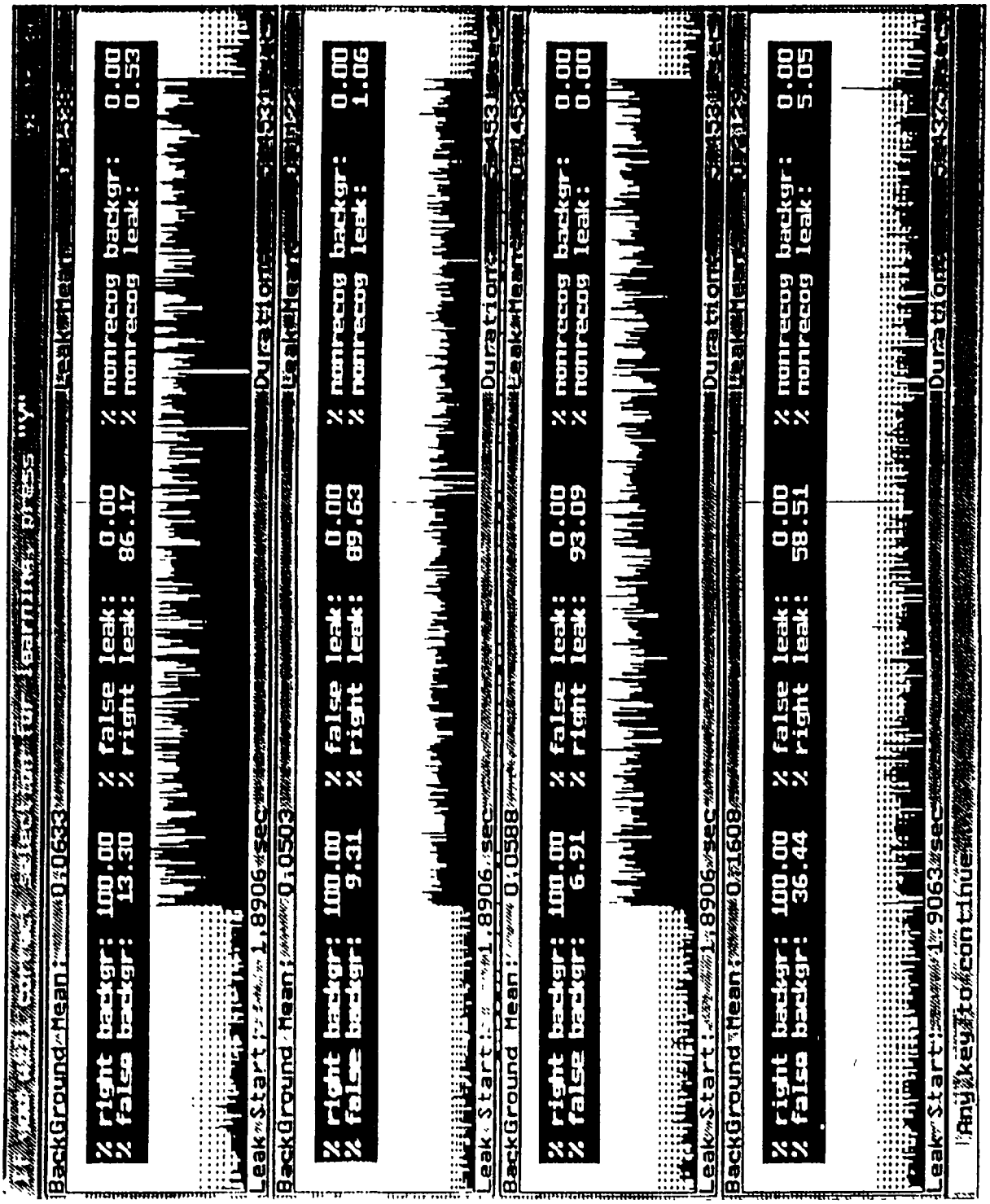

FIG. 24. Snap of the neural network output (Fifth tape)

TABLE 10. COMPARISON OF RESULTS (FIFTH TAPE)

Set No	S/N (dB)	Country	Onset of leak (s)	Duration of leak (s)	Ps (%)	Pm (%)
0	-12	Australia	1.87	5.63	-	-
		Japan	1.873	5.469	-	-
		India	1.7	5.5.	0.0	0.0
		Russia	1.8906	5.4531	0.0	6.9
		The Netherlands	1.877	5.500	-	-
		Actual	1.875	5.469	-	-
1	-20	Austrialia	1.23	4.16	-	-
		Japan	1.218	4.032	-	-
		India	1.1	5,3	41.4	30.0
		Russia	1.2500	4.7188	0.0	80.6
		Actual	1.23	4.0	-	-
2	-16	Australia	2.01	5.55	-	-
		Japan	2.015	5.390	-	-
		India	1.8	5.5	0.0	0.0
		Russia	2.03.13	5.375	0.0	8.5
		The Netherlands	2.016	5.390	-	-
		Actual	2.01	5.39	-	-
3	-6	Australia	1.60	5.66	-	-
		Japan	1.608	5.5	0.0	0.0
		Russia	1.6250	5.4844	0.0	10.2
		The Netherlands	1.609	5.500	-	-
		Actual	1.61	5.50	-	-
4	-24	Australia	2.30	4.64	-	-
		Japan	2.0	5.0	-	-
		India	2.8	4.6	11.1	71
		Russia	2.6875	4.0625	0.0	88.0
		Actual	2.29	4.50	-	-

Note: Onset time and duraiton of leak reported in the above Table are for channel No.2 in case of India and channel No.3 for Russia.

Ps: Probability of spurious detection
Pm: Probability of missing detection

which was successful for earlier data, did not give positive results for the present data. In estimation of leak location, the difference of start-up times among the leak pulses was not found. Therefore, an estimation method using time constants of the acoustic signal propagating paths based on the multivariate AR modelling technique is being developed.

(v) Russian analysis

The Russian analysis was done by applying the adaptive filtering and neural network methodology and could clearly recognize leak noise for S/N at least down to -16 dB. Neural network output for -12 dB data is shown in Fig. 24 for all four channels. The network output also lists the uncertainties (spurious and missing leak signals) in the detection. The detection was possible even in data with S/N of -24 dB but with poor discrimination.

Table 11. Comparison of results (Sixth Tape - PFR data)

Injection	Fluid	Location	Leak Rate (g/s)	Start (s)	Australia* (s)	France (s)	India (s)	Japan (s)	Netherlands (s)	Russia (s)
1	H_2	Bundle	0 05	1 95 - 2 01	N/A	8.49	1 88 - 2 11	1 9	-	-
2	Ar	Bundle	0 27	3 14 - 3 30	N/A	3 1	-	N/A	-	-
3	H_2O	Bundle	3 4	1 80 - 3 84	N/A	7 37	1 94	N/A	7 37	7 58
4	Ar	Interspace	0 5	4 46 - 4 65	N/A	5 13	-	N/A	4 83	5 43
5	H_2	Interspace	1 3	2 72 - 2 80	2 6**	2 65	2 71 - 2 99	N/A	2 61	2 77
6	H_2O	Bundle	7 65	2 40 - 6 40	N/A	5 41	4 70 - 7 03	2 4 - 5 5	5 3	5 53
7	Ar	Bundle	2 4	3 22 - 3 31	N/A	5 58	3 73 - 4 22	N/A	3 57	4 4
8	H_2O	Interspace	2 2	3 65 - 5 65	N/A	-	-	3 65	-	4 51

Notes The spread of detection times are based on results usisng different method and using data from different waveguides,
N/A - Not Analysed,
* Only used injection 5 to test seven different signal processing strategies,
** Typical Value
Onset times determined visually except by the Russian team who used an on-line technique

(vi) Netherlands analysis

The Netherlands participated for the first time in the CRP. The analysis reported that the data showed large pulses in background as well as in leak noise data and hence the signals could not be considered stationary in the usual sense. Hence the statistical tests resulted in a large number of anomalies of extremely short duration. This prohibited proper application of the Sequential Probability Ratio Test (SPRT) employed to detect the onset of a leak in the data. Autoregressive modelling of the noise signals which is sensitive to changes in the characteristics of the signals was also applied. Several statistical techniques were introduced to end up with an algorithm that could in principle be applied on-line to detect a leak in the signal very shortly after its inception.

Results from further analysis carried out after the 1994 RCM are included in Table 10. In this analysis, the residual signal of autoregressive modelling of the noise in the time domain was used to detect the leak signal. SPRT and χ^2 - tests were applied and leak signals could be detected in files with S/N down to -16dB. This analysis again showed the presence of several anomalies (spikes) of short duration in the background region.

(vii) UK presentation

The UK participant made a presentation on the acoustic background measurements on PFR evaporator 3 and superheater 3 and end-of-life acoustic leak detection experiments performed on PFR evaporator 3. A total of 142 injections (argon, hydrogen and steam/water) were carried out in evaporator 3 and data were recorded on analog tape during 115 injections. The injections were carried out at a low sodium flow in the SGU and without water in the SG tubes. He suggested that the test data for 1995 analysis can be prepared from the above experimental data.

3.4.5. PFR ALD experiments data

The test data were prepared from end-of-life ALD experiments carried out on PFR SGUs. Results from the analysis of this data were presented in the RCM held at Obninsk, Russian Federation from July 11-14 1995. Table 11 compares the results obtained by the participants.

(i) Australian analysis

Australian analysis compared the performance of seven different signal processing strategies. Two were derived from an autoregressive model of the process, whilst the rest were implemented in the frequency domain using either global spectral distance measures or more particular spectral measures used in conjunction with wavelet analysis. The approach adopted in the Australian analysis makes no assumptions about the nature of the signals from the injection. The signal processing techniques were tested on data synthesized by them by mixing linearly the evaporator full power background noise with the signal from injection 5, which is the best S/N test data. The results showed that a combination of the use of wavelets with spectral distance measures is the most effective method.

(ii) French analysis

A simple feature, RMS value of the signal in the 200-1000 Hz frequency band was used to determine the start time of injection. The ALD system developed for Super Phenix

operates in this range. The main thrust of French analysis was however directed to the problem of leak location using pulse timing and beam forming techniques. In the pulse timing method, time delays were calculated from cross correlation functions on 30 kHz high pass filtered data and accurate results were obtained for injection location. But the beam forming technique which used data in the 200-1000 Hz frequency range was not successful in correctly locating the leak, probably due to complex transmission paths in the PFR evaporator.

(iii) Indian analysis

For detection of the injection signal, features PSD-SUM and determinant and trace of the covariance matrix of the auto power spectral density were evaluated. As in the previous years, determinant and trace features were found to be very sensitive and could detect injection in five out of the eight test files. The Indian analysis further assessed the capability of these two features to detect the injections under full power conditions and concluded that the resulting RMS S/N (injection signal to full power background noise ratio) at the wave guide nearest to the leak for injections 5,6 and 7 fell within the detection capability of these two features. Efforts to predict the injection medium based on spectral features and leak location through cross correlation analysis did not yield positive results.

(iv) Japanese analysis

The Japanese analysis applied a whitening filter based on the univariate autoregressive model to detect the injection signal in injection files 1,6 and 8. The analysis concluded that this method with features whitening filter + RMS or whitening filter + time frequency PSD can reliably detect injection signals. The feature signal derived from time-frequency spectrum of the whitening filtered signal was found to be further capable of correctly classifying non-injection high amplitude pulses in the background region. A potential technique based on multivariate autoregressive model has also been proposed by them for leak location.

(v) Russian analysis

A processing technique based on a neural network was applied by the Russian team. The network was trained with data from injection 6, among the most powerful injection data made available for analysis. The same network was used for all four wave guides, whereas the weights were separately determined for each of the four wave guides. Injection signals were detected in six out of the eight files and detection reliability figures were also reported. The neural network trained on injection 6 also correctly recognized the full power background noise from evaporator 3 and superheater 3 without any false trips. Preliminary analysis showed that without additional training, the network would correctly detect a leak twice the size of injection 6 at full power.

(vi) Netherlands analysis

The Netherlands analysis was focused on the detection of the injection signal using an autoregressive model. A statistical test (χ^2 -test) considering the variance of the residual noise was applied to detect the presence of injection signal. In injection files 3 to 7, the signal could be clearly detected by this method. The analysis showed that the residual noise of all the signals exhibited a large number of spikes. An attempt was also made to locate the leak based on the relative increase in the variance of residual noise at different wave guides but the results were not encouraging.

(vii) UK presentation

The UK presentation covered details of injections used in the 1995 benchmark data and other injections carried out on PFR evaporator 3 and confirmed the representativeness of the benchmark data. The presentation described the sequence of events in various injections and indicated the injection medium and the onset time in each file prepared by them. The actual injection onset times given in Table 11 are subject to an uncertainty of about -0.1s. The spread in the onset times in the case of water injections in files 3 and 8 was attributed to the time taken for water to fill the injection line after the valve was opened, during which period argon gas flowed through the orifice. This phase lasted for 1.5 to 2 s during PFR experiments. In case of injection 6, the water line was initially blocked and full flow got established only after 4 s. The detailed UK analysis showed that the signal initially increased with injection rate and then reached a plateau value. Experiments at PFR have further shown that for 1g/s steam leak into the tube bundle region, the leak signal was of the order of 10 to 20% of full power RMS background noise level, whereas in the case of 1g/s leak into sodium interspace, higher signals in the range of 30 to 50% of full power background noise were observed. These are encouraging results from a leak detection point of view. The UK presentation further discussed the signal transmission characteristics of the evaporator unit. Injection medium, injection location and wave guide location determine the signal transmission characteristics to different wave guides in different frequency bands. However it was noticed from PFR acoustic experiments that the injection signal did travel to even the farthest waveguide which was nearly 5 m away from the injection zone.

3.5. Appraisal of results of sodium/water reaction detection

3.5.1. Detection sensitivity

A review of results from various analysis methods reported in this CRP conclusively proves that leak signals can be distinctly detected with good reliability for RMS signal to noise ratios down to -16 dB. This nearly meets the target value of -17 dB suggested by the UK for detecting a 1 g/s leak, based on their studies for the European Fast Reactor [6-8]. Furthermore, all the participants found little difficulty in reaching a decision concerning the onset of a leak within a second or two. Capabilities of the analysis techniques have been demonstrated on test tapes containing leak signals from different sources and covering a wide range of leaks from 0.05 g/s-3.8 g/s. Hence the conclusions drawn from the CRP are general in nature, having a wide scope of application.

Analysis methods are also able to detect leak signals even down to -24 dB S/N, but with less reliability. This can be improved using techniques described later. However, when the leak signal contains specific frequency bands, as observed in the Russian leak signal, discrimination and reliability are better even at such low S/N ratios. In this case, the participants have used some form of filtering techniques which imply prior knowledge of the nature of the signals concerned.

As reported in Section 3.4.5, various analysis methods have successfully detected the injection signal in five or six of eight test files created from PFR end-of-life acoustic experiments. This has established the capability of analysis methods developed on synthesized data to detect anomalies in real field data also.

The French team successfully demonstrated on the 1994 synthesized data the application of time domain beam forming technique for locating the leak even when the S/N

is -24 dB. This technique was however not successful on the PFR data due to the complex internal geometry of the PFR evaporator. Even in this case, the French analysis has successfully demonstrated the application of the pulse timing technique (through cross correlation of high frequency data) for leak location. Leak location enhances the detection reliability by confirming that the detected signal has its origin within the SGU and this advantage is derived from multichannel analysis. The precision of location can be enhanced with a better knowledge of the signal transmission characteristics and by using more sensors.

3.5.2. Need for prior knowledge of leak characteristics

In order to achieve the narrow band filtering required in certain analysis methods or to train neural networks, prior knowledge of the nature of the signals is needed. During the RCMs, there was discussion on whether the tapes should contain such clear samples of the leak and the background signals which were later to be mixed for the tests. There are, in fact, two schools of thought.

In the first case, it had been considered necessary to simulate the actual situation faced by the designer of leak detection equipment. He could be expected to have determined the nature of the signals to be detected so that he could design the detection equipment. This had been the approach used by the UK in specifying the passive leak detection system for EFR. Such also was the case with the EdF instrument tested by the French; it had been designed with narrow band filtering for the SPX1 reactor. On the other hand, not enough is known about the variety of sounds to be expected to achieve the optimum situation every time.

The other school of thought assumes that the nature of the leak noise will not be known, and so the analytical procedure must allow for this. The techniques used by the Indians, Russians and Australians are all adaptable. However, the adaptive learning network used by the Indians and the neural networks used by the Russians both involve a more or less extensive learning period, and whilst they may be capable of adapting to changes in conditions (they will certainly accommodate changes in background level), pre-cognition of typical leak sounds is necessary to set them up. However, the Indian team had evolved and tested a new approach to the ALN-technique in which the network is trained using background data [5]. Only the Australian team tackled directly the problem of total ignorance of the originating event signal with their use of wavelet filters. Again, this raises a difficulty - the instrument then becomes an anomalous event detector, and are water/steam leaks the only unusual events that will occur in a steam generator throughout its life?

With regard to the latter argument, for the European Fast Reactor design, the European Fast Reactor Users Group (formed by the relevant utilities) was already moving towards insisting on detection of water/sodium reaction being augmented by location of the leak; so that at least if a trip occurred, it was known that the acoustic signal originated from within the steam generator [6].

Another important consideration is that for the practical application of an acoustic leak detection system on SGUs, use of an in-situ calibration source could become necessary. In fact, such a system may be demanded by the licensing and operating agencies. The need for an in-situ calibration source was recognized in the Specialists' Meeting on Acoustic/Ultrasonic Detection of In-sodium Water Leaks on Steam Generators held at Aix-En-Provence, France in 1990 and the meeting recommended that work should be performed to develop such a source [8]. This source also provides data for training of networks and for tuning of filters in detection algorithms.

Noise generated by argon injection into sodium in a SGU is a candidate in-situ test source. Analysis of data from steam/water and argon injections in the PFR end-of-life experiments has shown that the similarity between steam and argon injections depends upon the injection location, transducer location and the frequency band considered. Reasonable similarity was obtained for injections both in the tube bundle region and in the interspace of PFR evaporator when comparisons were made in the low frequency band below 6.4 kHz. Results from PFR experiments further showed that similarity in RMS signal level for steam and argon injections is better when the results are normalized to volumetric flow rate rather than when they are compared on mass flow rate basis.

The differences observed between the signal from steam and argon injections can be attributed to the difference in solubility of hydrogen and argon in sodium. At present it can be concluded that care must be exercised when argon injection is used to simulate steam leaks for calibrating or for training an acoustic leak detection system. Further evaluation is required before such a simulation can be reliably applied.

3.5.3. Estimates of reliability of detection

In the tests on sodium-water reaction, the participants had not been asked to determine the spurious and failure-to-detect probabilities. To some extent this was because the figures could be misleading. A typical spurious trip rate required by an operator would be in the region of perhaps not more than once in ten years, and thus involve spurious trip probabilities of around 10^{-9} for most techniques. As was seen with the earlier boiling noise detection phase of the CRP, for some techniques this figure was below the resolution of the measurements, whilst for others (those relying on brief time samples of the data) the figure would be reached by a further stratagem, such as relying on "clusters" of events within a given time, a method that has been worked out in detail by both the Indian team with the n_o/N_o technique, and by the UK team [14]. These two techniques are described briefly below.

(i) Cluster analysis of spurious trip rate

This example is extracted from the UK analysis of the third tape. In order to give a suitable spurious trip rate, the mean and standard deviation of the background noise were calculated and used to give a detection threshold at 6σ above the mean. All the test records had a leak signal level which exceeded this threshold.

At this level for Gaussian noise, the probability of a sample exceeding this value is less than 1 in 10^8. With an analysis window of about 100 ms, this is equivalent to a spurious trip in 0.3 years. In order to provide a more robust trip decision, it is possible to take advantage of the fact that the leak noise is repetitive and requires more than one threshold crossing (a "cluster") in a given decision time window. The probability of a spurious trip can then be determined by using the Poisson distribution. Because of the very low initial probability of a 6σ crossing (<1 in 10^8), setting a requirement of two threshold crossings in say 5 seconds results in a very large value of spurious trip rate of 1 in 2.5×10^5 years. With this criterion for a trip, detection was still possible in all test records down to -22dB for the 64 Hz band width analysis, and down to -20 dB with the wider 800 Hz band width.

However, it was shown that a more likely cause of spurious trip is the intermittent appearance of extraneous acoustic pulses such as the one which appeared towards the end of record 2 in the third tape. The spurious trip rate due to background events was estimated to be not more than one event per minute, this having been judged from the test tape, and with

a measurement analysis time of 100 milliseconds, the probability of occurrence would be 1.67 x 10^{-3}. Cluster analysis can now be used to provide a sufficiently stringent requirement for a trip while still ensuring sensitivity to leaks. Figure 25 shows a plot of spurious trip rate as a function of number of events to be expected in a decision time window of 1, 2 and 5 seconds. The optimum choice would be dependent on more detailed knowledge of the signals involved than given by the test tapes, but as an example, a spurious trip rate of not more than 1 in 25 years with a decision window of 2 seconds would require a minimum of 5 events to be detected in the decision time. From an examination of the test tape data, detection with this stringent criterion was still possible at -16 dB and -20 dB signal to noise ratio for analysis with the 800 Hz and 64 Hz bands respectively.

(ii) n_0/No technique

This method is based on the criterion that the decision of detecting the anomaly is not based on a single estimate of the feature but on No estimates evaluated successively and checking whether n_0 or more estimates indicate anomaly.

If Ps is the probability of false alarm for a single estimate crossing the threshold, the probability of false alarm when n_0 or more estimates indicate anomaly is given by,

$$P_s = \Sigma\ [N_0!\ /\{\ (N_0\text{-}n)!\ .\ n!\}]\ .[\ (P_s)^n\ .\ (1\text{-}P_s)^{N0\text{-}n}\ ],\quad n = n_0,\ N_0.$$

Similarly if Pm is the probability of missing the anomaly when single estimate does not indicate the anomaly, the probability of missing the anomaly when (n_0-1) or less estimates out N_0 estimates do not indicate anomaly, is given by,

$$P_m = \Sigma\ [N_0!\ /\{\ (N_0\text{-}n)!\ .\ n!\}]\ [(P_m)^n\ .\ (1\text{-}P_m)^{N0\text{-}n}\ ],\quad n = N_0\text{-}n_{0\,+1},\ N_0.$$

From the above approach, it is always possible to achieve target probability values by selecting appropriate n_0/N_0 criterion for any value of Ps and Pm.

4. EXPERT SYSTEMS

Expert systems, although an objective of the CRP, were dealt with by only one of the participating countries. In Germany, an expert system has been developed for use with the KNK II reactor at Karlsruhe.

The general philosophy is illustrated in Fig. 25. The signal environment of the fast reactor produces raw data and a pre-processor produces formatted data. One part of this data stream (for example, noise signal) is the input for an intelligent signal processor which produces partial hypotheses in the context of the surveillance class *local diagnosis*. The expert system correlates these partial hypotheses. Another part of the formatted data (for example values of temperatures, speed of pumps, valve positions, etc.) is a direct input for the expert system. These inputs, the direct inputs and the partial hypotheses produce the dynamical facts as premises of the rules, given by the experienced knowledge. So the inference engine of the expert system can produce hypotheses in the context of a *global diagnosis*. These surveillance classes combine with a third, *post mortem diagnosis* to form the basis for the architecture of the complete system, known as DESYRE, (Diagnostic Expert System for Reactor surveillance). Further details have been published elsewhere [15]. Extensive tests of the

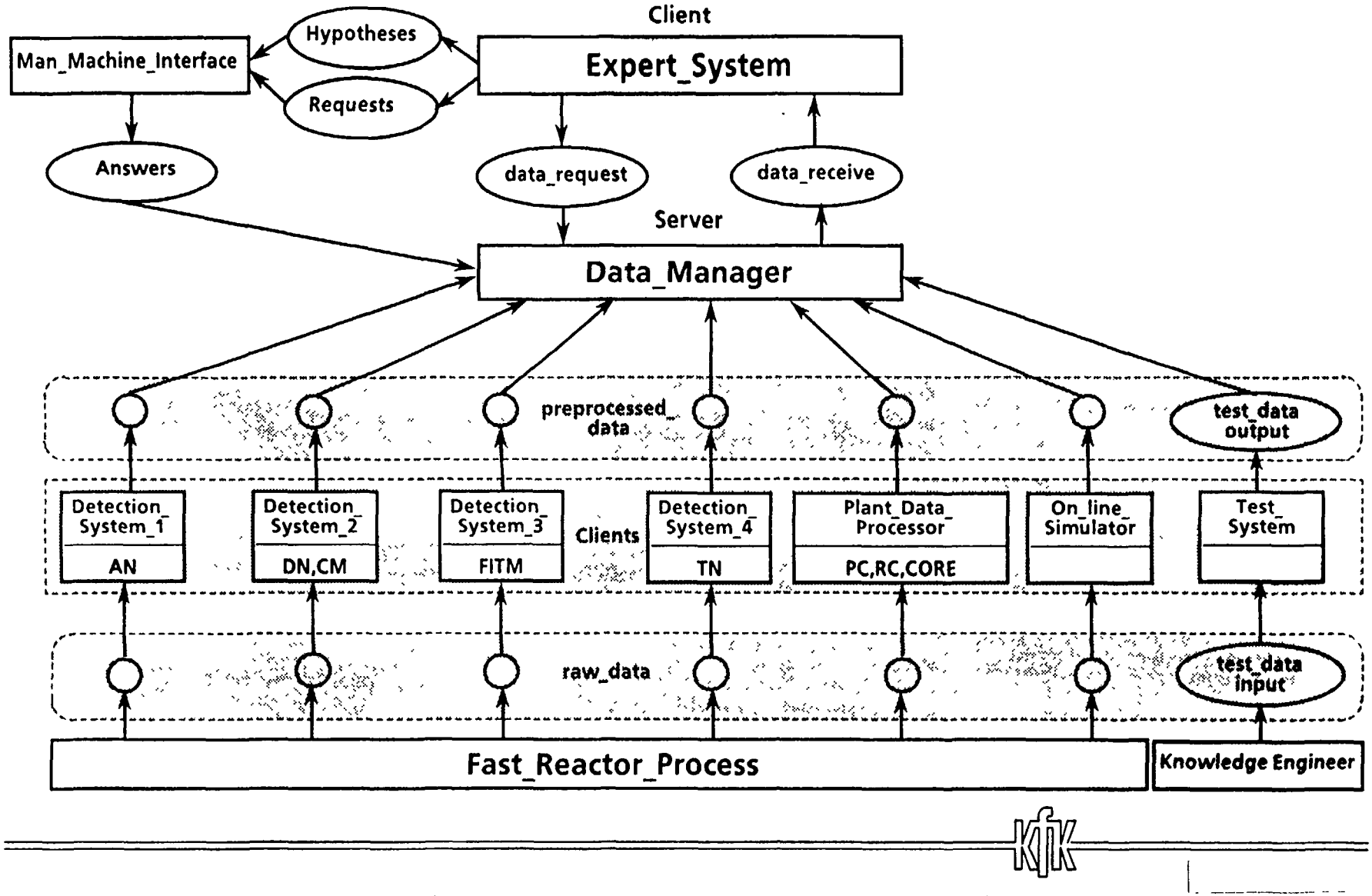

FIG. 25. **DESYRE: Diagnostic Expert SYstem for REactor Surveillance (Causality)**

running system have been performed and time related performance of the different tools including the data transfer from the detection system, like acoustic noise has been demonstrated in the expert system.

5. CONCLUSIONS

5.1. Techniques

This stage of the extended Co-ordinated Research Programme has seen further work on the detection of boiling noise signals and significant advances in techniques for detection of water/sodium reaction noise which would arise from leaks in fast reactor steam generators. In the latter case, the techniques have been tested with success on data from diverse sources and covering a wide range of leaks. This gives generality to the conclusions. The techniques developed / employed by different countries are:

- Mean square prediction error, distance in parameter space, and likelihood ratio tests based on autoregressive modelling approaches and wavelet functions of Australia.
- Bandpass filtering, time domain beam forming technique and pulse timing technique of France.
- Determinant and Trace of covariance matrix constructed from power spectral density, PSD Ratio and adaptive learning network methodologies of India.
- Twice squared processing of signals, background signal whitening filter based on univariate autoregressive modelling and its time frequency spectrum of Japan.
- Adaptive filtering and neural network methodology of the Russian Federation.
- Autoregressive modelling approach by the Netherlands.
- Pattern recognition, pulse counting and narrow band filtering by the UK.

5.2. Acoustic boiling noise detection

For boiling noise detection, it was found necessary to redefine the signal to noise ratio as compared to the earlier definition in the first stage of the CRP. The following specific points could be made:

- Most participants who analyzed the data were able to detect reliably boiling incidents when the RMS signal to noise ratio was as low as -12 dB. This lies just within the margin of detection expected to be required for a reactor trip system based on boiling noise detection.
- The detected boiling events were always detected within one second of the event occurring.
- All the participants had difficulty in detection when the S/N ratio was less than -12 dB. However, visual inspection of the output from the analysis techniques showed perceptible presence of boiling signals in the data.
- All the successful methods involved high frequency filtering of the signals.

5.3. Acoustic leak detection

From the results obtained by testing the various analysis techniques for acoustic leak detection on synthesized data and on PFR data, the following conclusions could be made:

5.3.1. Synthesized data

- Leak signals were distinctly detected with good reliability for RMS S/N down to -16 dB. This lies vary close to detection margin expected to be required for a fast reactor steam generator protection system.
- Analysis methods also detected leak signals even down to -24 dB S/N, but with less reliability. Discrimination and reliability get enhanced even at such low S/N ratios by filtering techniques if leak signals contain specific frequency bands.
- The response time of detection is always less than 1 s.
- Cluster analysis and n_0 / N_0 technique are the two methods available for improving the reliability of the detection system.
- Leak location was identified through time domain beam forming technique using multichannel analysis.

5.3.2. PFR acoustic experiments data

- The use of injection and background noise data measured with the same instrumentation and on the same installation has removed any uncertainty in the conclusions of previous exercises done on data prepared by mixing of signals obtained from different rigs.
- With a few exceptions, a satisfactory correspondence has been found between the times of onset of the injections determined by different methods and the actual values. Detection capability in real field conditions has been established. Techniques which were earlier successfully tested on synthesized data were effective in detecting the anomaly in real field data also.
- Mechanical wave guides terminating in accelerometers are found very suitable for leak detection.
- Acoustic signals from injection were transmitted to all the wave guides, including the farthest wave guide which was nearly 5 m away from the injection zone. However the frequency content at each waveguide was influenced by the injection medium and the transmission path.
- Leak location was difficult due to the complex internal geometry of PFR evaporator. Nevertheless French analysis based on cross correlation of 30 kHz high pass filtered data gave encouraging results.

5.4. General

The following general and important conclusions have emerged from the CRP.

- The CRP has evaluated different signal processing techniques both on synthesized data and real field data and hence the results could provide invaluable information to the designers of ALD systems. In the long run, this would lead to enhancing the economics of LMFRs through better surveillance on reactor cores and steam generators.
- The work carried out within the framework of this CRP has a general scientific value. Signal processing techniques developed in this CRP for anomaly (boiling or leak) detection can be applied for detecting other types of anomalies in thermomechanical equipments (like pump cavitation, rattling etc.) in fast and thermal reactors.

6. RECOMMENDATIONS FOR FUTURE WORK

The IAEA Co-ordinated Research Programme on Acoustic Signal Processing for the Detection of Boiling or Sodium-Water Reaction in LMFBR has covered two areas of great relevance to the LMFR safety and economics. The conclusions which have emerged from this CRP will provide valuable information to the designers of anomaly detection systems in LMFRs and also other types of reactors. However it is recognized that there are certain areas which require further evaluation before reliable acoustic detection systems can be incorporated as part of reactor/steam generator protection systems. Some of the recommendations of the CRP outlined below are intended to address these areas.

- Further analysis for establishing detection capability at full power, for leak location and for identifying the injection medium should be carried out on the 1995 data from PFR end-of-life acoustic experiments. During this exercise, particular attention should also be paid to the question of the suitability of the method for implementation in an on-line detection system.
- More attention should be paid to the development of automatic detection algorithms and expert systems which can be implemented in an on-line detection system. Such a system should satisfy the requirements of detection speed and reliability.
- Studies in the areas of mathematical modelling of the physical processes involved and feasibility of using argon injection for in-situ testing of ALD system are essential.
- A concise monograph on the signal processing methods developed for boiling and leak detection in this CRP may be published in order to disseminate the information to other potential users.

ABBREVIATIONS

ABND	-	Acoustic Boiling Noise Detection
ALD	-	Acoustic Leak Detection
ALN	-	Adaptive Learning Network
APSD	-	Auto Power Spectral Density
CDM	-	Computerized Decision Making
CRP	-	Co-ordinated Research Programme
DESYRE	-	Diagnostic Expert SYstem for REactor Surveillance
DT	-	Digital Tape
EFR	-	European Fast Reactor
LMFR	-	Liquid Metal Fast Reactor
PDF	-	Probability Density Function
PFR	-	Prototype Fast Reactor (UK)
Pm	-	Probabilities of missing the boiling detection
Ps	-	Probabilities of spurious the boiling detection
PSD	-	Power Spectral Density
PSD-SUM	-	Sum of PSD values of selected frequency regions
RCM	-	Research Co-ordination Meeting
RMS	-	Root Mean Square Methods
SD	-	Standard Deviation
SGU	-	Steam Generator Unit
S/N	-	Signal over Noise
SPRT	-	Sequential Probability Ratio Test
SPX	-	Superphenix
SWLR	-	Small Water Leak Rig

REFERENCES

[1] International Atomic Energy Agency, Signal Processing Techniques for Boiling Noise Detection, IWGFR/68, Vienna, 1989.

[2] Ledwidge T.J., and Black J.L., Signal Processing Strategies for On-line Diagnostics, Proc. Australian Instrumentation and Measurement Conference, Adelaide, 1989, pp 130-135.

[3] Srinivasan G.S., and Om Pal Singh, New Statistical Features Sensitive to Sodium Boiling Noise, Annals of Nuclear Energy, Vol 17, No. 3, 1990, pp. 135-138.

[4] Srinivasan G.S., Om Pal Singh, Vyjayanthi R.K., and Prabhakar R., New Statistical Features for Sodium Boiling and Leak Noise Detection in LMFBRs under poor S/N - Ratio Conditions, Annals of Nuclear Energy, Vol 20, No.2, 1993, pp. 101-116.

[5] Vyjayanthi R.K., Prabhakar R., Srinivasan G.S., and Om Pal Singh, Application of Adaptive Learning Network Technique to Detection of Sodium Boiling Noise in Fast Reactors, Prog. Nuclear. Energy, Vol. 27, No. 1, 1992,pp. 77-82.

[6] Lennox T., McKnight J.A., and Rowley R., The Application of Acoustic Instrumentation for use in Liquid Metal Fast Breeder Reactors, Nuclear Energy, Vol 33 No 1, Feb., 1993.

[7] McKnight J.A., Rowley R., and Beesley M.J., Acoustic Surveillance Techniques for SGU Leak Monitoring, IWGFR/79 (ed. JPh Girard), IAEA, Oct. , 1990.

[8] Rowley R., Airey J., Analysis of Acoustic Data from the PFR SGU Condition Monitor, ibid /7/

[9] Rowley R., McKnight J., and Airey J., Analysis of Acoustic Data from UK Sodium/Water Reaction Test Facilities, ibid /7/

[10] Rowley R., and Airey J., Acoustic Transmission in SGUs: Plant and Laboratory Measurements, ibid /7/

[11] Heckl M., Sound Propagation in the Steam Generator - a Theoretical Approach, ibid /7/

[12] Yughay S., and Kozlov F.A., Noise Spectrum when Water leaks into Sodium, Atomnaya Energiya, Vol 65, No 1, July, 1988, pp 17-20.

[13] Daubechies I., The Wavelet Transform - Time-Frequency Localisation and Signal Analysis, IEEE Trans. on Information Theory, Vol 36, No 5, Sept. 1990, pp961-1005.

[14] Macleod I.D., Beesley M.J., Firth D., Rowley R., Taylor C.G., and Waites C., Acoustic Surveillance Systems for LMFBRs, Science and Technology of Fast Reactor Safety, Vol 2. BNES, London, 1986, pp 371-376.

[15] Eggert H., Scherer K.P., Schleisiek K., Stiller P., Schöller H., and Rohnacher P., An Intelligent Diagnostic System for the Experimental Fast Reactor KNK II, International Conference on Fast Reactors and Related Fuel Cycles (FR'91), Kyoto, Japan, Oct. 28-Nov. 1, 1991.

EXPERIMENTAL SGU BACKGROUND AND IN SODIUM WATER LEAK NOISE DATA PROVIDED BY THE ELECTRICITE DE FRANCE R&D ORGANIZATION FOR IAEA BENCHMARK TAPES

C. JOUNEAU
Centre d'Etudes Nucléaires de Cadarache,
Saint-Paul-lez-Durance,
France

Abstract

The paper describes the data which have been provided to Mr Shinohara (JAERI) and which have served to generate the Fourth Stage Analysis Benchmark Test Tapes distributed in August 1993

1 PFR Background Noise Data

Mr. Rowley and Mr McKnight of AEA Technology (United Kingdom) have conducted numerous background measured the 19th of July 1991 on the Steam Generator Units of the Prototype Fast Reactor at Dounreay. From those, they provided to the CRP data measured on Superheater 2 and Superheater 3 PFR Superheaters are 1 6 m diameter 11 7 m high U tube SGUs. During those measurement, the plant was running at 650 MW thermal (245 MWe)

The tape prepared by JAERI used only one sensor from Superheater 2 - sensor 9 situated at 1 9 m from bottom level , orientation South-South West - and one sensor from Superheater 3 - sensor 4 located at middle of the unit (4.1m high) not far from a rattling noise source which has been observed over years. (see Figure 1 from [1])

Those two transducers have roughly the same sensitivity (33.4 and 28.5) and were recorded with the same gains, so are comparable

5 other transducers per unit are available to the CRP on each unit. For example on Cell 3, the accelerometers attached to Waveguides (WG) number 4, 6, 9, 7, 8 and 10 (see Figure 1) were recorded
The following table show the available measurement points :

Superheater 2	Superheater 3
Sensor 9 (Level 1.9m SSW)	Sensor 4 (Level 4.1 m W)
Sensor 7 (Level 1.9m NNW)	Sensor 6 (Level 4.1m SSE)
Sensor 8 (Level 1.9 m E)	Sensor 9 (Level 1.9m SSW)
Sensor 10 (Level 0, W)	Sensor 7 (Level 1.9m NNW)
Sensor 12 (Level 0, SSE)	Sensor 8 (Level 1.9m E)
Sensor 11 (Level 0, NNE)	Sensor 10(Level 0 W)

Those data should enable the CRP in a following stage to do multi sensor analysis It could also be possible to train a method on one unit and test it on the other This would assure that the detection is not specific to a certain data set

At the 1991 Coordinated Research Meeting held at Chester,U.K.[2], France had also provided background noise tapes from Superphénix 1 SGU "D" recorded the 27th of June 1989 while the plant was operating at 1140 MWe. 4 transducers have been recorded. They are situated on the same generant of the helical SGU shell at the altitudes of 21 m, 25 m, 29 m, 33 m.

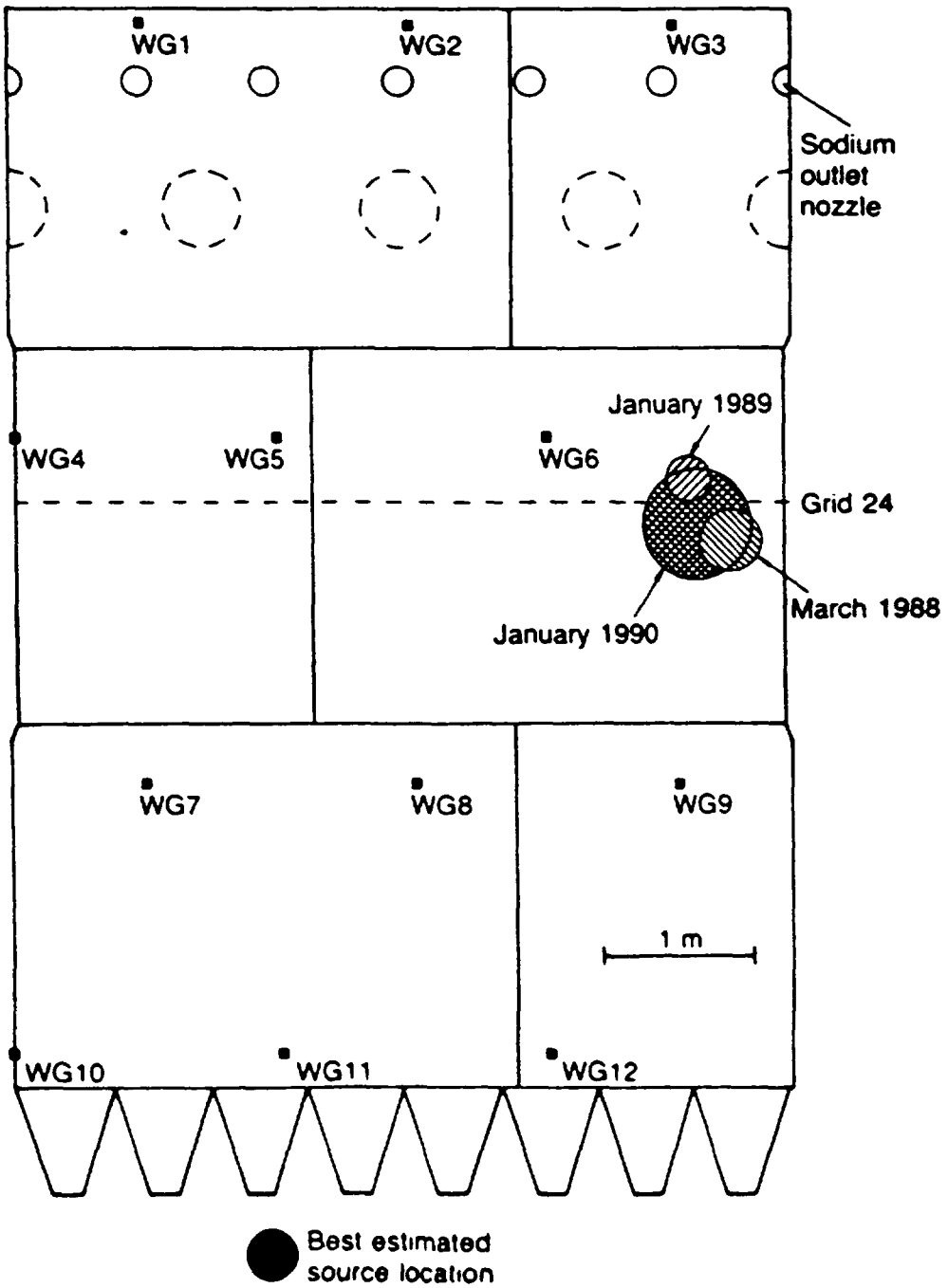

Figure 1 : Location of Waveguides on PFR Superheater 3
and location of acoustic source, from [1]

2. Sodium Water Reaction Leak Noise

In sodium water leaks have been conducted on the ASB loop by Interatom (now a part of SIEMENS KWU) at Bensberg in the Federal Republic of Germany. This loop has a 4.6 m high 0.6 m inner diameter Reaction Test Vessel in which water can be injected in stagnant sodium.

Acoustic measurement have been conducted in December 1991 by a British team, as part of the EFR R&D collaboration, on this loop during two tests corresponding respectively to 1.8 g/s and 3.8 g/s water injections.

Figure 2 presents the transducers layout.

3 sensors are 90° apart about 0.4 m above the leak position, while 3 others (4,5,6) were installed 0.85 m below the injector. It must be noted that there is a dummy tube plate between the injector and the lower transducers.

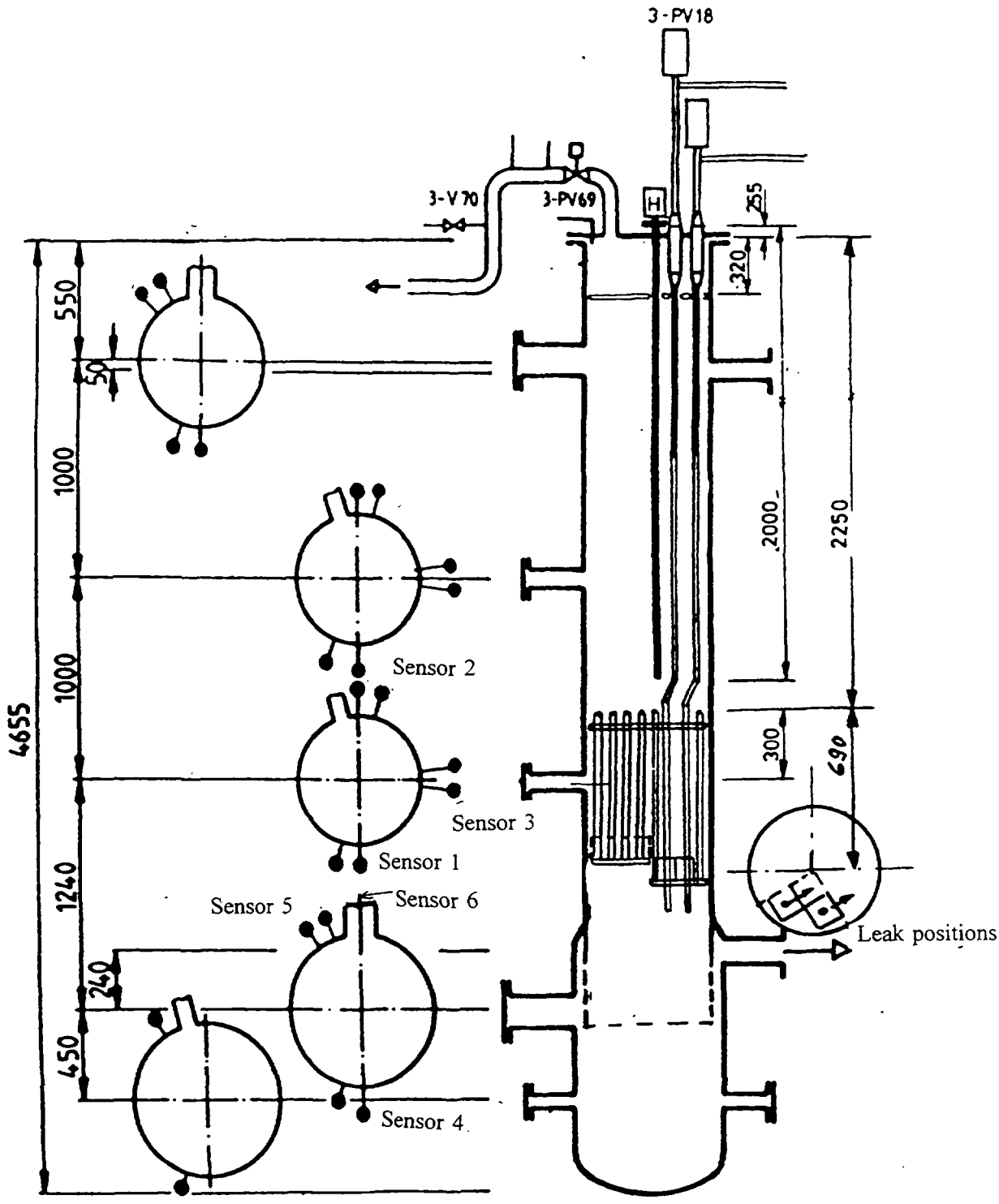

Figure 2 : Superposition of PFR and ASB geometries'

The tape produced by Drs. Shinohara and Hayashi of JAERI used only sensor 1 which is the nearest from the leak positions , which are at about ± 30° from this waveguide. Between the first test (1.8 g/s) and the second (3.8 g/s) the sensor gain has been lowered of 5 dB.

This experiment present the "advantage" that the leak initiation is a quite noisy mechanical event : The leaky tube is pulled up. Thus the sequence of event is : background, mechanical noise (not to be detected by an Acoustic Leak Detection System), leak noise.

3. Multi channel acoustic analysis

At the 1992 Coordinated Research Meeting it was recommended that multi-track data be studied. This is closer to the situation that would happen on an operating Acoustic Leak Detection System were several transducers would be attached to each unit.

Thus, I propose that the next tape to be issued as a benchmark for the CRP uses this multi-sensor properties. The signal processing may analyse the channels independently and , only at the end, propose a vote between the various transducers, or use all transducers - or subsets- for a multichannel analysis.

Since we don't have yet background and leak noise data obtained on the same unit, the superposition of background and leak noise will be a bit awkward. Thus I suggest that we provide to the participants a multi-track tape containing :

- PFR Background data
- ASB Leak noise data
- A superposition of PFR and ASB data with signal to noise ratios ranging from -6 to -24 decibels. (Fig. 3).
- A superposition of leak noise with artificial incoherent noise from noise generators , at the same signal to noise ratios.

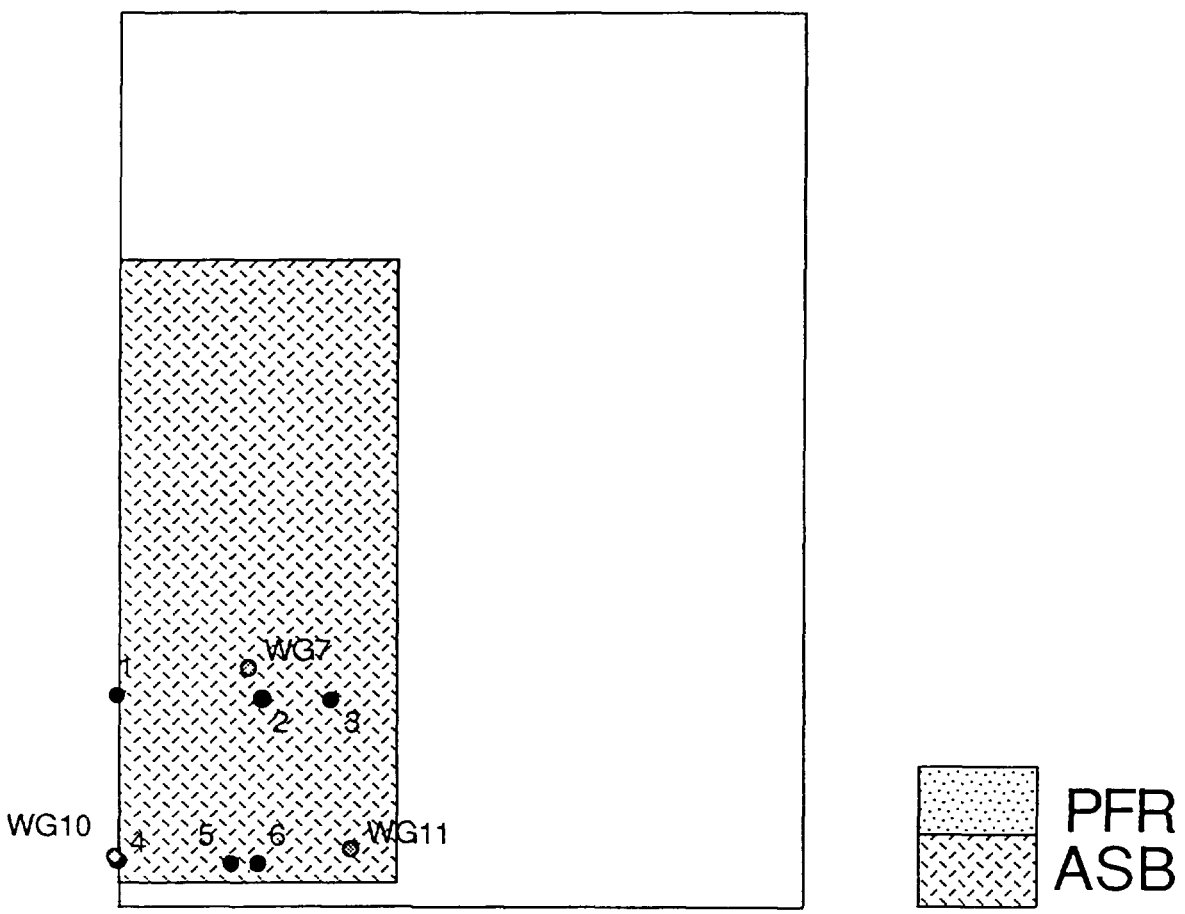

Fig. 3: Superposition of PFR and ASB geometries.

4. PFR End of Life Experiment

In April 1994, the Prototype Fast Reactor at Dounreay, Scotland is to be definitively stopped. End of Life experiments have been planned and, in particular, water shall be injected in an evaporator while, among others, acoustic measurements will be taken.

This type of experiment is not expected to happen again in the near future. Furthermore it is an unique opportunity to test acoustic leak detection algorithm with real leak and background noises, either directly or by mixing the measured data with amplified evaporator background noise tapes.

It is proposed that the CRP request the British for access to measurements to be make during this unique experiment and uses it to validate the various algorithm.

As part of those end of life experiments, a long term monitoring of PFR background noise is been done on the last months of its life. If the British agree to distribute some of those data, it could be interesting to test the methods with some of the strange background noises that appear now and then on an operating reactor.

ACKNOWLEDGEMENTS

The data used to established this benchmark were provided in March 1993 by Mr. Ray Rowley and Mr. Jim McKnight of AEA Technology.

The Prototype Fast Reactor is operated by AEA Technology

Superphénix1 is operated by the European consortium NERSA

The ASB experiment was operated by Interatom GmbH

REFERENCES

[1] T. Lennox, J.A. McKnight, R. Rowley "Application of Acoustic Instrumentation for use in Liquid Metal Fast Breeder Reactors", Nucl.Energy 32, n°1, pp.29-40 (Feb 1993)

[2] C.Journeau " Superphénix1 SGUs Background measurements" IAEA IWGFR Coordinated Reaserch Meeting held at Chester,U.K (1991)

ACOUSTIC LEAK DETECTION EXPERIMENTS PERFORMED IN PFR, MARCH 1993 TO JUNE 1994

R. CURRIE
Reactor Technology Department,
Dounreay, United Kingdom

Abstract

In this paper emphasis is given to describing how the data that has been recorded during each experiment may be used to generate further test cases for acoustic leak detection techniques. It should be also noted that the detailed analysis of this data is currently in progress and therefore there is a short description of the analysis of the data in this paper.

1.0 Introduction

A series of experiments aimed at obtaining acoustic noise data for developing and validating acoustic leak detection techniques for LMFBR steam generators was performed in PFR during the last year of operation, culminating in a series of gas and steam injections shortly after the final shutdown of the plant.

The background noise in one evaporator and one superheater were continuously monitored during the last year of operation, allowing data to be collected on the similarities and differences in the acoustic background noise in these two different types of steam generator at all operating states. This data was recorded digitally, with data capture being triggered by measurement of a significant pulse.

Additionally, analogue tape recordings of acoustic background noise in these units were made periodically to obtain data on the differences and similarities of the background noise in these units at full power, at different times, and at part load and shutdown conditions. Over and above the normal range of operating conditions which naturally occurred, some special sets of conditions were set up to enable data to be obtained to allow the factors contributing to the overall background to be separated out.

An experiment previously reported[1] on the transmission of sound through a PFR Superheater was repeated with the sound source in a different location. This new experiment was designed to provide further data on the acoustic transmission path in a steam generator (SGU) with internal baffles.

An experiment on the long term behaviour of an active acoustic leak detection system was performed on a PFR superheater. This experiment was carried out by CEA, France, using CEA equipment. The analysis of the results from this experiment is being performed by CEA.

An injection device was installed into a PFR evaporator which enabled injections of gas and water/steam to be performed into two locations: one inside the tube bundle; the other in the sodium interspace between the vessel shell wall and the wrapper baffle around the tube bundle. A total of 142 injections were performed:

85 argon injections
53 water/steam injections
4 hydrogen injections.

Passive acoustic data was recorded on an analogue tape recorder for 115 injections and active acoustic data was recorded by CEA during 26 injections.

In this paper emphasis is given to describing how the data that has been recorded during each experiment may be used to generate further test cases for acoustic leak detection techniques. It should be noted that the detailed analysis of this data is currently in progress and therefore there is little description of the analysis of the data in this paper.

1. Rowley and Airey: Acoustic Transmission in SGUs: Plant and Laboratory Measurements: IAEA IWGFR Specialists Meeting, Aix-en-Provence, 1-3 October 1990

2.0 Passive Acoustic Data Recorded During Injections into PFR Evaporator 3

In Figure 1, the positions of the waveguides attached to the outside of the shell of PFR Evaporator 3 are shown. The lengths of Waveguides WG7 and WG10 were reduced in order to increase their resonant frequency to about 4 kHz, which is above the expected frequency of signals from bubbles (0 - 2 kHz). Endevco 7704-A-17 accelerometers were fitted to WG3, WG5, WG6, WG7, WG8 and WG10. WG12 was used to input the pulses for the CEA active experiment and was not used to collect passive data.

The passive acoustic signals during the injections were recorded in analogue form using a tape recorder running at 120 inches per second, set to Wideband 1. The bandwidth of the recorded signals was 0 to 80 kHz.

The normal procedure was to record some background noise just prior to commencing the injection.

The status of the plant during these injections was the steamside pressurised with argon at low pressure and therefore the steamside contribution to "normal" background noise was not present. Background noise measurements made at various pump speeds with the steamside at this condition had shown that above a threshold value, a significant impulsive sound occurred, which was not representative of full power operation. It was therefore decided to perform these experiments with a pump speed set below this threshold value and to obtain leak noise data in a generally quiet steam generator. The possibility exists to mix the leak noise with background noise recorded at different plant operating states.

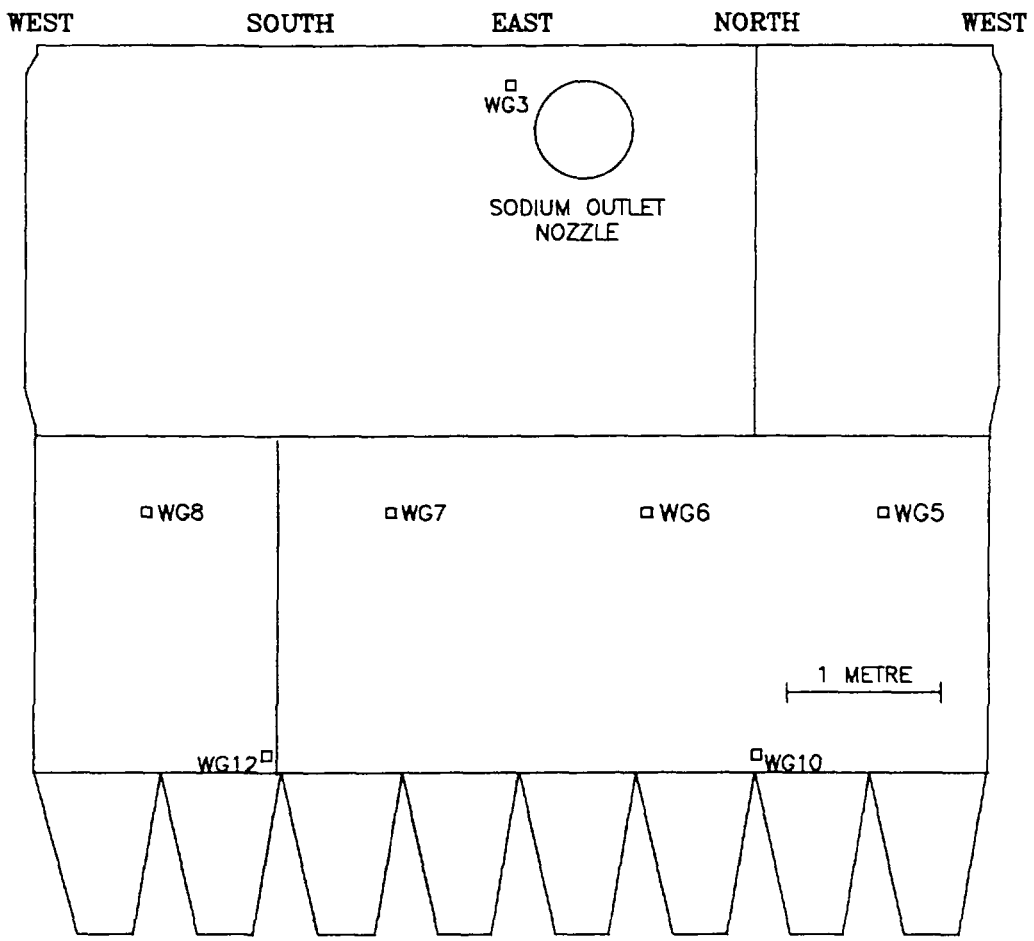

Figure 1 PFR Evaporator 3 – Waveguide Positions (outside view of vessel shell)

The injection system consisted of a device installed into the evaporator which contained 18 injection lines, each initially sealed by a bursting disc to prevent sodium entering the line, 9 terminating in the sodium interspace between the shell wall and the tube bundle wrapper and 9 terminating in the tube bundle region - Figure 2. These injection lines were of internal diameter 2.26 mm and 6 were fitted with 0.5 mm orifices and 6 with 1.0 mm orifices, to enable a wide range of injection rates to be achieved. These injection lines were connected 6 at a time to an injection system (Figure 3) which was capable of selecting a line and injecting gas or water at a controlled pressure for a controlled period followed by an automatic low pressure argon purge to maintain the line open after the injection period. In this way several injections were achieved through each injection line. During argon and hydrogen injections, the injection rate was derived from the pressure drop between two pressure transducers in the injection line and for water injections, the injection rate was measured by an ultrasonic level meter measuring the residual mass of water in the injection bottle.

The injections during which passive acoustic measurements were made are summarised in Tables 1 - 8. As can be seen from these tables, acoustic data has been obtained which allows the following to be performed:

- Comparison between the acoustic noise produced by argon compared to water/steam injections
- Investigation of the relationship between acoustic noise and injection rate for argon and water/steam
- Determination of dominant acoustic transmission path as a function of location of leak and gas being injected
- Determination of relationship between leak location and fluid with attenuation of acoustic signals in the steam generator
- Comparison of acoustic noise produced by leaks of the same mass flowrate, but with different driving pressures for both argon and water/steam
- Effect of sodium temperature on acoustic noise - e.g. effect of different rates of hydrogen dissolution during water/steam injections.

It can be seen that the data recorded during these injections provides a unique database for testing the performance of acoustic leak detection techniques and for developing "calibration" techniques for systems installed in a plant.

3.0 Background Acoustic Noise Measurements

The background acoustic noise measurements made in PFR since March 1993 are summarised in Table 9. Two steam generators have been monitored in particular, Superheater 3 and Evaporator 3. It can be seen that data has been collected which allows investigation of the following:

- Variations over a period of time in the background noise in each unit at nominal full power conditions
- Background noise in each unit at different power levels
- Contribution of waterside/steamside conditions of evaporator on background noise
- Contribution of sodium pump speed / sodium flowrate on background noise in each unit
- Similarities in characteristics of background noise in these two units which have different geometries and operating conditions
- Differences in characteristics of background noise in these two units which have different geometries and operating conditions
- Potential false trip frequencies of different acoustic leak detection systems.

This database can be used to produce tapes containing leak noise from the injections performed in PFR Evaporator 3 with background noise in the evaporator or superheater at different operating conditions.

The data has been recorded in analogue form on magnetic tape recorders. The bandwidth of the recordings were either DC to 40 kHz or DC to 80 kHz. The location of waveguides and the type of transducers used are shown in Figures 4 and 5.

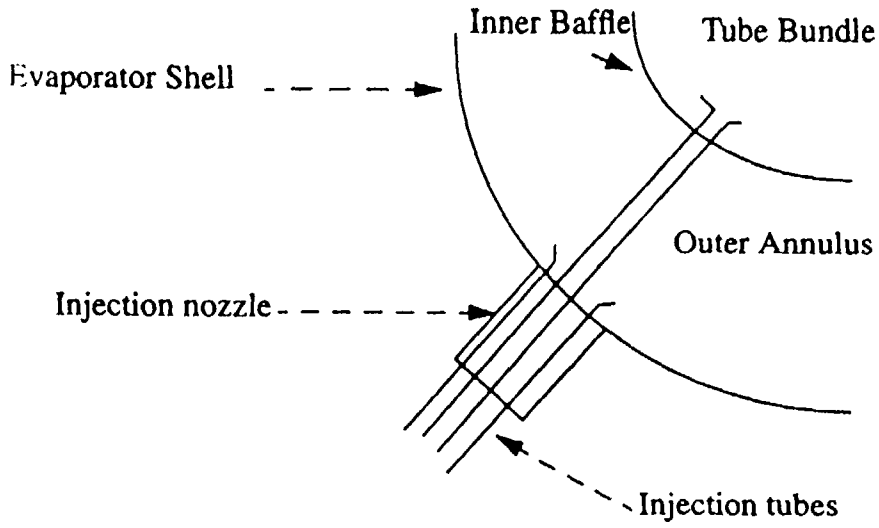

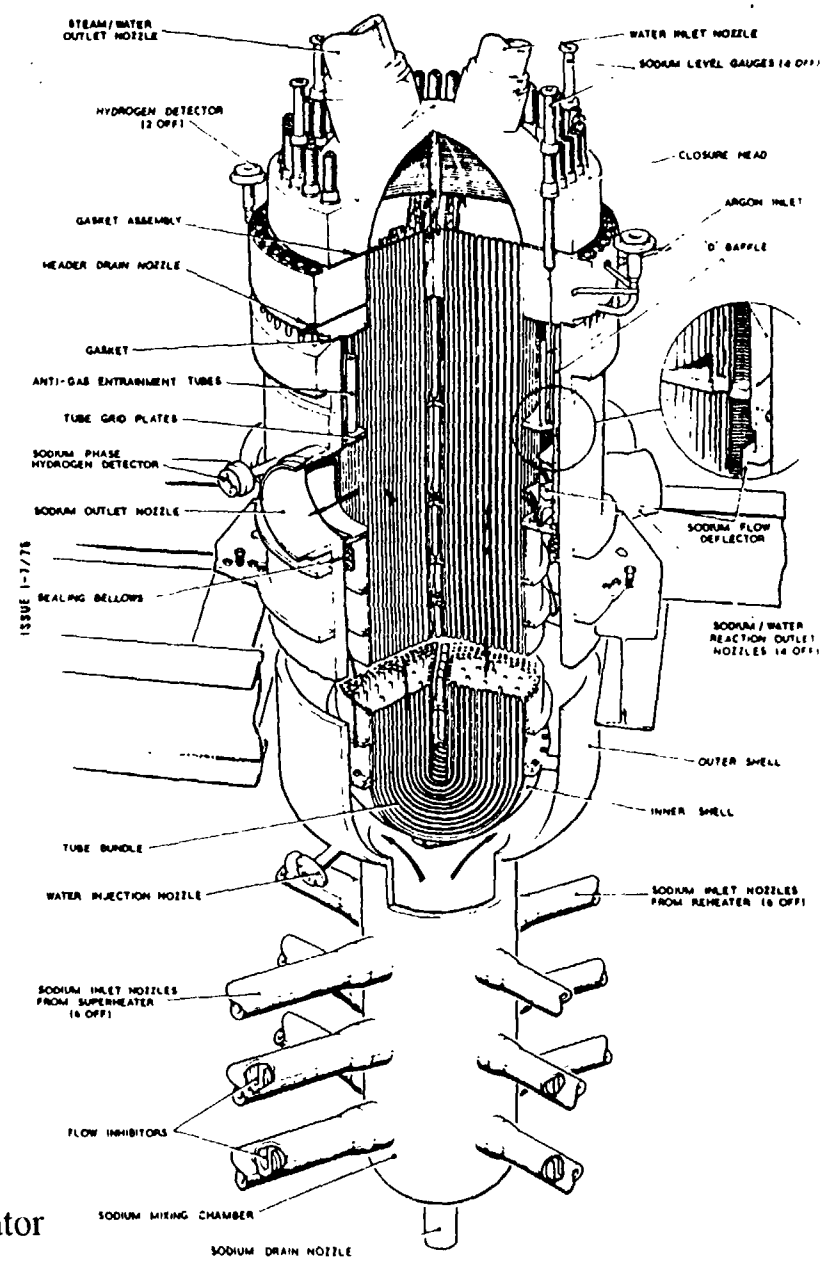

FIGURE 2 Evaporator

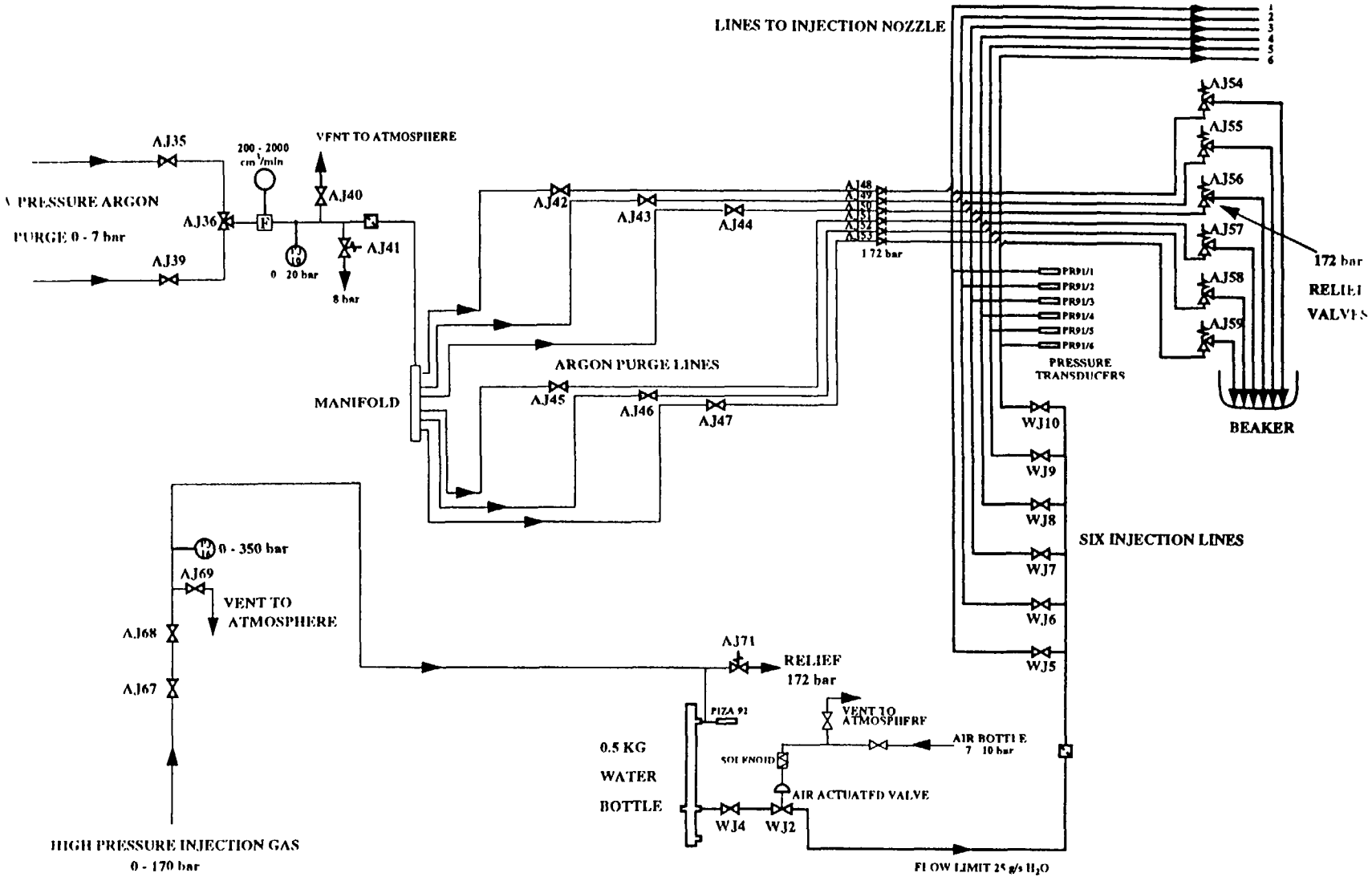

FIGURE 3 Diagram of flow paths in LDS5 injection system

Table 1: Argon Injections into Tube Bundle at 300°c

Injection Rate (gs^{-1})	Duration (s)	Source Pressure (bars)	Nozzle Diameter (mm)	Test Number
0.25	240	10	0.5	067
0.25	240	10	0.5	040
0.32	240	10	2.26	061
0.45	420	10	1.0	048
1.3	1.3	50	0.5	041
2	90	50	2.26	062
2	90	50	0.5	068
2	90	50	1.0	049
2.4	45	100	0.5	042
3.3	30	140	0.5	043
3.8	45	100	0.5	069
4	45	100	2.26	063
4.1	45	100	1.0	050
4.1	4.1	170	0.5	044
5.5	30	140	0.5	070
5.5	30	140	2.26	064
5.7	30	140	1.0	051
6.4	30	170	0.5	071
6.7	30	170	2.26	065
7	30	170	1.0	052

In addition to the data recorded on magnetic tape on the various dates shown in Table 9, background noise on two waveguides in each of Superheater 3 and Evaporator 3 was continuously monitored during the final year of operation of the plant and the detection of pulses exceeding a predetermined size triggered recording of the data digitally.

This data coupled with the database of all of the data from all PFR instrumentation allows correlations between plant events and significant acoustic events to be determined. This data will be important for assessing the potential false trip frequency of various acoustic leak detection techniques.

Table 2: Argon Injections into Sodium Interspace at 300°c

Injection Rate (gs^{-1})	Duration (s)	Source Pressure (bars)	Nozzle Diameter (mm)	Test Number
0.24	240	10	1.0+	092
0.24	480	10	0.5	002
0.25	240	10	0.5	030
0.36	240	10	2.26	102
0.5	240	10	1.0	016
0.6	240	10	2.26	024
0.8	90	50	1.0+	093
0.8	90	50	0.5+	090
1.3	90	50	0.5	031
1.3	90	50	0.5	003
1.5	45	100	1.0+	094
1.6	45	100	0.5+	089
1.9	30	140	0.5+	088
2	30	140	1.0+	095
2	90	50	1.0	017
2.3	90	50	2.26	025
2.3	30	170	1.0+	087
2.3	30	170	0.5+	096
2.4	90	50	2.26	103
2.5	45	100	0.5	032
2.5	45	100	0.5	004
3	30	140	0.5	005
3.3	30	140	0.5	033
4	30	170	0.5	006
4.1	30	170	0.5	034
4.2	45	100	1.0	018
4.6	45	100	2.26	026
4.7	45	100	2.26	104
5.9	30	140	1.0	019
6.3	30	140	2.26	105
6.5	30	140	2.26	027
7	30	170	1.0	020
7.5	30	170	2.26	028

Note: + signifies that an additional resistance was used in the injection line to enable smaller injection rates to be achieved.

Table 3: Argon Injections into Tube Bundle at 350°c

Injection Rate (gs^{-1})	Duration (s)	Source Pressure (bars)	Nozzle Diameter (mm)	Test Number
0.17	240	10	0.5+	107
0.27	240	10	1.0+	129
0.35	240	10	1.0	138
0.75	90	50	0.5+	108
0.86	40	50	1.0+	130
0.86	90	50	1.0+	133
0.86	90	50	1.0+	132
0.86	90	50	1.0+	131
1.4	45	100	0.5+	109
1.55	45	100	1.0+	134
1.8	30	140	0.5+	110
2	90	50	1.0	139
2	30	140	1.0+	135
2.1	30	170	0.5+	111
2.4	30	170	1.0+	136
4	45	100	1.0	140
5.5	30	140	1.0	141
6.6	30	170	1.0	142

Note: + signifies that an additional resistance was used in the injection line to enable smaller injection rates to be achieved.

Table 4: Water/Steam Injections into Tube Bundle at 300°c

Injection Rate (gs^{-1})	Duration (s)	Source Pressure (bars)	Nozzle Diameter (mm)	Test Number
3.4	30	10	0.5	075
3.85	20	20	0.5	076
5.5	15	30	0.5	079
11.1	15	40	0.5	078
11.1	10	35	1.0	054
11.6	10	40	1.0	056
13.1	15	50	0.5	077
16	10	60	1.0	057

Table 5: Water/Steam Injections into Sodium Interspace at 300°c

Injection Rate (gs^{-1})	Duration (s)	Source Pressure (bars)	Nozzle Diameter (mm)	Test Number
0.22	600	170	0.5+	085
0.41	240	170	0.5+	084
0.71	150	170	1.0+	097
0.75	120	170	0.5+	081
0.83	120	170	0.5+	083
1.31	100	170	0.5+	082
1.65	20	20	0.5	011
2.2	30	10	0.5	010
2.7	10	30	0.5	012
5	10	30	0.5	058
9.3	10	40	0.5	013
10	10	30	1.0	037
11.3	10	50	0.5	014
13.4	10	40	1.0	038
29.3	15	170	2.26	059

Note: + signifies that an additional resistance was used in the injection line to enable smaller injection rates to be achieved.

Table 6: Water/Steam Injections into Tube Bundle at 350°c

Injection Rate (gs^{-1})	Duration (s)	Source Pressure (bars)	Nozzle Diameter (mm)	Test Number
0.21	90	20	0.5+	115
0.6	90	50	0.5+	116
1.06	65	60	1.0+	143
1.22	55	110	1.0+	144
1.52	50	170	1.0+	145
1.78	90	10	0.5+	113
4.5	30	10	2.26	152
5.9	20	17	2.26	153
7.65	20	24	2.26	154
10.6	10	35	2.26	155
12.2	10	42	2.26	156
14.3	10	50	2.26	157
21.2	10	100	2.26	158
28.5	10	170	2.26	159

Note: + signifies that an additional resistance was used in the injection line to enable smaller injection rates to be achieved.

Table 7: Water/Steam Injections into Sodium Interspace at 350°c

Injection Rate (gs^{-1})	Duration (s)	Source Pressure (bars)	Nozzle Diameter (mm)	Test Number
4.5	30	10	2.26	147
7.15	20	17	2.26	148
9.1	20	24	2.26	149
12.5	10	35	2.26	150

Table 8: Hydrogen Injections at 300°c

Injection Rate (gs^{-1})	Duration (s)	Source Pressure (bars)	Nozzle Diameter (mm)	Location	Test Number
0.04	120	10	0.5	Inter-space	009
0.05	120	10	0.5	Tube Bundle	053
1.3	30	170	2.26	Inter-space	101

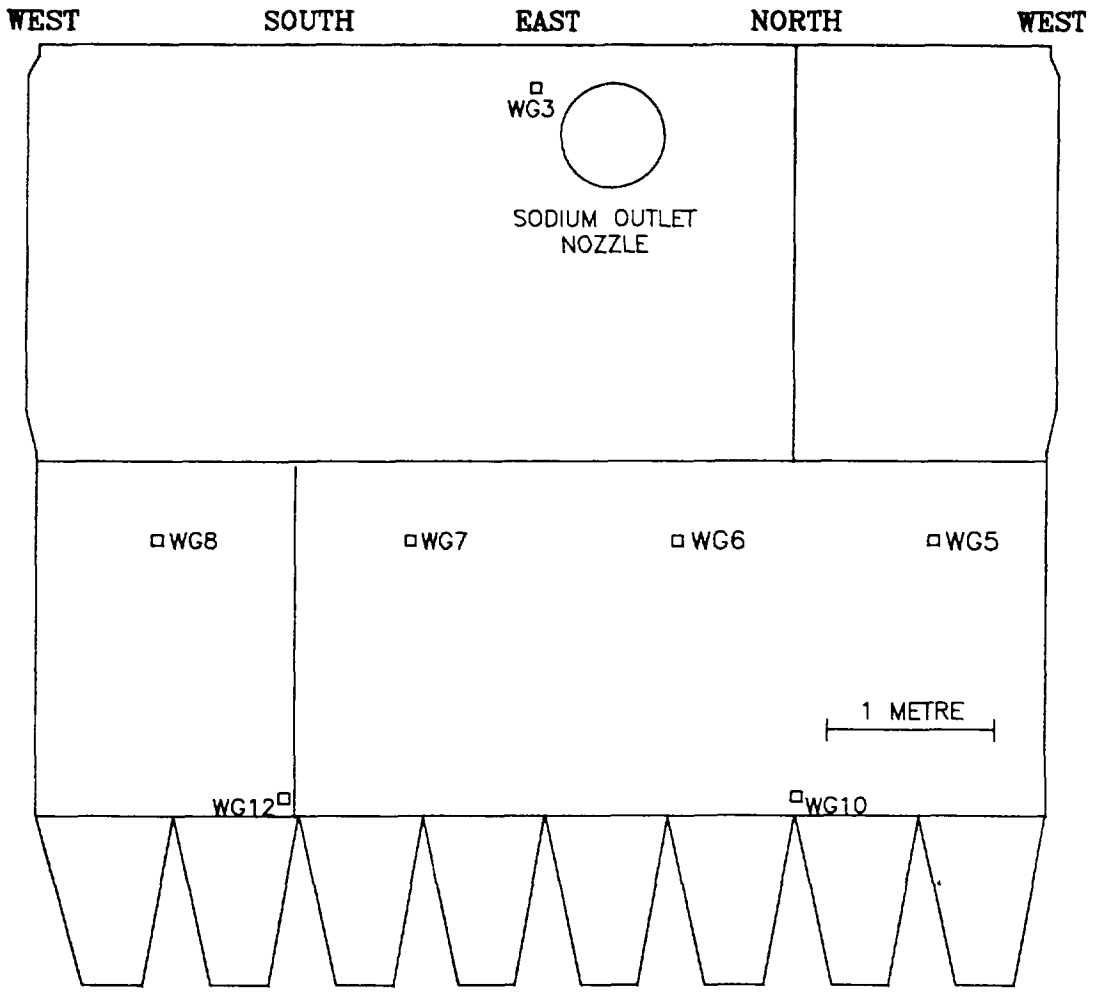

Types of Transducers fitted to Waveguides :

March 1993 to August 1993 – All waveguides fitted with Birchall A/120 accelerometers.

August 1993 to April 1994 – As above except waveguides 7 & 10 which were fitted with Endevco 7704A–17 accelerometers.

April 1994 to July 1994 – All waveguides fitted with Endevco 7704A–17 accelerometers.

Birchall A/120 accelerometers:
Sensitivity 28 uA/g; Resonant Frequency 27.5 kHz.

Endevco 7704A–17 accelerometers:
Sensitivity 17 pC/g; Resonant Frequency 45 kHz.

Figure 4 PFR Evaporator 3 – Waveguide Positions (outside view of vessel shell) and Transducer Details

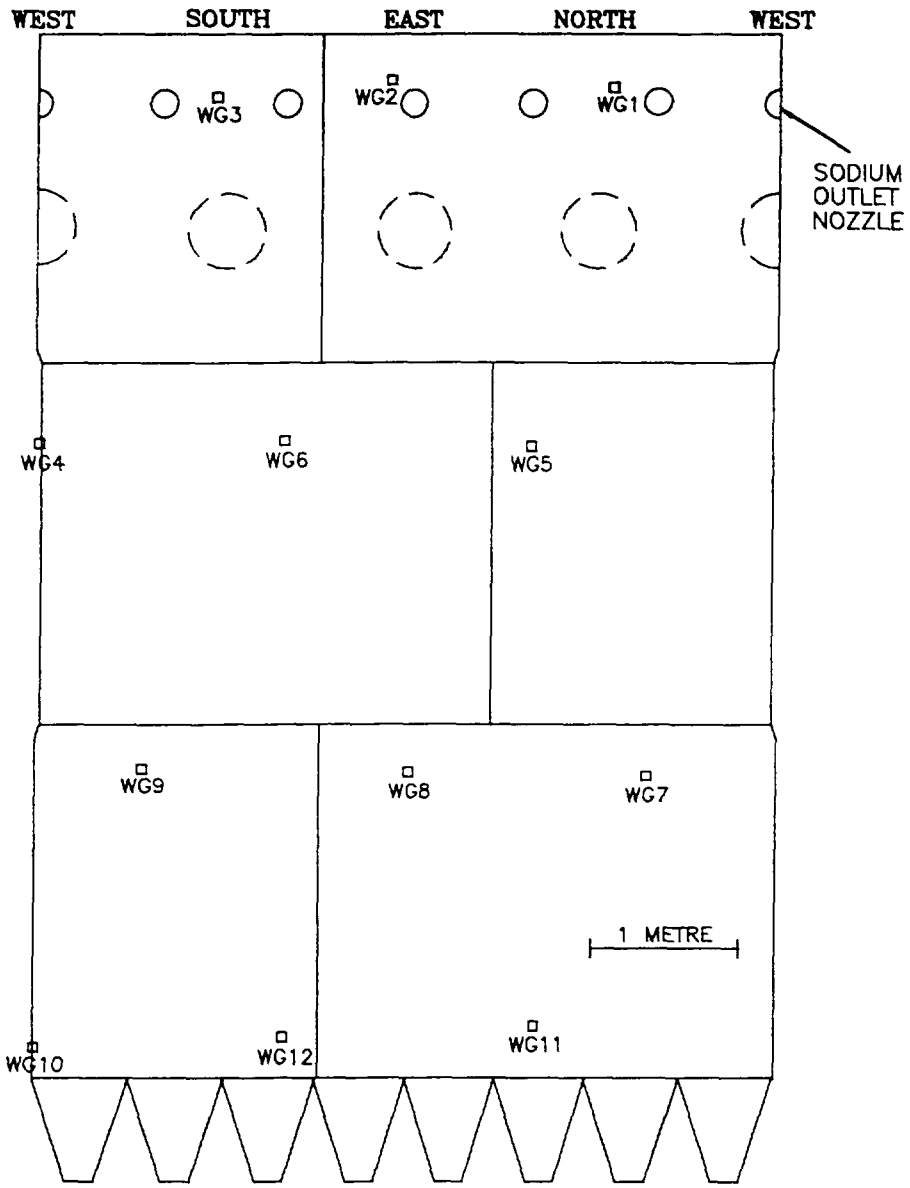

Types of Transducers fitted to Waveguides:

March 1993 to August 1993 – All waveguides fitted with Birchall A/120 accelerometers.

August 1993 to April 1994 – As above except waveguides 2 & 6 which were fitted with Endevco 7704A–17 accelerometers.

April 1994 to July 1994 – All waveguides fitted with Birchall A/120 accelerometers.

Birchall A/120 accelerometers:
Sensitivity 28 uA/g; Resonant Frequency 27.5 kHz.

Endevco 7704A–17 accelerometers:
Sensitivity 17 pC/g; Resonant Frequency 45 kHz.

Figure 5 PFR Superheater 3 – Waveguide Positions (outside view of vessel shell) and Transducer Details

Table 9: Background Noise Measurements

Date	Power (MW(th))	Plant State	Number of evaporator waveguides	Number of superheater waveguides	Bandwidth (kHz)
23/4/93	630	Full Power	11	12	40
25/693	628	Full Power	11	12	40
9/12/93	632	Full Power	6	12	40
12/1/94	0	Evaporator Argon Pressurised Sodium Pump Speed Effect	6	0	80
12/1/94	0	Evaporator Argon Pressurised Sodium Pump Speed Effect	6	0	80
2/2/94	647	Full Power	6	12	40
15/10/93	0	Evaporator Argon Pressurised	3	3	40
16/10/93	0	Evaporator Steam Pressurised	3	3	40
17/10/93	0	Evaporator On-Line	3	3	40
18/10/93	155	Power Raising	3	3	40
18/10/93	250	Power Raising	3	3	40
18/10/93	450	Power Raising	3	3	40
18/10/93	600	Full Power	3	3	40
13/12/93	634	Full Power	6	0	40
9/1/94	0	Evaporator Argon Pressurised	3	3	80
14/1/94	52	Power Raising	3	3	80
14/1/94	174	Power Raising	3	3	80
14/1/94	201	Power Raising	3	3	80
15/1/94	339	Power Raising	3	3	80
15/1/94	420	Power Raising	3	3	80
15/1/94	503	Power Raising	3	3	80
16/1/94	634	Full Power	3	3	80
15/6/94	0	Evaporator Argon Pressurised Sodium Pump Speed Effect	6	0	80

4.0 Conclusions

AEA Technology have performed a series of experiments at Dounreay, in PFR, which have generated data relevant to the development and validation of acoustic leak detection systems. Data has been collected on the nature of typical steam generator background noise under a wide range of operating conditions. Acoustic data has also been recorded during injections of argon, hydrogen and water/steam into a PFR Evaporator under acoustically quiet conditions. The members of the Coordinated Research Project are invited to discuss this data and agree what data would be of value in further testing the acoustic leak detection systems being developed by them.

1995 BENCHMARK DATA BASED ON EXPERIMENTAL RESULTS FROM THE PROTOTYPE FAST REACTOR AT DOUNREAY

R. CURRIE, P.J. WRIGHT, I.R. WIDDOWSON,
P. RAMSAY, R.E. SHALLCROSS
AEA Technology,
Risley, United Kingdom

Abstract

During the final year of operation of the Prototype Fast Reactor (PFR) at Dounreay and during the first 3 months following its closure on March 31 1994, a series of experiments was conducted to obtain data on the performance of leak detection systems. In June 1994, a series of injections of argon, hydrogen and steam was performed in Evaporator 3. Two injection locations were studied: one within the tube bundle region and one in the flowing sodium interspace between the tube bundle wrapper and the steam generator shell. During 113 injections, acoustic noise measurements were made at 7 transducer locations, spatially distributed on the shell of the Evaporator. These transducers were mounted on waveguides, welded to the shell Data from two argon injections, two steam injections and one hydrogen injection in the tube bundle and from 1 argon, 1 steam and 1 hydrogen injection in the sodium interspace, recorded at 4 transducer locations, were selected for the IAEA 1995 Benchmark exercise. The plant state during these injections was such that the acoustic background noise was lower than at full power operating conditions. It was agreed at the meeting to discuss the 1994 Benchmark results and to agree the 1995 Benchmark data, that it would be preferable not to mix these injection signals with full power background noise, but to include some separate full power background noise data for the Evaporator and for a Superheater. Accordingly, full power data recorded at two transducer locations in each unit have been included with the injection data. The task set was to: (a) compare and characterise the background noise from the evaporator and the superheater, (b) characterise and identify the type of leak noise signals (steam or argon or hydrogen), (c) estimate the onset of and duration of the leak in the injection data files, (d) evaluate the transmission characteristics of the leak noise signals from leak location to the transducers, and (e) locate the leak. In this paper, details of the injections in the Benchmark test are given. Additionally, the main characteristics of the data from these injections are compared with the other injections in the series to enable the representativeness of the Benchmark data to be assessed and to present the trends observed during the experiments.

DESCRIPTION OF THE INJECTION EXPERIMENT IN PFR EVAPORATOR 3

PFR has three secondary sodium circuits, each containing an evaporator, a superheater and a reheater - Figure 1. The heat exchangers are of the shell and U-tube design with the sodium flowing on the shell side and the water/steam flowing inside the tubes. Acoustic data from the evaporator and superheater in circuit 3 are included in the 1995 Benchmark Test Cases. These units are shown in Figures 2 and 3. The acoustic transducers were installed on the outside end of steel waveguides attached to the shell walls. The locations of the transducers used for the Benchmark are shown in Figures 4 and 5. In Figure 6, the locations of all of the transducers used during the injections into the evaporator are shown for completeness. The transducers used were Endevco Type 7704A-17, having a typical sensitivity of 17 pC/g and a resonant frequency of 45 kHz. The acoustic data was originally recorded in FM Wide Band 1 mode at a tape speed of 120 inches per second, giving a nominal frequency range of 0 to 80 kHz.

To enable the injections to be performed, an injection device was installed through a nozzle at the lower end of Evaporator 3. The location of this nozzle, which was used for

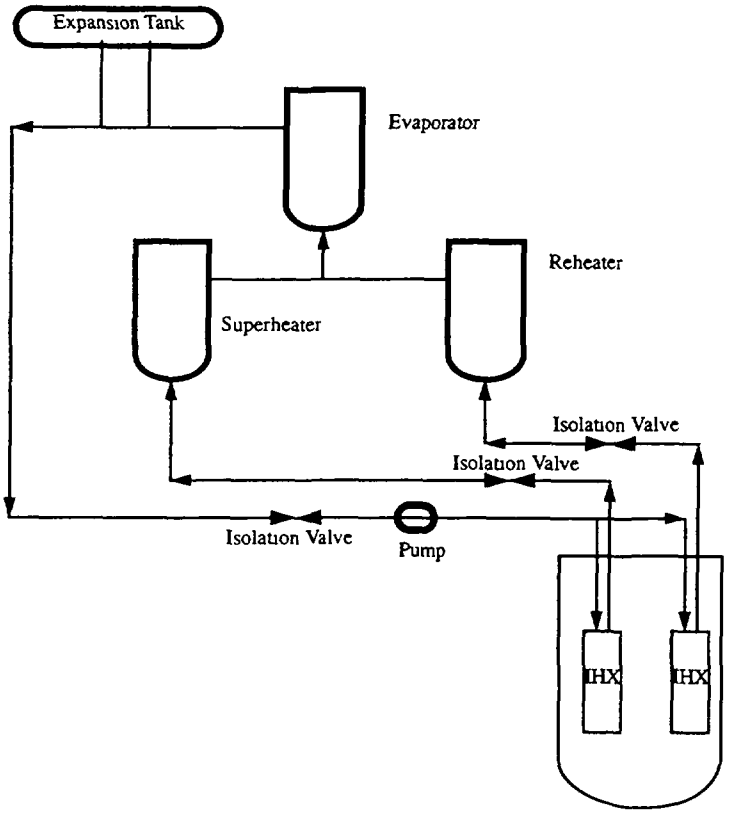

Figure 1 PFR Secondary Sodium Circuit

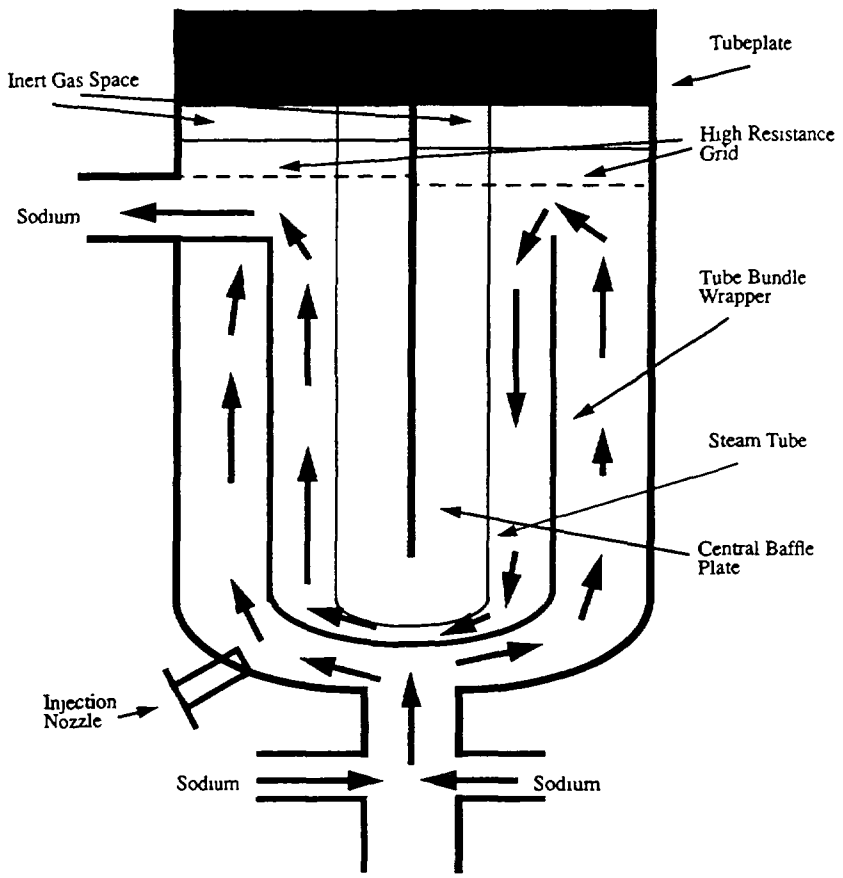

Figure 2
Main Design Features of an Evaporator

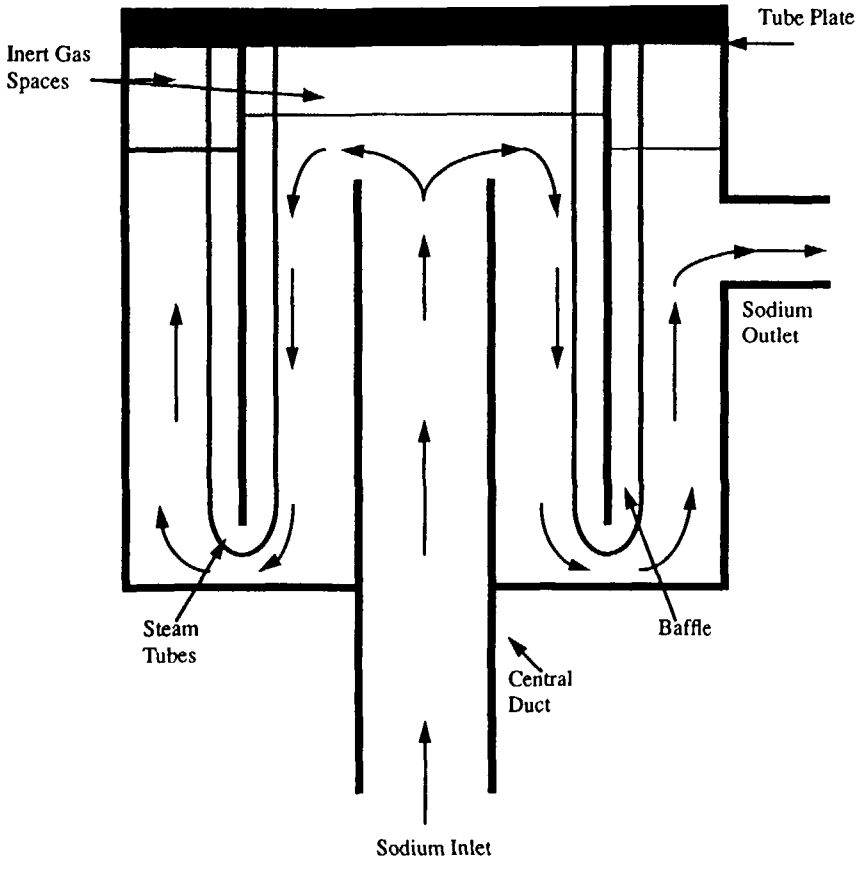

Figure 3
Main Design Features of a Superheater

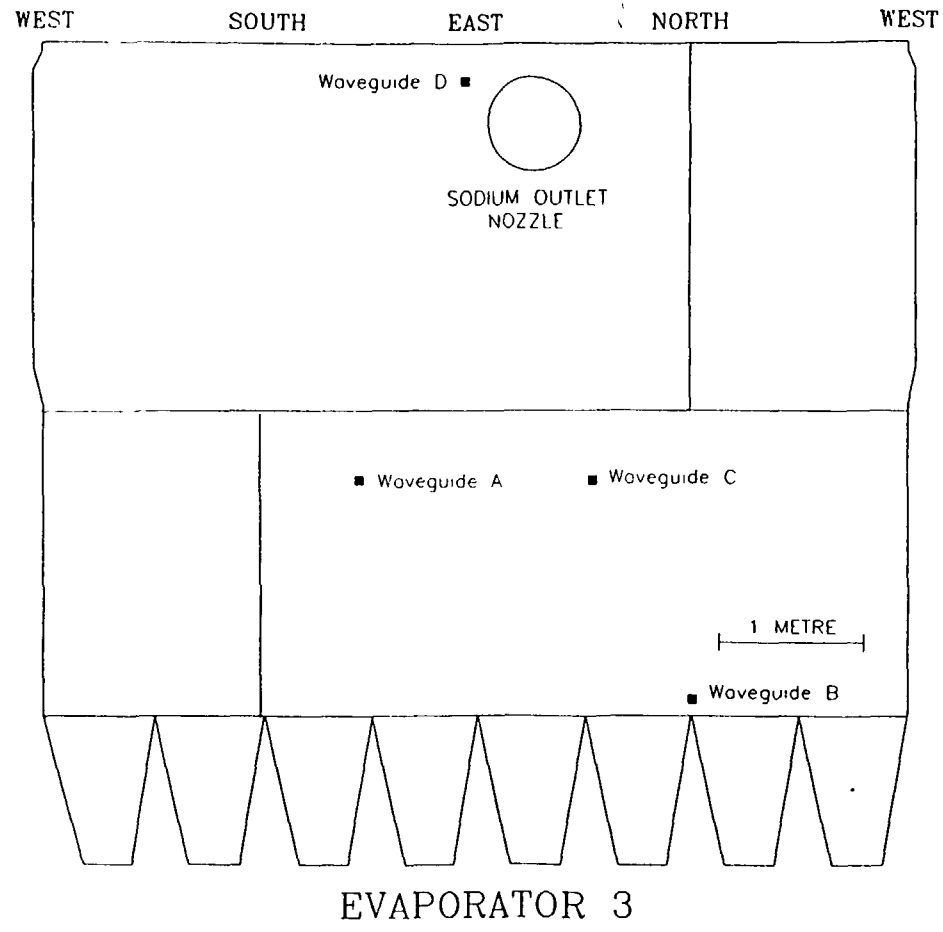

Figure 4
Location of Waveguides/Transducers on Evaporator 3 used for the IAEA Benchmark

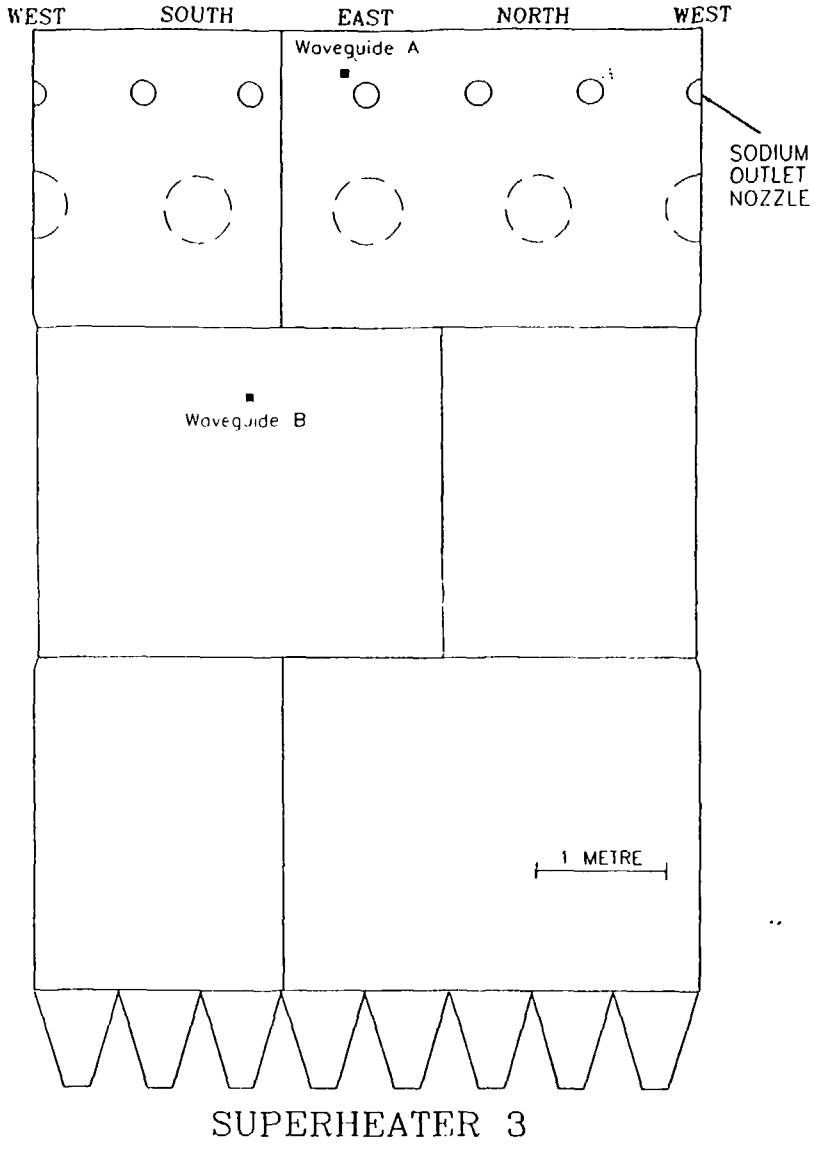

Figure 5
Location of Waveguides/Transducers on Superheater 3 used for the IAEA Benchmark

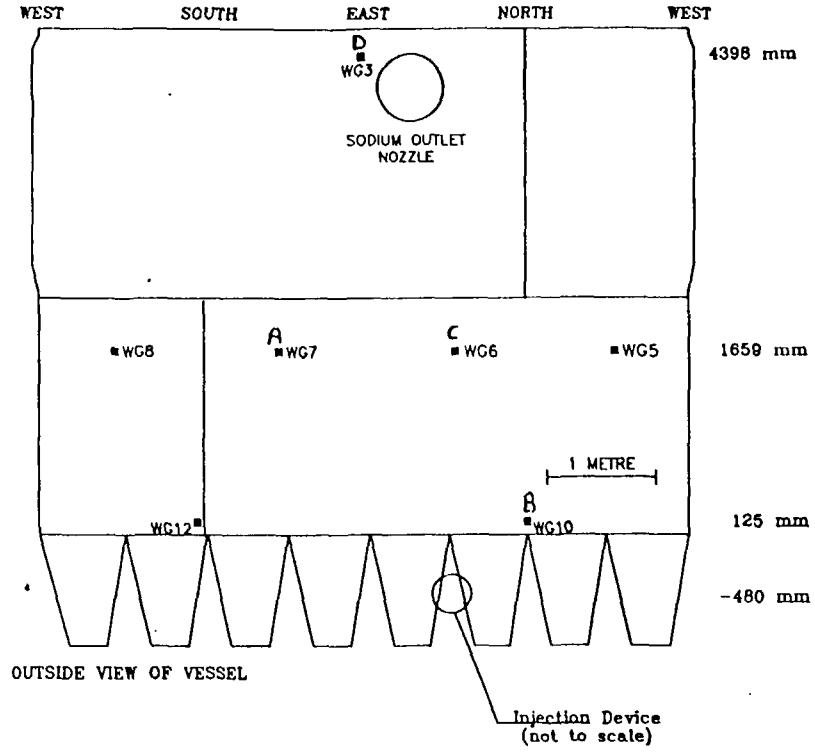

Figure 6 Schematic of Evaporator 3 showing the positions of the waveguides and the injection device

hydrogen injections during the commissioning of PFR, is shown in Figure 2. During the commissioning experiments, injections of steam were not allowed and the injections of hydrogen were only into the flowing sodium interspace between the tube bundle wrapper and the shell. In order to perform injections directly into the tube bundle region, a technique to cut a hole in the tube bundle wrapper, 12.7 mm wall thickness, was developed. This allowed an injection device containing 9 tubes which terminated in the interspace and 9 tubes which terminated in the tube bundle to be installed. This injection device is shown in Figure 7. The injection tubes were each 2.26 mm in diameter. Three tubes in each location had 0.5 mm nozzles, three tubes in each location had 1.0 mm nozzles and three tubes in each location had 2.26 mm nozzles at the end terminating in the evaporator. These nozzles were protected by bursting discs to prevent sodium entering the injection lines. In Figure 8, the location of the injection device and of the transducers are given in a 3-D coordinate system. These positions are summarised in Table 1. The position of the injection device shown in Figure 8 and Table 1, is the point at which the tubes penetrated the inner wall of the shell. The injection tubes were inclined at an angle of 30^0, with the 9 tubes terminating in the interspace being very close to the shell wall and the 9 tubes terminating in the tube bundle being just inside of the inner wall of the tube bundle wrapper. The distance from the point at which the injection tubes penetrated the inside wall of the shell and the inside wall of the tube bundle wrapper was 223.7 mm. For completeness, the wall thickness of the shell was 48mm.

The injection fluids were supplied to the injection lines in the injection device using an injection system previously used for sodium-water reaction injections in rigs. A flow diagram of the injection system is shown in Figure 9. Six injection lines at a time were connected to the injection system which was capable of selecting a line and injecting gas or water at a controlled pressure for a controlled period followed by an automatic low pressure argon purge to maintain the line open after the injection period. In this way several injections were achieved through each injection line. The injection system was originally designed to inject water from the water bottle into sodium, using a high pressure driving gas. Injections of argon and hydrogen were performed with the water bottle empty of water and using the appropriate high pressure driving gas (argon or hydrogen). During argon and hydrogen injections, the injection rate was derived from the pressure drop between two pressure transducers in the injection line and for water injections, the injection rate was measured by an ultrasonic level meter measuring the residual mass of water in the injection bottle.

Acoustic background noise measurements at various plant operating conditions had shown that at high sodium pump speeds with the steamside of the steam generators pressurised by low pressure argon, the situation during these injections, considerable tube vibration occurs and the acoustic noise is high and very impulsive and not representative of full power conditions. It was therefore decided to perform these injections at a sodium pump speed below the threshold for significant tube vibration. A value of 300 RPM compared to the full power value of 900 RPM was used. At this pump speed, the background noise was in the range of 10 - 20 mg RMS , compared to about 60 mg RMS at full power.

Approximately half of the injections were performed at a sodium temperature of 300 ^{o}C and half at 350 ^{o}C.

The experimental procedure was to rupture the bursting disc on a line and then to perform a series of injections of different fluids through that line, with a low pressure argon purge between each injection. Background noise was recorded for a period prior to the start of each injection.

It was observed that in the case of argon injections, the acoustic noise after an injection took several minutes to return to the pre-injection value, whereas in the case of steam and

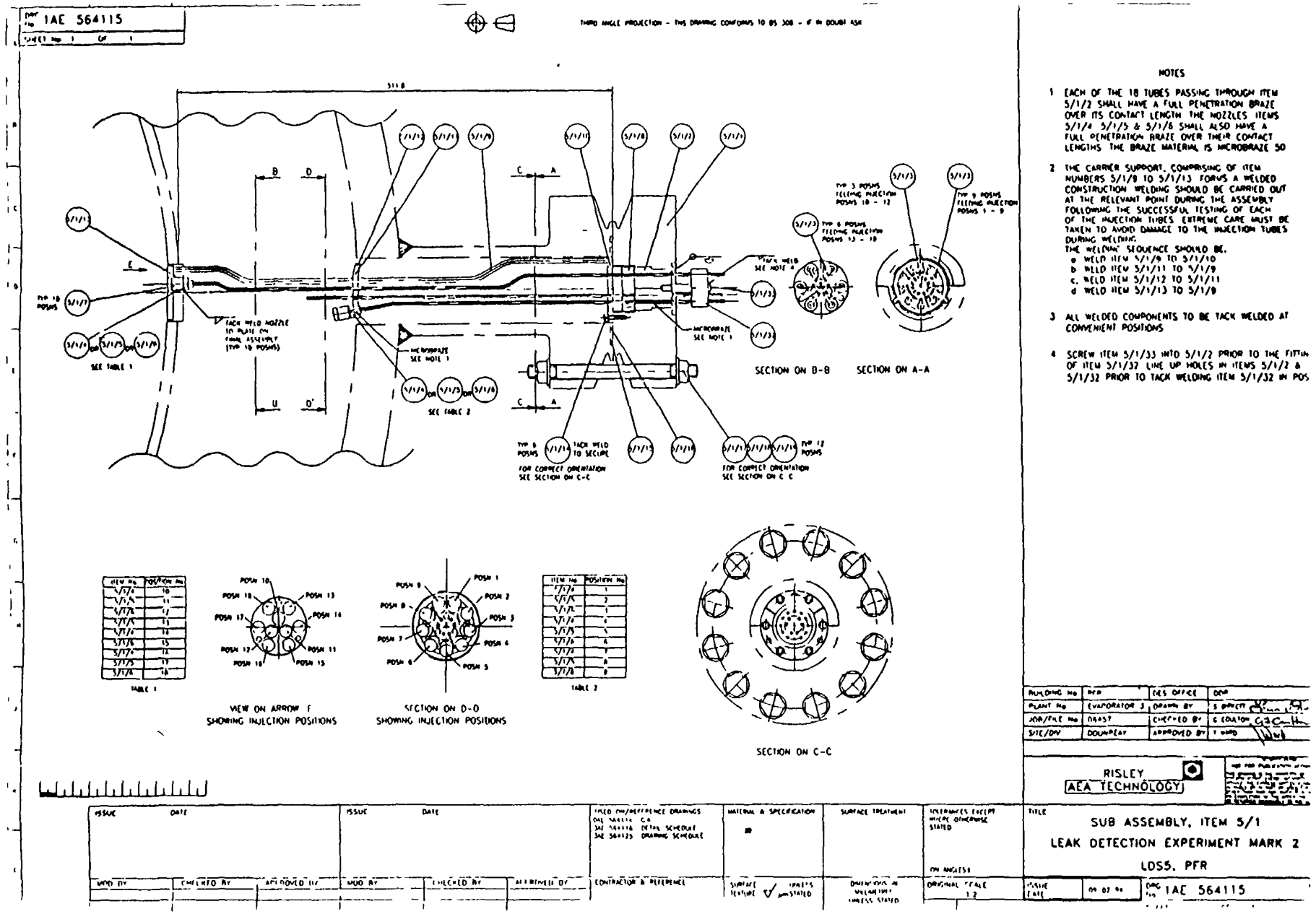

Figure 7 Second Injection Device (Installed April/May 1994)

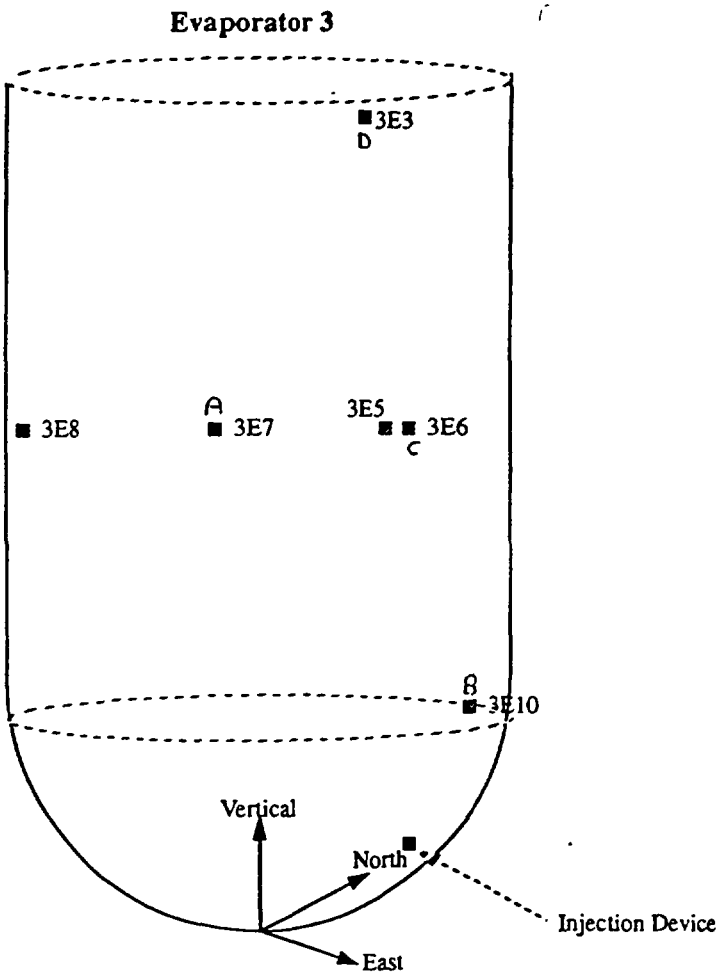

Figure 8 Three Dimensional Co-ordinate system (not to scale)

Table 1

POSITION OF WAVEGUIDES AND INJECTION DEVICE

Item	East (mm)	North (mm)	Vertical (mm)
Waveguide D	957.0	-63.0	5357.0
Waveguide C	634.0	720.0	2618.0
Waveguide A	632.0	-721.0	2618.0
Waveguide B	1.0	959.0	1084.0
Injection Device	588.0	588.0	479.0

hydrogen injections the noise returned to normal almost immediately. This was taken into consideration when selecting argon injections for the Benchmark, to ensure that the pre-leak background noise was not strongly influenced by the impulsive noise generated by undissolved gas bubbles.

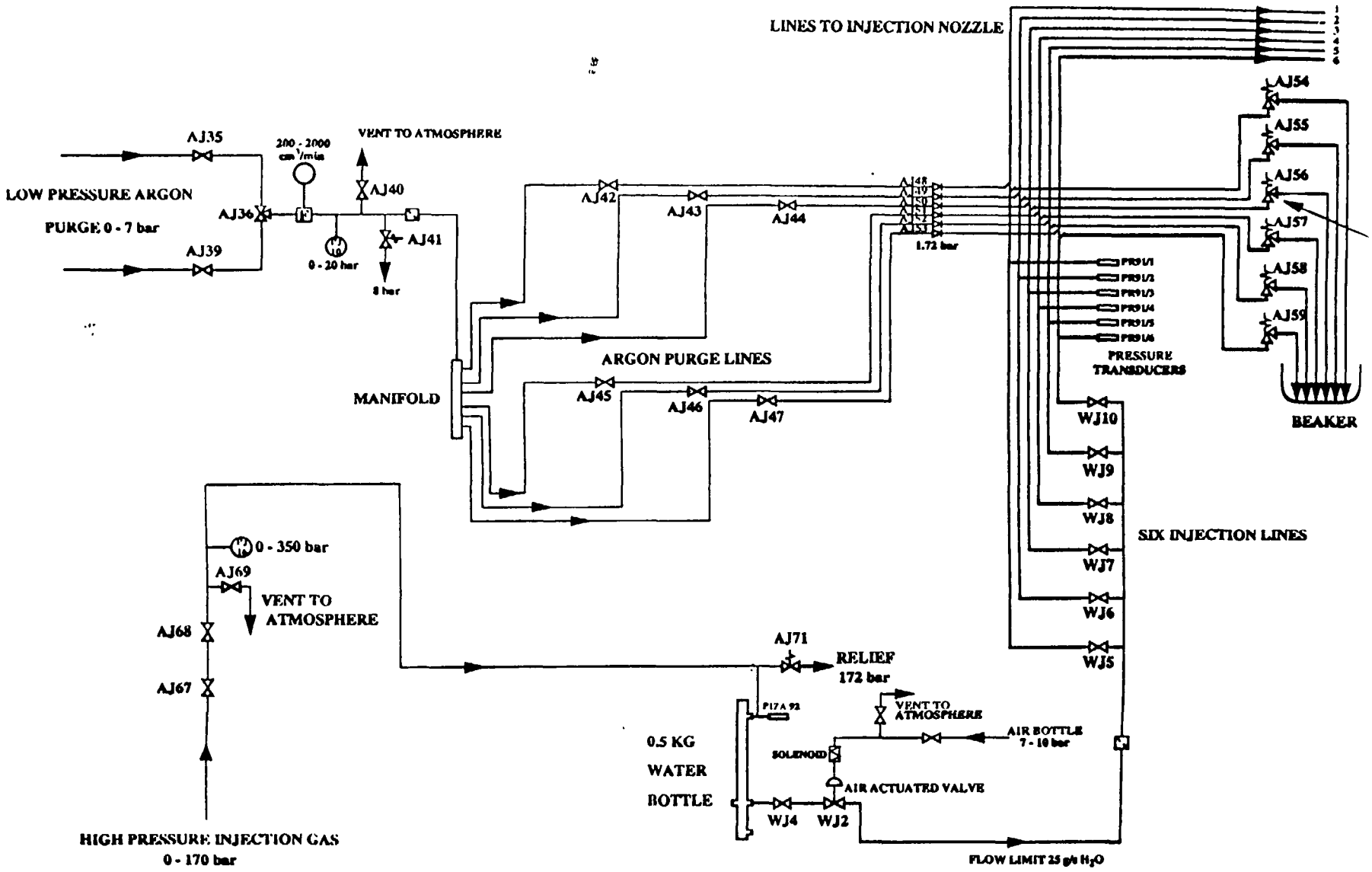

FIGURE 9: DIAGRAM OF FLOW PATHS IN LDS5 INJECTION SYSTEM

DIGITISATION OF THE ACOUSTIC DATA FOR THE BENCHMARK TEST CASES

To allow leak location to be attempted, it was important that the acoustic data from the four transducers was digitised synchronously. With the limitations of the equipment available, this could only be achieved by digitising the data in pairs, with each pair having one common transducer.

The problems associated with handling very large data files were recognised and it was decided to use two digitisation rates: a low sampling rate which could be used for FFT purposes and a high sampling rate for time delay measurements and signal visualisation. Therefore for each injection there are three pairs of digitised data at each sampling rate.

The low sampling rate was 160,000 samples per second per channel, with the signals being filtered via a low-pass filter set at 72 kHz. The high sampling rate was 2,000,000 samples per second per channel, with the signals being filtered via a low-pass filter set at 71.68 kHz

In order to ease the problems of distributing the very large quantity of data resulting from this exercise to the participants, the data was recorded onto CDs. This enabled all participants to obtain data at both sampling rates for all transducers and all injections and to select which data they required for their own particular analysis techniques.

A README file was included on each CD giving details of the digitisation technique and the nature of the data files.

The signals were replayed from the tape recordings and were digitised two channels (the signals from two transducers) at a time, using the two inputs of an LSI DSP32-C Digital Signal Processing Card installed in a PC. The resultant data from one digitisation run was stored in a single data file. This data file was then processed to produce a resultant data file where,

- the data values are stored in two-byte integer binary form (least significant byte first)
- the first two bytes are the first value from channel A, the next two bytes are the first value from channel B, the next two bytes are the second value for channel A, and so on
- the data values are normalised (for amplifier gain) and are in integer units, where one unit is equal to 0.1 mg (i.e. 0.0001 g, where g is the acceleration due to gravity)

The data files were named:

TTPPD.DAT

where:

TT	represents the experiment type	
	BE	Evaporator background
	BS	Superheater background
	I1 to I8	An injection (numbered 1 to 8) into the Evaporator
PP	represents the waveguide pair - See Figures 4 and 5	
	P1	Waveguides A and B
	P2	Waveguides C and B
	P3	Waveguides D and B
D	represents the digitisation speed	
	L	Low speed digitisation
	H	High speed digitisation
	.DAT	signifies a data file.

For example, the data file BEP1H.DAT contains data for evaporator full power background from waveguides A and B, digitised at the high speed.

The data was recorded onto a set of 5 CDs for each participant. The data recorded on each Volume was as follows:

Volume 1:	BEP1H.DAT, BEP1L.DAT, BSP1H.DAT, BSP1L.DAT
Volume 2:	I1P1H.DAT, I1P2H.DAT, I1P3H.DAT, I1P1L.DAT, I1P2L.DAT, I1P3L.DAT, I2P1H.DAT, I2P2H.DAT, I2P3H.DAT, I2P1L.DAT, I2P2L.DAT, I2P3L.DAT
Volume 3:	I3P1H.DAT, I3P2H.DAT, I3P3H.DAT, I3P1L.DAT, I3P2L.DAT, I3P3L.DAT, I4P1H.DAT, I4P2H.DAT, I4P3H.DAT, I4P1L.DAT, I4P2L.DAT, I4P3L.DAT
Volume 4:	I5P1H.DAT, I5P2H.DAT, I5P3H.DAT, I5P1L.DAT, I5P2L.DAT, I5P3L.DAT, I6P1H.DAT, I6P2H.DAT, I6P3H.DAT, I6P1L.DAT, I6P2L.DAT, I6P3L.DAT
Volume 5:	I7P1H.DAT, I7P2H.DAT, I7P3H.DAT, I7P1L.DAT, I7P2L.DAT, I7P3L.DAT, I8P1H.DAT, I8P2H.DAT, I8P3H.DAT, I8P1L.DAT, I8P2L.DAT, I8P3L.DAT

It should be noted that the data on Waveguide C during Injection 2, i.e. the data from Channel A in P2 from injection 2 (I2P2H.DAT and I2P2L.DAT), is distorted and overloaded. This was the case on the MASTER tape recording and was ascribed to a temporary instrument fault on the plant. This fault rectified itself, without operator intervention. This data has been included in the Benchmark because a leak detection system on an operating plant will experience similar faults during its operation and trip algorithms will require to be able to discriminate between such data and "real" signals. It is however recognised that an instrument fault simultaneous with a real leak event should be a low probability event.

INJECTION DATA INCLUDED IN THE 1995 BENCHMARK TEST CASES

The injections included in the 1995 Benchmark Test Cases are summarised in Table 2.

For each injection, the data was digitised for a duration of 10s, encompassing some length of time before the opening of the injection valve. Also for each injection, 6 pairs of digitised data were produced, as described earlier. Although the data for each pair is synchronised, the pairs are not precisely synchronised for each injection, although the digitisation was attempted to be commenced at nominally the same time for each. The start time of the injection in each pair of data for each injection is given in Table 3. In each case, the actual injection proceeded beyond the end of the digitisation period. Therefore the injection duration in the test cases is 10 s minus the start time, for each data pair. As can be seen from Table 3, the length of background signal preceding the injection was in the range of 1.78s to 4.64s, so that injection durations are in the range of 5.36s to 8.22s.

It should be noted that in the case of water/steam injections, there is an initial period, of approximately 1s during which the injection line between the valve and the nozzle is filling with water. During this period, there is a flow of argon through the nozzle and a high flowrate of water/steam inside the line. The acoustic noise during this period will not necessarily be representative of that during the initiation of a real leak in a steam generator.

Table 2

SUMMARY OF INJECTIONS

Injection No	Fluid	Pressure (bars)	Nozzle (mm)	Sodium Temperature (^oC)	Location	Injection Rate (gs^{-1})
1	H_2	10	0.5	298	Bundle	0.05
2	Ar	10	1.0+	346	Bundle	0.27
3	H_2O	10	0.5	301	Bundle	3.4
4	Ar	10	1.0	299	Interspace	0.5
5	H_2	170	2.26	324	Interspace	1.3
6	H_2O	24	2.26	344	Bundle	7.65
7	Ar	100	0.5	298	Bundle	2.4
8	H_2O	10	0.5	299	Interspace	2.2

+ Indicates that an additional flow restricting valve was used

Table 3

INJECTION START TIMES FOR EACH DATA PAIR

Injection No	P1H (s)	P1L (s)	P2H (s)	P2L (s)	P3H (s)	P3L (s)
1	1.96	2.0	1.96	1.96	1.96	1.98
2	3.14	3.15	3.14	3.15	3.13	3.20
3	1.79	1.81	1.78	1.83	1.78	1.84
4	4.46	4.64	4.46	4.47	4.46	4.50
5	2.75	2.73	2.75	2.79	2.75	2.78
6	2.40	2.41	2.40	2.42	2.40	2.43
7	3.25	3.30	3.25	3.23	3.25	3.26
8	3.67	3.69	3.68	3.66	3.68	3.71

FULL POWER BACKGROUND NOISE DATA INCLUDED IN 1995 BENCHMARK

A 25s sample of full power background noise data from Waveguides A and B, Figures 4 and 5, for each of the evaporator and superheater was included at both digitisation rates in the Benchmark data. These measurements were made at full power conditions on 16 January 1994

of 634 MWth, with a sodium pump speed of 894 RPM. These data are considered to be typical of the normal PFR background in these units. It should be noted that in the Evaporator, water is boiled and a 20% steam/water mixture is produced. In the case of the Superheater, there is no boiling. There are also differences in the sodium flow paths (Figures 2 and 3) and in the sodium flowrates through the units (approximately 1000 kgs^{-1} through the Evaporator, approximately 700 kgs^{-1} through the Superheater). It has been observed that although the main characteristics of the full power background noise in both units are essentially invariant with time, impulsive events can occur at some locations. For example, impulsive events have been recorded at various power levels, including full power, on Waveguide A in the Evaporator. It has also been observed that the general magnitude of the background noise at full power in the Evaporator is greater at the top of the unit than at the bottom.

COMPARISON OF DATA FROM BENCHMARK INJECTIONS WITH OTHER INJECTIONS

It is instructive to compare the data from the injections selected for the 1995 Benchmark with the data from the other injections in the series, to determine how representative the selected injections are and to observe trends in the overall data. AEA Technology performed detailed analysis of a selection of injections of each fluid in each location, covering the full range of injection rates. The injections selected for the IAEA 1995 Benchmark were chosen from the list of injections which were subjected to detailed analysis.

The data from the injections of Argon into the Tube Bundle are summarised in Table 4 and into the Sodium Interspace in Table 5. The data from Water/Steam injections are summarised in Tables 6 and 7, Tube Bundle and Sodium Interspace respectively and the Hydrogen injections are summarised in Table 8.

In Tables 4 - 8, the average RMS signals in the low frequency range (0 - 6.4 kHz) and over the full frequency range (0 - 100 kHz) are given for each injection. These values have been computed taking the pre-injection average background RMS in these frequency ranges into account. The equation used was:

$$\text{Leak Signal RMS} = \text{SQRT}[(\text{Injection RMS})^2 - (\text{Background RMS})^2]$$

The detailed analysis of the data used a different set of waveguides than used for the Benchmark exercise. Therefore comparisons are only given for Waveguides B, C and D, which were common to both.

The injections included in the Benchmark are highlighted. It can be seen that their characteristics are similar to the other injections of that fluid, in that location, at similar injection rates.

It should be noted that the 29.3 gs^{-1} injection of Water/Steam into the Sodium Interspace (Table 7) produced significant impulsive noise which caused an overload on the low frequency measurements.

Examination of the data in Tables 4 - 8, gives an insight into the power of the signal in the low and high frequency range for each fluid and each location and also on the transmission of the signal in the different frequency bands. By normalising the injection rates in terms of volumetric flowrate, by multiplying the Argon injection rates by 0.45, it is also possible to directly compare Argon with Steam/Water to determine the applicability of Argon for calibrating detection systems.

It can be seen that, as expected, more powerful signals were recorded during injections in the sodium interspace than in the tube bundle.

It can also be seen, that for all injection fluids, in both locations, the leak signal initially increases with leak rate, but quickly reaches a plateau value, resulting in the signals from a 15 gs^{-1} steam leak not being much different in terms of average RMS from that of a 5 gs^{-1} leak. Average RMS leak signal values for leaks of 1 gs^{-1} into the Tube Bundle are of the order of 10 - 20% of the normal, full power RMS in PFR evaporators and superheaters. In the case of leaks into the Sodium Interspace, even higher leak signals are observed, in the range of 30 - 50% of the normal background.

The dominant acoustic transmission path in the case of injections into the sodium interspace would be expected to be through sodium to the shell and through/along the shell to the waveguides and hence to the transducers. Waveguide B is closest to the point of injection and Waveguide D, near the sodium outlet at the top of the unit, is furthest from the point of injection. As expected for injections into this location, in general, higher signals were recorded at Waveguide B than at Waveguide D, for all injection fluids. Similarly, signals recorded at Waveguide C were generally higher than those at Waveguide D. However, in some cases, the signals recorded at Waveguide C were higher than those recorded at Waveguide B.

Table 4

ARGON INJECTIONS INTO TUBE BUNDLE - RMS SIGNALS IN mg

Injection Rate (gs^{-1})	Waveguide B		Waveguide C		Waveguide D	
	0 - 6.4 kHz	0 - 100 kHz	0 - 6.4 kHz	0 - 100 kHz	0 - 6.4 kHz	0 - 100 kHz
0.25	4.42	5.28	6.46	6.32	0.00	4.55
0.25	7.05	7.91	8.40	8.67	3.77	7.39
0.27	1.49	3.81	0.11	0.00	2.26	4.15
0.32	4.08	5.33	0.01	0.01	0.00	5.44
0.45	10.62	6.90	8.22	6.84	1.25	2.94
0.75	8.85	18.65	8.16	7.80	3.13	6.52
0.86	5.99	7.91	0.11	0.72	4.03	11.72
1.3	10.26	29.19	12.38	14.44	3.96	9.29
2.0	3.58	61.43	12.61	24.27	5.22	15.55
2.4	14.03	20.72	19.69	20.59	6.56	10.84
3.3	14.65	17.95	19.97	19.12	6.13	9.72
4.0	12.98	62.15	16.13	22.90	6.76	14.96
4.1	14.07	17.37	20.13	21.24	5.27	6.82
5.5	11.87	90.22	18.78	31.80	3.88	14.31
6.6	15.12	94.06	22.35	31.98	6.95	18.99

Table 5

ARGON INJECTIONS INTO SODIUM INTERSPACE - RMS SIGNALS IN mg

Injection Rate (gs^{-1})	Waveguide B		Waveguide C		Waveguide D	
	0 - 6.4 kHz	0 - 100 kHz	0 - 6.4 kHz	0 - 100 kHz	0 - 6.4 kHz	0 - 100 kHz
0.24	8.02	14.68	9.34	11.61	5.85	8.65
0.24	2.98	3.26	3.20	4.49	3.32	4.95
0.25	5.68	12.99	7.48	4.02	7.07	8.75
0.36	4.71	9.24	10.47	9.75	8.61	10.52
0.5	9.56	13.66	11.63	10.13	6.81	11.52
0.6	2.13	9.10	7.71	7.05	7.03	10.11
0.8	2.86	0.00	3.69	5.37	0.00	0.00
1.3	25.66	35.66	43.55	42.10	1.69	15.44
2.0	25.94	34.42	34.11	33.13	10.01	17.06
2.3	18.27	41.01	21.55	24.13	9.34	17.74
4.7	59.20	59.99	102.2	112.8	22.36	24.89
6.3	73.21	77.21	125.7	117.5	26.70	29.63

Table 6

WATER/STEAM INJECTIONS INTO TUBE BUNDLE - RMS SIGNALS IN mg

Injection Rate (gs^{-1})	Waveguide B		Waveguide C		Waveguide D	
	0 - 6.4 kHz	0 - 100 kHz	0 - 6.4 kHz	0 - 100 kHz	0 - 6.4 kHz	0 - 100 kHz
0.21	5.03	3.62	1.64	6.50	1.21	1.64
0.6	0.00	14.84	0.00	1.73	0.28	2.29
1.06	0.00	13.85	5.13	3.37	0.00	7.86
1.52	4.43	5.62	10.78	9.25	3.21	11.09
3.4	17.43	16.66	25.46	21.91	9.29	14.68
7.65	26.50	30.52	29.77	29.55	10.97	24.25
13.1	24.71	22.15	34.57	32.37	13.30	23.28
28.5	31.61	57.55	39.59	34.29	19.45	31.73

Table 7

WATER/STEAM INJECTIONS INTO SODIUM INTERSPACE - RMS SIGNALS IN mg

Injection Rate (gs^{-1})	Waveguide B		Waveguide C		Waveguide D	
	0 - 6.4 kHz	0 - 100 kHz	0 - 6.4 kHz	0 - 100 kHz	0 - 6.4 kHz	0 - 100 kHz
0.22	3.41	11.34	3.00	10.54	0.43	11.89
0.41	0.00	3.50	0.00	8.33	3.67	3.68
0.83	11.97	25.19	18.03	33.52	8.00	21.19
2.2	29.04	30.96	42.92	46.06	14.08	25.37
4.5	41.23	43.02	46.96	52.44	19.98	40.64
7.15	87.38	65.13	45.40	58.53	0.00	42.55
13.4	37.62	31.53	57.95	50.47	18.89	34.65
29.3	5852.8	30.28	228.8	124.9	322.5	111.8

Table 8

HYDROGEN INJECTIONS - RMS SIGNALS IN mg

Injection Rate (gs^{-1})	Waveguide B		Waveguide C		Waveguide D	
	0 - 6.4 kHz	0 - 100 kHz	0 - 6.4 kHz	0 - 100 kHz	0 - 6.4 kHz	0 - 100 kHz
0.04[a]	21.98	37.77	26.43	26.51	14.48	29.79
0.05[b]	0.00	2.54	0.00	0.00	1.01	0.00
1.3[c]	83.41	88.85	104.5	102.4	36.75	55.26

a. Injection into Sodium Interspace
b. Injection into Tube Bundle
c. Injection into Sodium Interspace

In terms of frequency components, the signals recorded during steam injections in the Sodium Interspace at Waveguide D were predominantly high frequency, whilst at Waveguides B and C, low frequencies dominated for injection rates less than about 1 gs^{-1}, with high frequencies dominating at the higher injection rates. In the case of Argon injections, high frequencies predominated at Waveguide B, low frequencies at Waveguide C and although low frequencies dominated at Waveguide D, high frequency components were important during some injections.

The acoustic transmission path for injections into the tube bundle would be through sodium to the wrapper, then either through the wrapper to sodium to the shell and hence the

waveguides or along the wrapper to the tube plate and then to the shell and hence to the waveguides. In reality, both of these transmission paths would contribute to the received signals.

During argon injections into the tube bundle, the received signals at Waveguide D, furthest from the injection point, were predominantly in the high frequency range. At Waveguide B, closest to the injection point, there was a significant low frequency component up to an injection rate of 0.75 gs^{-1} (0.34 gs^{-1} steam equivalent). At Waveguide C, this transition from low frequency to high frequency was not so pronounced. In fact, there was little attenuation in low frequency signals between Waveguides B and C, but there was a significant reduction in the high frequency power of the signals. Therefore the transmission paths were such that high frequency components reached Waveguides B and D, but only low frequency components reached Waveguide C.

During steam/water injections into the tube bundle, low frequencies generally dominated at Waveguides B and C, whilst high frequencies dominated at Waveguide D.

The dominant frequency band of the signals recorded on each waveguide for each injection fluid and each injection location is summarised in Table 9. In this Table, "Low" indicates that the average RMS in the 0 - 6.4 kHz range was similar to that over the entire 0 - 100 kHz, indicating that the power was concentrated in this low frequency range, whilst "High" indicates that the average RMS in the 0 - 100 kHz range was much higher than that in the 0 - 6.4 kHz range, indicating that the power was concentrated above 6.4 kHz.

The interpretation of the results above is complicated by the fact that the nature of the source signal and the exact transmission path to each waveguide are not known. One approach is to examine if the results are consistent with commonly held theories about the source signal produced by a leak and the attenuation caused by the various possible fluid and steel interfaces/ transmission paths.

Two of the significant sound sources are the jet decompression noise, which is broad band in nature and the noise caused by bubbles being born, oscillating and collapsing, generally low frequency. In addition to being a source of noise, bubbles can attenuate acoustic signals. This latter effect may explain the observation that the signals tend to reach a plateau

Table 9

SUMMARY OF DOMINANT FREQUENCY BAND

Leak Location	Tube Bundle			Sodium Interspace		
Waveguide	B	C	D	B	C	D
Steam						
Small Rates	Low	Low	High	Low	Low	High
Large Rates	Low	Low	High	High	High	High
Argon						
Small Rates	Low	Low	High	High	Low	Low
Large Rates	High	Low	High	High	Low	Low
Hydrogen	High		Low	Low	Low	High

value as the injection rate increases. As the injection rate increases, the gas bubble volume local to the leak position will increase and hence could prevent the larger jet noise at the source from being propagated to the waveguides.

It is generally accepted that significant attenuation occurs, particularly in the higher frequency range, when an acoustic signal travels from liquid to steel and then to liquid. It is also generally accepted that, particularly in the higher frequency range, the attenuation of a signal transmitted along the structure of the steam generator is less that one which experiences several sodium-to-steel interfaces.

The effect of leak location in the case of steam injections appears to be that the presence of the tube bundle wrapper suppresses the high frequency components observed at Waveguides B and C during the higher injection rates in the Sodium Interspace from being observed during injections into the tube bundle. This is consistent with expectation if it is assumed that the transmission path to these two waveguides for a leak in the Tube Bundle is sodium-to-Wrapper -to-sodium-to the shell. There is little effect on the signals observed at Waveguide D in terms of frequency component, which suggests that the transmission path may be different in this case, perhaps involving a more important contribution from transmission along the Wrapper itself.

The effect of leak location in the case of argon injections is most pronounced at Waveguide D, furthest from the leak position, with high frequencies dominating for leaks in the tube bundle and low frequencies dominating for leaks in the Sodium Interspace. In the case of argon injections, the gas bubbles do not dissolve [hydrogen bubbles generated by a steam leak rapidly dissolve]. If the transmission path from a leak inside the tube bundle to this waveguide is to the Wrapper and then to the shell via the Tubeplate, the high frequency component generated by the jet may be received at this location. The high frequency signals observed at this waveguide during steam injections inside the tube bundle are consistent with this model. If it is assumed that the transmission path to Waveguide D during a leak in the Sodium Interspace is through sodium to the shell in the vicinity of the waveguide, then the presence of undissolved gas bubbles would attenuate the high frequencies, as observed. In the case of steam injections in the Sodium Interspace, the bubbles would dissolve and would be less effective in attenuating high frequencies, as observed during these injections. Additionally, argon gas bubbles would be expected to produce more low frequency noise over a significant length of the flow path, compared to the quickly dissolving hydrogen bubbles. This would again favour low frequencies predominating the signals reaching Waveguide D during argon leaks in the Sodium Interspace.

On the basis of these results, it would appear that the dominant transmission paths are as summarised in Table 10. The most interesting observation is that the dominant transmission path to Waveguide D, the furthest away from the leak location, during injections into the Tube Bundle is in the structure of the steam generator. This has the effect of reducing the effect of undissolved bubbles in the sodium on the received signal compared to all of the other cases.

Comparing Argon with Steam, it can be seen that the agreement depends on the location of the leak, the location of the transducer and the frequency band considered. Agreement for leaks in the Sodium Interspace of wideband signals recorded at Waveguide D is excellent (Figure 10), reducing to good when considering low frequencies only, because although the argon signal is low frequency, a significant high frequency component exists in the steam signal. However, agreement is poor for injections into the tube bundle for wideband signals recorded at Waveguide B (Figure 11), improving to reasonable when considering only low frequencies due to the removal of the significant high frequency component in the argon signals.

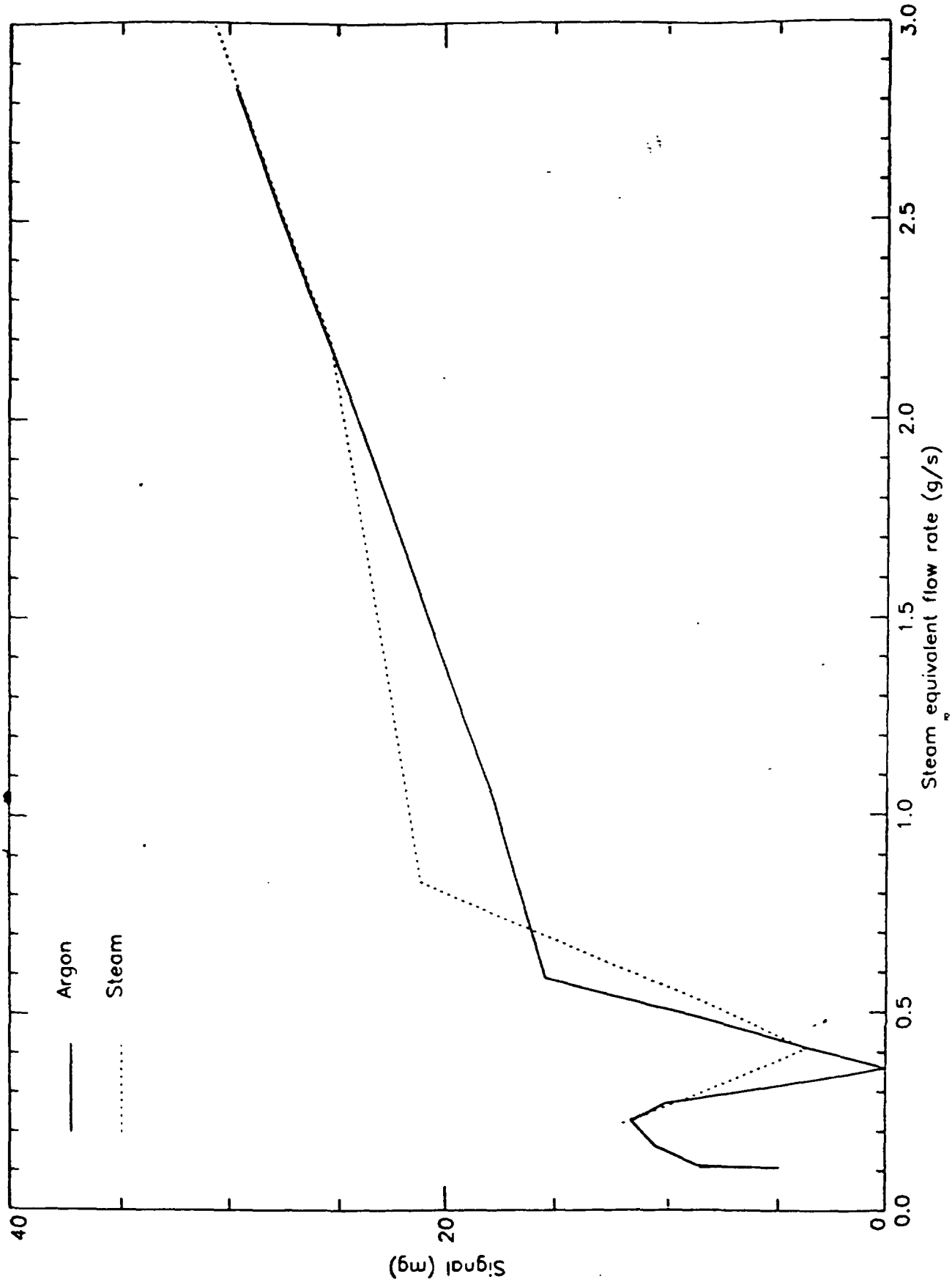

Figure 10
Comparison between Argon and Steam Injections into Sodium Interspace
Average RMS leak signals recorded at Waveguide D : 0 to 100 kHz

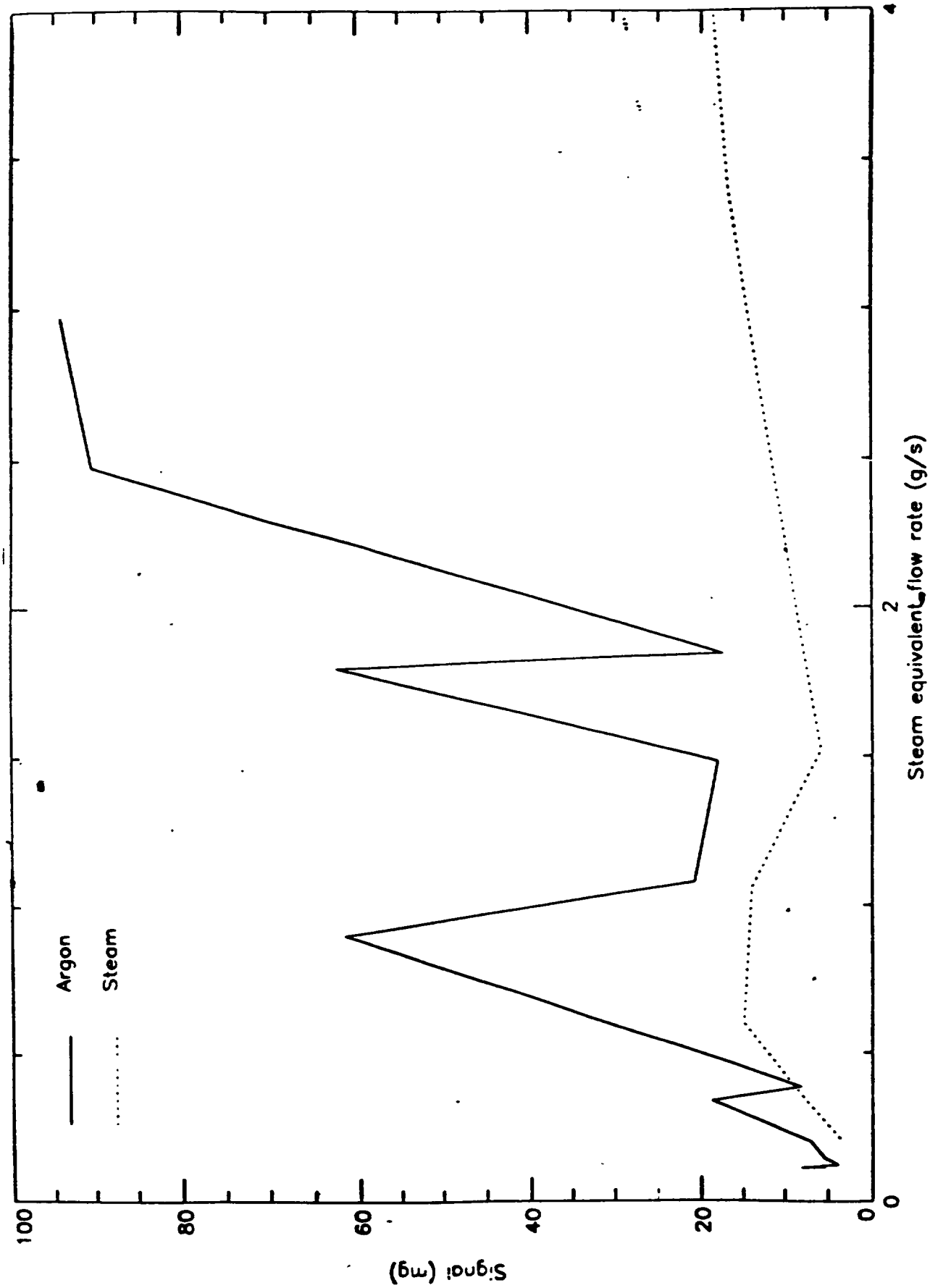

Figure 11
Comparison between Argon and Steam Injections into Tube Bundle
Average RMS leak signals recorded at Waveguide B: 0 to 100 kHz

Table 10

DOMINANT TRANSMISSION PATH

Leak Location	Waveguide		
	B	C	D
Tube Bundle	Sodium **Through Wrapper** Sodium Shell Waveguide	**Sodium** **Through Wrapper** Sodium Shell Waveguide	Sodium **Along Wrapper** **Tubeplate** Shell Waveguide
Sodium Interspace	**Sodium** Shell Waveguide	**Sodium** Shell Waveguide	**Sodium** Shell Waveguide

Note: The media shown in **bold** are the most important in determining the characteristics of the signals received at the waveguides.

It can therefore be seen that care must be exercised when using Argon to simulate steam leaks to calibrate a leak detection system. The differences can probably be explained on the basis of the difference in behaviour of argon and hydrogen bubbles. Hydrogen bubbles rapidly dissolve in the sodium, whilst argon bubbles are essentially insoluble. Undissolved bubbles in the sodium will attenuate the acoustic noise transmitted through the sodium, but will not affect the part of the signal being transmitted through steel.

CONCLUSIONS

The injection fluids, locations, rates and start times have been presented for the test cases included in the 1995 Benchmark.

It has been demonstrated that the selected injection data are consistent with the rest of the data recorded during the series of experiments in PFR.

Some trends in the signals recorded during the PFR experiments have been presented. In particular it has been shown that the leak signals increase initially with leak rate but quickly reach a plateau and that there are differences in the nature of the signals generated by steam and argon leaks, in terms of frequency components. The plateauing tendency of the signals means that detection of 15 gs^{-1} leaks would not be significantly easier than detection of 5 gs^{-1} leaks, using systems based on RMS . However, the strong RMS leak signals measured during leaks of steam of about 1 gs^{-1} into the tube bundle are encouraging from the leak detection point of view. The fact that argon bubbles do not dissolve in sodium, whilst hydrogen bubbles rapidly dissolve is probably significant in explaining the observed differences between the signals recorded during argon and steam injections.

A COMPARISON OF SOME GENERIC STRATEGIES FOR FAULT DETECTION IN LIQUID METAL FAST BREEDER REACTORS

S.E.F. ROFE, T.J. LEDWIDGE
University of Southern Queensland,
Mooloolaba, Queensland,
Australia

Abstract

Data from the 1994 and 1995 bench mark tests were used to compare the performance of seven different signal processing strategies proposed for the detection of boiling or a sodium/water reaction in LMFBR The general signal processing strategy relies on the signals from the normal background noise and the fault being additive, which gives rise to changes in the signal model in the time, frequency or probability domain Two of the specific signal processing strategies are derived from an autoregressive model of the process, whilst the rest are implemented in the frequency domain using either global spectral distance measures or more particular spectral measures used in conjunction with wavelet analysis The emphasis throughout the work reported in this report has been to make no assumptions about the nature of the fault to be detected other than the principle of the additive nature of the signals from a fault and the background noise

1.0 INTRODUCTION

The detection of faults in liquid metal cooled fast reactors is in the same class as the detection of faults in any industrial process, but differentiated from them by the high power density usually associated with fast reactors. If left unchecked, a fault in a fast reactor could lead to considerable damage to the plant and become a threat to human life. Therefore the early detection of incipient mal-function is of paramount importance in the operation of all fast reactors. The two components of the plant which are of significant concern are the reactor core and the heat exchangers. Protection of the core is important because of the high power density, and the heat exchanger presents special threats because of the possible interaction between water and sodium in the event of a leak in any of the tubes in the heat exchanger.

It may be possible, by extensive in-plant testing, to characterise the features of defined fault conditions in a particular plant and design a fault detection strategy around the data obtained in this way. Srinivasan and Singh [1990] demonstrated a method showing impressive discrimination by using a selected set of individual frequencies from a spectral estimate in a covariance matrix. However, it may not always be possible to transfer the results of these in-plant tests to another situation with a high degree of confidence unless the plants are identical in design.

In this work, generic fault detection strategies are examined in order to determine which ones are applicable to the detection of incipient malfunction in a liquid metal cooled fast reactor. Ideally a generic strategy for fault detection should not make any assumptions about the nature of the fault conditions. Whilst this means the strategy is an anomalous event detector, it has the

advantage that faults not previously considered may be identified, otherwise these faults may pass unnoticed.

The data, used to test a variety of generic fault detection strategies, were provided as part of the IAEA coordinated research programme on acoustic signal processing for the detection of boiling or sodium /water reaction in a liquid metal cooled fast breeder reactor.

2.0 THE TEST DATA

Test data were supplied in 1993 and 1994 in the form of signals from the superheater in the prototype fast reactor (PFR) in Scotland mixed with signals from an experimental rig in Bernsberg in Germany. The test data supplied in 1995 were obtained from the PFR during de-commissioning and comprised background signals from both the evaporator and superheater in secondary circuit number three operating at full power, and a separate set of recordings made whilst injecting argon or hydrogen or water into the evaporator whilst the PFR was shut down.

The 1993 data (supplied by the United Kingdom Atomic Energy Authority). consisted of a calibration signal followed by 12 recordings, the first two of which were the background noise from the PFR superheater number two and a five-second sample of the sodium-to-water injection at a rate of 1.8 g/s. The next four records consisted of the signals from the background noise and the noise from an injection starting at an arbitrary time with a signal-to-noise ratio set at one of the values from a maximum of -12dB to a minimum of -24dB. This arrangement of test data was repeated with PFR superheater number three and a five-second sample of a sodium-to-water injection at a rate of 3.8 g/s.

The 1994 data provided multichannel recordings prepared by CEA, Cadarache, France. Using the original 1993 data, four channels of test data were generated by mixing the noise of a leak detected by four sensors attached to waveguides on the test vessel in Germany with four sensors attached to waveguides on the PFR superheater number two. Five signal-to-noise ratios from -6dB to -24dB were used to prepare the test data from analogue signals sampled at 131 kHz.

Although similar waveguides and sensors were used in both the 1993 and 1994 benchmark tests, an uncertainty remained on the general applicability of the findings because the signals from a simulated fault were obtained in a different plant to that from which background signals were obtained and the usefulness of these trials rested on identifying signal processing strategies that show potential for use in real industrial situations.

The 1995 test data were provided by the Atomic Energy Authority, Reactor Technology Department, Dounreay, Caithness, Scotland and used precisely the same waveguides and sensors on the same item of plant used under normal operation and test conditions respectively. Thus the uncertainly associated with

the use of different plant for the generation of background and fault signals was removed.

The steam generators in the PFR are of the shell and 'U' tube design with water or steam flowing through the tubes and sodium flowing over the outside of the tubes. Three essentially identical secondary circuits each comprise an evaporator, a superheater and a reheater.

The data sets used in this work are derived from recordings of the output of four accelerometers attached to waveguides on secondary circuit number three. The accelerometers were Endevco type 7704A-17 having a typical sensitivity of 17 pC/g and a resonant frequency of 45 kHz. The signals from each of the four accelerometers were recorded in FM mode at a tape speed of 120 inches per second, giving a nominal frequency range of 0 to 80 kHz. These signals were subsequently digitised two at a time by using a LSI DSP32-C digital signal processing card in a Dell 486D/33 PC computer. In order to overcome the limitations of using only two signals at a time and to facilitate the use of multichannel methods of fault detection and location, signals were digitised synchronously in pairs. The first pair were sensors A and B, the second pair C and B, and the third pair D and B. In this way the original synchronised recordings of all four sensors could be reconstructed.

3.0 GENERAL SIGNAL PROCESSING STRATEGY

The development of a generic signal processing strategy is based on two assumptions. It is assumed that the background noise is spatially distributed around the plant giving rise to a signal at a sensor which is sampled appropriately to generate a series $x[j]$. Conversely, the noise associated with a fault is assumed to be localised and thus is not necessarily correlated with the background noise. The noise associated with the fault gives rise to a signal at the sensor which is similarly sampled to generate a series $y[j]$ which is regarded as the target signal.

In general, the sampled signal from the sensor may be written as

$$z[j] = x[j] + \delta * y[j],$$

where $\delta = 0$ corresponds to no fault and
$\delta = 1$ corresponds to fault conditions.

Although this model is simple it has significant implications for generic fault detection strategies because the fault acts in an additive sense and will produce a change in the structure of the signal model which can be observed from the sensor. Because no other a priori information is required additive changes in descriptions of $z[j]$ in the time, frequency or probability domains can be deduced.

3.1 SPECIFIC SIGNAL PROCESSING METHODS

Seven different signal processing methods are reviewed in this section and compared against the use of the mean square to judge the effectiveness of the more sophisticated techniques. Three of the methods use wavelet analysis, two use spectral distance measures and two are based on autoregressive modelling.

3.1.1 Wavelet Analysis

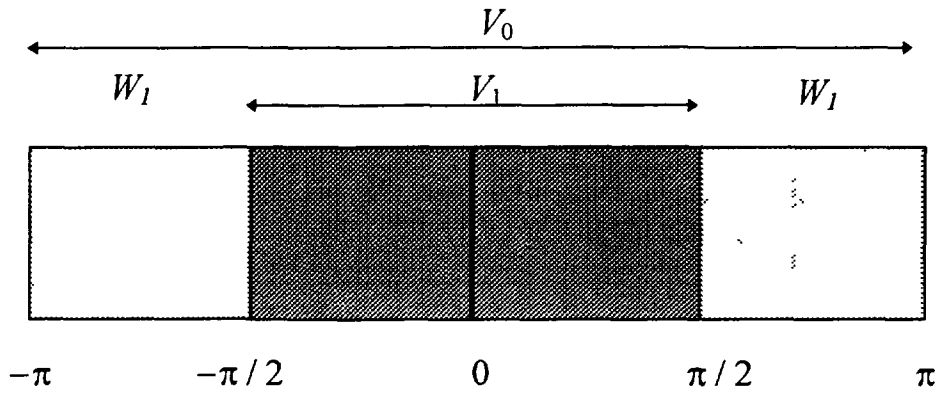

Figure 1 Division of space V_0 into subspaces V_1 and W_1

The wavelet transform decomposes a signal space into a series of subspaces usually by filtering. This concept is illustrated in Figure 1 in which a signal $x[j]$ in the space V_0 is decomposed into an *approximation* signal in V_1 together with some added *detail signal in* W_1. The space V_1 contains all that part of the signal limited to the range $(-\pi/2, \pi/2)$ and may be regarded as the output of an ideal low-pass filter. W_1 contains the rest of the signal, which from a signal processing perceptive may be taken as the output of an ideal band-pass filter. The frequency scale $(-\pi, \pi)$ may be considered the folding frequency on a normalised frequency scale.

In general, the signal space V_0 may be divided or decomposed into a number of related subspaces by sub-sampling. In this work every alternate sample was used. Subsampling by two being used for convenience here although it is possible to take every third sample or select any sample set. The major advantage in subsampling by taking every second sample is that the wavelets generated are orthonormal and hence the different decomposition signals are (ideally) independent.

Sub-sampling is of fundamental importance to the discrete wavelet transform since it allows the same filter coefficients to be used at each level of decomposition rather than scale the filter to match the bandwidth of concern. In the current work the wavelet transform was implemented using the filter coefficients $h[j]$ provided in a paper by Daubeches [1988] using the computational scheme shown in Figure 2 where the *detail* outputs are

equivalent to constant percentage band-pass filters. Outputs corresponding to the *approximation* of the input are not necessary in this case.

The mean squares of the outputs of the equivalent constant percentage band-pass filters form a feature that may be used to detect the onset of an anomalous event. In practice attention would be focussed on those wavelets in which the energy associated with the anomalous event predominantly lay.

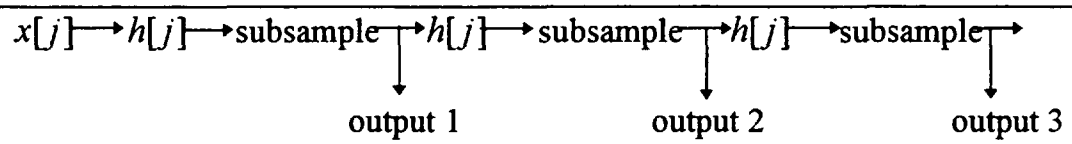

Figure 2 Part of the discrete wavelet transform filter with subsampling by two

3.1.2 Spectral Density Measures

A direct way to attempt to detect the onset of fault conditions is to compare the spectral components of a reference block of data to that of test blocks throughout the signal record. This method is generic in that it does not use any a-priori information. However, it may incorporate significant redundancy and loss of resolution by including all parts of the frequency spectrum in the analysis.

It is possible to combine the comparative method inherent in the above with the use of wavelets, thereby exploiting the band-pass characteristics of wavelets, whilst maintaining a generic approach by noting that wavelets cover the entire frequency spectrum of the sampled signal.

Two variations are possible using this approach and for convenience are called the *direct spectral distance measure* and the *normal spectral distance measure*. Both these variations are defined in the following sections.

3.1.3 Direct Spectral Distance Measure

This method compares the frequency components of the fast Fourier transform (FFT) of a reference set of data to that of test blocks for each of the wavelet decomposition signals by forming each of the FFTs into a vector of size P.

In this method the original signal is divided into a number of blocks of data each containing M samples, and the wavelet decomposition being performed on each block of data. Depending on the size of M, it may be necessary to further subdivide to facilitate the use of available FFT algorithms and take the average over these sub-divisions. The resulting vector of the spectral components at the i^{th} level of decomposition is written as $X_i(f)$ and the distance measure for the detail signal at this level is given as:

$$D_i(j) = \sum_{k=1}^{M} \left[\left| X_{i,ref}[k] \right| - \left| X_{i,test}[k] \right| \right] \quad j = 1,2,3,\ldots,K.$$

This spectral distance method can also be implimented without using wavelets and is calculated in precisely the same way as illustrated in the following example, in which 20,000 samples of the original signal were selected for analysis. These samples were divided into 78 contiguous blocks each containing 256 samples, thereby using 19,968 of the available data set. The choice of 256 samples in each block facilitated the use of a standard FFT algorithm to generate the FFT of each of the 78 blocks. The FFT of the individual blocks is

$$X_i[f] = FFT\{x_i[j]: i = 1.2,\ldots,78\}$$

$$\text{for } j = 1.2,\ldots,256$$

$$\text{and } f = 1,2,\ldots,128.$$

Note that the range for the frequency f is only taken to 128, corresponding to the folding frequency. The 78 FFTs were then averaged to produce a vector with elements at each of the 128 frequencies. This process was implemented for both the reference and test signals to yield the following vectors

$$\boldsymbol{X}_{ref} = \left[X_{ref}[1],\ldots,X_{ref}[128]\right],$$

$$\boldsymbol{X}_{test} = \left[X_{test}[1],\ldots,X_{test}[128]\right].$$

The feature is then the Euclidean distance between the reference and test vectors given as

$$\left\|\boldsymbol{X}_{ref} - \boldsymbol{X}_{test}\right\| \quad .$$

3.1.4 Normal Spectral Distance Measure

One view of the spectral distance measure first proposed by Black [1993] is that differences in the direction of the reference vector only reflect an increase in the volume of the background signal and thus may not be indicative of the on-set of fault conditions. He proposed that a distance measure based on deviations normal to the reference vector would indicate a change in shape of the power spectral density function and be more likely to signal the on-set of fault conditions.

If the reference and test vectors are denoted by $\boldsymbol{r}$ and $\boldsymbol{t}$ respectively and a vector orthogonal to $\boldsymbol{r}$ in the direction of $\boldsymbol{t}$ is $\boldsymbol{q}$, then it can be shown that,

$$\boldsymbol{x=t-q-r}$$

where $\boldsymbol{x}$ is a vector in the direction of $\boldsymbol{r}$. A two dimensional example is shown in Figure 3.

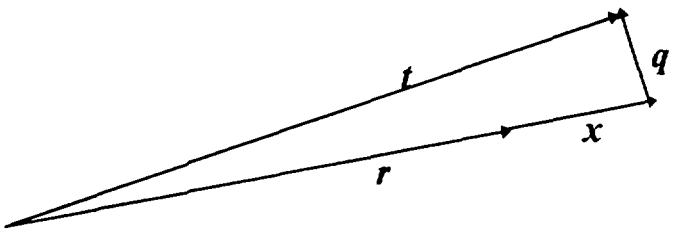

Figure 3 Illustration of normal spectral distance measure

The feature proposed by Black was the square of the magnitude of the normal and given as

$$|\boldsymbol{q}|^2 = \boldsymbol{t}.\boldsymbol{t} - \left[\frac{\boldsymbol{r}.\boldsymbol{t}}{|\boldsymbol{r}|}\right]^2,$$

representing the magnitude of deviation of the test vector in a direction normal to the reference vector. This expression can be written with the same convention as used earlier as

$$\text{feature} = \quad X_{test}.X_{test} - \left[\frac{X_{ref}.X_{test}}{|X_{ref}|}\right].$$

Note that the normal spectral distance measure may be implemented either with or without the use of wavelets as in the application of the direct spectral distance measure.

3.1.5 Autoregressive Modelling

Autoregressive (AR) modelling has been developed extensively over a number of years for modelling linear stochastic processes. The AR model consists of a set of parameters which can be used for either prediction or spectral estimation. The pth order AR linear predictor is given as

$$x[j] = -\sum_{k=1}^{p} a[k]x[j-k] + u[j],$$

where $a[k]$ are the AR parameters and $u[n]$ is a zero mean white Gaussian distributed process with variance σ^2. The spectral estimate is given as

$$P_{AR}(f) = \frac{\sigma^2}{1 + \sum_{k=1}^{p} a[k]e^{-j2\pi kf}}.$$

There are several methods which may be used to determine the parameters of the AR model; for example, those of Kay and Marple [1981], Marple [1987] and Kay [1988]. Of these methods the modified covariance method minimises the average of both the forward and backward prediction errors, as opposed to the autocorrelation or covariance method which minimises the forward prediction error only.

The two variables which must be set in determining the AR model are the order p and the number of samples used in the estimate.

Model Order Selection

The problem of model order selection has been dealt with in considerable detail by Akaike [1970], Rissanen [1983], Kay and Marple [1981], Marple [1987], and Kay [1988]. In general, if the model order is too low, the result will be a high prediction error and a smoothed spectrum. Conversely, if the model order is too high, spectral peaks will result in an attempt to model the noise process. (Kay 1988). Optimal criteria have been developed by Akaike and Rissanen independently. Akaike developed the final prediction error (FPE) and the Akaike information criterion (AIC) whilst Rissanen developed the minimum description length (MDL) criterion. These are defined as follows:

$$FPE(p) = \frac{N+p}{N-p}\tilde{\rho}_p$$

$$AIC(p) = \log\tilde{\rho}_p + \frac{2p}{N}$$

$$MDL(p) = \log\tilde{\rho}_p + \frac{2p}{N}\log N,$$

where $\tilde{\rho}_p$ is the error variance estimate for model order p, and N is the number of samples used for the estimate. Sometimes a minimum can be found when applying these criteria, but often the results are simply monotonically decreasing. In that case the choice of the model order is a question of judgement; a value of p being chosen such that the results of applying the criterion shows insignificant decreases above that value. In this work, all three criteria gave very similar results as shown in figure 6 As this figure shows all three criteria decrease rapidly initially and level off around a model order of 22, this model order was used for all subsequent analysis for the 1995 data. It had been necessary to use a model order of 32 for the 1994 data.

Data Length

A key factor in the decision making process is the time taken to recognise a fault condition. This decision time is directly related to the number of samples used in any estimation scheme. Examination of the variation of each of the AR

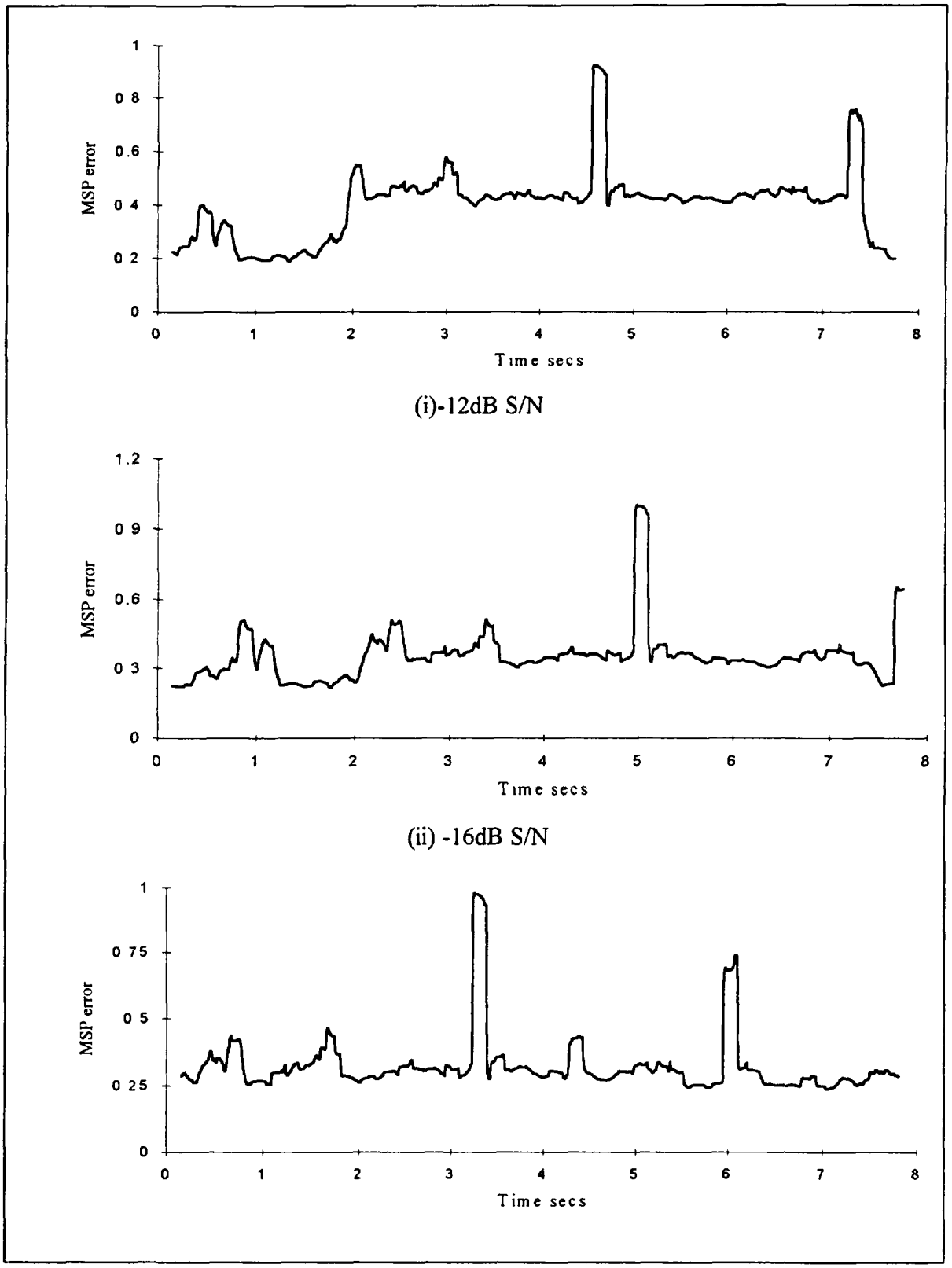

Figure 4 showing the MSP error at three signal-to-noise ratios v.time using **1994 data**.

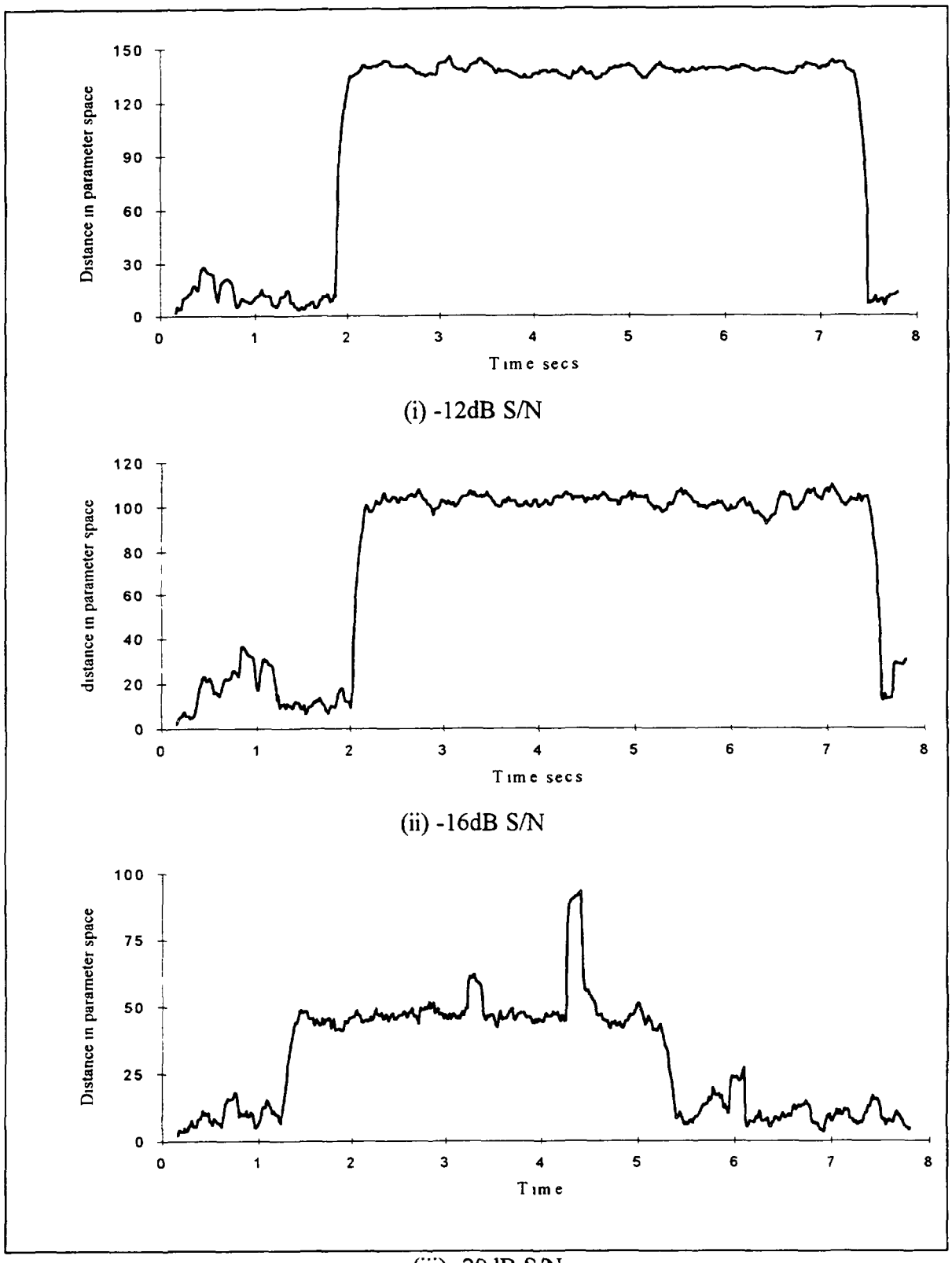

Figure 5 distance-in-parameter-space at three signal-noise-ratios v time using **1994 data**

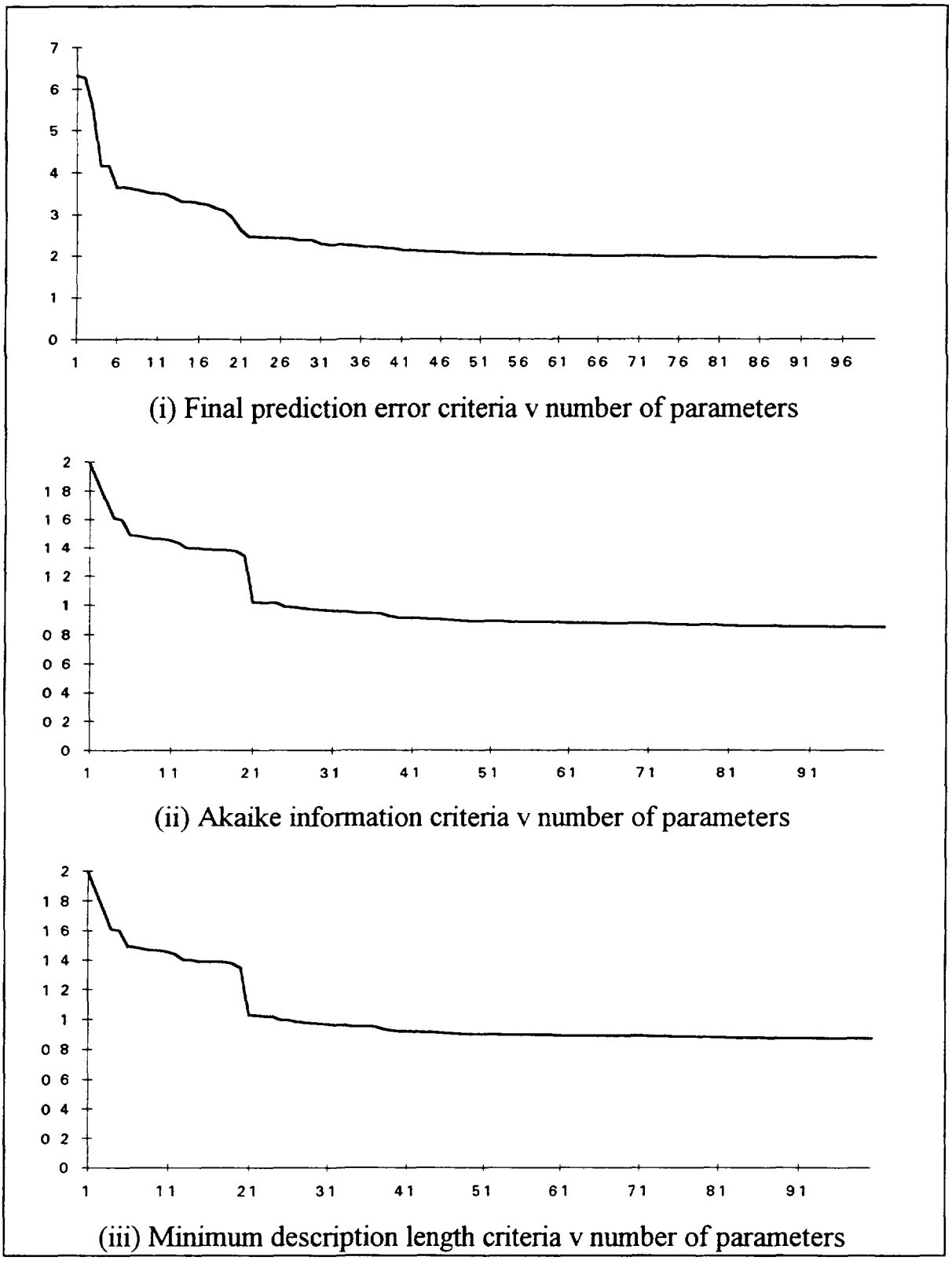

Figure 6 Comparison of some optimal criteria using **1995 data**

parameters showed that, for the autocorrelation method, as the sample size was increased, no convergence occurred over the maximum length of sample used, indicating that this method was not suitable for the context. Conversely, the modified covariance method resulted in only gradual change to the parameters after some 20,000 samples. Subsequently, all analysis was computed using 20,000 samples.

Fault Detection Strategies using AR Models

The underlying assumption with all fault detection strategies that employ any form of modelling is that the occurrence of a fault changes the model structure of the received signal. A direct comparison between parameter estimates obtained under 'normal" operating conditions and those obtained during any further operational conditions may indicate the onset of an anomaly. Two of the different detection strategies used in this work are explained in the following sections.

3.1.6 Mean Square of Prediction Error

The AR model of order p gives the parameters of the pth order linear predictor. Using this model as a one-step-ahead predictor, the prediction error variance over a suitable averaging time is determined. It is expected that this error variance will be larger during fault conditions than during normal operating conditions. The mean square prediction error (MSPE) averaged over M samples is given as

$$MSPE = \frac{1}{M}\sum_{j=1}^{M}\left|e[j]\right|^2$$

$$MSPE = \frac{1}{M}\sum_{j=1}^{M}\left|x[j]-\tilde{x}[j]\right|^2,$$

where $\{x[j]: j = 1,2....,N\}$ is the actual signal value, $\{\tilde{x}[j]: j = 1,2....,N\}$ is the predicted value, N is the total number of samples of the signal, and the error term at any value j is given by the difference between the observed and predicted values.

The predicted values are obtained by using the estimated model parameters $\{\tilde{a}[k]: k = 1,2,...,p\}$ in the following expression:

$$\tilde{x}[j] = -\sum_{k=1}^{p}\tilde{a}[k]x[j-k].$$

Note that the mean square of the prediction error is dependent on the model order p and the number of samples M. This latter parameter effectively determines the total time taken to reach a decision whether or not an anomalous event has occurred .

3.1.7 Distance-in-parameter-space

A more direct method is to use a feature which incorporates the prediction error variance as follows:

$$\textbf{Feature}=\left\| \frac{a_{ref}}{\sigma_{ref}} - \frac{a_{test}}{\sigma_{test}} \right\|,$$

where a_{ref} and a_{test} are vectors of the estimated reference and test parameters, and σ_{ref} and σ_{test} are the standard deviations of the reference and test signals respectively. The reference is obtained from signals at the start of the file which are known to be 'normal' and the test is obtained from signals at all subsequent times. The basic assumption used in this method is that the model structure will be different under fault conditions from that found in 'normal' operation. The standard deviation is used in this feature to normalise the dimensions of the feature.

4.0 RESULTS OF THE FEATURE EXTRACTION STRATEGIES

The results presented in graphical form in the figures that follow relate to trials of the feature extraction strategies with data from the 1994 and 1995 benchmark tests. In order to compare the various signal processing strategies under conditions as closely similar as possible, the 1995 data was modified by mixing the background noise from the evaporator with the noise from a typical injection. The results reported here for the modified 1995 data are for injection number 5 using sensors A and B only to limit the volume of the data processing to manageable proportions. The methods investigated may be extended to the other injections and other sensors directly without any need for further modification.

The signal processing strategies compared in the following set of results are:

- Autoregressive models
  - mean square prediction error
  - distance-in-parameter-space
- Spectral distance measures
  - direct spectral distance
  - normal spectral distance
- Wavelet analysis
  - mean square of the wavelet decomposition signals
  - direct spectral distance of wavelet decomposition signals
  - normal spectral distance of wavelet decomposition signals.

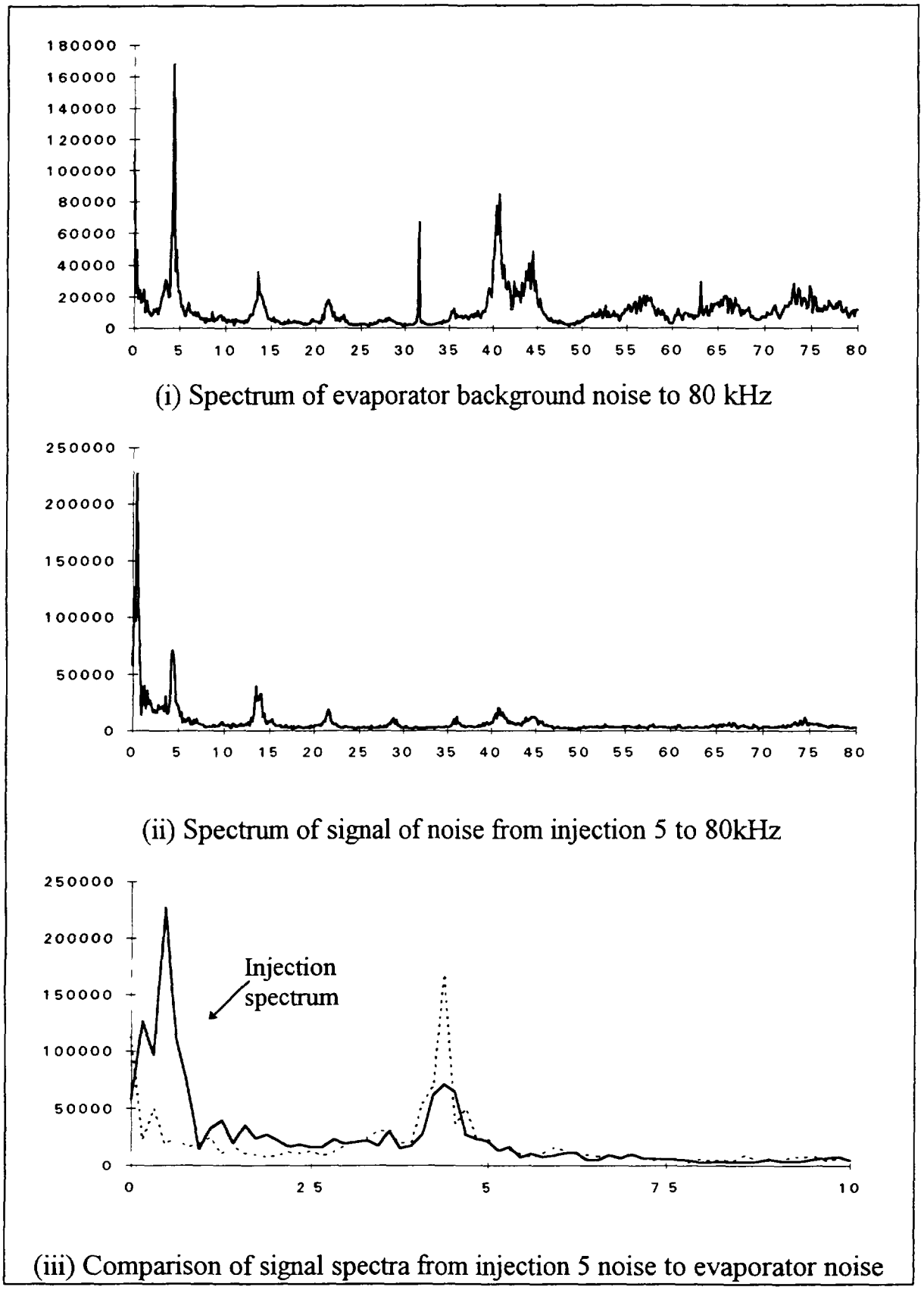

Figure 7 Frequency spectra of noise from evaporator and injection 5 using **1995 data**

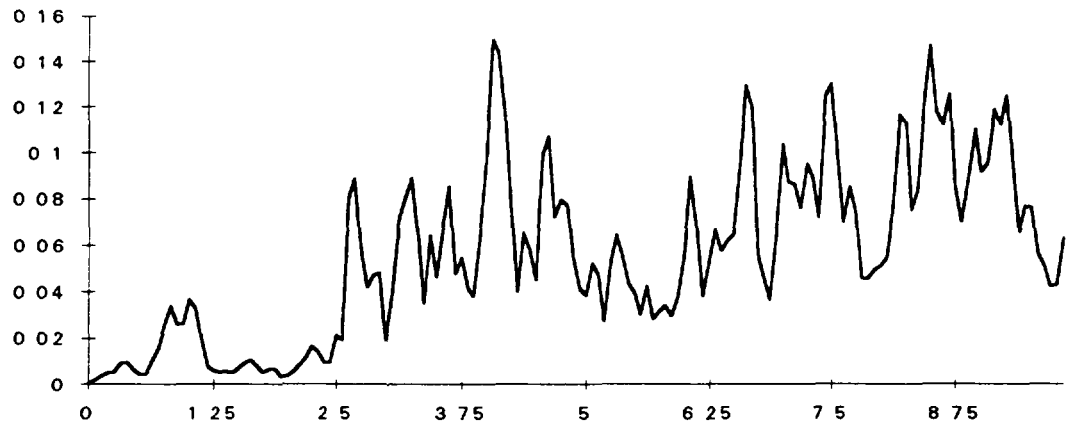

(I) Distance-in-parameter space v time for inoise from njection 5 and evaporator background

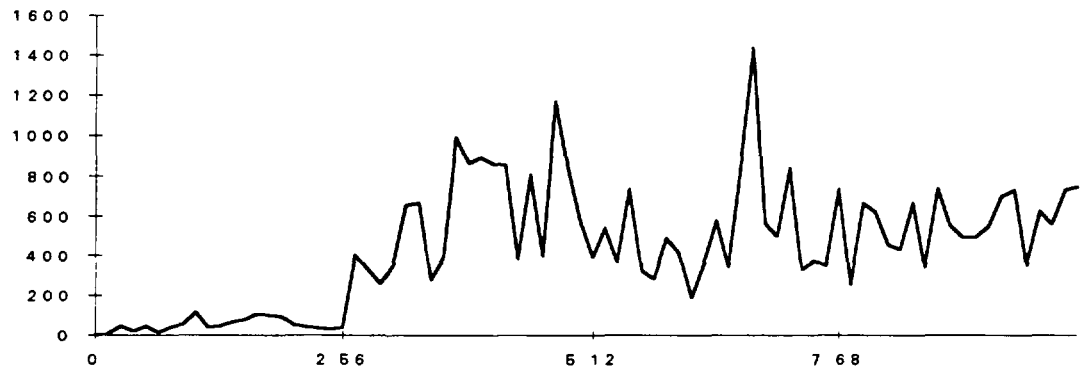

(ii) Direct spectral distance v time for noise from injection 5 and evaporator background

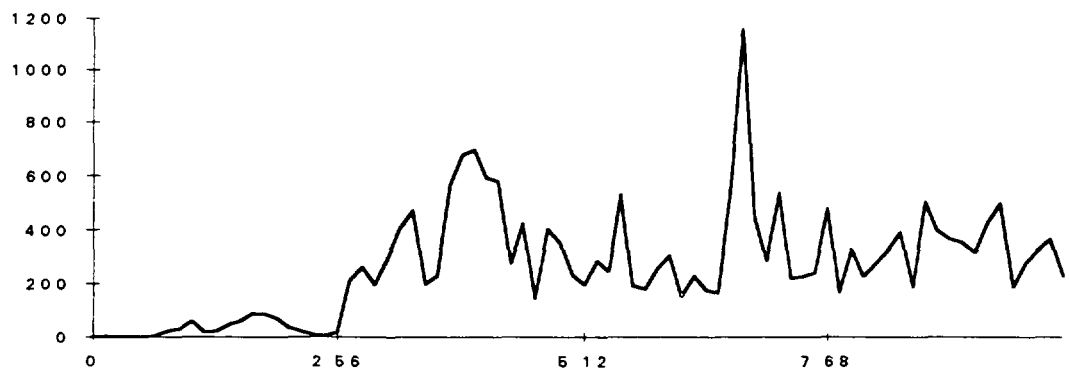

(iii) Normal spectral distance v time for noise from injection 5 and evaporator background

Figure 8 Comparison of three signal processing strategies **using 1995 data**

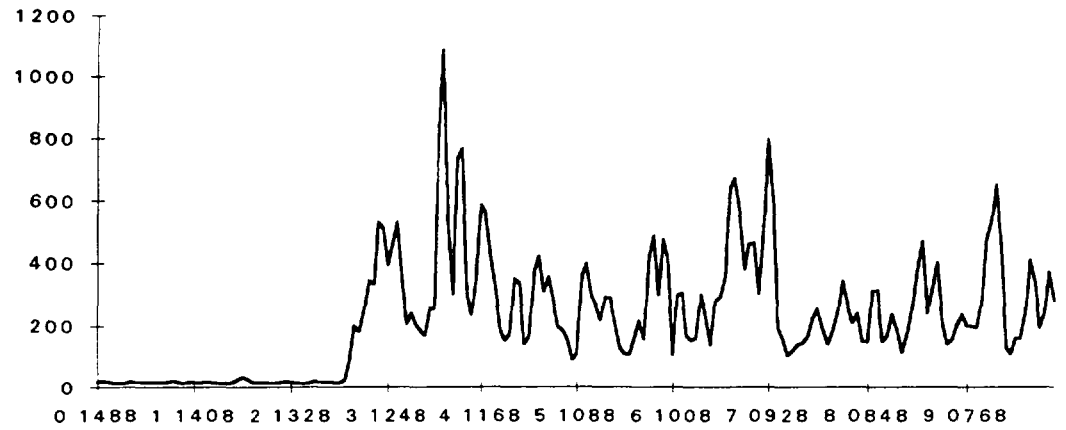

(i) Variance of the output of wavelet decomposition level 6 v time

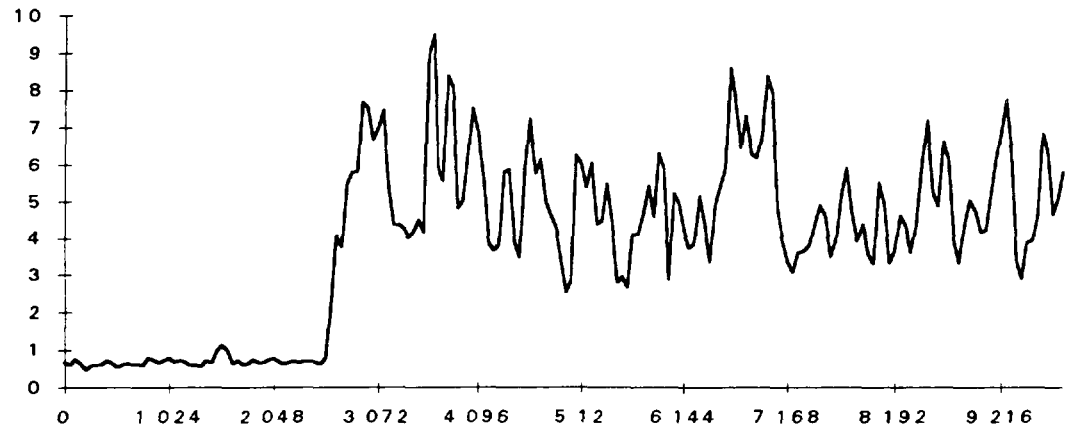

(ii) Direct spectral distance at the output of wavelet decomposition level 6

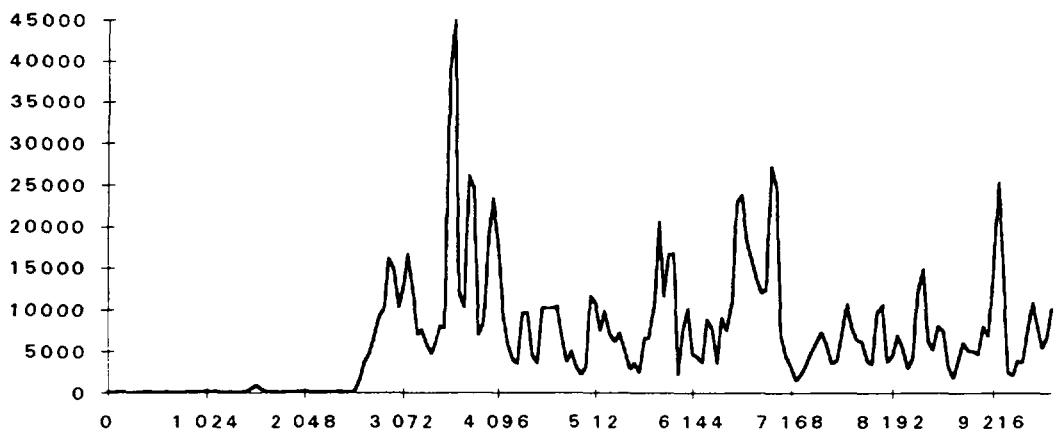

(iii) Normal spectral distance at the output of wavelet decomposition level 6

Figure 9 Comparison of variations with wavelets: injection 5 plus evaporator background using **1995 data**

5.0 CONCLUSIONS

- In this work, the three optimal criteria used to establish a suitable value for the order of an AR model all show similar results
- The energy associated with a test leak in the PFR evaporator lies predominately in a frequency band below1 kHz
- .The mean square prediction error (MSPE) is the least effective method of fault detection and may only be used with confidence with signal-to-noise ratios greater than -12 dB
- The Distance-in-Parameter-Space Method is considerably superior to the MSPE method
- A combination of the use of wavelets with spectral distance measures is the most effective method for detecting the onset of an anomaly of the type that existed in the benchmark tests.

REFERENCES

Akaike, H 1970, 'A new look at statistical model identification', *IEEE Transactions on Automatic Control*, AC-19, pp. 716-723.

Black, J L, Rofe, S E F & Ledwidge, T J *IAEA Extended Co-ordinated Research Programme on Acoustic Signal Processing for the Detection of Boiling or Sodium/Water Reaction in LMFBR*: Report to a meeting of the research co-ordination meeting, Vienna, Austria, 9-10 december 1993.

Daubechies, I 1988, 'Orthonormal Bases of Compactly Supported Wavelets', *Comm. in Pure and Aplied Math.*, Vol 41, No 7, pp. 909-996.

Kay, S M & Marple, S L 1981, 'Spectrum analysis - a modern perspective', *Proceedings of the IEEE*, 69 (11), pp. 1380-1419.

Kay, S M 1988, *Modern Spectral Estimation: Theory and Applications*, Prentice Hall.

Marple, S L 1987, *Digital Spectral Analysis: with applications*, Prentice Hall.

Rissanen, J 1983, 'A universal prior for integers and estimation by shortest data description', *Annals of Statistics* 11 (2), pp. 416-431.

Rofe, S E F & Ledwidge, T J 1994, *IAEA Extended Co-ordinated Research Programme on Acoustic Signal Processing for the Detection of Boiling or Sodium/Water Reaction in LMFBR*: Report to a meeting of the research co-ordination meeting, Kalpakkam, India, 1-3 November 1994.

Srinivasan G S & Singh O P 1990, 'New Statistical Features Sensitive to Sodium Boiling Noise', *Annals. of Nuclear. Energy* v 17, no 3, pp 135-138.

SODIUM/WATER REACTION DETECTION CONFIRMATION AND LOCATION WITH TIME DOMAIN BEAM FORMER

C. CORNU
Centre d'Etudes Nucléaires de Cadarache,
Saint-Paul-lez-Durance,
France

Abstract

The CEA studied the validity of a time beamforming method for the detection and location of Sodium/water reaction in steam generators of breeder reactors. In the context of the RCM, we apply this method on recorded data during a water injection in Sodium in ASB loop, artificially mixed with PFR background.

Despite the severity of experiment conditions (the signal to noise ratio is between -6 and -24 dB), we show that the employed method , completed with a low frequency pass band filter, allows us to locate the injection with a precision of 30% of the diameter of the loop

Using the method in the course of time allow us to coarsely locate the start time and the duration of the leak

The good functionning of the method is however perturbed by uncertainty about the wave celerity in the sodium, about wave propagation in waves guides that are mounted with the sensors and in the structure of the loop.

1. Introduction

The passive acoustical location method was firstly used in 1968 for the detection of leaks in steam generators of fast reactors. This method consists in detecting an acoustical source from its generated signal. Later on, for EFR program, while the CEA was studying an active method, the AEA members applied themselves to the studying of the performance of passive methods The CEA synthetised this various approaches after the AEA interrupted their research program in Risley

This RCM allowed the CEA to test, parallel to its own research, some passive methods.

The aim of this paper is to sum up the results obtained by the CEA as regards leak detection and location in steam generators with an antenna acoustical method on the data achieved by C.Journeau in Feb. 1994, which were distribued to all participants.

The AEA experience in this domain allowed us to make a choice between all possible passive methods.

The British team had studied several beamforming methods [1] (that is a combination of signals issued from several sensors) as part of an experiment in water. The time domain beamforming method achieved the best precision for the location of the source (a microphone) and a raising of the signal of 8 dB, but the source was impulsive boiling noise

So we choosed to apply this method on our data

We will apply ourselves, after reminding the principles of the beamforming method, to study the characteristics of the mixed data, and then to show that this method allow us to locate a leak in very severe conditions.

2. Beaforming methods

While an active method consists in studying the response of a surroundings to a signal emitted by the operator after its propagation, a passive method simply consists in studying the signal that is emitted by the observed surroundings. It is obvious that a passive method asserts itself in the case of a rapid detection of a Sodium/water reaction in steam generators.

Four passive methods were studied by the British team that we briefly remind

The time domain beamforming is the easiest to understand
We suppose that the signal which is received by the sensor is the addition of to components, the background noise and the leak noise The acoustical source in the surroundings emits a signal which is not in phase on all sensors because of the different propagation ways We have to suppose that the celerity is well known Then we can focuss the antenna to a certain point of the surroundings applying a correct phase displacement to all sensors The phase is calculated with the transit time from the point to the sensors Then the signal issued from this point is in phase for all sensors Then we can reconstruct the signal emitted by this point and calculate its power
While focussing on each point of the surroundings, we can reconstruct the power distribution of the source, and then we visualize the location of the source if it does exist

The frequency domain beamformer is equivalent to filter the signal on a particular frequency and then to achieve an operation similar to the time domain beamforming The dephasing term is multiplicative and is also obtained from the calculation of the duration of propagation and the power distribution of the source is obtained We can find with this method several maxima, but the study of several frequencies is a way to choose the good solution

The orthogonal beamformer is interesting if the signal to noise ratio is very different from one sensor to another That can arrive if if the middle is highly attenuating or if one channel is disturbed with some background noise This method requires the previous knowledge of the cross spectral density matrix of the background The comparison of the cross spectral density of the background and of the current response permits to detect the presence of a leak

If the background noise is not known, we can apply the optimal beamformer which is as powerful as the orthogonal beamformer We have to make an hypothesis on the background, we have to suppose it uncorrelated from one channel to another Than we can modelize the background noise and achieve the same technic than previously

The characteristics of the data do not justify the use of an optimal beamformer A time domain or frequency domain beamformer is sufficient
Beacuse of its simplicity and its reliability, we choosed the time domain beamformer

The mathematical principles are briefly exposed now

2 2 Mathematical aspects of the time domain beamformer

We suppose that the celerity in the propagation middle is well known

For one point of the observed zone rs, the dephasing term on sensor j will be

$$T_j = E((|r_j - r_S|/(c\delta t)))$$

where

E integer part operator
rj position of sensor j
rs position of the focussed point
c celerity
dt time sample

Then the beamformed signal from the source point rs is

$$P_s(t) = 1/n \sum_{j=1}^{n} P(t - T)$$

where

n: number of channels
Pj: recorded data from sensor j
t: time point

Then we can achieve the power distribution of the source in the inspected zone:

$$\mu(r_s)^2 = 1 / N \sum_{t=1}^{N} P_s(t_i)^2$$

where

μ^2: power of the source
N: number of samples

Another for the calculation of μ^2 is the use of cross correlation matrix:

$$C_{jk}(T) = 1 / N \sum_{i=1}^{N} P_j(t_i + T) P_k(t_i)$$

Then:

$$\mu^2(r_s) = 1 / n^2 \sum_{j=1}^{n} \sum_{k=1}^{n} C_{jk}(T_j - T_k)$$

It is the solution we choosed for the calculation of μ.

3. Preliminary study of the data

We studied the root mean square value with 1024 or 2048 samples blocks for the visualisation of the background, of the leak noise and all the set files.
Figure 1 shows that there is an important peak on block 500 of the leak noise (1024 samples a block). This corresponds to a violent shock on the vessel while manipulating it and is not representative of the injection

The rms of set number 3 (see Figure 2) shows an increasing from block 150 (2048 samples a block) and this is cler on channel 2. This observation allows us to situate the leak between the times 2.3 seconds and 6.2 seconds. This observation is good comparing to the solution.

Unfortunatlv, this observation is not possible on the other sets which present stable rms values. The leak is not discernable.

In conclusion, we can sav that set number 3 has the highest signal to noise ratio (-6 dB). A more sophisticated signal processing is necessarv for the extraction of the leak noise in such severe conditions of signal to noise ratios.

The frequency domain studying of the leak noise is interesting: we achieve the fast Fourier transform on 1024 samples blocks and we obtain figure 3. The energy of the signal is concentrated on frequency 1000 Hz. We can see this maximum also on background noise drowned in the large band.

So it is iudicious to filter frequencies higher than 1000 Hz before applving the beamforming, in order to increase the signal to noise ratio. We choosed to use a finite impulsive response filter with cut frequencies of 200 and 1000 Hz that preserve phase characteristics.

4. Results

Calculation were achieved on a SUN station with the mathematical librarv MATLAB.

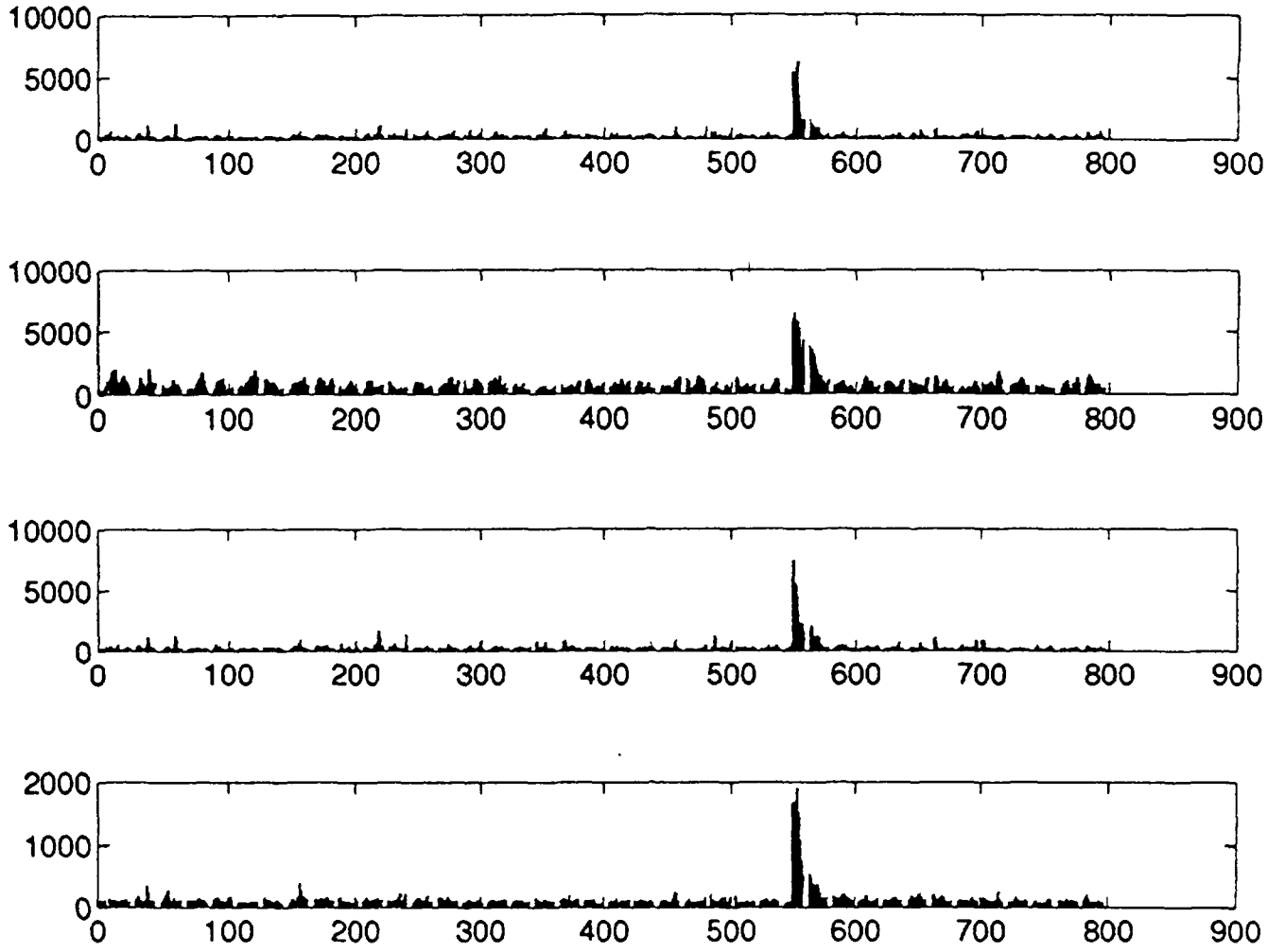

Figure 1: RMS on leak data

We essentially applied ourselves on the testing of the performance of the location method is order to use it as a way of detect the leaks. The power source distribution will not be the same in the presence of a real source -we can see a high intensity zone. and in the presence of a diffuse background. A detection technic would be to realize some successive pictures with the time of the distribution of the power of the source with N samples blocks of recorded data. The studying of the pictures allow us to decide if there is a source or not and where it is located. We can also determine the start time of the leak.

In our case. the location will be achived on the vessel of the German loop. Its geometry is well known (diameter. position of the sensors).
The wave length of the leak signal is 2.4 m approximately with a celerity of 2400 m/s (celerity in the Sodium).
1024 samples are sufficient for the representation of several periods of the signal (that is a duration of 7.6 ms).
We achieved the beamforming describing horizontal planes of the loop. the length of a spatial sample was approximately 1 cm.

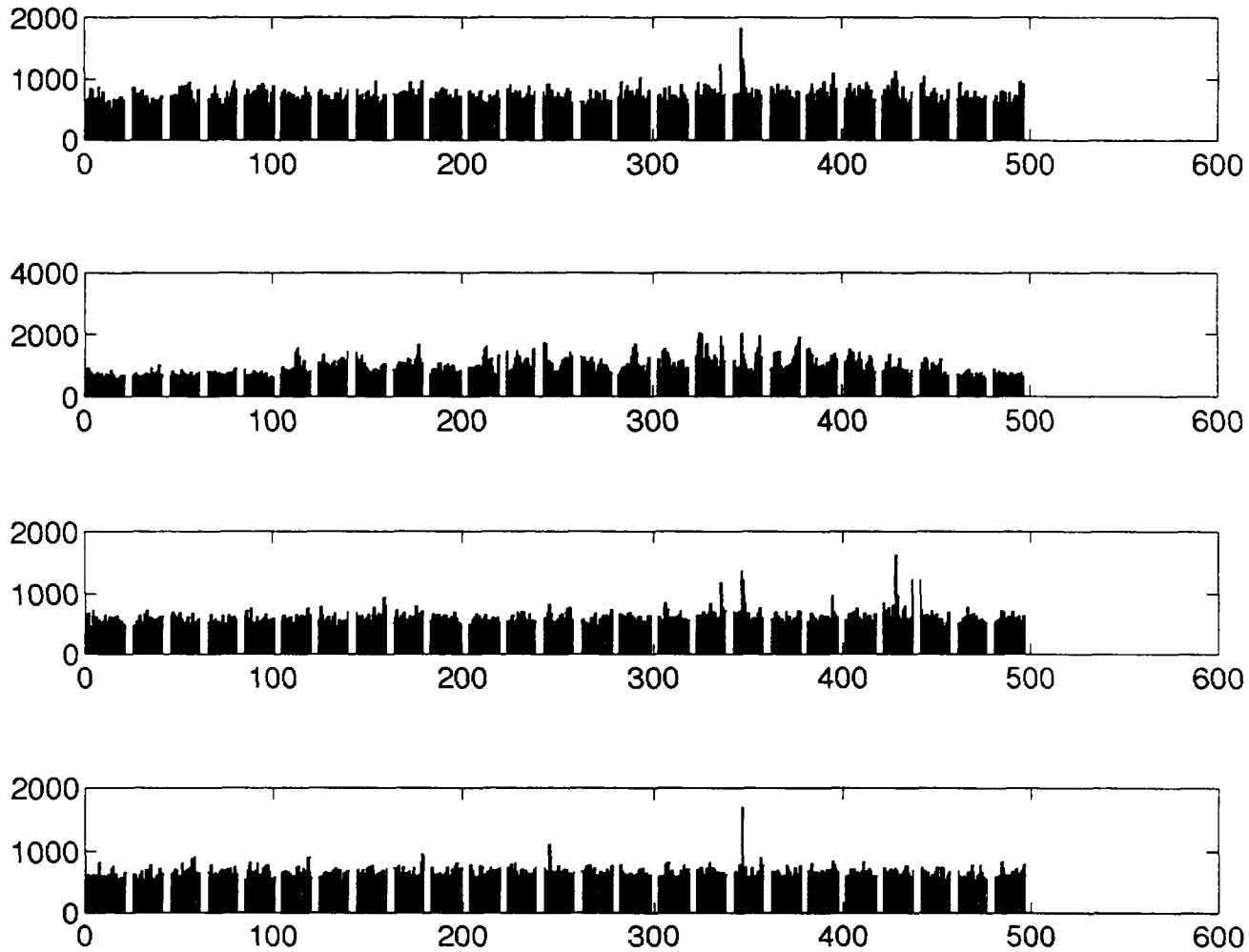

Figure 2: RMS on data set3

We validated the beamforming program with leak files. Figures 4. 5. 6 show the result of the treatment on a 1024 samples block on planes which are situated 0.85m. 0.3 m and 0.1 m above sensor 4 We can remark a clear zone that corresponds to the maximum of the power of the source The position of the leak is near sensor 1. which is correct compared to the real position of the injector. The intensity of the source decrease while going away from level 0.85 m
We can conclude on the good functionning of the algorithm

We obtained the same result with set3 (see figure 7) with a lowest intensity of the source because of the background The position of the source remains consistent with the previous figure. The calculation was realized on level 0 85 m above sensor 4 with the 1024 samples block number 750 We demonstrated that the filtering reduces the dimension of the source zone and increase the power of the signal of 6 dB. which corresponds to in increasing of the signal of 3 dB

The listening of the mixed data allowed us to find some characteristics of the leak noise in set 3. 1 and 2 In set3 we could hear distinctivelv the flow noise of the injection. Set 4 was the most silencious and we can imagine that it corresponds to the lowest signal to noise ratio. that is -24 dB.

So we decided to test the method on this set to see if a beamforming method can extract signal -24 dB bellow the background
In figure 8 we can see a zone near sensor 1 The location is in this case less precise than with set3 In this figure. we can distinguish the cone shaped leak noise and the cylinder shaped background. The level of the power of the source is as high as in the case of set 3. so the signal was 24 dB increased with this method

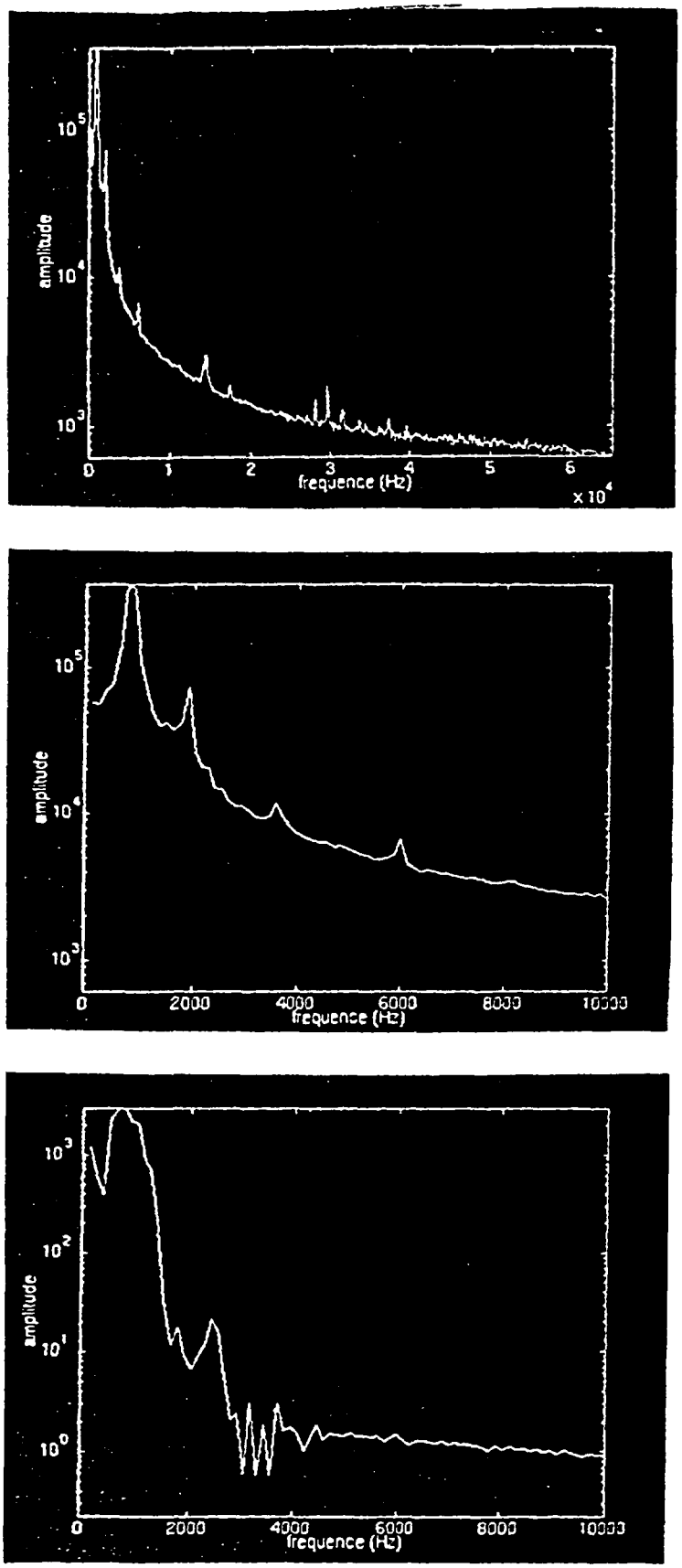

Figure 3 Fast Fourier transform of leak noise and filtered leak noise

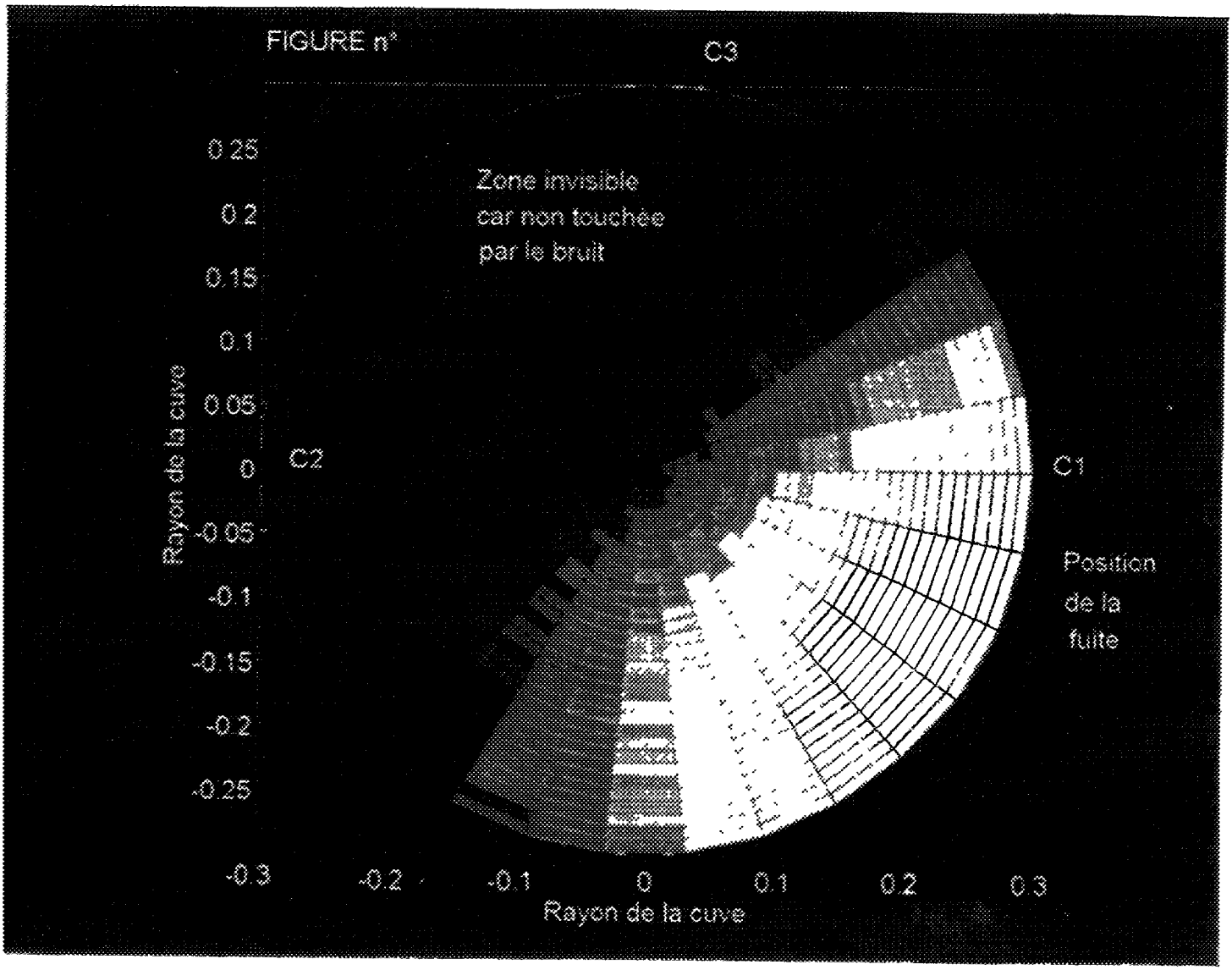

Figure 4 location of the leak with leak data 0.85 m above sensor 4

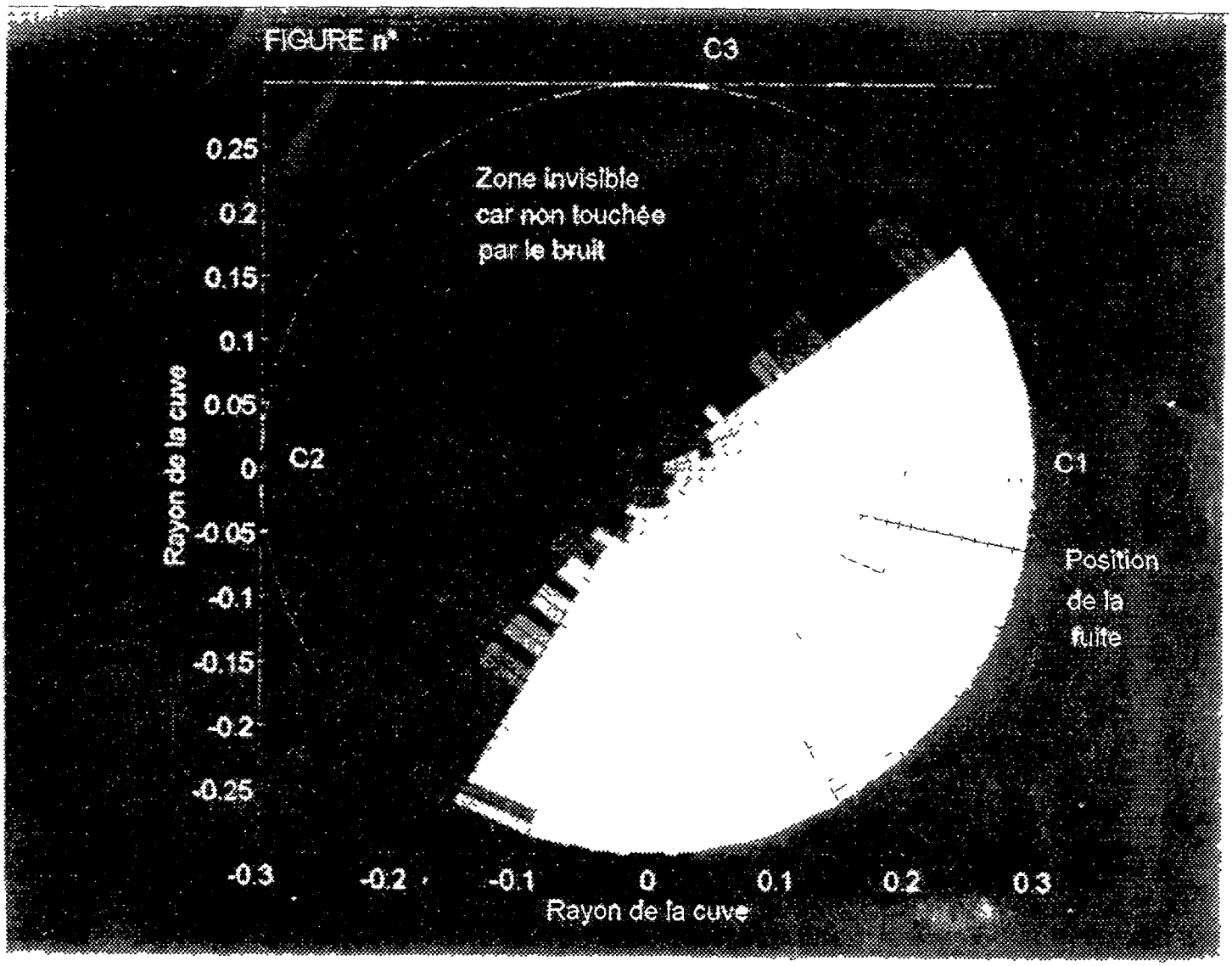
FIGURE n°
C3
Zone invisible
car non touchée
par le bruit
C2
C1
Position
de la
fuite
Rayon de la cuve
0.25
0.2
0.15
0.1
0.05
0
-0.05
-0.1
-0.15
-0.2
-0.25
-0.3
-0.2
-0.1
0
0.1
0.2
0.3
Rayon de la cuve

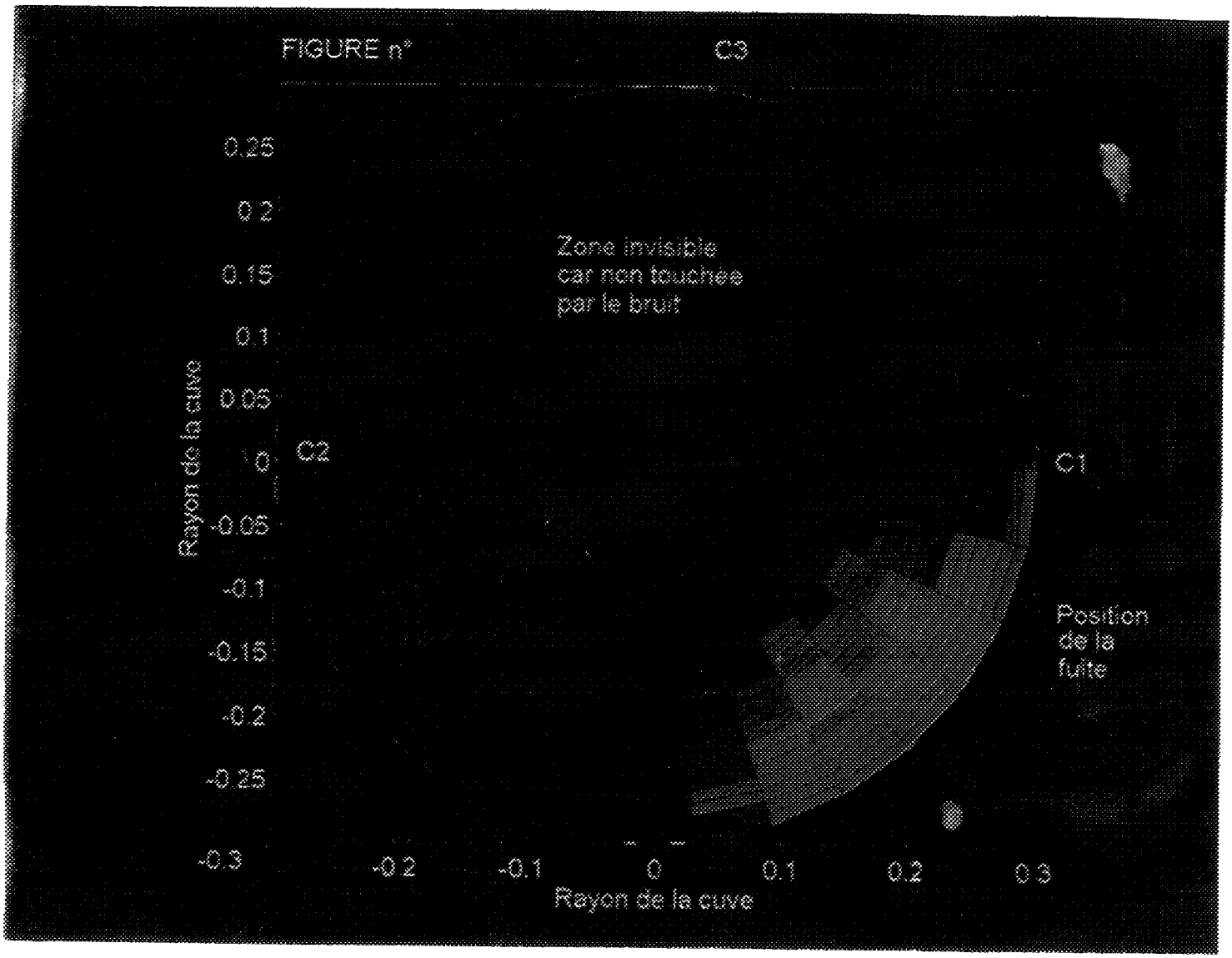

Figure 5: location of the leak with leak data. 0.3 m above sensor 4

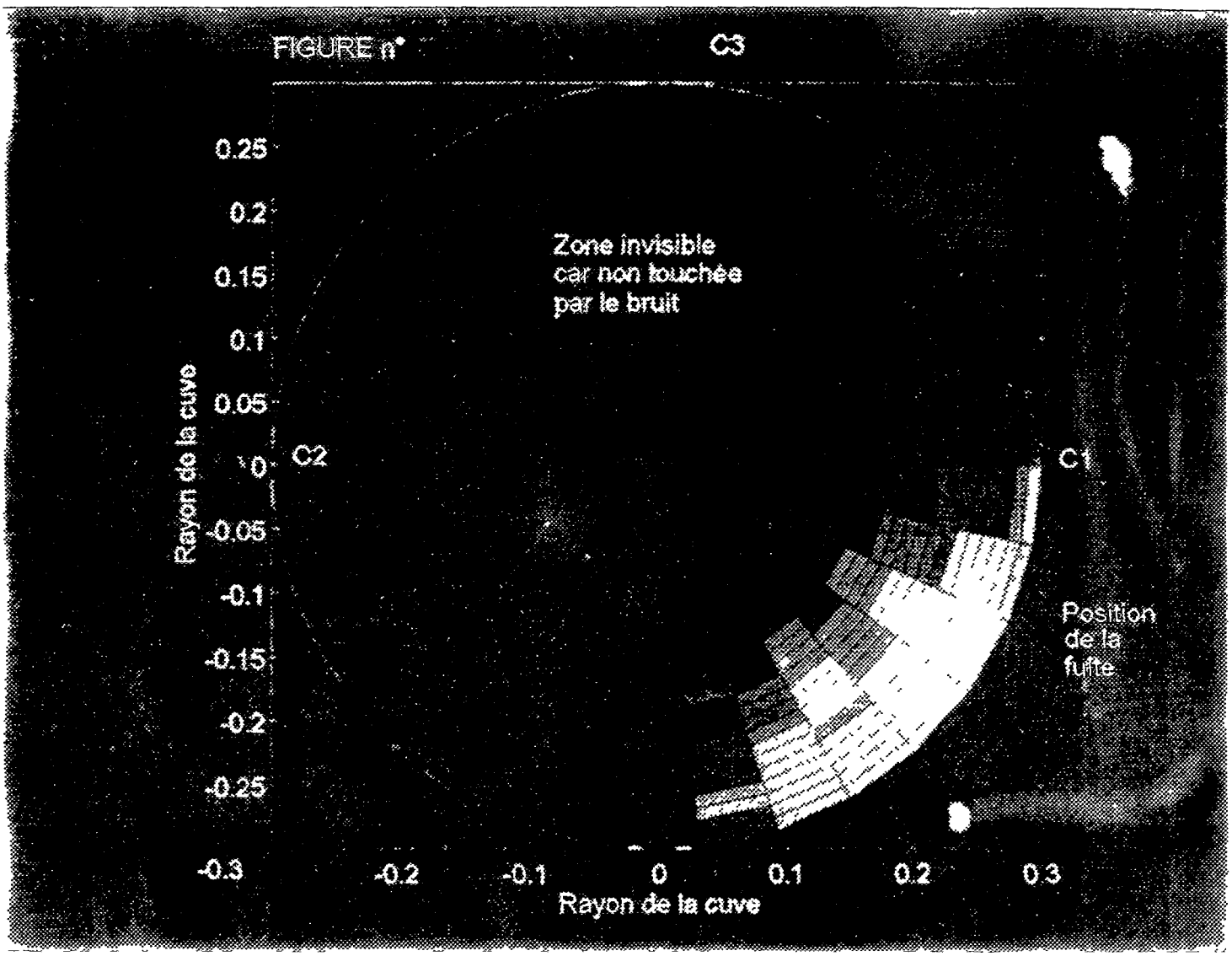
FIGURE n°
C3
0.25
0.2
0.15
0.1
0.05
0
-0.05
-0.1
-0.15
-0.2
-0.25
Rayon de la cuve
Zone invisible
car non touchée
par le bruit
C2
C1
Position
de la
fuite
-0.3
-0.2
-0.1
0
0.1
0.2
0.3
Rayon de la cuve

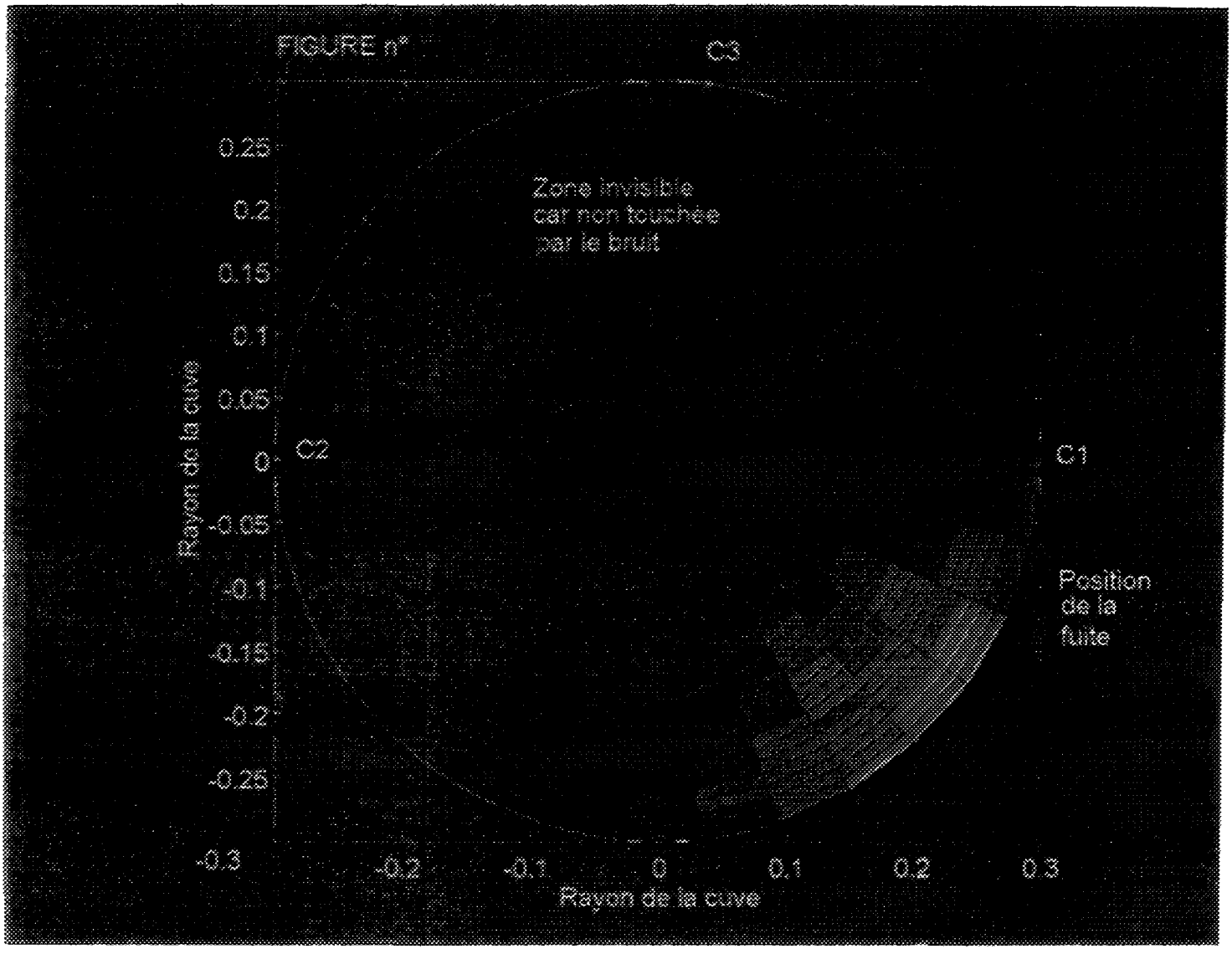

Figure 6 location of the leak with leak data, 0.1 m above sensor 4

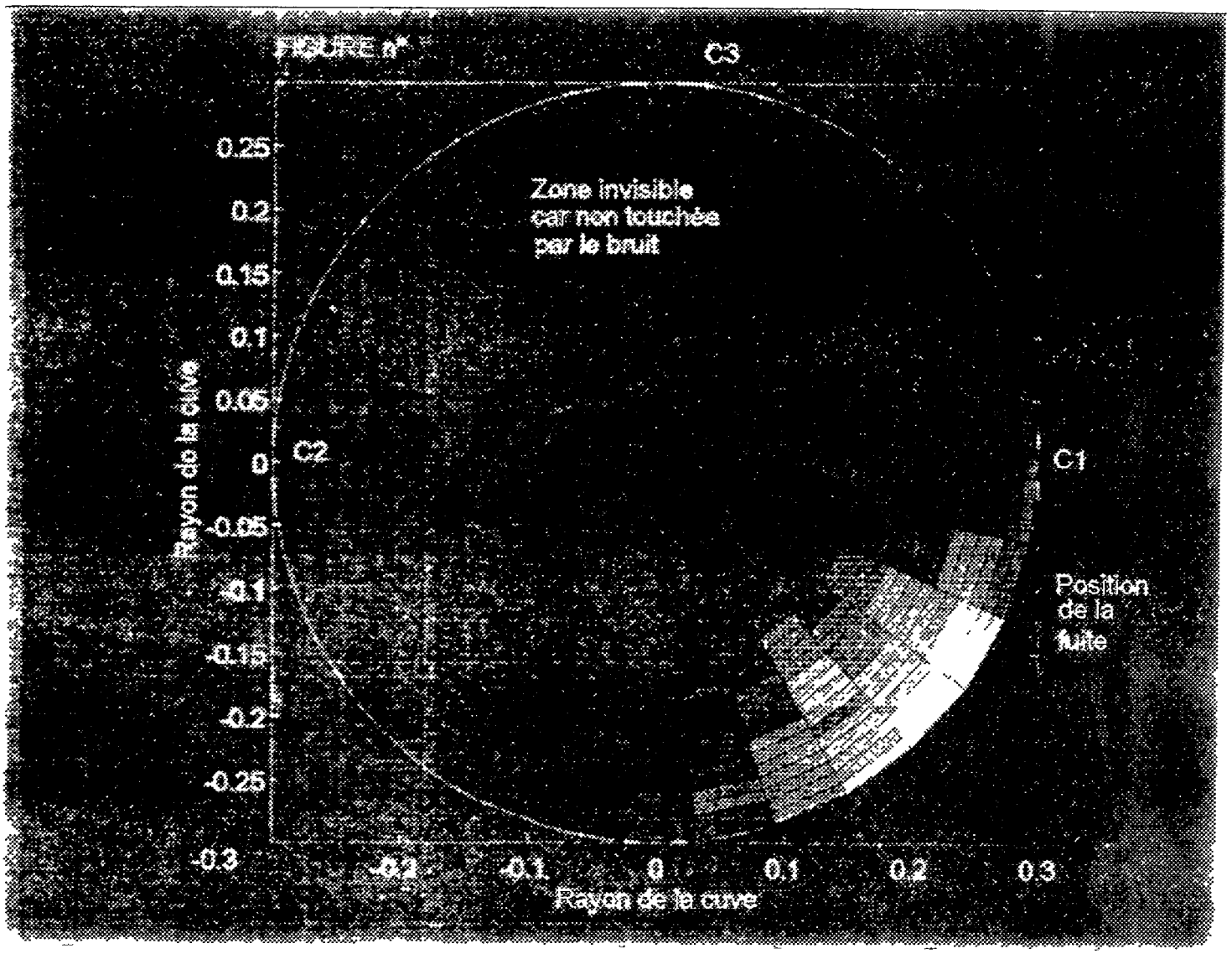
FIGURE n°
C3
C2
C1
Zone invisible
car non touchée
par le bruit
Position
de la
fuite
Rayon de la cuve
Rayon de la cuve
0.25
0.2
0.15
0.1
0.05
0
-0.05
-0.1
-0.15
-0.2
-0.25
-0.3
-0.2
-0.1
0
0.1
0.2
0.3

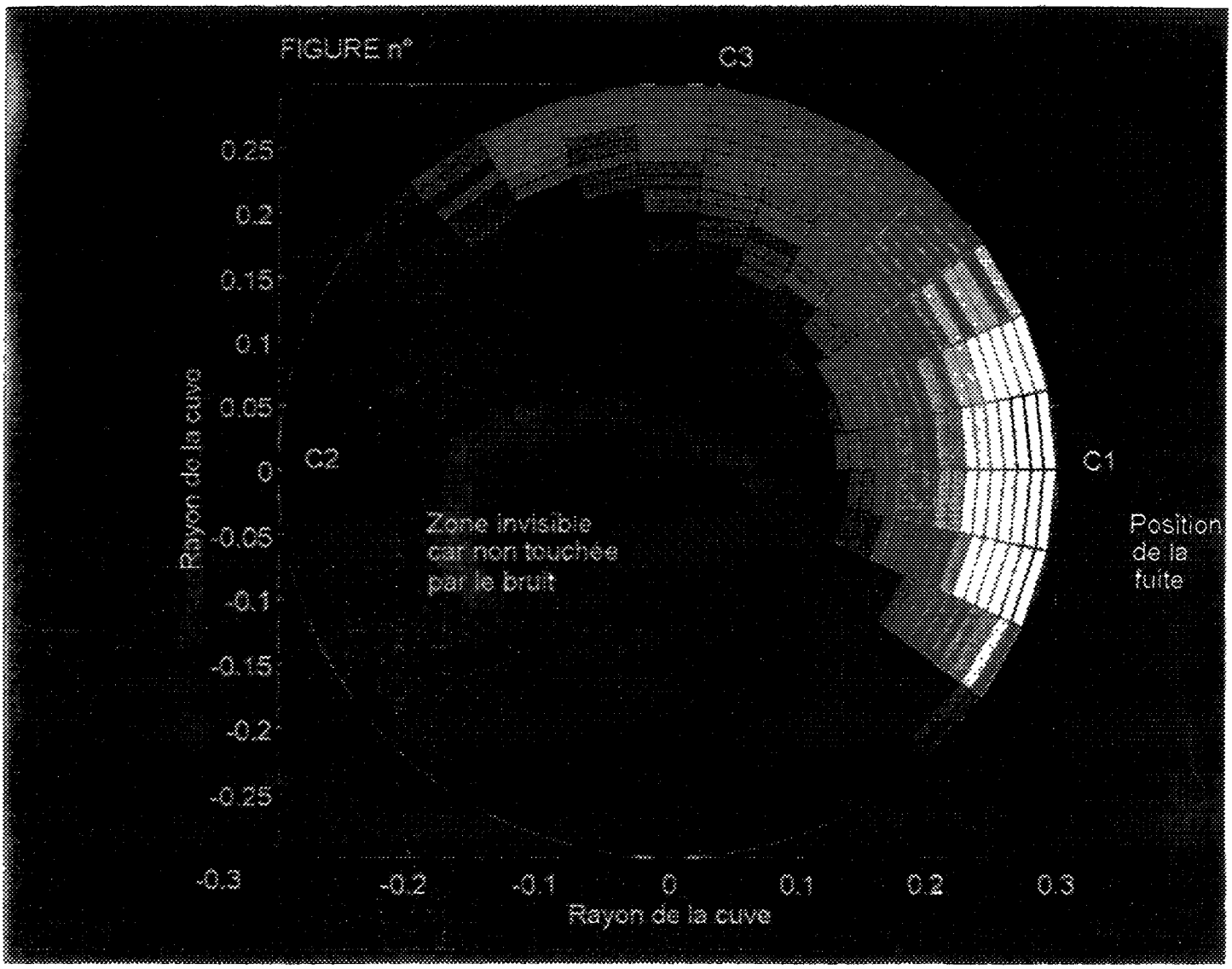

Figure 7: location of the leak with set3, 0.85 m above sensor 4

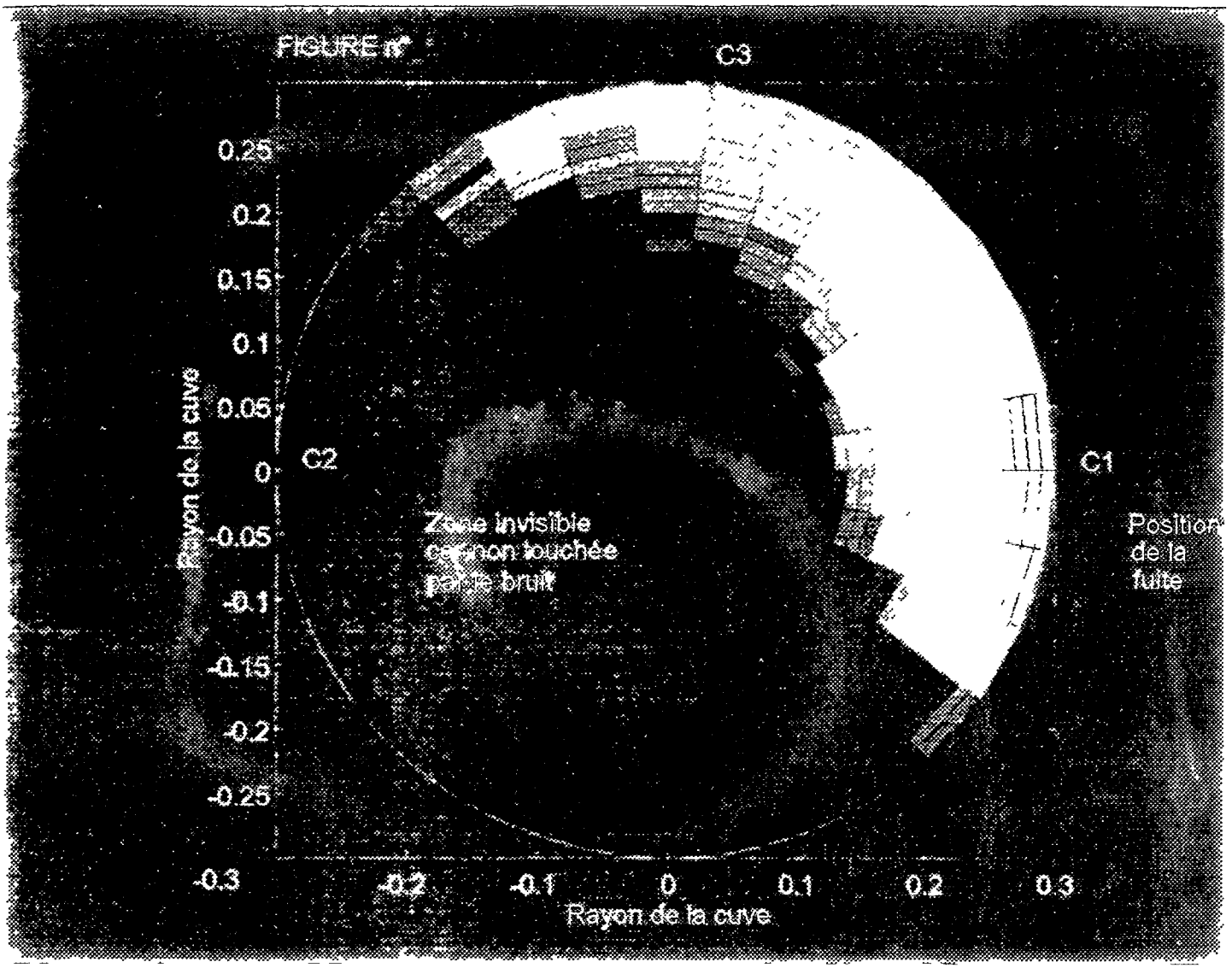
FIGURE n°
C3
C2
C1
0.25
0.2
0.15
0.1
0.05
0
-0.05
-0.1
-0.15
-0.2
-0.25
Rayon de la cuve
Zone invisible car non touchée par le bruit
Position de la fuite
-0.3
-0.2
-0.1
0
0.1
0.2
0.3
Rayon de la cuve

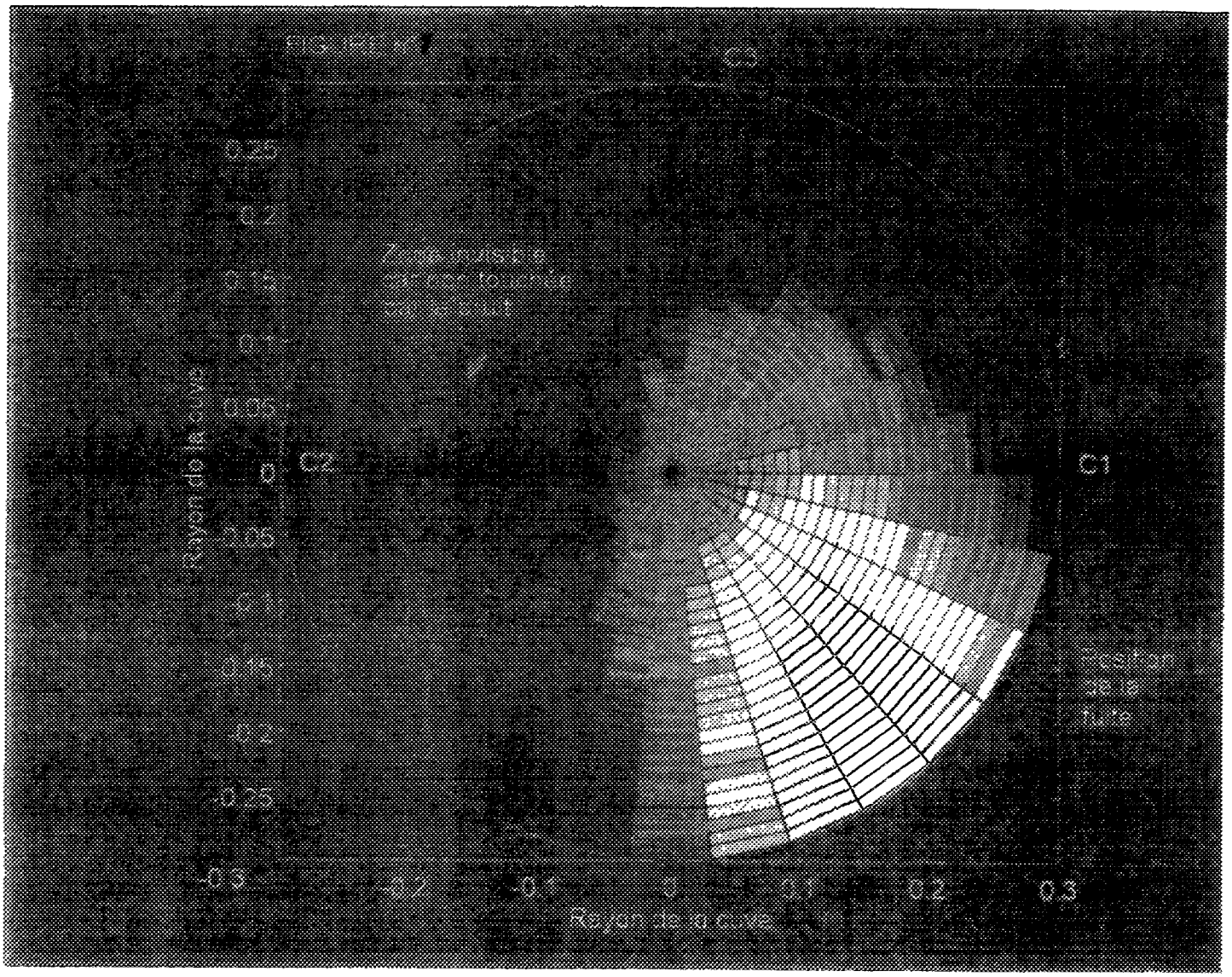

Figure 8: location of the leak with set4. 0.85 m above sensor 4

In conclusion, we found with the time domain beamformer a leak -24 dB bellow the background. The precision of the location is nearly 0.2 m, that is 30% of the diameter of the loop. We used the minimum number of sensors for a three dimensionnal location in this experiment, and we can imagine that an increasing of the number of sensors would increase the precision of the location.

It must be noted that the presence of waveguides during the experiment can affect the phase of the signal, unless we work with low frequency signal. A more precise study of the filtering of the waveguides would be important to improve the result.

5. Conclusion

We showed that time domain beamforming was capable to extract and locate leak signal -24 dB bellow the background. The knowledge of the frequency characteristics of the leak noise and the pass band filtering were necessary for the good working of the method.
However, the studies of C.Journeau in this domain show that this band of frequencies was common for all the Sodium/water reaction in several plants. The systematic using of this filter is not completly impossible.

The precision of the method depends on many factors: number of sensors for example. The British team used a 10 sensors device and obtained a precision better than 6% of the dimension of the vessel.
The knowledge of the celerity is also important. In our case, we used the value of the celerity in Sodium considering that the middle was homogeneous. But the calculation of the phase terms is pertubed by the presence of the tubes and by the dummy plate. We also do not really know the influence of the vessel and of the wave guides.

Amelioratıons in signal processing and in programming remain necessary before an application of this method as an automatical procedure for leak detection and location in steam generators. Location method should complete the application of a detection method in nuclear plants.

references

[1] I D Macleod, M Beesley, D Firth, R Rowley, C G Taylor, C Waites, "Acoustic surveillance of fast reactor Systems for LMFBRs", BNES Conf. on Science and technology of Fast Reactor Safety, Guernsey May 1986.

DETECTION OF SODIUM/WATER REACTION IN A STEAM GENERATOR: RESULTS OF A 1995 BENCHMARK TEST

L. ORIOL
Centre d'Etudes Nucléaires de Cadarache,
Saint-Paul-lez-Durance,
France

Abstract

The CEA analysis of the 1995 benchmark test has been focused on the location of the injections. Two techniques have been tested: the pulse timing technique, and the time-domain delay and sum beamforming technique. The two methods gave coherent locations of the injector even if there was a difference of 25 % of the SGU height between the vertical locations. Prior to that analysis, the RMS values of the signals were calculated in different frequency bands. The results obtained in the 200-1000 Hz were used to draw a rough estimation of the beginnings of the injections in order to determine the parts of the records on which the location signal processing can be carried out.

1. Introduction

As far as acoustic leak detection in Fast Reactor SGUs is concerned, the CEA has been studying, for the last five years, alternative acoustic methods to reduce the spurious trip rate of the classical Passive Acoustic Leak Detection (PALD) technique. Two methods have been investigated for that purpose :
- the Active Acoustic Leak Detection (AALD) technique which consists in monitoring the damping of an ultrasonic signal emitted in the SGU due to the absorption of the sound by the hydrogen bubbles produced by the water/sodium reaction [1],
- leak location techniques in order to discriminate against PALD spurious trips due to noises coming from outside of the SGU.

Thus the acoustic surveillance system proposed by the CEA for Fast Reactor SGUs is based on the following association of the three acoustic techniques : a leak is detected if it is detected by the PALD method and if this detection is confirmed by the AALD method and/or the location method.
The confirmation by the location is obtained by a rough location of the leak inside of the SGU.

The CEA analysis of the IAEA CRP 1995 benchmark test has been focused on the location of the injections using pulse timing and time-domain beamforming methods.
Prior to that analysis very simple signal processing has been applied to the data in order to determine beginnings of the injections.

All the signal treatments were carried out on SUN workstations using the Visual Numerics PV-WAVE software.

2. Preliminary benchmark records processing

PFR Evaporator 3 dimensions implies flight delays between sensors of less than 2 ms i.e. 320 samples for the **160 kHz** sampling frequency which was the one chosen for all our analyses. It is thus of great importance to have the four channels synchronized for the location studies.

For each injection, the synchronization of the four channels was carried out by evaluating the delay between channel B of a record and channel B of another record. More precisely, as only two delays are required to synchronize the four channels, delay between pair 1 and pair 2 (d_{12}) and delay between pair 1 and pair 3 (d_{13}) have been determined.

The delay between channel B of a pair record and channel B of another one was assessed thanks to the measurement of the peak delay in the cross-correlation function of the two signals.

The following table shows the delay d_{ij} calculated between pair i and pair j records ($d_{ij} < 0$ means that pair i record is in advance of pair j record, and thus that dij samples must be taken off from the beginning of pair i signals) :

Table 1 : Synchronization delays

Injection number	d_{12}	d_{13}
1	3730	465
2	-4228	-3741
3	1258	1885
4	-2106	-2471
5	-2557	-4166
6	-1730	-261
7	2228	8054
8	-1457	929

These delays have been obtained for a block of signals taken in the middle of the records (sample number 800000). It has been however noticed that variations can be observed considering another part of the records, that is to say that the speed of the magnetic recorder was slightly different from an acquisition to another one.
The resulting shift was of about 500 samples for injection 2, and less than 50 samples for the other ones.

3. Detection of the injections

A simple detection of the injection was performed in order to determine the onset time of each injection. The RMS value of the four channels in different frequency bands was calculated summing the corresponding components in the autospectra of the signals. Autospectra were calculated on 4096 samples frames, using an Hanning window. The result was median smoothed in order to eliminate impulses.

We were especially interested in the 200 Hz - 1000 Hz frequency band which corresponds to the one that was found to have the best signal-to-noise ratio for Argon injections performed in an SGU of the French Super-Phénix plant.

The analysis of the resulting RMS signals (figure 1 represents those obtained for the injection 7) gives the following times for the onset of the injections.

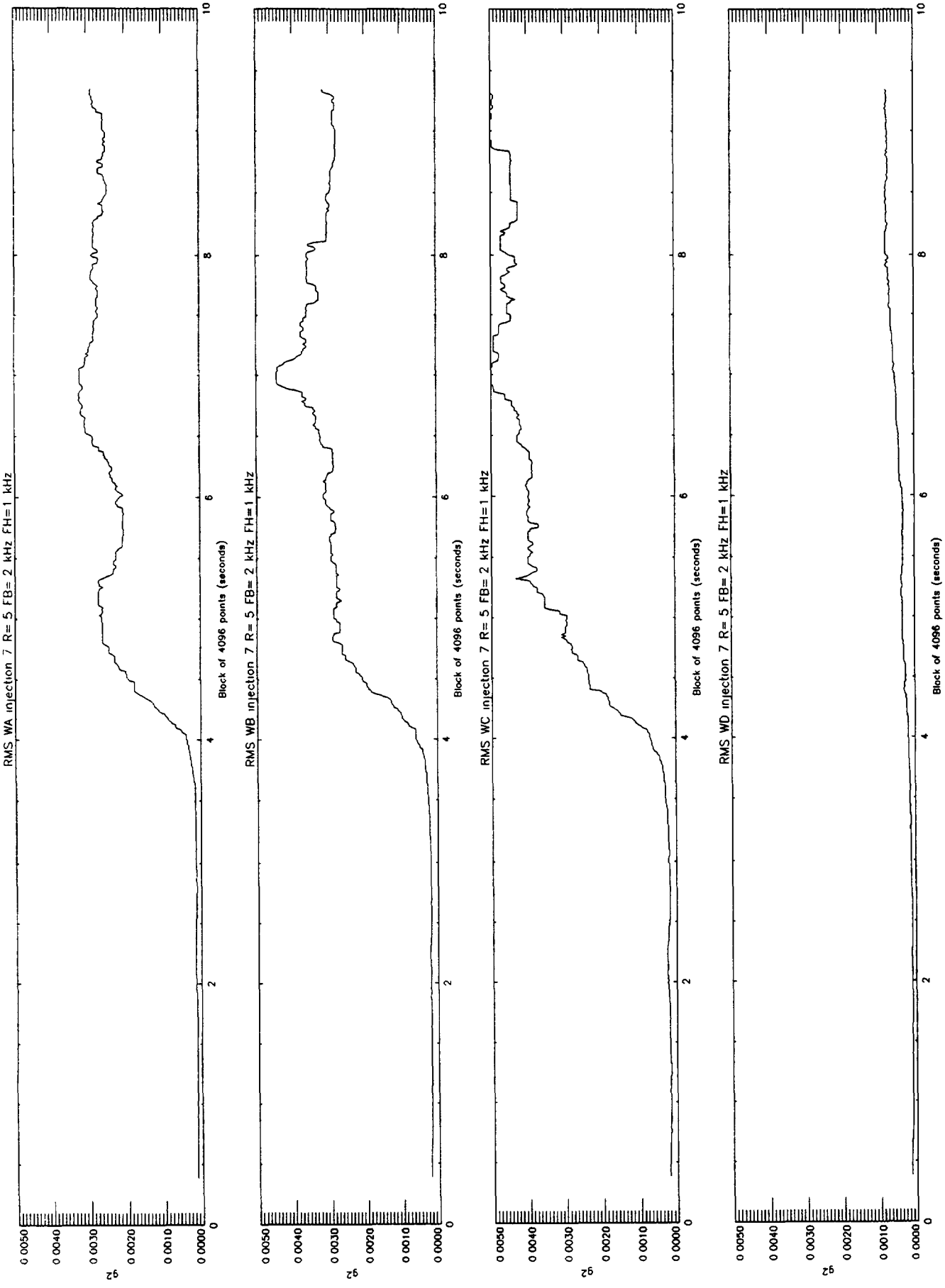

Figure 1 : RMS in the 200 Hz - 1000 Hz frequency band signals for injection 7

Table 2 · Injections onset times

Injection number	Injection onset time (s)
1	8.49
2	3.81
3	7.37
4	5.13
5	2.65
6	5.41
7	5.58
8	not found

We did not manage to read channel C signal on the CD-ROM for injection 2.

A second increasing edge can be observed in the RMS signals calculated in the highest frequency bands for injections 3, 6, and 7 (see figure 2 for injection 7). It looks like as if the injection stopped and then started again. We don't know how to explain this phenomenum. We will see with the solution of the benchmark if it is linked with the fluid injected.

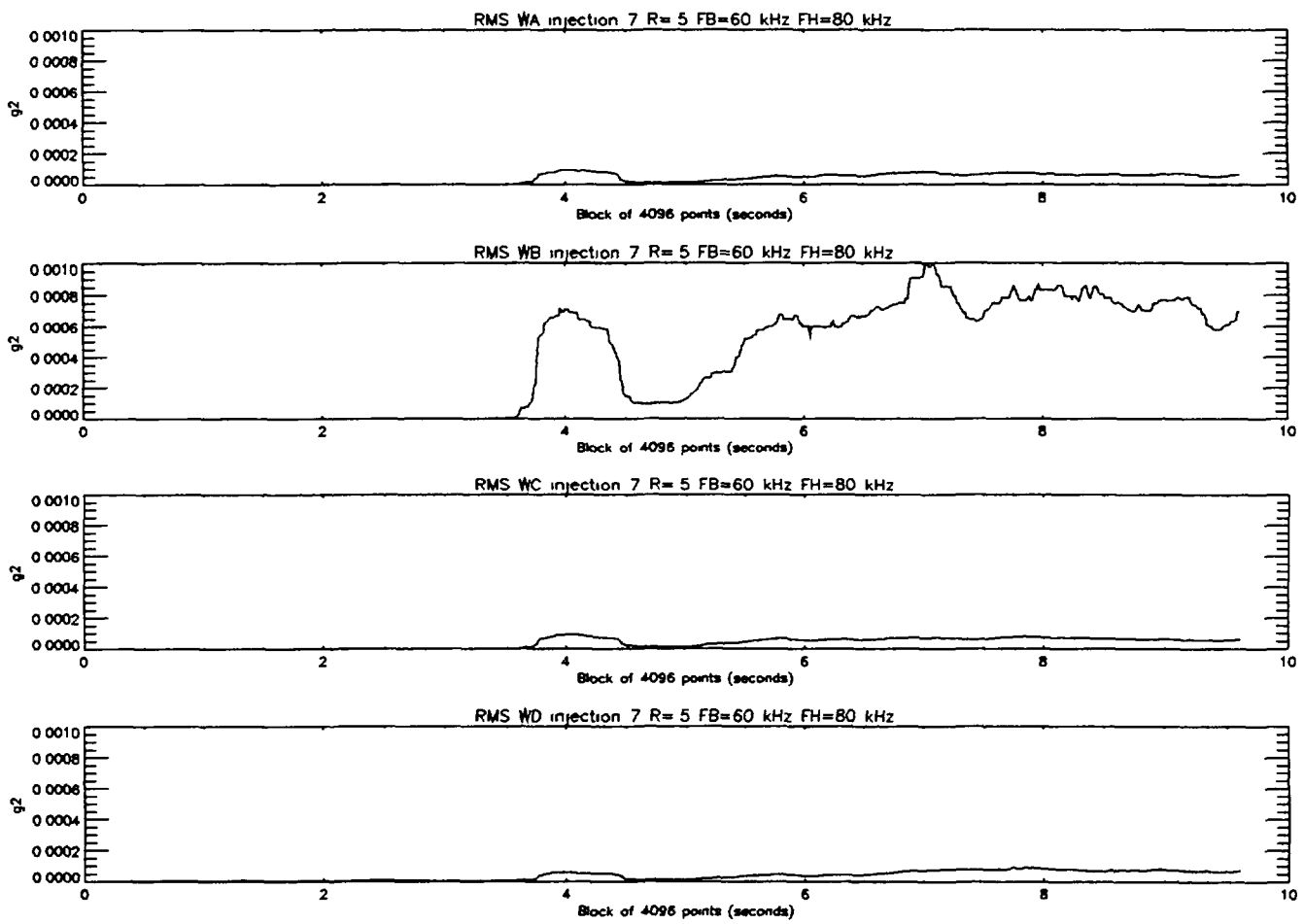

Figure 2 RMS in the 60 kHz - 80 kHz frequency band signals for injection 7

An other conclusion that can be drawn from an over-simple analysis of the RMS signals is a rough location of the injection in the SGU. As the signal received on sensor D is largely the weakest, injector should be in the lower part of the SGU underneath sensors A and C. As signals on sensors B and C are bigger than the one on sensor A, we can suppose that the injector in located in the north or north-east sector of the SGU.

4. Location of the injections

4.1. Pulse timing

4.1.1. Description of the method

Pulse timing is the simplest method that can be applied when the signals are clear, for example a large anomalous pulse. Location is then determined by a direct comparison of the signals from the detectors to determine the difference in the transmission time of the signal to each of a pair of transducers.
Once again these time differences can be drawn by a cross-correlation method.

4.1.2. Results

We calculated the cross-correlation functions on signals filtered in different frequency bands.
Figures 3a and 3B show some results obtained in low frequency bands. It is not possible to draw a proper correlation peak from these results.
However we obtained nice correlation peak for 30 kHz high-pass filtered signals. Figure 4 shows the cross-correlations calculated for the injection 7. Similar results have been obtained for the other injections.

Considering sodium-borne transmissions, and taking a sound velocity of 2400 m/s (sodium temperature between 300°C and 350°C), the results of this high-frequency pulse timing analysis is that the injector was in average 1.20 m (0.5 ms) closer from sensor B than sensor C, and also in average 1.44 m (0.6 ms) closer from sensor B than sensor A. The cross-correlations between signals received on B and D show different peaks from about 2 ms to about 4 ms, and it is difficult to chose the good one.

Assuming first that the SGU is still a cylinder 1.5 m underneath waveguide B, and secondly that the direct paths between waveguides B,C and A through the sodium are close from the ones in the shell , the hyperbola drawn from these results are represented on figure 5.
The injection is thus located in the hemi-spherical part of the SGU with a rough precision due to the hypotheses we had to make.

4.2. Time domain beamforming

4.2.1. Description of the method

As for the IAEA CRP 1994 benchmark test, we used the simplest beamformer, the delay and sum one, to attempt to locate the leak.

In that method, the correlation value is obtained by calculating the distance from the point of focus to each of the sensors on the shell. We also assume here that the sound takes direct paths through the sodium from the focus point to the sensors. The distances are then divided by the velocity of sound (also taken here of 2400 m/s) to give the transit times which in turn are

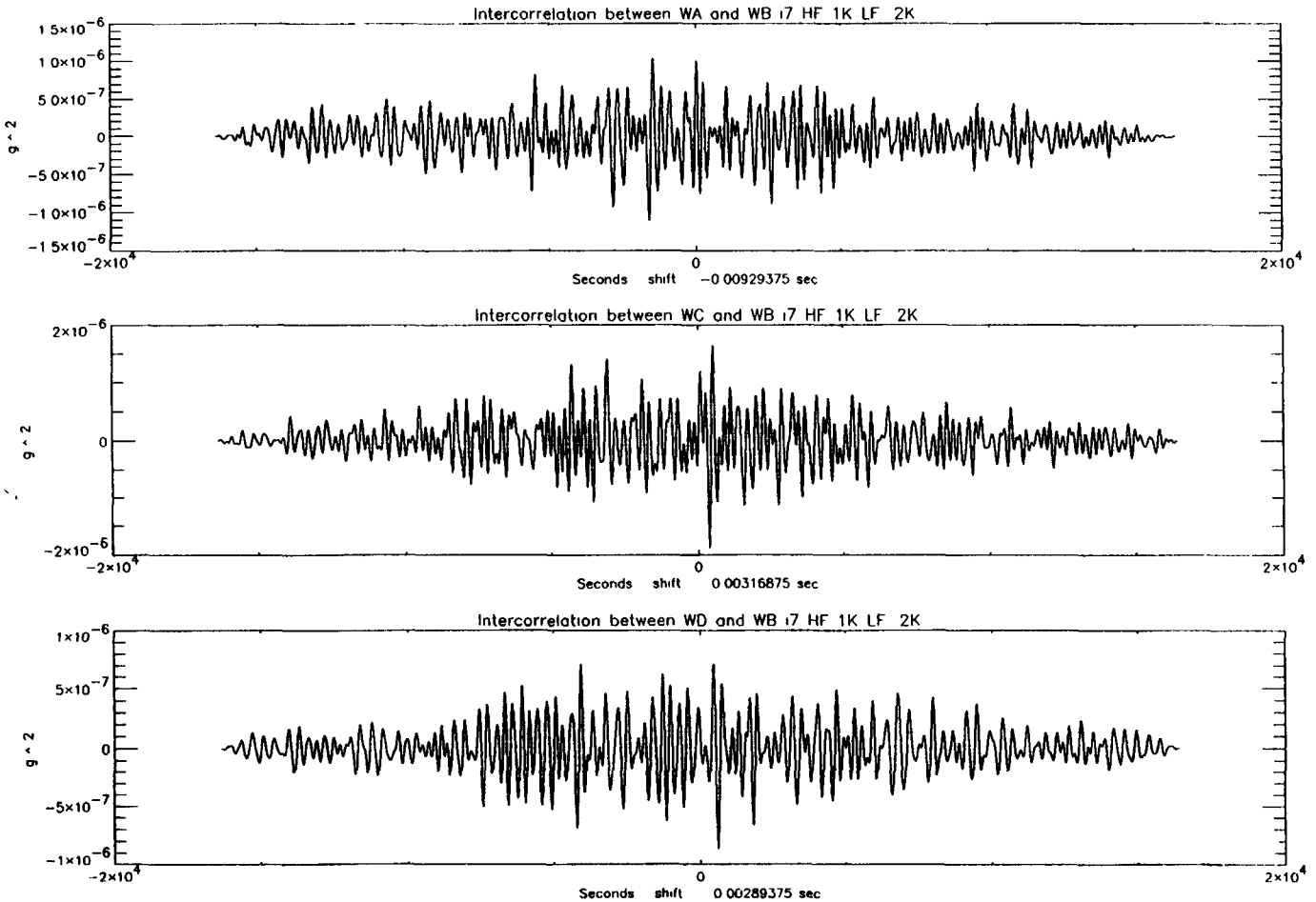
Intercorrelation between WA and WB i7 HF 1K LF 2K
1.5×10^-6
1.0×10^-6
5.0×10^-7
0
-5.0×10^-7
-1.0×10^-6
-1.5×10^-6
g^2
-2×10^4
0
2×10^4
Seconds shift -0.00929375 sec
Intercorrelation between WC and WB i7 HF 1K LF 2K
2×10^-6
0
-2×10^-6
g^2
-2×10^4
0
2×10^4
Seconds shift 0.00316875 sec
Intercorrelation between WD and WB i7 HF 1K LF 2K
1×10^-6
5×10^-7
0
-5×10^-7
-1×10^-6
g^2
-2×10^4
0
2×10^4
Seconds shift 0.00289375 sec

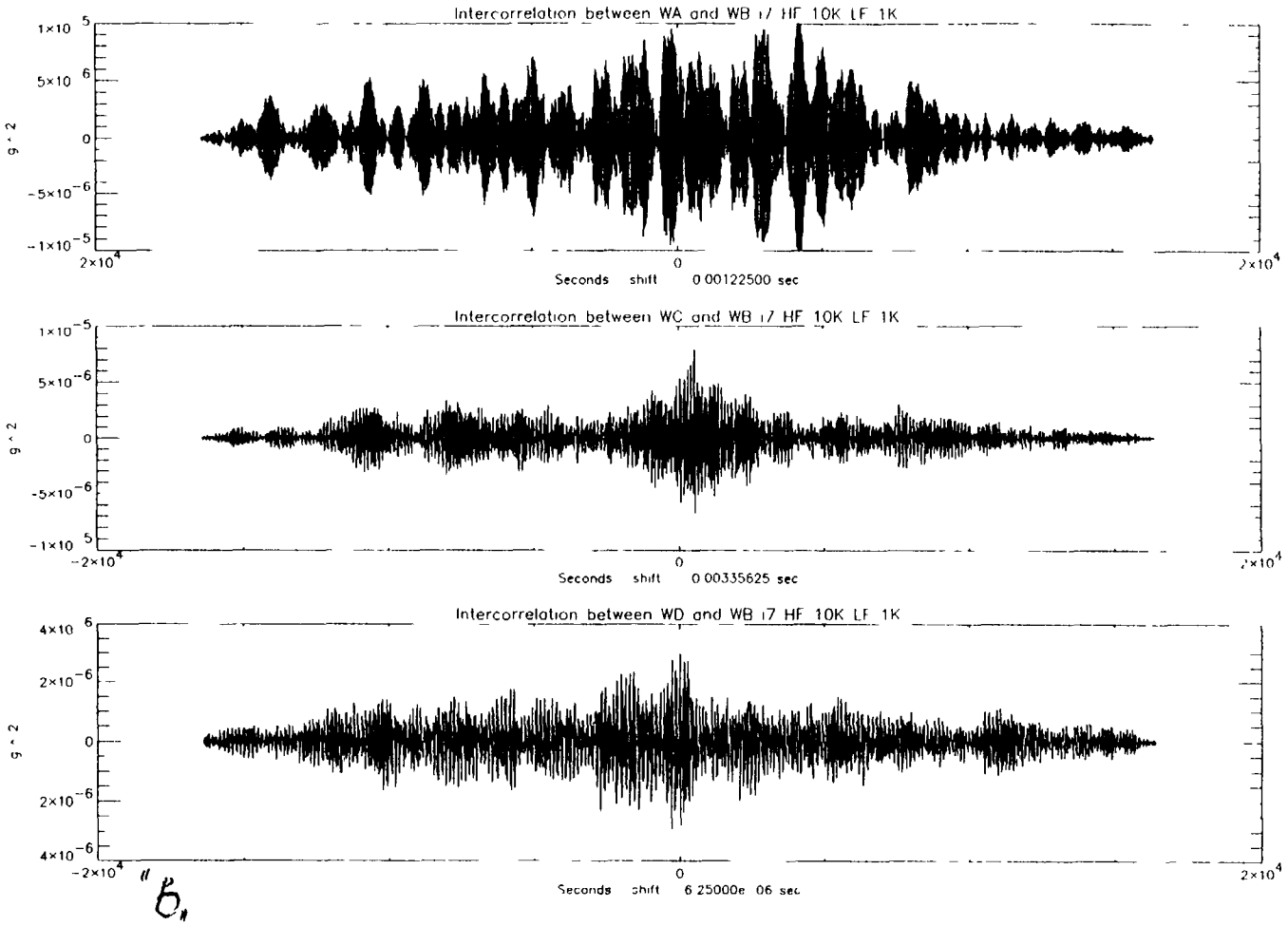

Figure 3 : Cross-correlation fonctions for injection 7 in the lower frequency band

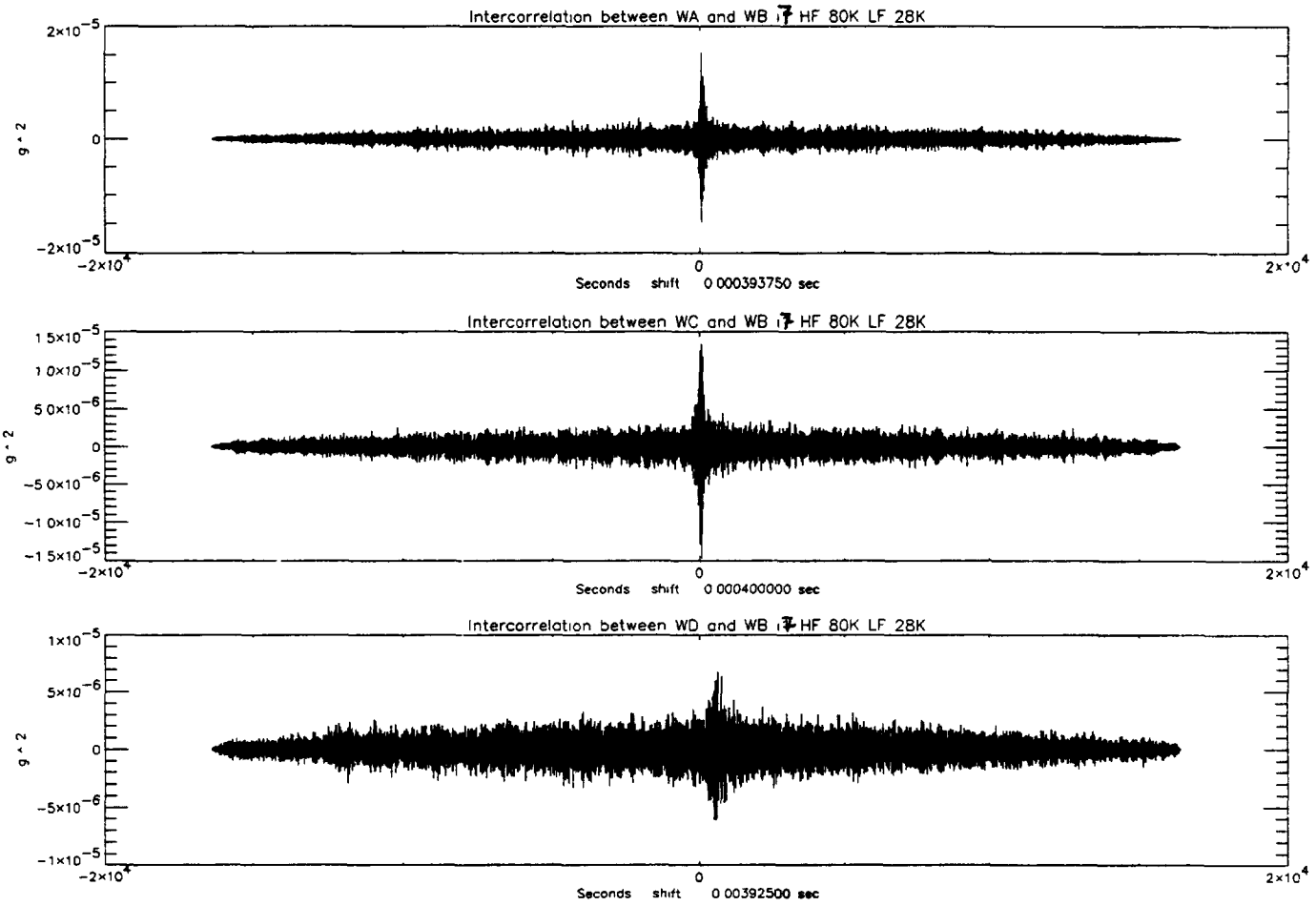

Figure 4 : Cross-correlation fonctions for injection 7 in the higher frequency band

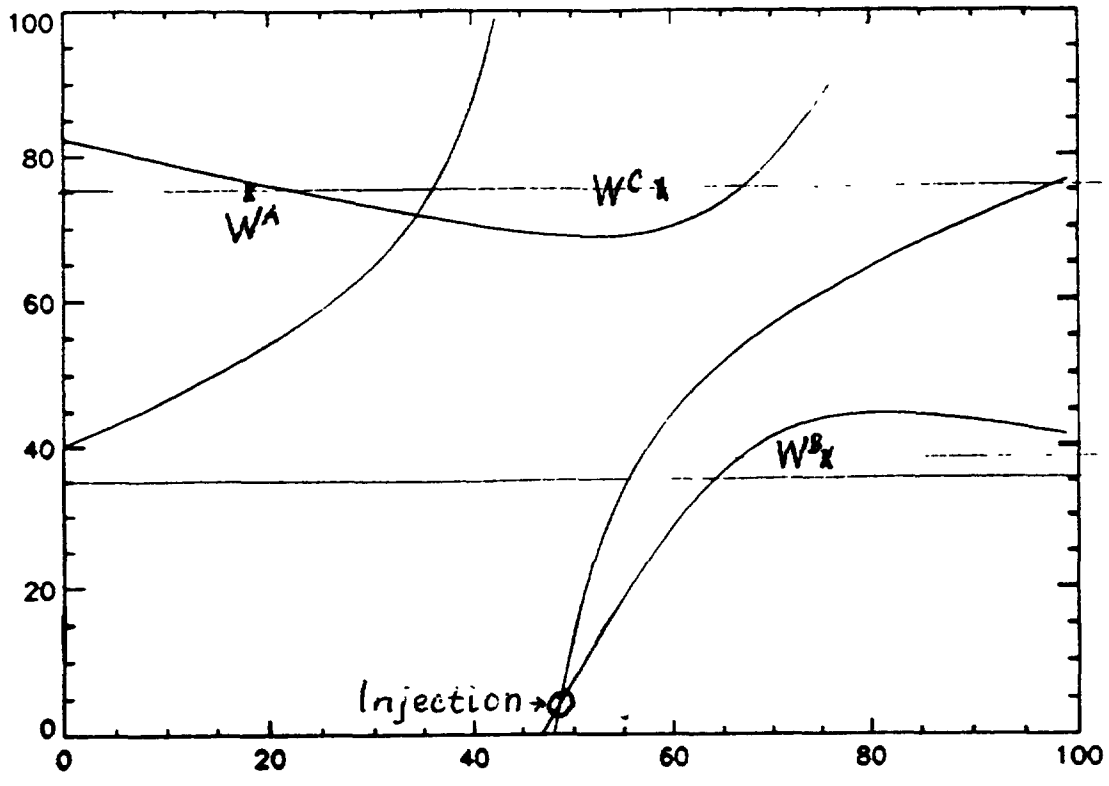

Figure 5 : Pulse timing location of the injection

divided by the sampling interval used in the digitizing process to express the transit times as numbers of time points in the digitized records. The records can then be shifted by these amounts so that a signal emanating from the focus point will appear at the same time point in all records. The records are then added and squared to give a measure of the acoustic power from that point.
See the CEA 1994 benchmark test report for more details concerning the mathematical aspect of this beamformer.[2]

The volume inside Evaporator 3 was gridded with a rectangular grid, but only horizontal sections of this volume are shown in the figures of this report. The levels of these sections were measured from the lower point of the hemi-spherical part of Evaporator 3. Horizontal axes were chosen in such a way that the north direction was up and the east direction was to the right. Moreover the color images obtained on the workstation screens to represent the beamformed acoustical intensity maps are replaced here by contour plots.

The signals were digitally filtered using FIR band-pass filters in the 200 Hz - 1000 Hz frequency. This frequency band was determined for geometrical reasons as well as for the fact that it was found to be optimal for the detection of argon injections at the Super-Phénix plant.
Although the leak signal frequency determines the resolution that can be achieved in its location (the higher is the frequency, the greater is the resolution), if it corresponds to a wavelength smaller than the spacing between sensors, then subsidiary peaks due to space aliasing will be introduced in the plot of correlation.
Each sensor being at most about 2.5 meters away from its nearest neighbor, we should not exceed a maximum frequency of 1 kHz. We actually observed such aliasing effects on the benchmark test records for which a location was achieved in the lower frequency band.

4.2.2. Results

The main result of our study is that it is much more difficult to locate an injection occurring in an actual SGU than in a rig. It is likely due to the fact that the transmission of sound through an actual SGU is much more complex, especially in PFR Evaporators which have a double shell.

Figure 6 represents the correlation plots obtained at different levels of the SGU, at the same moment, for the injection number 7 considered from the 4.0 s time point to the 4.0125 s time point (2000 samples). Level 0 is 0.5 m high (above the lower point of the hemi-spherical part of Evaporator 3), and the spacing between levels is 0.25 m. The sharpest correlation peak is observed at level 7, that is to say at 2.25 m high. That is much more higher than the location determined by high frequency pulse timing, but the north-east orientation is confirmed.

We then tried to obtain successive pictures of the acoustic intensity field at the level where the injection was located. Figure 7 represents the correlation plots obtained on injection 7 for the samples from the 4.0 s time point to the 4.00625 s time point (1000 samples), and then for the samples from the 4.00625 s time point to the 4.0125 s time point (1000 samples). The event located during the first interval has faded away during the second one.

That shows that the beamforming technique can only locate very precise noisy events which have to be detected prior to the location search. It can be easily understood that the longer the signal to locate is, the more the presence of paths between source and sensor other than directly through the sodium impede the performance of the beamformer. Studies are in progress to detect significant events automatically.

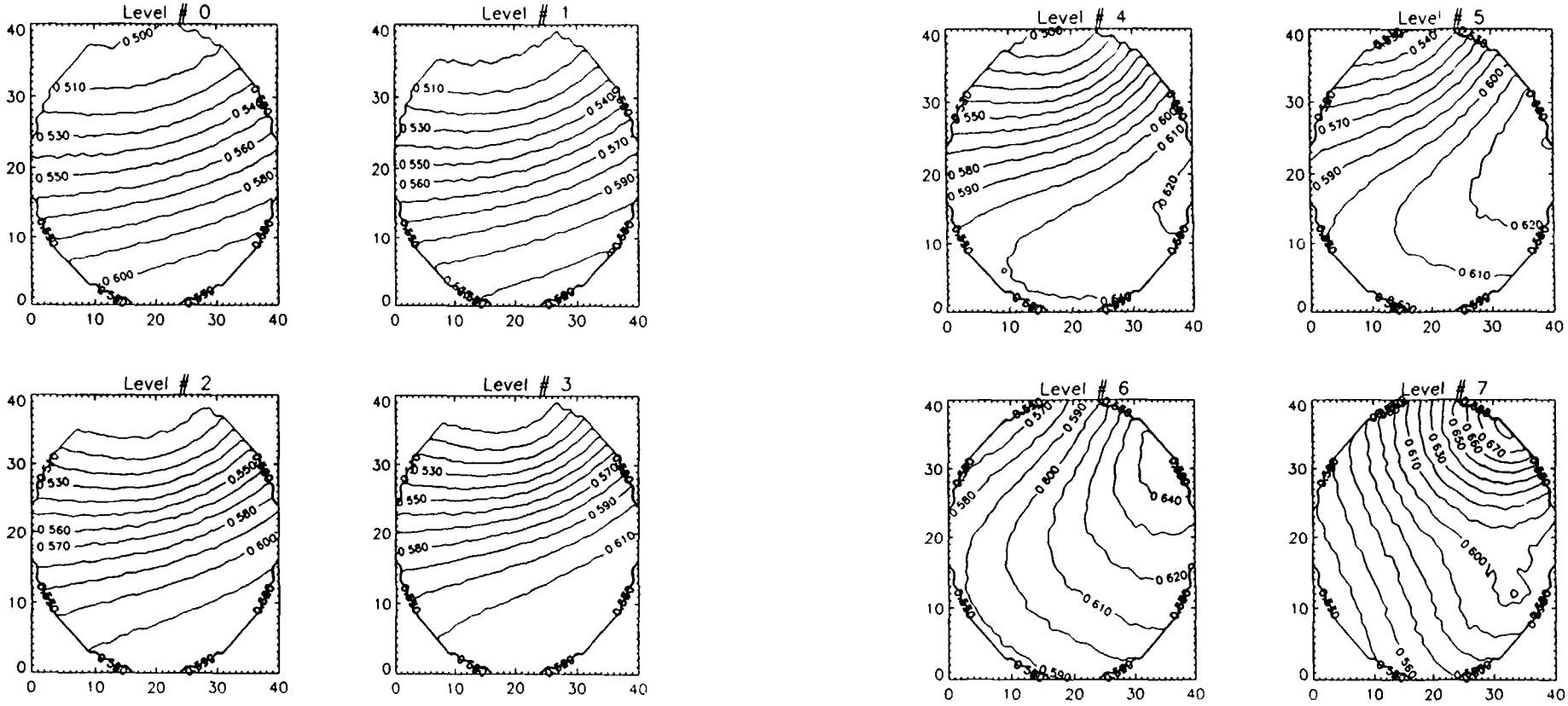

Figure 6 · Beamformed correlation plots for injection 7 at different levels

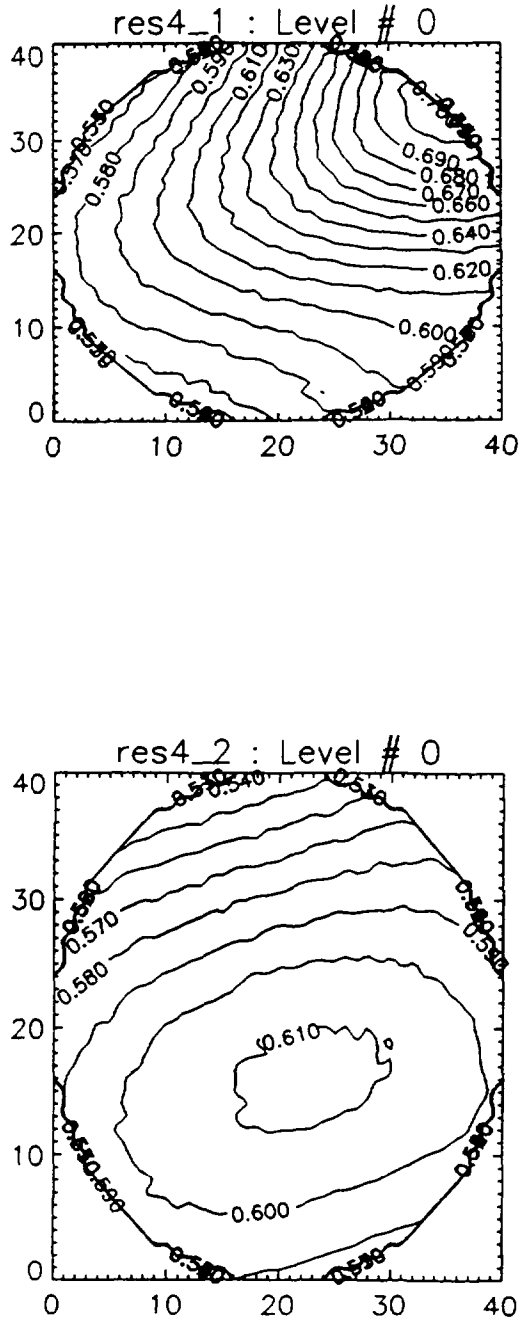

Figure 7 : Successive beamformed correlation plots at the 2m level for injection 7

The same 2 meter high, north-east oriented location was found for two or three other injection by chance. Figure 8 represent two examples corresponding to injections 1 and 3.

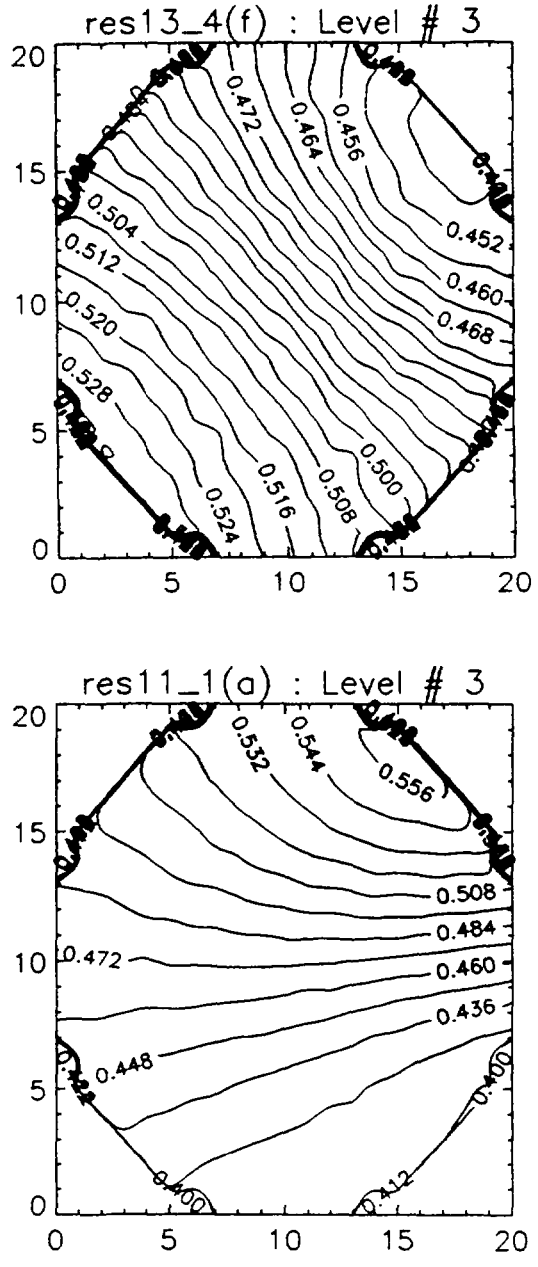

Figure 8 : Beamformed correlation plots obtained at the 2m level for injection 1 (a) and injection 3 (b)

5. Conclusions

We had more difficulties for that benchmark test than for the last one to achieved location of the injections. It should be reminded first that the conditions of the test were much more stringent. The fact that injections were performed in an actual SGU and not in a rig is not the only reason of the difficulties we met.

First of all, the design of a PFR evaporator with its double shell makes the transmission of the sound through the SGU more difficult to understand and thus to represent, since it multiplies the possibilities of different acoustical paths from source to sensor. In particular, the hemi-spherical double-shell part of the SGU was not easy to take into account in our calculations.

The layout of the transducers on the shell was not ideal either. We know that the performance of the beamformer decreases as the distance of the source from the transducer plane increases, unless the scan volume is comprised between two transducer planes. Because it was simpler to analyze, we were interested in correlation plots in horizontal sections although the transducer plane was rather vertical.

The lessons we learn from that benchmark test are :
– improvements should be obtained working with higher frequency signals since we observed sharper peaks in the cross-correlation functions when increasing the frequency. But it will require to have much more sensors on the shell of the SGU to monitor.
– we understood that it was necessary to develop signal processing techniques to extract from the signal the short significant acoustical manifestations of the leak that can be located.

REFERENCES

[1] L. ORIOL, Ch. JOURNEAU. Active Acoustic Leak Detection in SGUs of Fast Reactors. SMORN VII Proceedings, Avignon (France), June 1995.

[2] C. CORNU. Report for the IAEA CRP 1994 benchmark test.

VERIFICATION AND IMPROVEMENT OF THE SIGNAL PROCESSING TECHNIQUE USING EXPERIMENTAL DATA

O.P. SING, G.S. SRINIVASAN,
R.K. VYJAYANTHI, R. PRABHAKAR
Indira Gandhi Centre for Atomic Research,
Kalpakkam, India

Abstract

International Atomic Energy Agency (IAEA) has organised the Co-ordinated Research Programme (CRP) on Acoustic Signal Processing for the Detection of Boiling or Sodium/Water Reaction in LMFR over the period 1990–1995. This was an extension of an earlier CRP on Signal Processing Techniques for Sodium Boiling Noise Detection which ended in 1988. The objectives of the extended CRP were to evaluate the suitability of signal processing techniques for the detection of boiling noise under very poor signal to noise ratio conditions and then to develop the techniques further to cover leak detection in the Steam Generator Units of Liquid Metal Fast Reactors.

The Indian analysis showed that Determinant and Trace features and Adaptive Learning Network technique were able to detect with very good discrimination boiling signals down to a signal to noise ratio (S/N) of −12 dB. Determinant and Trace features were very sensitive to boiling noise and could detect signals even down to −21 dB S/N, but with a lower reliability of detection. Among the various analysis techniques evaluated by India on the acoustic leak noise data during the period 1991-1994, Determinant and Trace of covariance matrix constructed from auto power spectral density proved to be the most sensitive features for leak noise detection. These features have detected leak signals even down to −24 dB S/N, but with reduced reliability of detection below −16 dB.

The data for the final year of the CRP (1995) were generated from the end-of-life acoustic leak experiments on the evaporator unit of the Prototype Fast Reactor at Dounreay, United Kingdom. The Indian analysis on this data pertained to the detection of onset and duration of leak signal, to the identification of injection medium, to the determination of leak noise transmission characteristics and to the detection of leak location.

1.0 INTRODUCTION

International Atomic Energy Agency (IAEA) has organised the Co-ordinated Research Programme (CRP) on Acoustic Signal Processing for the Detection of Boiling or Sodium/Water Reaction in LMFR and the initial objectives of this CRP were formulated in a consultants' meeting in 1989. This became an extended programme of the earlier CRP on Signal Processing Techniques for the Sodium Boiling Noise Detection organised during 1983-1988. The initial objectives of the

new CRP were to investigate the suitability of the signal processing techniques for detecting boiling signals buried in background noise under very poor signal to noise ratio (S/N) conditions and to develop them further to cover leak detection in Steam Generator Units (SGU) of LMFRs. The other objectives which evolved during the progress of the CRP included application of multichannel analysis, testing of localisation techniques and testing of analysis techniques on field data from the Prototype Fast Reactor (PFR) at United Kingdom.

The Indian analysis evaluated a number of statistical features and analysis techniques for both boiling noise detection and leak detection. Determinant and Trace of covariance matrix constructed from auto power spectral density of the data were found to be very sensitive to the boiling noise and could detect boiling noise with good reliability in data with S/N down to −12 dB. These features could also *detect boiling signals down to −21 dB S/N but with reduced reliability.* A two generation Adaptive Learning Network (ALN) technique was also evolved and this could detect boiling down to −12 dB. Among the various analysis techniques evaluated on the acoustic leak noise data, Determinant and Trace proved to be the most sensitive features for leak noise detection. These features have detected the leak signals even down to −24 dB S/N, but with reduced reliability below −16 dB.

The data made available to the participants during the final year of the CRP (1995) were prepared by UK using the data from background noise measurements on PFR SGUs and from the end-of-life acoustic leak experiments carried out on PFR evaporator-3. In these experiments, argon, hydrogen and water/steam injections were carried out and acoustic noise was measured at different locations. This was the first set of data in which both the background and leak noise signals were obtained from the same unit. Analysis carried out on this data by the Indian team pertain to the detection of onset and duration of leak, to the identification of injection medium, to the determination of leak noise transmission characteristics and to the detection of leak location.

This report contains a brief resume on the status of acoustic surveillance technology for SGU leak detection and a summary of results obtained from Indian analysis of ASB loop leak noise data in 1993 and of multichannel leak noise data in 1994. The report then discusses in detail the results obtained from the Indian analysis of data from PFR end-of-life experiments. The final part of the report includes conclusions and recommendations for future programme.

2.0 STATUS OF ALD DEVELOPMENT

The existing fast reactors depend on in-sodium hydrogen detectors for detecting steam leaks in SGUs and in some fast reactors, in-cover gas hydrogen detectors have been additionally used. These detectors have long detection times and hence do not provide protection against all leak rates. Acoustic Leak Detection (ALD) system which is faster in response, is emerging as a promising supplementary method and is being developed in all the countries interested in fast reactor programme. Experimental ALD systems have been installed and tested in reactors like Prototype Fast Reactor (UK), Phenix and Super Phenix (France), KNK-II (Germany), Monju (Japan), BOR-60 and BN-600 (Russia) and Fast Breeder Test

Reactor (India). These systems are basically passive devices which respond to the noise generated due to leak. In France, an active ALD system is also being developed which depends on the effect of changes in the transmission characteristics due to hydrogen bubbles on ultrasonic sound beam. Details on world-wide development programmes are available in the Proceedings of the Specialists' Meeting on Acoustic/Ultrasonic Detection of in Sodium Water Leaks on Steam Generators, IWGFR/79, Oct., 1990.

In the Indian fast reactor programme also, the need for acoustic leak detection system in SGUs has been well recognised. The ALD system is required to play a supplementary role to in-sodium and in-cover gas hydrogen detectors. Faster response of ALD system and its ability to detect leaks, even in stagnant regions within the SGU have prompted this approach.

An experimental ALD system has been installed on one of the four steam generator modules in the 40 MW(t) Fast Breeder Test Reactor at Kalpakkam [1]. Background noise measurements at power levels upto 10.2 MW(t), which is the maximum power attainable with the present small carbide core, and simulation experiments have indicated that at such low power levels, a steam leak greater than 0.3 g/s can be detected with a simple feature like RMS value [2]. At higher power levels, background noise would increase and more involved signal processing techniques would be required to detect the leak signal. The IAEA-CRP has successfully demonstrated the suitability of various analysis techniques for detecting leak signals even under very poor S/N conditions and the on-line PC-based leak detection system under development here would incorporate such techniques.

Experiments to establish an in-situ test method using low pressure argon injections in the steam generator module have yielded encouraging results.

3.0 SUMMARY OF WORK DONE DURING 1993

The test data were prepared by mixing leak noise from ASB loop, Bensberg, Germany with background noise from PFR superheater-2. Similar measuring equipments were used in both the experiments. The S/N in four records ranged from −8 dB to −20 dB. The special feature of this data was that two sets of synthesised data were prepared, with leak rates of 1.8 g/s and 3.8 g/s respectively and this provided an opportunity to check whether processing techniques are influenced by the leak rate.

Results from the Indian analysis are reported in Ref.3. The Determinant and Trace of the covariance matrix constructed from auto power spectral density emerged as two sensitive features and could detect clearly both the onset and duration of leak signals in files with S/N of −12 dB and −16 dB. These features were sensitive for both the leak rates. The presence of leak noise in data with S/N of −20 dB was identified, but the detection could not be claimed to be reliable. Analysis also showed that Determinant and Trace features evaluated through diagnolisation of the covariance matrix were relatively more sensitive.

4.0 SUMMARY OF WORK DONE DURING 1994

The test data contained four channels in which leak noise data (3.8 g/s) measured at four locations in ASB loop were mixed with background noise measured on PFR superheater at four waveguide locations. Similar measuring equipments were used in both the experiments. S/N in the test files ranged from −6 dB to −24 dB.

Results from Indian analysis are reported in Ref.4. Features PSD-SUM (sum of PSD values in selected frequency bands), Determinant and Trace indicated that detection was best for channel 2, followed by channels 3,1 and 4. Detection of leak noise was possible even for the case of −24 dB in channel 2 using Determinant feature. Determinant and Trace features detected leak signals with better detection margins. The PSD-SUM feature could detect the leak signals only to −16 dB.

Cross correlation technique and cross power spectrum density phase plots did not give positive results for determining the leak location. Sinusoidal profile was observed in cross correlation plots which was attributed to the presence of strong sinusoidal component at around 1 kHz in the data. After the 1994 Research Co-ordination meeting at Kalpakkam, India, delay and sum beam forming technique was tested. The leak location was identified to be in the plane 0.868 m above the sensor-4 plane and this matches well with the French results [5,6].

5.0 RESULTS FROM ANALYSIS OF 1995 DATA

5.1 Description of Test Data

The test data were prepared by UK using the data from background noise measurements on PFR evaporator 3 and superheater 3 when the reactor was running at full power and from the end-of-life acoustic leak experiments carried out on evaporator 3. In these experiments, argon, hydrogen and water/steam were injected into sodium and acoustic noise was measured at different waveguide locations. During the injection experiments, the reactor was in shutdown condition with the steam generator tube side padded and the secondary sodium pump running at a reduced speed. All the acoustic data were obtained using accelerometers fitted on waveguides.

Data contained following files:

- Evaporator background noise from two waveguides
- Superheater background noise from two waveguides
- Data from four waveguides for two different hydrogen injection rates
- Data from four waveguides for three different argon injection rates
- Data from four waveguides for three different water injection rates

The data were supplied in digital format at two speeds of digitisation, the faster speed data being specifically prepared for time delay measurements.

Following objectives were defined for the analysis:

- **Detect onset and duration of injection signal**
- **Identify the injection medium**
- **Determine the signal transmission characteristics**
- **Locate the injection spot**
- **Characterise the evaporator and superheater background noise at full power**

It is interesting to note that the following parameters were varied during the end-of-life acoustic leak experiments at PFR [7] and the CRP participant did not have a prior knowledge of the parameters which existed during the injections pertaining to test data.

- **Injection medium**
- **Injection rate**
- **Injection pressure**
- **Location of injection (interspace or tube bundle)**
- **Diameter of orifice**
- **Sodium temperature**

5.2 Onset Time and Duration of Injection

The injection data files contain in the beginning background noise due to sodium flow in the evaporator and then the injection signal. For detecting the injection signal, statistical features like variance, PSD-SUM, Determinant and Trace were evaluated for all the four waveguides. Variance was not found to be a sensitive feature.

5.2.1 PSD-SUM Feature

For the present analysis, PSD-SUM is defined as the sum of the power in the first 30 frequency lines in the PSD which covers a frequency band upto approximately 5 kHz. This was found to be a sensitive frequency band for detecting leak signals in the CRP analysis during 1992-94.

PSD-SUM could detect distinctly the injection signal at all the four waveguides for Injection File 5 (Fig.1) and at waveguide C in Injection Files 6 and 7.

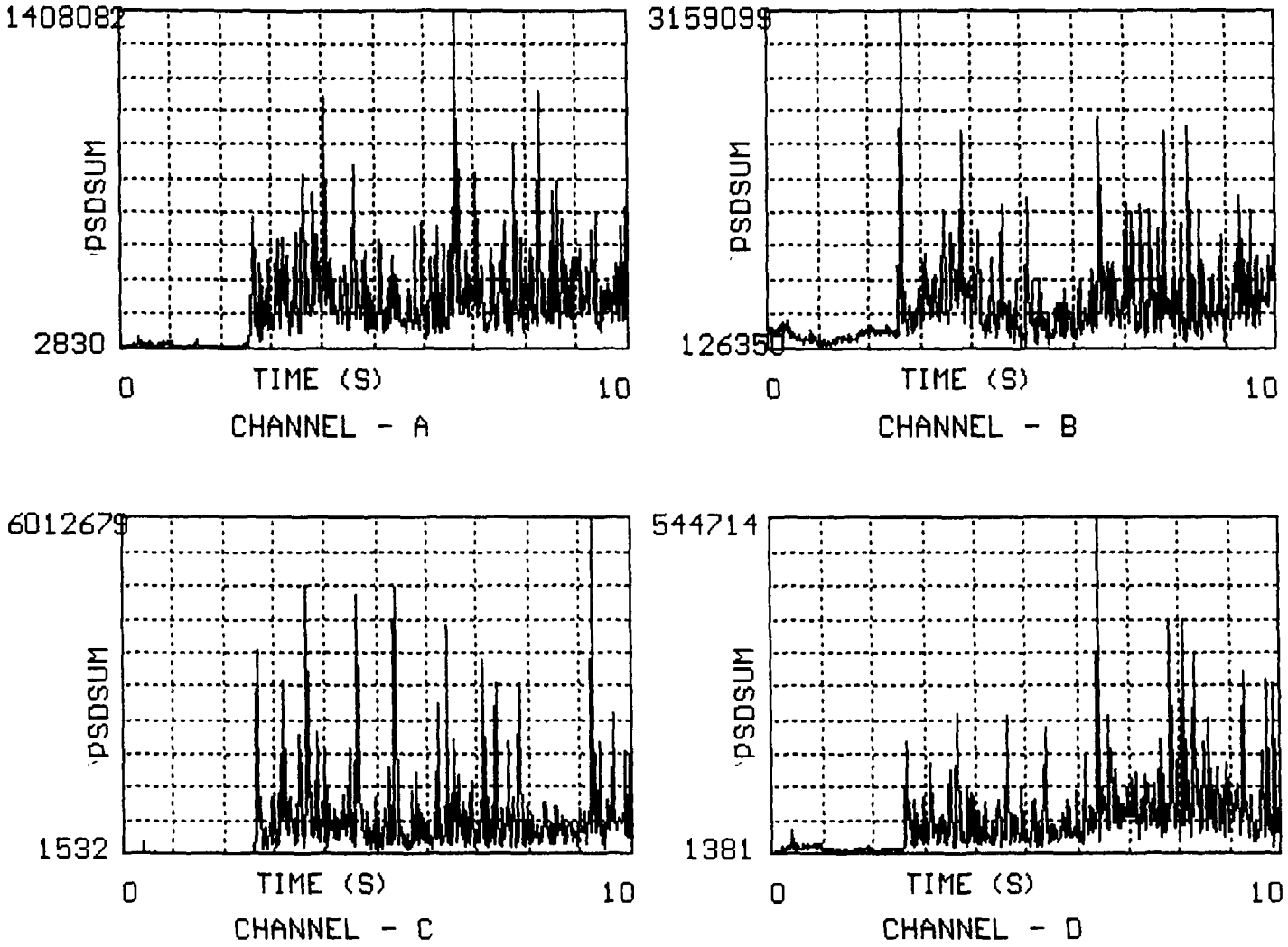

FIG.1 : PSDSUM VALUE VS. TIME FOR INJECTION5

In the case of Injection File 3, an increase is seen towards the end of the file in waveguides A, B and C long after the initiation of the injection.

Results from PSD-SUM are given in Table 1.

5.2.2 Determinant and Trace

As mentioned earlier in this report, Determinant and Trace features are very sensitive for detecting the leak signal. These are calculated by forming the covariance matrix from the auto power spectral density. For the present analysis, 512 line PSD was calculated in the known background region and in an assumed injection region. At each frequency line, the ratio of power in the two regions was estimated and the best ten spectral lines were identified for each leak and waveguide. The APSD values at these frequencies formed the input to the covariance matrix.

Fig.2 to Fig.9 show the results obtained from Determinant feature for the eight injections and 4 waveguides. Similar results were obtained for Trace feature also. Tables 2 & 3 give the onset time, duration and discrimination (ratio of features in injection and background regions) for Determinant and Trace respectively. The results demonstrate that these two features have detected the injection signal in five out of the eight injection cases; at all the four waveguides for Injection Files 5 and 6 and at atleast two waveguide locations in Files 1 and 7.

5.3 Injection Medium

5.3.1 Review of Literature

Noise produced by leak of steam/water into sodium in a SGU can be considered to be due to sources like jet noise (due to turbulence in the steam jet and its impingement on a target), reaction noise (including noise from sodium boiling under larger leak rates) and bubble noise (due to oscillations of hydrogen bubbles and bubble entrained flow noise). However in the case of argon injection, the reaction noise would be absent. In addition to acting as a source of noise, gas bubbles (hydrogen or argon) also tend to attenuate the noise in certain frequency bands. During their passage with the flowing sodium, hydrogen bubbles tend to go into solution depending on the sodium temperature, whereas the argon bubbles remain in sodium till they can escape into a cover gas space. Because of these phenomena, the characteristics of the noise produced can depend on the injection medium.

Many experimental results comparing different injection media have been published in literature and some of the results are highlighted below:

- Studies in experimental sodium loops in France showed an acceptable similarity between the noise produced by steam leak into sodium and the noise produced by injection of inert gas through a small orifice. Their results show similar power spectral densities for argon and water injections at the same mass flow rate in sodium at 773K through a 0.8 mm diameter orifice [8].

Table 1 Detection of Leak (PSD-SUM)

Injection Number	Waveguide A			Waveguide B			Waveguide C			Waveguide D		
	Onset	Duration	Detection Margin	Onset	Duration	Detection Margin	Onset	Duration	Detection Margin	Onset	Duration	Detection Margin
1	–	–	–	–	–	–	–	–	–	–	–	–
2	–	–	–	–	–	–	–	–	–	–	–	–
3	–	–	–	–	–	–	–	–	–	–	–	–
4	2.25	7.55	13.27	1.96	–	–	–	–	–	–	–	–
5	2.61	7.19	28.66	2.67	7.13	9.53	2.66	7.14	43.92	2.66	7.14	20.65
6	–	–	–	–	–	–	5.29	4.51	15.15	–	–	–
7	–	–	–	–	–	–	3.63	6.17	10.14	–	–	–
8	–	–	–	–	–	–	–	–	–	–	–	–

NOTE:

Onset and Duration in seconds.

Detection Margin in dB

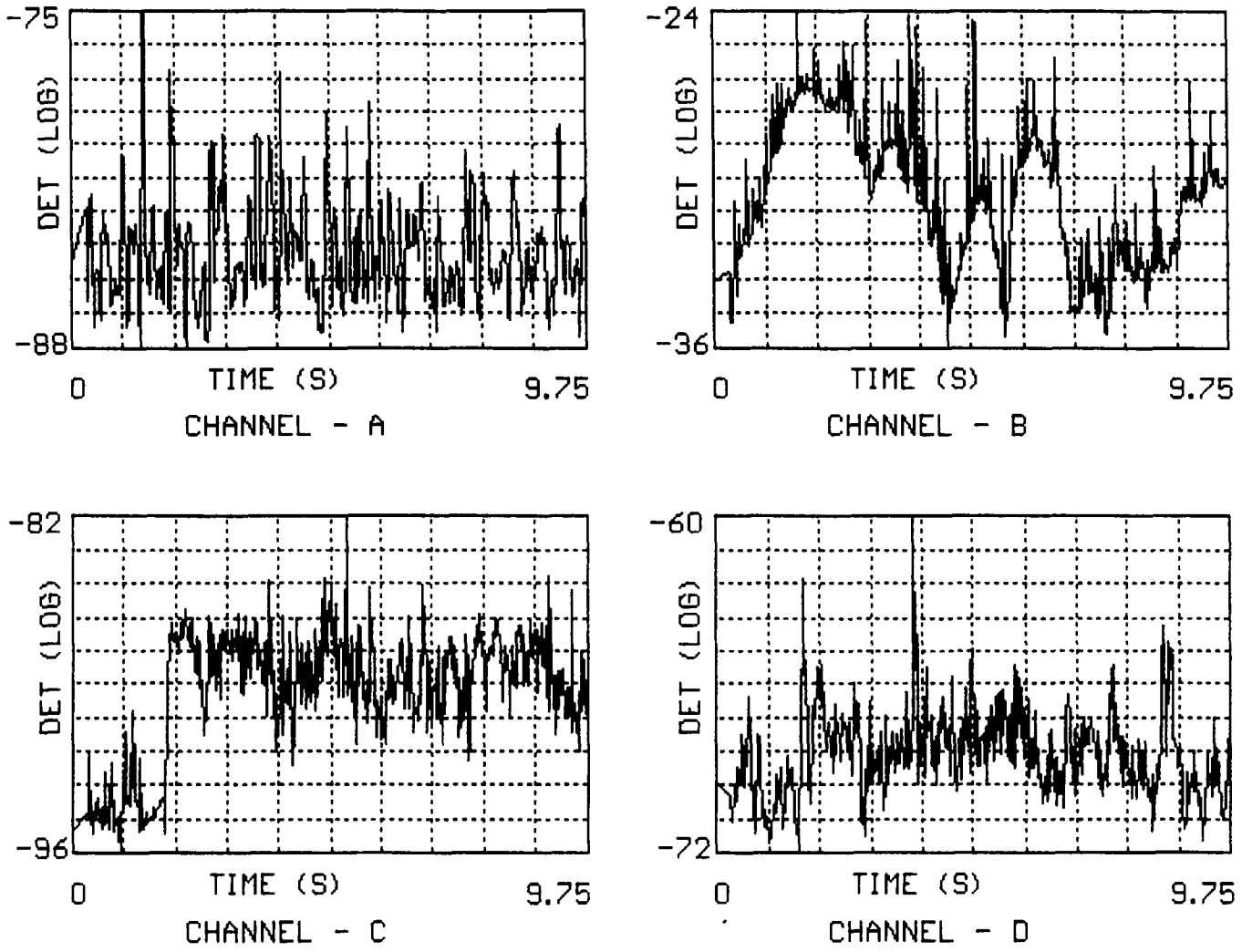

FIG. 2 : DETERMINANT VALUE VS. TIME FOR INJECTION 1

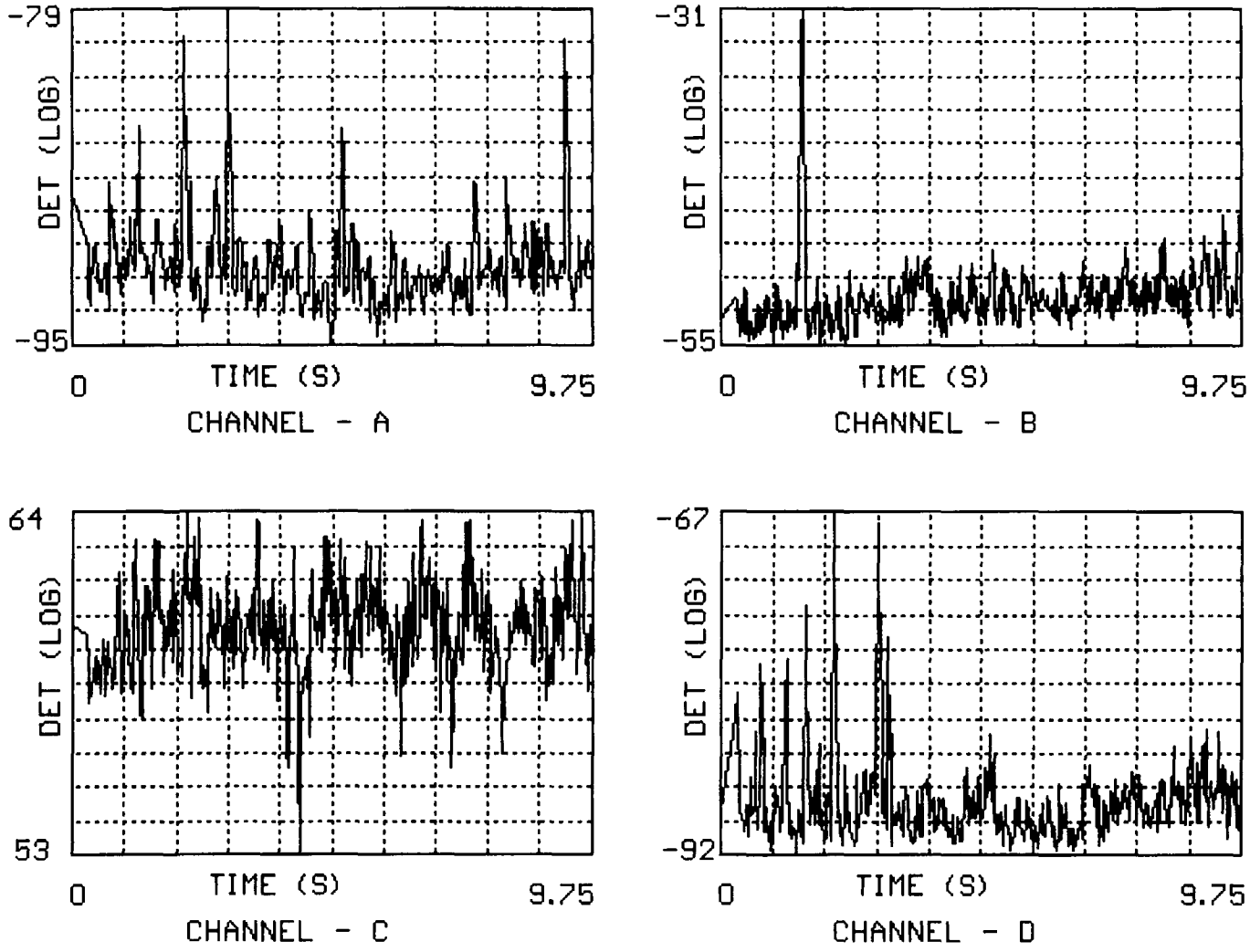

FIG.3 : DETERMINANT VALUE VS. TIME FOR INJECTION 2

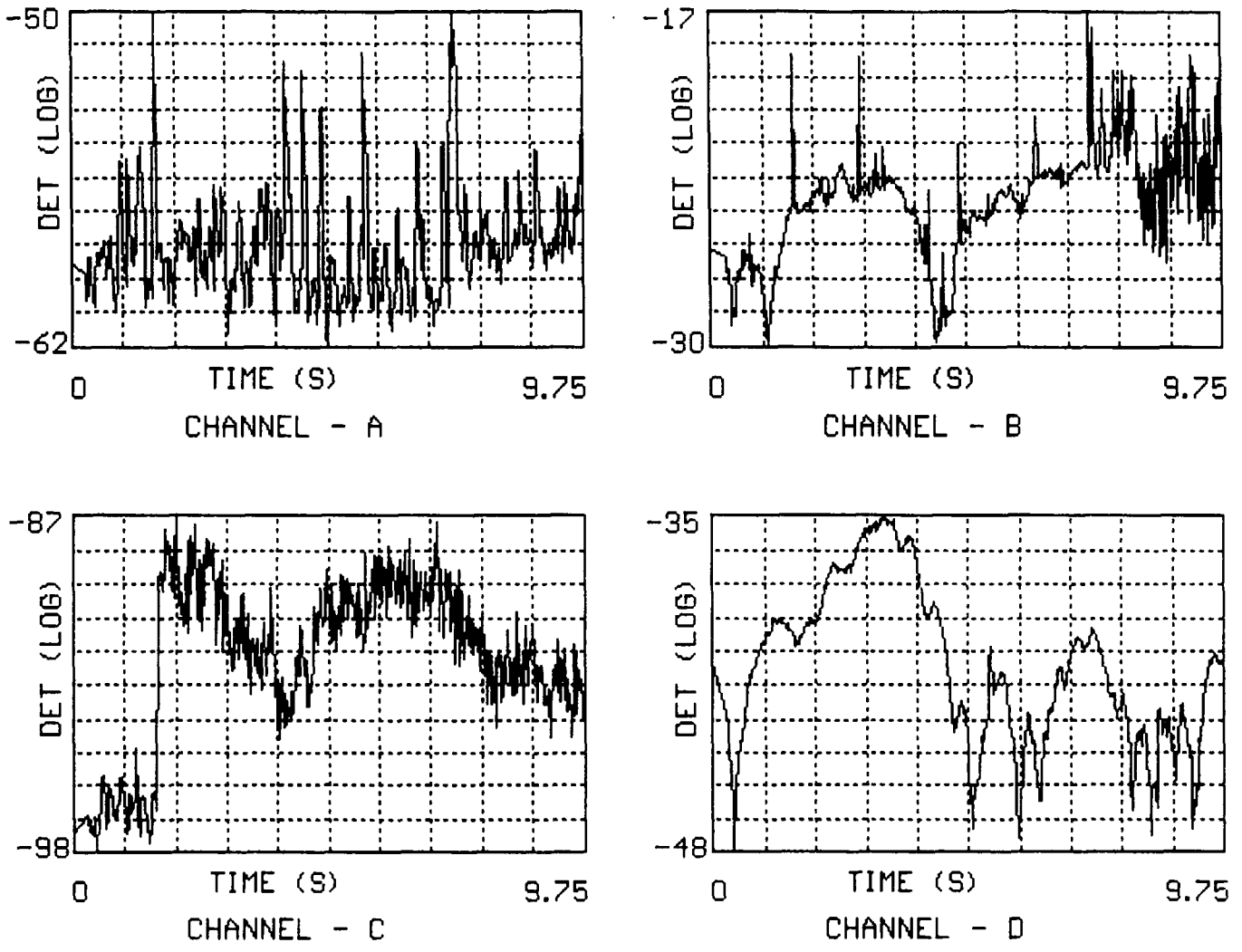

FIG.4 : DETERMINANT VALUE VS. TIME FOR INJECTION 3

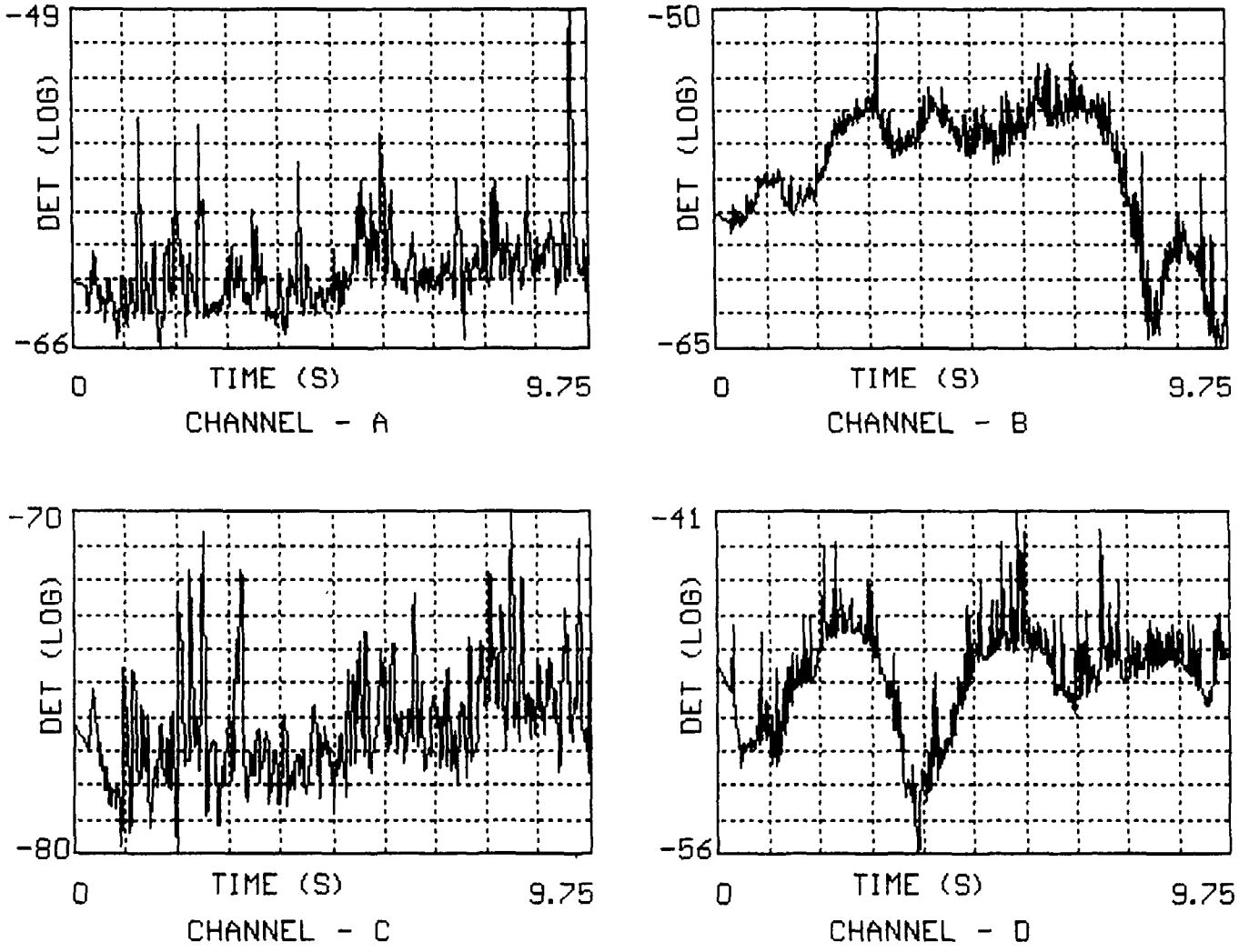

FIG.5 : DETERMINANT VALUE VS. TIME FOR INJECTION 4

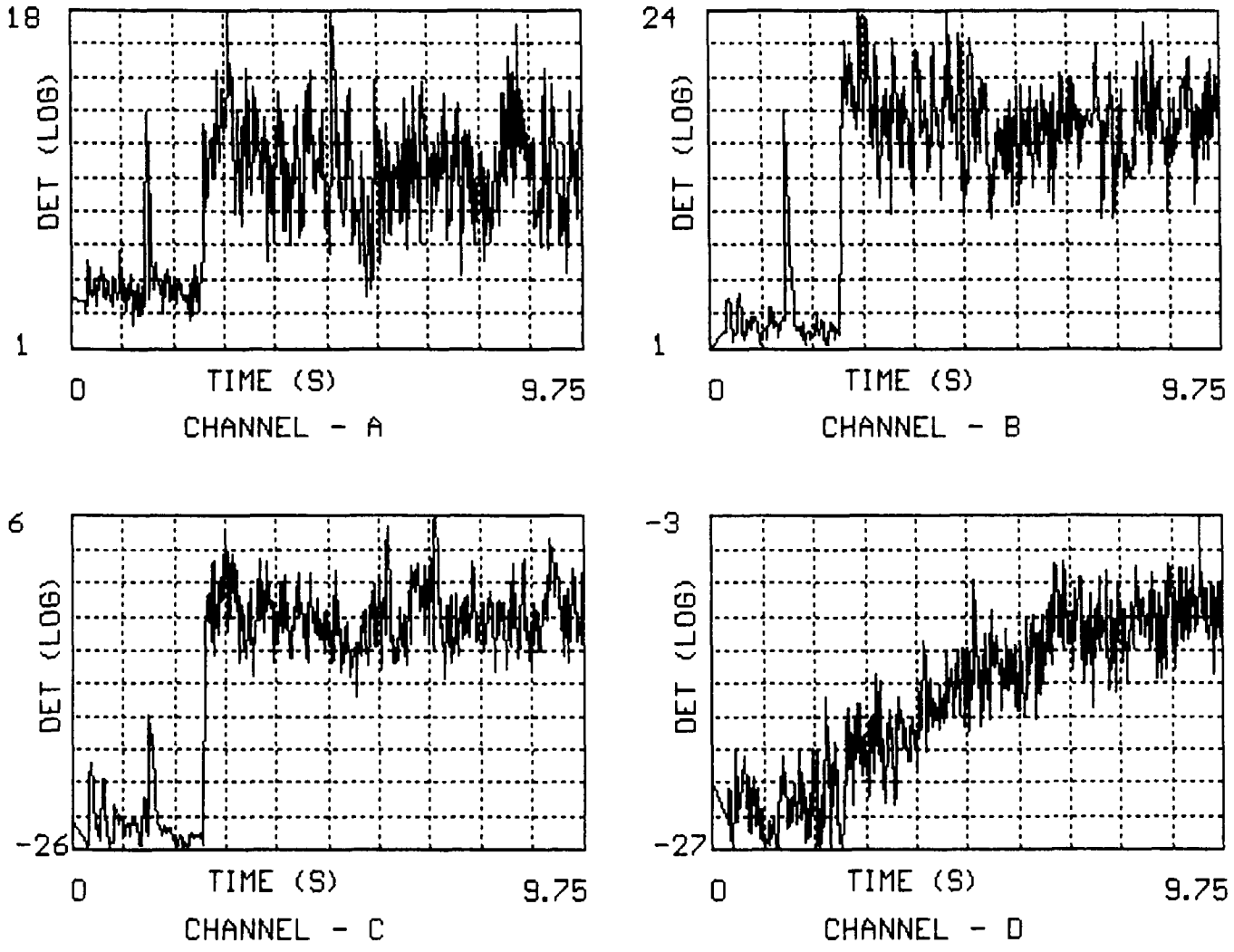

FIG.6 : DETERMINANT VALUE VS. TIME FOR INJECTION 5

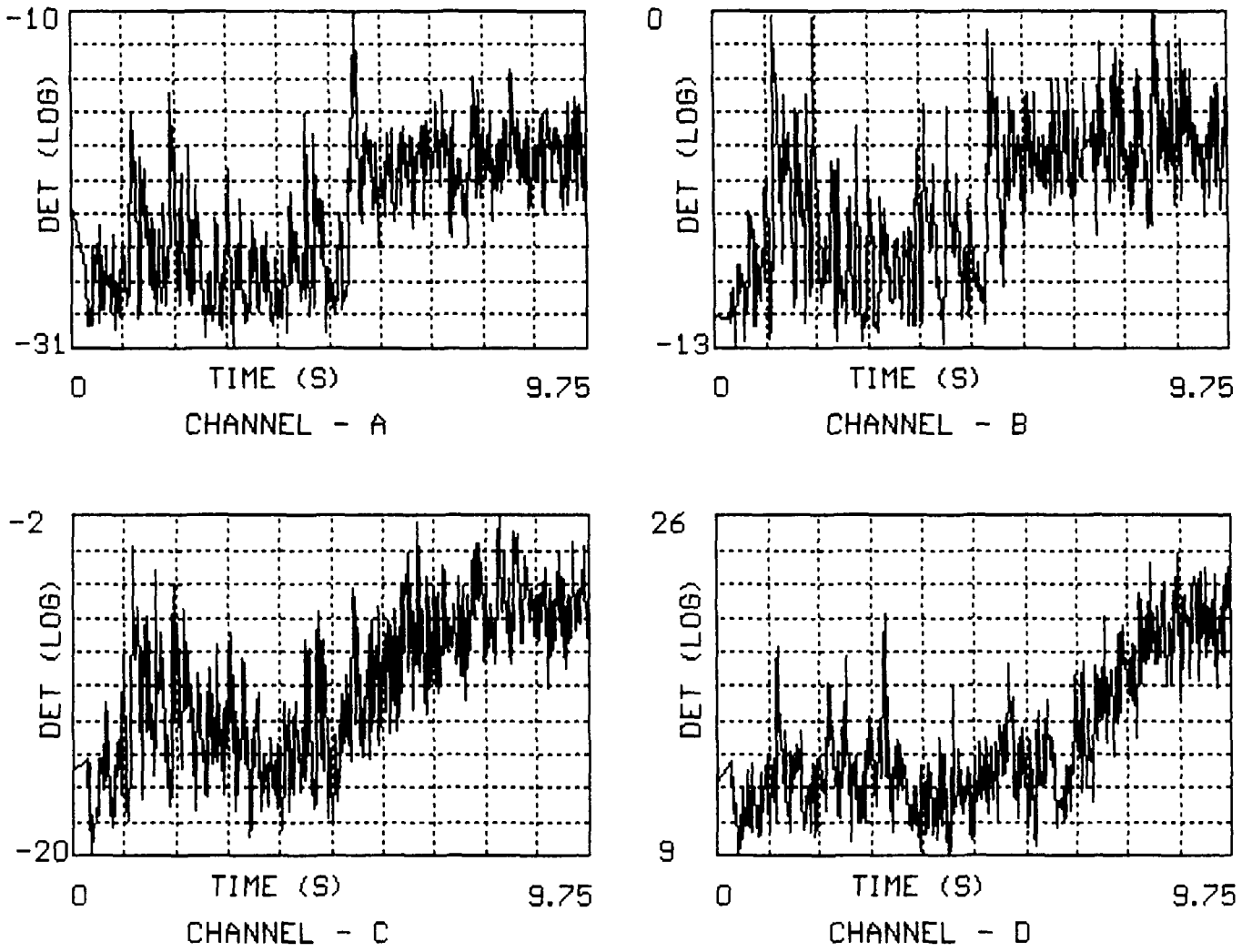

FIG.7 : DETERMINANT VALUE VS. TIME FOR INJECTION 6

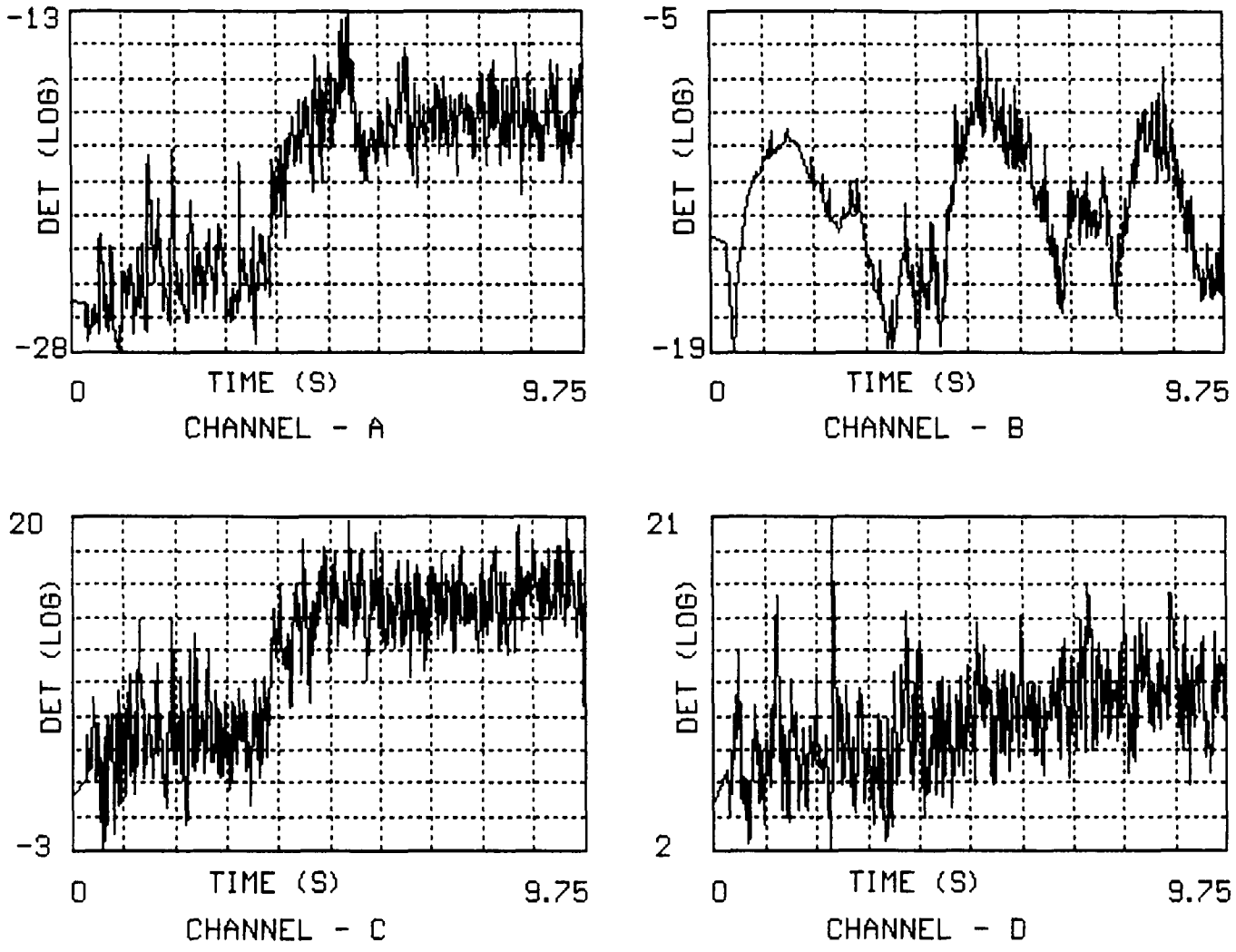

FIG.8 : DETERMINANT VALUE VS. TIME FOR INJECTION 7

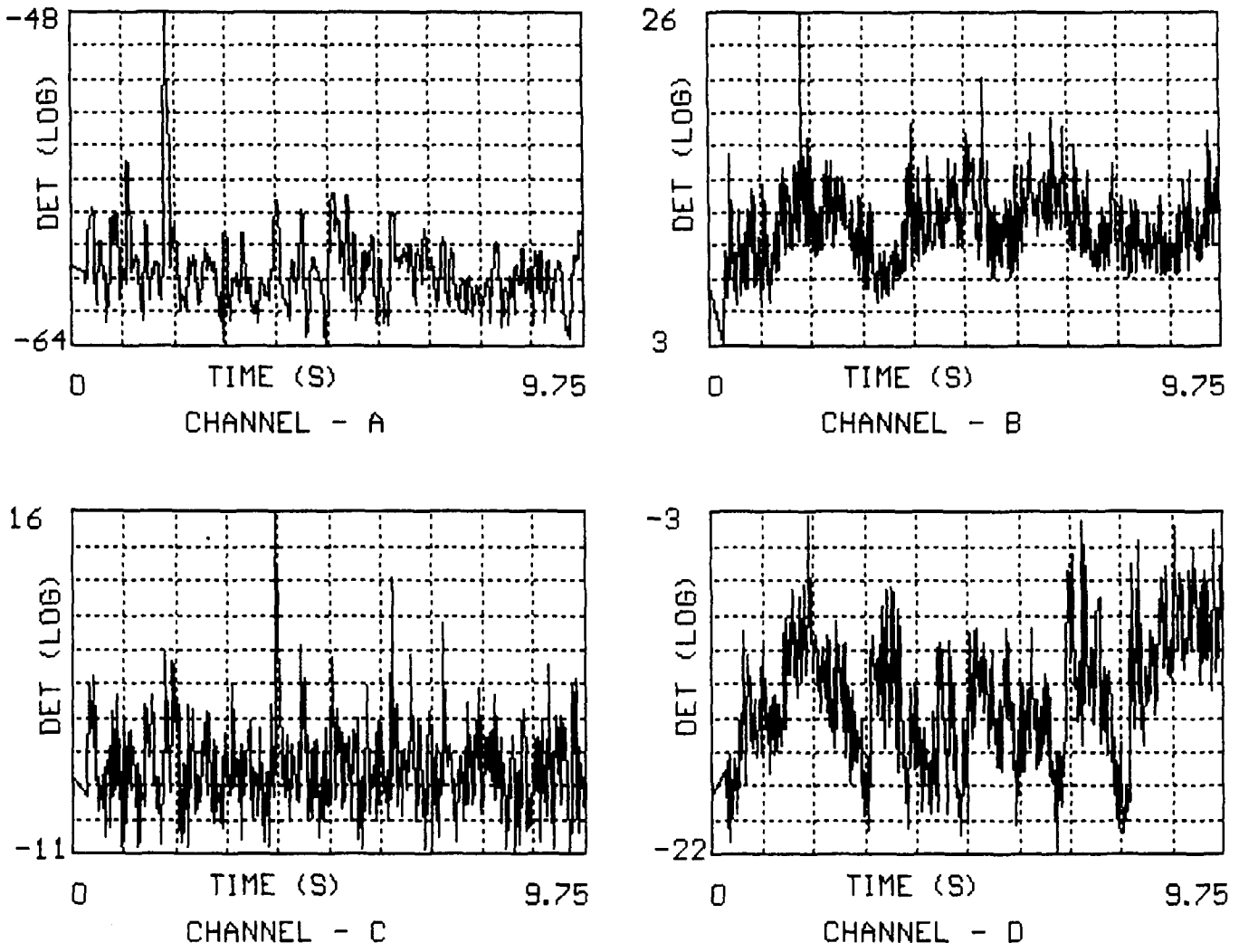

FIG. 9 : DETERMINANT VALUE VS. TIME FOR INJECTION 8

Table 2 Detection of Leak (Determinant)

Injection Number	Waveguide A			Waveguide B			Waveguide C			Waveguide D		
	Onset	Duration	Detection Margin	Onset	Duration	Detection Margin	Onset	Duration	Detection Margin	Onset	Duration	Detection Margin
1	–	–	–	–	–	–	1.79	7.96	42.8	1.63	7.24	32.6
2	–	–	–	–	–	–	–	–	–	–	–	–
3	–	–	–	–	–	–	1.62	8.13	54.7	–	–	–
4	–	–	–	–	–	–	0.95	8.8	31.0	–	–	–
5	2.39	7.36	86.4	2.49	6.85	148.3	2.5	7.25	198.1	2.44	7.31	123.3
6	5.24	4.51	72.6	5.17	4.58	46.7	5.11	4.64	78.0	6.44	3.31	80.3
7	3.79	5.96	72.1	–	–	–	3.76	5.99	90.5	3.41	6.34	38.3
8	–	–	–	–	–	–	–	–	–	–	–	–

NOTE:

Onset and Duration in seconds

Detection Margin in dB

Table 3 Detection of Leak (Trace)

Injection Number	Waveguide A			Waveguide B			Waveguide C			Waveguide D		
	Onset	Duration	Detection Margin	Onset	Duration	Detection Margin	Onset	Duration	Detection Margin	Onset	Duration	Detection Margin
1	–	–	–	–	–	–	1.79	7.28	8.0	1.56	7.22	1.59
2	–	–	–	–	–	–	–	–	–	–	–	–
3	–	–	–	–	–	–	1.62	8.13	16.9	–	–	–
4	–	–	–	–	–	–	–	–	–	–	–	–
5	2.54	7.21	37.3	2.49	7.26	67.6	2.43	7.32	93.4	2.44	7.31	40.4
6	5.24	4.51	10.12	5.17	4.58	3.0	4.38	5.37	2.0	6.71	3.04	25.9
7	3.72	6.03	19.6	–	–	–	3.9	5.85	13.1	3.6	6.15	11.4
8	–	–	–	–	–	–	–	–	–	–	–	–

NOTE :

Onset and Duration in seconds.

Detection Margin in dB

- Experiments in the ASB loop at Bensberg, Germany showed that for a given injection pressure and orifice diameter (15 MPa and 0.8 mm) argon injection gives a lower noise output as compared to steam injection [9].

- Experiments in SOTA-15 facility in Russia showed that at comparable argon (0.32 ml/s) and hydrogen (0.3 ml/s) injection rates, the signal level (in frequency bands upto 200 kHz) for hydrogen injection considerably exceeds the signal level due to argon injection [10].

- Experiments on BOR-60 micromodular steam generator showed that for the test conditions, the spectra from steam leak (0.04 g/s) and argon injection (0.032 g/s) are similar [11].

- Low pressure injection experiments at FBTR showed that the noise produced by hydrogen injection is more than that produced by argon injection for the same mass flow rate. The acoustic power is concentrated in lower frequencies below 5 kHz for low pressure injection.

- In the leak evolution tests carried out in Small Water Leak Rig at Dounreay, UK, it was observed that acoustic noise (10-100 kHz) from argon injection fell close to the best fit line for steam injection. Large scatter was noticed in some other experiments in this facility [12].

- When argon is injected into sodium, a decrease in signal can be observed at some transducer locations due to attenuation of the background noise by argon bubbles. This has been noticed in the experiments at Phenix, France [13] and at FBTR, India.

From the above results, it can be broadly concluded that at a given mass flow rate, steam and argon injections give similar noise output and hydrogen injection results in higher noise as compared to argon injection.

5.3.2 Identification of Injection Medium

Patterns of the injection spectra and Determinant feature for various injections were evaluated to identify the injection medium.

i) Based on PSD:

A study was made to establish whether any significant differences are seen in the power spectrum density at a given waveguide for different Injection Files. After identifying the injection region through one of the features described earlier, PSDs were calculated in the known background and injection regions. The injection spectrum was then calculated as the difference of these two spectra and this spectrum is considered to represent the acoustic power contributed by the injection process at different frequencies.

Fig.10 and Fig.11 show the injection spectrum at the four waveguides for Injection Files 5,6 and 7. It is clearly seen that the spectral shapes are very similar except for magnitude in all the cases. However the only main difference observed

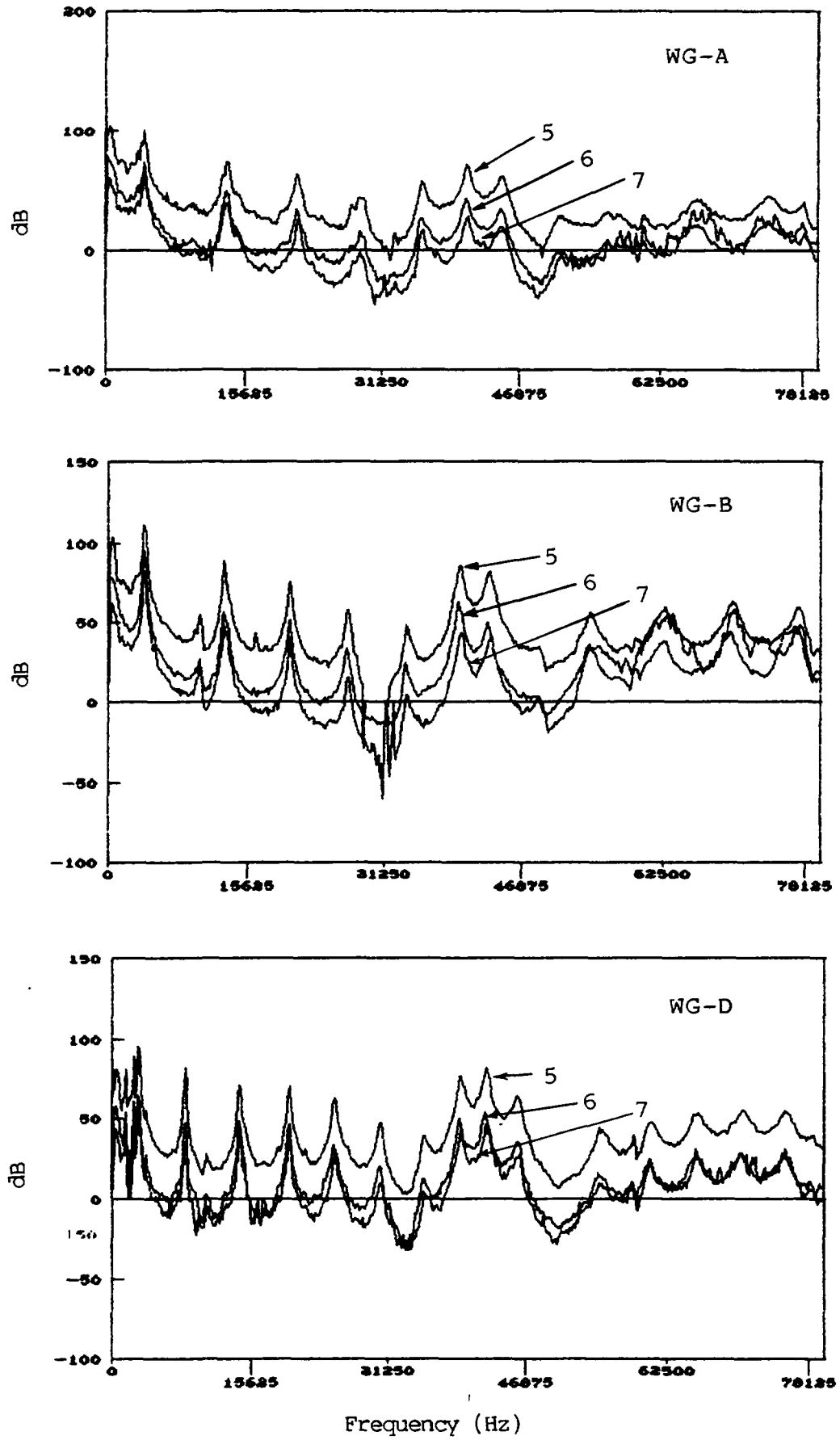

FIG. 10 INJECTION SPECTRA

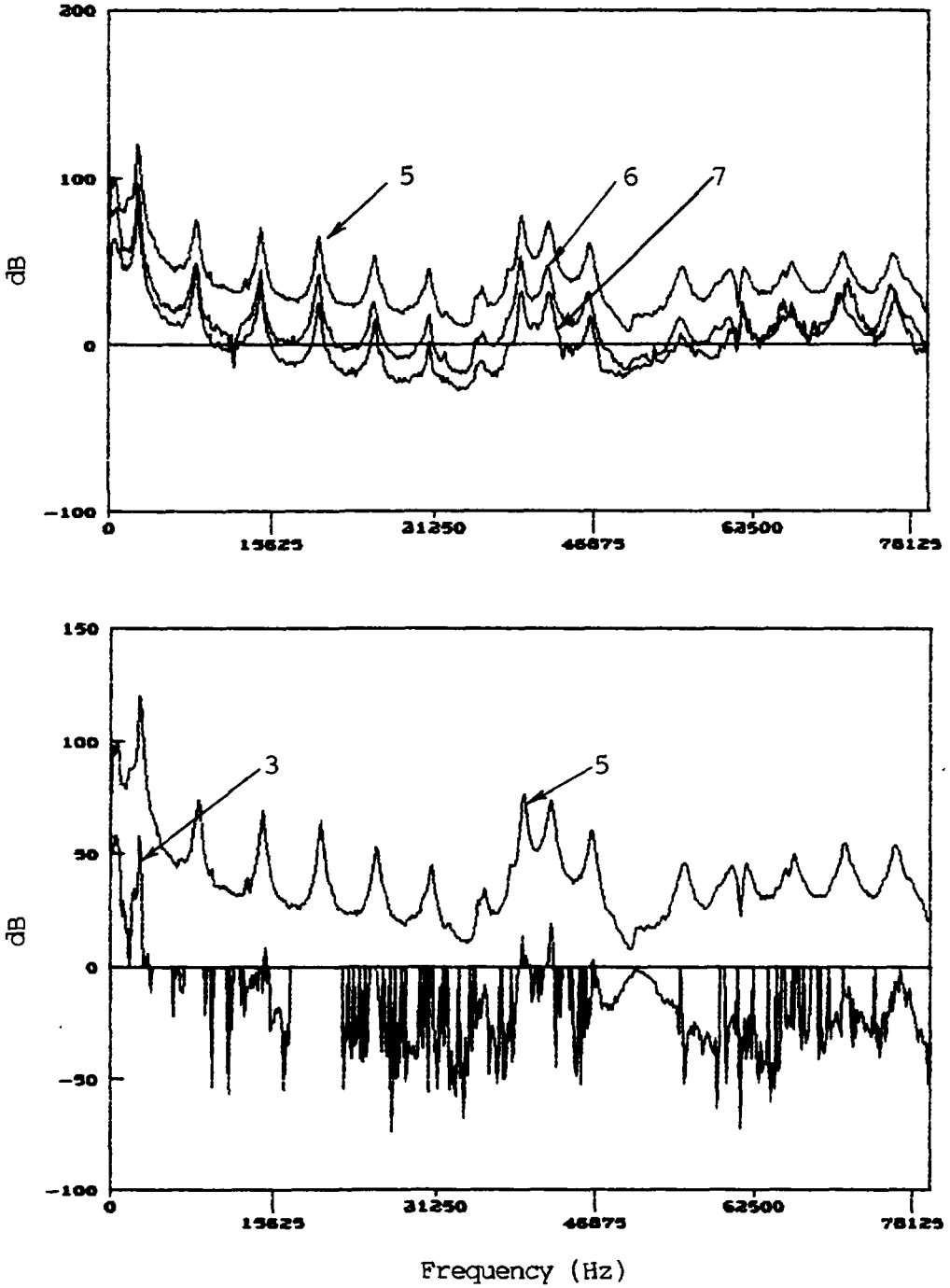

FIG 11 INJECTION SPECTRA : WG–C

was a strong attenuation of background signal at waveguide B during injection over the frequency band 29 kHz to 31.5 kHz for Injection File 5. Based on the general similarity noted in the PSDs, it is postulated that Files 5,6 and 7 contain water or argon injection signals.

Fig.11 also compares the injection spectra at waveguide C for Injection Files 3 and 5. It is seen that in the case of injection 3, the injection signal is concentrated only below 3 kHz. Based on our experiments at FBTR, Injection File 3 is identified as a low pressure gas injection (argon or hydrogen).

ii) Based on Determinant Feature:

The pattern of the Determinant (Vs) time plots at waveguide B looks similar for injections 1,3 and 7. There is a cyclic variation (repeated increase and decrease) over the data length. Waveguide B is the nearest to the injection zone. Based on this pattern, it is postulated that injections 1,3 and 7 are of same medium. It is probable that during these injections, the orifice periodically got plugged due to reaction products and such a scenario would suggest water or hydrogen as the injection medium in Files 1,3 and 7.

At waveguide D, which is the farthest from injection zone, a ramp increase is seen in the Determinant feature for injections 5 and 6. This could be due to bubble entrained flow noise building up at this waveguide, as the bubbles are carried by sodium towards it. This observation suggests that injections 5 and 6 could be with argon.

iii) Results:

Based on the indications from PSD plots and Determinant feature as discussed in this section, the following injection media are predicted, as the best possible estimate.

Injection No.	Likely Medium
1	Water or Hydrogen
3	Hydrogen
5	Argon
6	Argon
7	Water

5.4 Signal Transmission Characteristics

The injections were carried out near the evaporator bottom and waveguide B is the nearest to the injection zone and waveguide D at top is the farthest. Waveguides A and C are at the same plane nearly 2 m above B. The injection zone was either in the tube bundle region or in the annulus between the outer shell and the inner baffle. The participant did not have a prior knowledge of the injection location. Noise signal due to injection would get transmitted to the waveguides through the evaporator internals. The injection nozzle seems to be acoustically coupled to the outer shell and hence in addition, some noise due to injection would propagate through the outer shell to the waveguides. Transmission characteristics were assessed with respect to injections 5 and 6 which were detected at all the waveguides.

Taking waveguide B as the reference, ratio in RMS value between other waveguides and reference waveguide was calculated and the values are given in Table 4 for Injection Files 5 and 6. Injection signal measured at D is only 50% less compared to waveguide B for these two injections, indicating only a low attenuation along the evaporator height. This is an encouraging observation for the ALD system design.

Table 4 Ratio of RMS Injection Signal at Different Waveguides

Injection Number	WG-A / WG-B	WG-C / WG-B	WG-D / WG-B
5	0.75	0.992	0.565
6	0.622	1.145	0.518

Comparison of injection spectra 5 and 6 at different waveguides clearly shows that the spectra extend upto 80 kHz at all the waveguides. To see whether attenuation at farther waveguides is frequency dependant, ratio of acoustic power at waveguides A, C and D to waveguide B was computed at each spectral line. Due to slight offset in the individual frequency peaks in the spectra from different waveguides, the computed ratio spectra showed zig-zag profile and did not yield any useful data. The offset in frequency peaks could be due to different waveguide characteristics.

5.5 Leak Location Analysis

In the time period available, it was not possible to retrieve the data from CD-ROM files for time delay measurements to detect the leak location. Instead, cross correlation analysis was carried out on low speed digital data from the tapes. As observed during 1994, the cross correlation functions contained periodic profiles and did not show the time delay as a distinct peak. A sample result is shown in Fig.12.a and 12.b for Injection File 6 and for waveguide pair B and D.

5.6 Leak Detection at Full Power in PFR Evaporator:

The 1995 data also contained evaporator 3 background noise data measured at two waveguide locations (A and B) when the reactor was operating at full power. Table 5 compares the RMS value of the above background noise with the RMS value of the injection noise at waveguides A and B from Files 5 and 6. Injection noise was obtained by subtracting the background component due to sodium flow from the signal in the known injection region by square law method. The resulting signal to noise ratio, if the injections were carried out at full power, are also given in Table 5. For injection 6, at waveguides A and B, S/N is –9.6 dB and –6.4 dB respectively. These S/N values are well within the detection capabilities of Determinant and Trace features. For injection 5, signal levels were still higher. It is

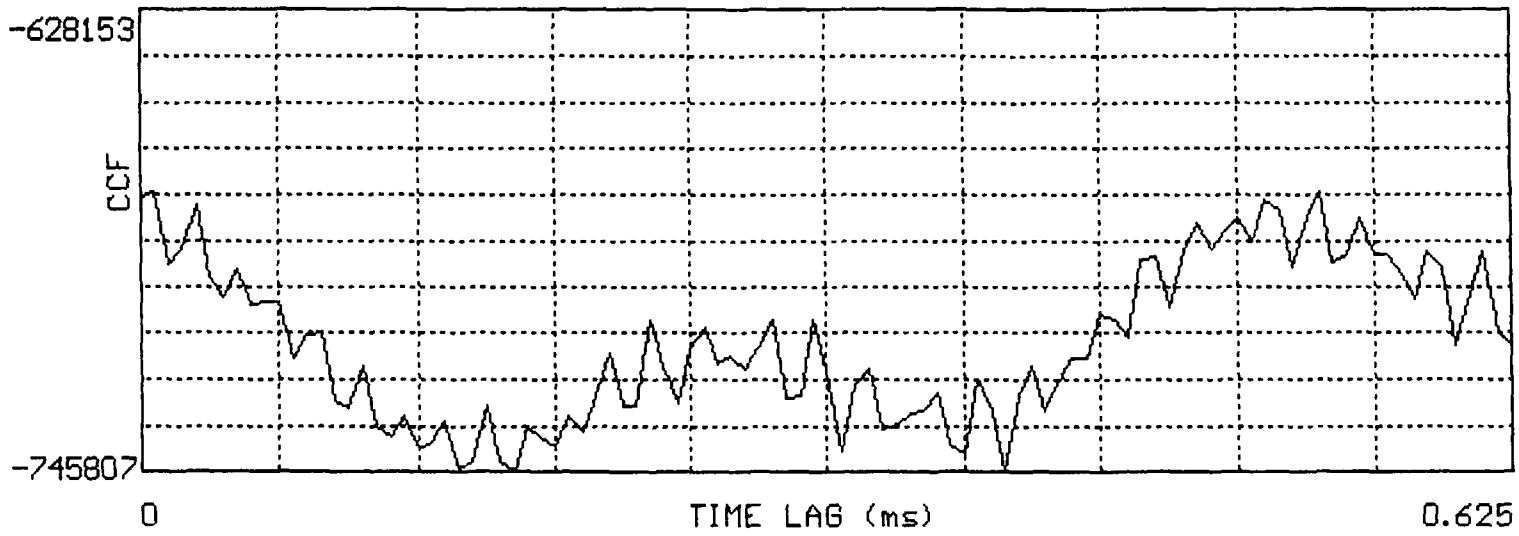

FIG.12a CCF VS. TIME LAG (I6P3S, CH-D DELAYED)

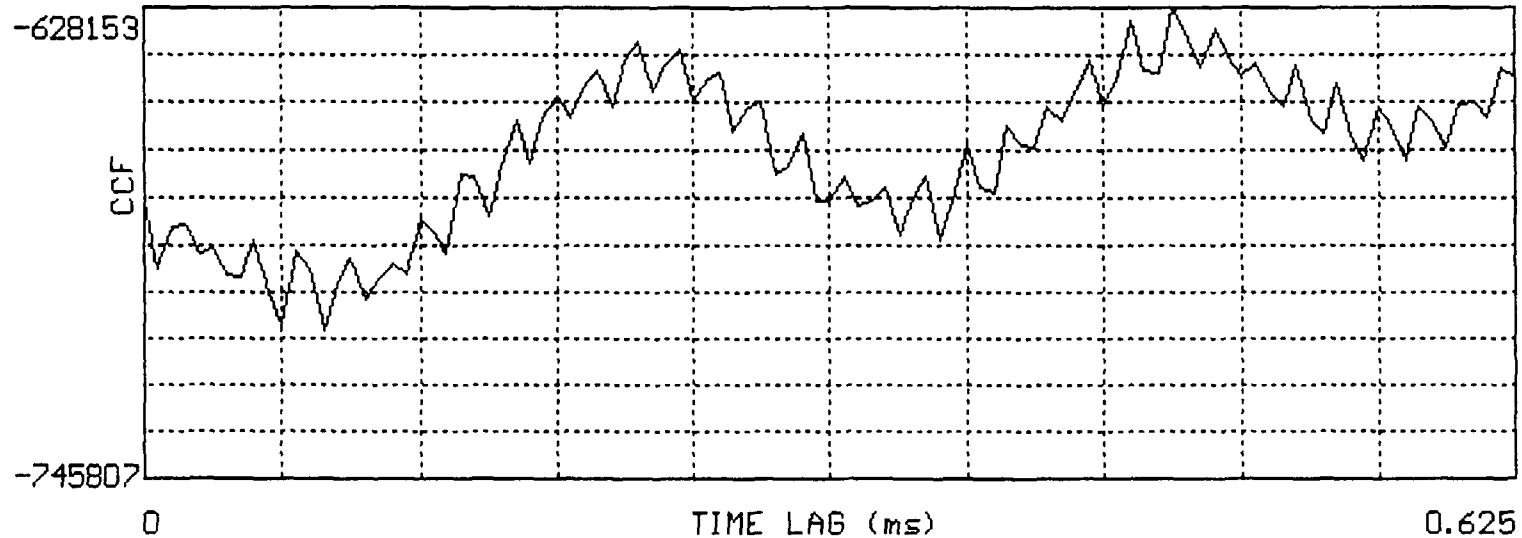

FIG.12b CCF VS. TIME LAG (I6P3S, CH-B DELAYED)

Table 5 Comparison Between Evaporator Background Noise and Injection Signal Level

Noise Source	Waveguide–A		Waveguide–B	
	RMS	S/N	RMS	S/N
Background at Full Power	583	–	646	–
Injection-5	739	+2.1dB	982	+3.6 dB
Injection-6	193	–9.6dB	310	–6.4 dB

also seen that in the case of injection 7, at waveguide B which is near the leak zone, the resulting S/N would be –11 dB and this injection can also be readily detected with these features at waveguide B.

Fig.13 compares the PSD of the background noise and injection noise from Files 5 and 7 at waveguides A and B respectively. It is interesting to note that the full power background spectrum is similar to injection spectrum, except for magnitude, at both waveguides A and B. Similar observation was made for Injection File 6 also, which is not shown in the figure. It is clear that the spectra measured are basically determined by the system and waveguide frequency response characteristics. At waveguide A, the injection noise from File 5 is more than the background noise at low frequencies upto about 4.5 kHz.

Since the injection spectra seem to be influenced by the system characteristics, no comparison is made between injection and superheater background noise spectra. Comparison between evaporator and superheater background spectra in Fig.14, however shows that the superheater background noise contains less power at higher frequencies in waveguide A. Similar behaviour is observed at waveguide B also.

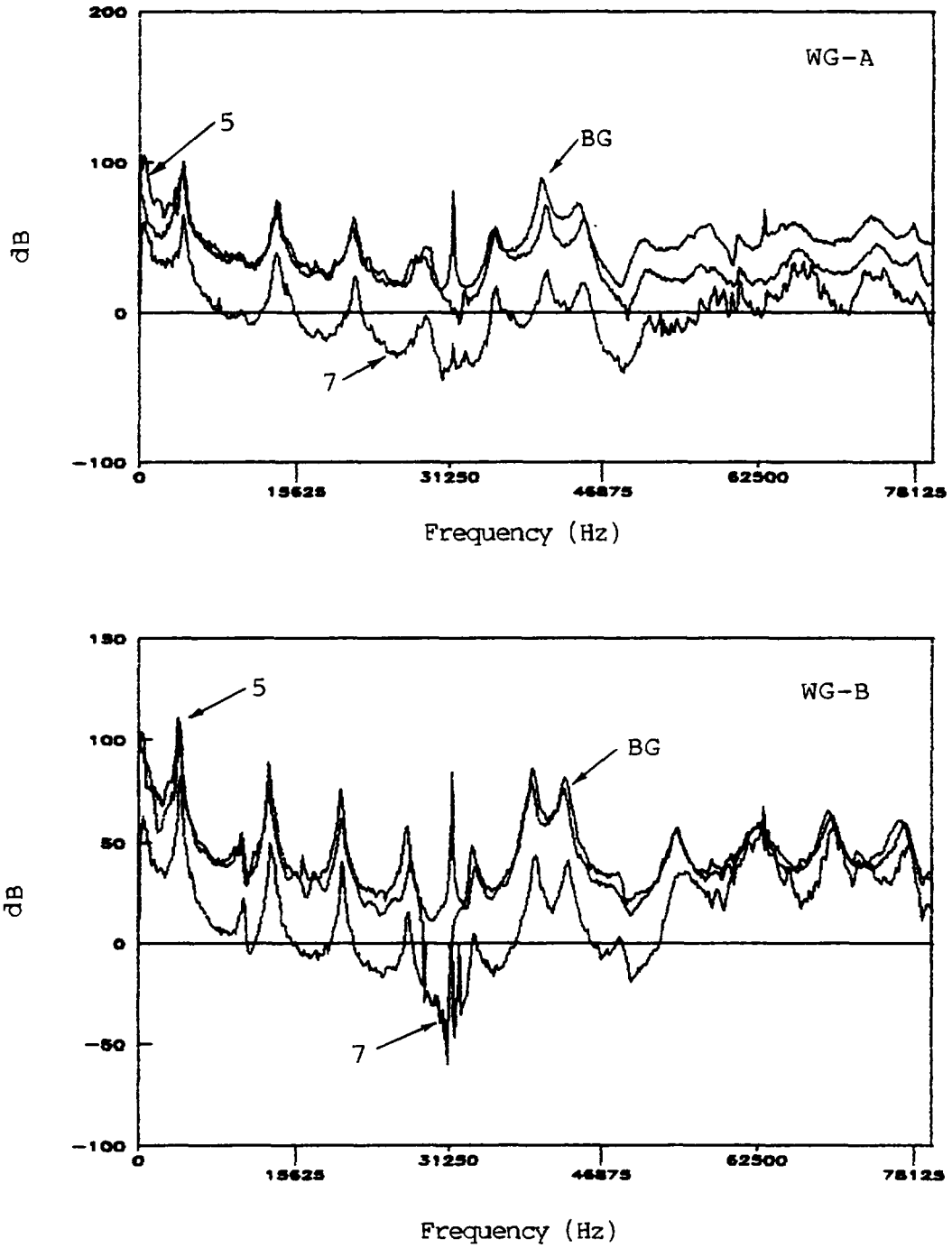

FIG 13 EVA.BG & INJ-5&7 SPECTRA

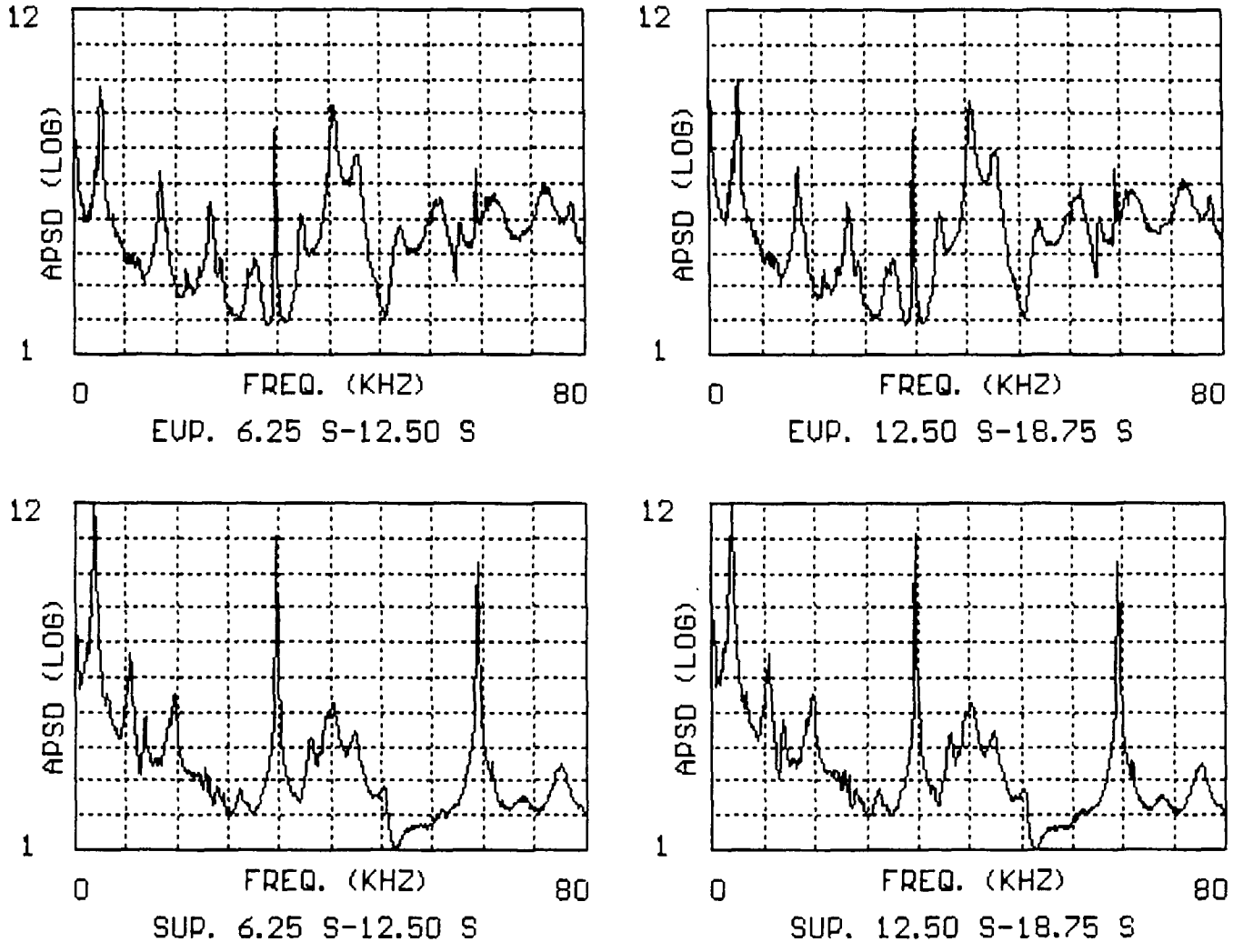

FIG.14: AVERAGE APSD FOR EUP. & SUP BACKGROUND - CHANNEL A

6.0 CONCLUSIONS

Based on the analysis of data from PFR end-of-life acoustic experiments, the following conclusions can be drawn.

1. Leak Detection: Features which could earlier detect anomaly signals in synthesised data can also detect anomaly signals in real plant situations, as demonstrated on PFR SGU injection data. As observed earlier, Determinant and Trace features derived from covariance matrix of power spectral density have been found to be very sensitive on PFR data also.

2. Injection Medium: Based on an evaluation of the patterns of injection spectra and Determinant feature, likely medium of injection in five files has been predicted.

3. Signal Transmission: For injections 5 and 6, the injection RMS value measured at waveguide D at top is only 50% less than the RMS value at waveguide B, which is the nearest to the leak at the bottom of the evaporator. Such a low attenuation is a very encouraging result for the design of an ALD system.

4. Leak Location: Cross correlation analysis on data digitised at low sampling speed has not yielded any positive results for identifying signal time delays between waveguides.

5. Full Power Background Noise: Comparison of evaporator background noise spectra at full power with injection spectra (injections 5,6 and 7) clearly indicates that all these spectra are similar, except for magnitude, and seem to be basically determined by the waveguide and system characteristics. A comparison of the RMS values of the injection noise(5,6 and 7) with the background noise at full power indicates that at waveguide B, which is near the injection zone, the resulting S/N values are within the detection capabilities of Determinant and Trace features.

7.0 RECOMMENDATIONS FOR FUTURE ACTIVITIES

The need for an ALD system as part of the steam generator surveillance and protection system has been well recognised by the fast reactor community. The IAEA extended CRP has convincingly demonstrated that diverse signal processing techniques can detect leak signals even under very poor S/N condition in synthesised and real field data. However in order to consolidate the achievements of the CRP further, the points suggested below deserve to be considered:

1. Evaluation of signal processing techniques on injection data from SGU while the plant is operating near rated power.

2. Studies on evolving an in-situ calibration method for the ALD system

3. Based on suggestions 1 and 2 above, there is a merit in considering the extension of the CRP by one more year.

4. **The analysis carried out so far have been restricted to short term background data. It is known that the background noise is not stationary. Hence there is a need to create at IAEA a FR-SGU Background Noise Data Bank, collecting samples of noise data measured over a long period of time from different countries.**

5. **Due to the efforts put in by the participants of two CRPs, several new techniques for detecting boiling and leak signals have emerged and these signal processing techniques could be useful in other allied disciplines also. Therefore it is desirable to bring out an IAEA Monograph covering the studies done during 1983-1995 in the two CRPs. If necessary, the Indian team is ready to share the major responsibility in this task.**

6. **Acoustic techniques have potential for detecting various anomalies like boiling, cavitation, leak and loose part impacting in fast reactors. An IAEA Technical Committee Meeting may be organised, inviting specialists in these areas, to review the status and to identify areas where further thrust is required.**

7. **Development of expert systems for boiling and leak detection.**

REFERENCES

1. **R.Prabhakar, R.K.Vyjayanthi and R.D.Kale, "*Detection of Steam Leaks into Sodium in Fast Reactor Steam Generators by Acoustic Techniques - An Overview of Indian Programme*", IWGFR/79 (ed.JPh.Girard), IAEA, Oct., 1990.**

2. **R.Prabhakar, R.K.Vyjayanthi and R.D.Kale, "*Experimental Acoustic Leak Detection System in FBTR Steam Generator Module, Int. Topical Mtg. on Sodium Cooled Fast Reactor Safety*", Obninsk, Russia, Oct. 3-7, 1994.**

3. **Om Pal Singh, R.Prabhakar, G.S.Srinivasan and R.K.Vyjayanthi, "*Fourth Year Progress Report to RCM at Vienna*", Dec.9-10, 1993.**

4. **Om Pal Singh, R.Prabhakar, G.S.Srinivasan and R.K.Vyjayanthi, "*Fifth Year Progress Report to RCM at Kalpakkam*", Nov.1-3, 1994.**

5. **S.Marimuthu, G.S.Srinivasan and Om Pal Singh, "*Investigation of Leak Location in SGUs using Beamforming Technique, Internal Document*", RPD/SNAS-77, May, 1995.**

6. **C.Cornu, "*Sodium-Water Reaction Detection Confirmation and Location with Time Domain Beamformer*", Report to RCM at Kalpakkam, Nov.1-3, 1994.**

7. **R.Curry, "*Acoustic Leak Detection Experiments Performed at PFR, March 1993 to June 1994*", Report to RCM at Kalpakkam, Nov.1-3, 1994.**

8. N.Kong, M.Brunet, P.Garnaud and D.Ghaleb, "*Water Leak Detection in Steam Generator of Super Phenix*", IWGFR/79 (ed.JPh.Girard), IAEA, Oct., 1990.

9. J.Voss and N.Arnaoutis, "*Recent Experiments on Acoustic Leak Detection, IAEA-IWGFR Specialists' Mtg. on Theoretical and Experimental Work on LMFBR Steam Generator Integrity and Reliability with a Particular Reference to Leak Development and Detection*", The Hague, Netherlands, Nov.9-11, 1983.

10. A.A.Petrenko and V.M.Poplavsky, "*Experimental Studies on Acoustic Detection of Sodium-Water Steam Generator Leaks in the USSR*", IWGFR/79 (ed.JPh.Girard), IAEA, Oct., 1990.

11. V.M.Sokolov, V.V.Golushko, V.A.Afanas'ev, Yu.P.Grebenkin and A.B.Muralev, "*Acoustic Noise from Steam Generators in the BOR-60 Reactor During Simulation of Leaks by Argon and Steam*", Atomnaya Energiya, Vol.59, No.5, pp 327-330, Nov., 1985.

12. R.Rowley, J.A.Mcknight and J.Airey, "*Analysis of Acoustic Data from UK Sodium/Water Reaction Test Facilities*", IWGFR/79 (ed.JPh.Girard), IAEA, Oct., 1990.

13. M.Carminati, L.Martin and A.Sauzaret, "*Acoustic Sodium-Water Reaction Detection of the Phenix Steam Generators*", IWGFR/79 (ed.JPh.Girard), IAEA, Oct., 1990.

AUTOREGRESSIVE TECHNIQUES FOR ACOUSTIC DETECTION OF IN-SODIUM WATER LEAKS

K. HAYASHI
Japan Atomic Energy Research Institute,
Tokai-mura, Naka-gun, Ibaraki-ken,
Japan

Abstract

We have been applied a background signal whitening filter built by univariate autoregressive model to the estimation problem of the leak start time and duration. In the 1995 present benchmark stage, we evaluated the method using acoustic signals from real hydrogen or water/steam injection experiments. The results show that the signal processing technique using this filter can detect reliably the leak signals with a sufficient signal-to-noise ratio. Even if the sensor signal contains non-boiling or non-leak high-amplitude pulses, they can be classified by spectral information. Especially, the feature signal made from the time-frequency spectrum of the filtered signal is very sensitive and useful.

1. Introduction

The Coordinated Research Program on Acoustic Signal Processing for the Detection of Sodium Boiling or Sodium/Water Reaction in LMFBR was started in December 1989.

Table 1. Previous and Present Benchmark Tests

Year	Objective	Boiling/Leak Signal	Background Signals
1990	Boiling Detection	KNS-1, Germany	Artificial Noise
1991	Leak Detection	Exp-Facility, Russia	SGU-2 of PFR, UK SGU-3 of PFR, UK
1992	Leak Detection	Exp-Facility, Russia	SGU-2 of PFR, UK SGU of SPX1, France
1993	Leak Detection	ASB, Germany	SGU-2 of PFR, UK
1994	Leak Detection (Location Estimation)	ASB, Germany (Multi-channel)	SGU-2 of PFR, UK
1995	Leak Detection (Location Estimation)	SGU of PFR, UK (Hydrogen, Argon and Water injection)	SGU of PFR, UK

The first benchmark test in **1990** used the test data that were synthesized in UK using the sodium boiling acoustic noise signals obtained at KNS 1 loop in FRG. The second benchmark test in **1991** used the test data synthesized also in UK using the sodium/water reaction acoustic noise signals, or leak noise signals, supplied by Russia and the background noise signals from two different steam generator units of PFR supplied by UK. The third test in **1992** used two kinds of test data that were synthesized in UK. The first one uses the background noise from a PFR steam generator unit and the leak noise from a Russian leak test facility. The second one contains a leak noise example from the UK and the background noise from a steam generator unit of SPX1 in France. The fourth test in **1993** used the test data synthesized in Japan using the sodium/water reaction acoustic noise signals, or leak noise signals, from a UK leak test facility (ASB Loop experiment) and background noise from two different PFR steam generator units. Then the test data was distributed to the participants as well as the information sheets. The fifth test in **1994** was focused on not only estimations of the start time and duration but also the location estimation of sodium/water reaction in SGU. The multi-channel digital recorded test data were distributed to participants for this benchmark test.

Through the benchmark tests from 1990 to 1993, we had developed and evaluated the Twice-Squaring method [1,2,3,4] for detecting sodium boiling or sodium/water reaction. The principle of this method is a band-limited nonlinear amplification focusing on the pulsive nature of the boiling or the leak noise signals to enhance the signal-to-noise ratio. Its advantages are a high sensitivity, a real time capability and a relatively simple processing. It was concluded from the results of analysis that the Twice Squaring method can detect reliably the leak signals with signal-to-noise ratio down to -16 dB by using a decision time of 0.5 second and a detection margin 0 dB. In the 1994 benchmark test, we newly applied and evaluated autoregressive (AR) technique [5] to the signal processing for leak detection and for location estimation. The results showed that the signal processing using univariate AR background signal whitening filter can detect reliably the leak signals with signal-to-noise ratio down to about -20 dB. Even if the sensor signal contains the non-boiling or non-leak large pulse components with a frequency range similar to the leak noise, they can be classified by spectral information. It also suggested that an estimation method using the time constants of the acoustic signal propagating paths based on the multivariate AR modeling techniques is capable to estimate the leak location.

The present **1995** benchmark test has been focused on the analysis of real experimental data instead of artificially synthesized data. This report describes the results of the benchmark test analysis using the autoregressive techniques.

2. Data and Tasks of the 1995 Benchmark Test

2.1 Test Data

The 1995 benchmark test data were prepared by UKAEA from their experimental data [6] measured at the steam generator unit (SGU) in the Proto-type Fast Reactor (PFR), UK. The data are derived from a total of 10 experiments performed at the evaporator and the superheater in secondary circuit number 3 of the PFR, as shown in **Table 2**.

Table 2 Data Set of 1995 Benchmark Test

Data set number	Location	Experiment (leak rate)	Reactor	Sensor
Background-1	Evaporator	None (Background)	Full-power	2
Background-2	Superheater	None (Background)	Full-Power	2
Injection-1,2	Evaporator	Hydrogen (2 rates)	Shut-down	4
Injection-3,4,5	Evaporator	Argon(3 rates)	Shut-down	4
Injection-6,7,8	Evaporator	Water/Steam(3 rates)	Shut-down	4

The sensor locations are shown in **Fig.1.** Each acoustic accelerometer is fitted to the external surface of the shell of each SGU using waveguide that projects radially outwards. They have a typical sensitivity of 17 pC/g and a response frequency of 45 kHz.

The test data was prepared with a digital format and distributed to participants of the present benchmark test by CD-ROM or QIC-80 magnetic tape. For the case of injection experiments, each pair of waveguide signals was digitized synchronously and four signals were recorded on three files separately, i.e., {WA, WB}, {WC, WB} and {WD, WB}. Sampling conditions are shown in **Table 3**.

2.2 Tasks

The participants in the benchmark test should address the following points in their analysis:

a) Compare and characterize the background noise from evaporator and superheater
b) Characterize and identify the type of leak noise signals (water/steam or argon or hydrogen)
c) Estimate the onset of leak and duration in all leak files

d) Evaluate the transmission characteristics of the leak noise signals from leak location to the transducers
e) Locate the leak

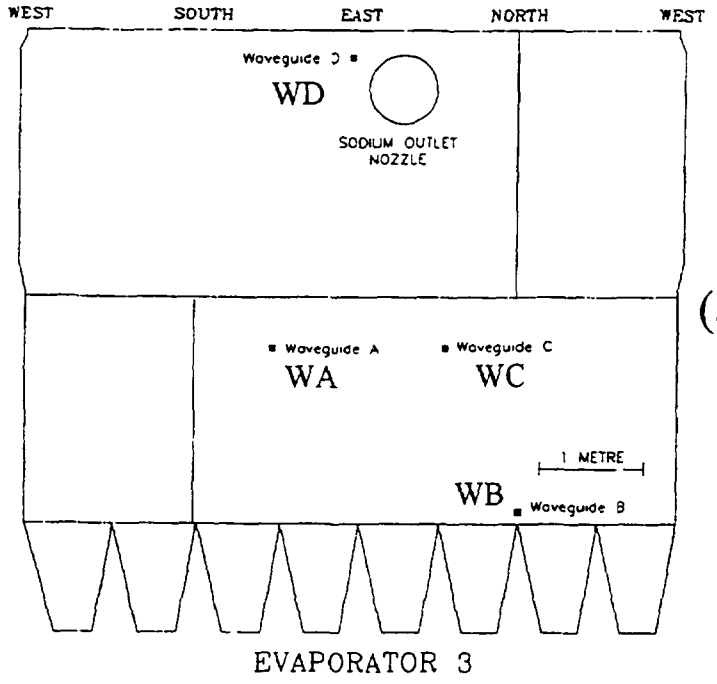

(a) Sensor location in Proto-type Fast Reactor Evaporator-3

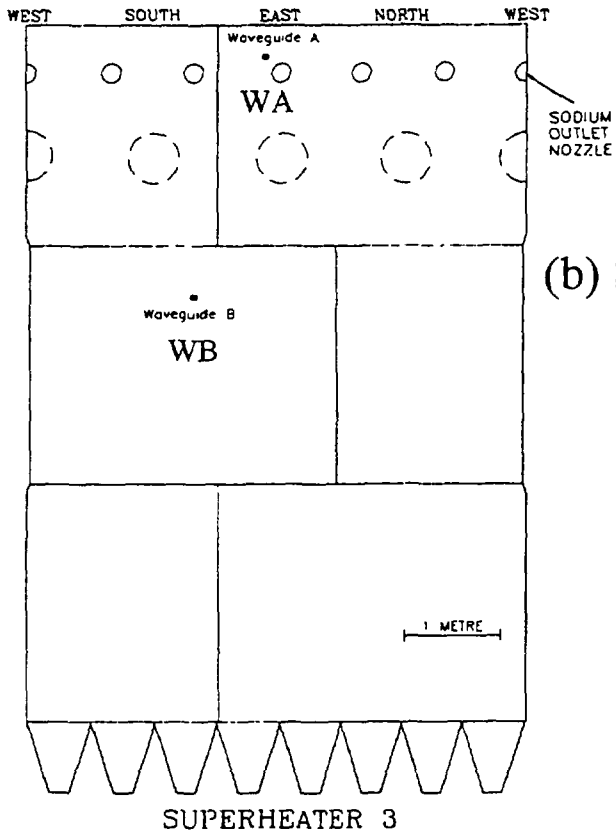

(b) Sensor location in Proto-type Fast Reactor Superheater-3

Fig.1 Sensor Locations

Table 3 Sampling Conditions of data file

Data set	Mode	Time	Rate	Samples	LPF
Background	High speed	25 s	2 MHz/ch	99,999,744	71.68 kHz
	Low speed	25 s	160 kHz/ch	7,987,200	72 kHz
Injection	High speed	10 s	2 MHz/ch	39,985,152	71.68 kHz
	Low speed	10 s	160 kHz/ch	3,194,880	72 kHz

2.3 Selection of Data Sets and Tasks

A great deal of experimental data sets was supplied us in the present benchmark test. This may be very useful for us to evaluate our signal processing methods near future. However, it is impossible for us to analyze all data and to answer all tasks in the present time because the analysis time permitted for us was very limited and insufficient. Therefore, we decided to choose several data sets, containing typical or our interesting cases, from the benchmark test data sets.
The following files were chosen for the preliminary analyses described in next chapter.

(1) BEP1L, BEP1H ..... Background signals of Evapolator
(2) I1P1L,I1P2L,I1P3L Injection-1 (Hydrogen-1)
(3) I3P1L,I3P2L,I3P3L Injection-3 (Argon-1)
(4) I6P1L,I6P2L,I6P3L Injection-5 (Water/Steam-1)
(5) I7P1L,I7P2L,I7P3L Injection-6 (Water/Steam-2)
(6) I8P1L,I8P2L,I8P3L Injection-7 (Water/Steam-3)

Furthermore, analysis of the onset of leak and duration using the UAR background whitening filter was performed only for the data sets of (2) Injection-1, (4) Injection-6 and (7) Injection-8.

3. Preliminary Analyses of the Benchmark Test Data

3.1 Checking of the data files

First, we made a data conversion program for SUN Sparc station and confirmed the validity of the data restored from the CD-ROM we received. The numerically dumped list for the BEP1L.DAT file was checked by the information sheet of benchmark test.

3.2 Signal characteristics : Wave-forms, RMS and PSD

Furthermore, in order to check the signal behaviors in both time and frequency domains, we plotted (a) the signal recordings for several files, (b) their RMS values and (c) their power spectral density (PSD) functions, as shown in **Figs.2** through 7. The RMS value was calculated with a time interval 25.6 ms (4096 samples).

(1) Background signals of Evaporator

The background signal of the waveguide-A (WA) in the evaporator is very noisy. It seems nonstationary. They contain many relatively large pulses. The signal WB contains two very high pulses.

(2) Injection-1: Hydrogen-1

The wave-forms of acoustic signals in the data set of Injection-1 show large DC changes. This means that the signal state is a transient and the statistical property is a nonstationary. They contain many large pulses.

The RMS analysis gives no useful information on the injection. This means that hydrogen injection generates a very weak acoustic noise or the leak rate was very low.

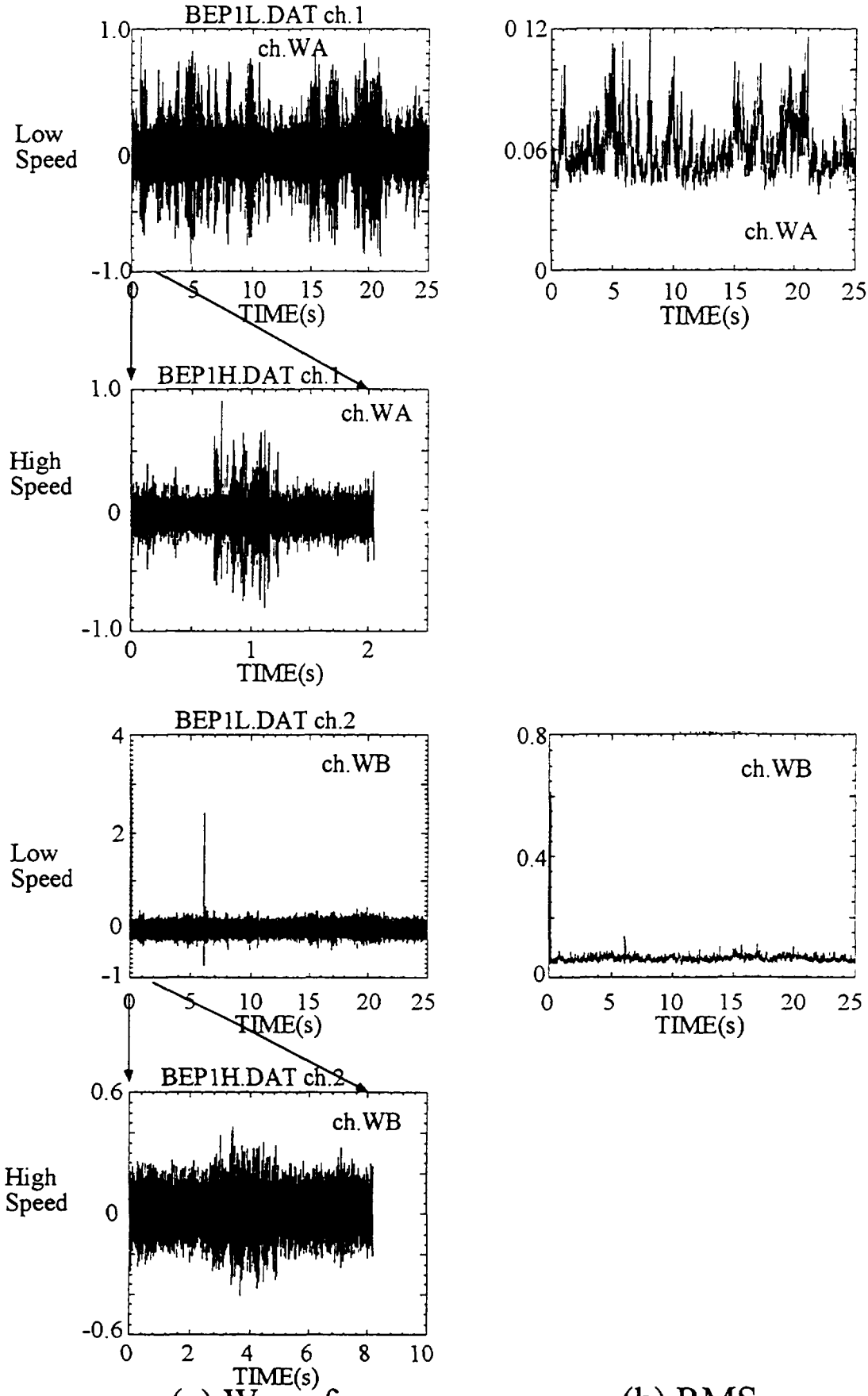

(a) Wave-form (b) RMS

Fig. 2 Statistical features of data set Background-1 (Evaporator, Full Power)

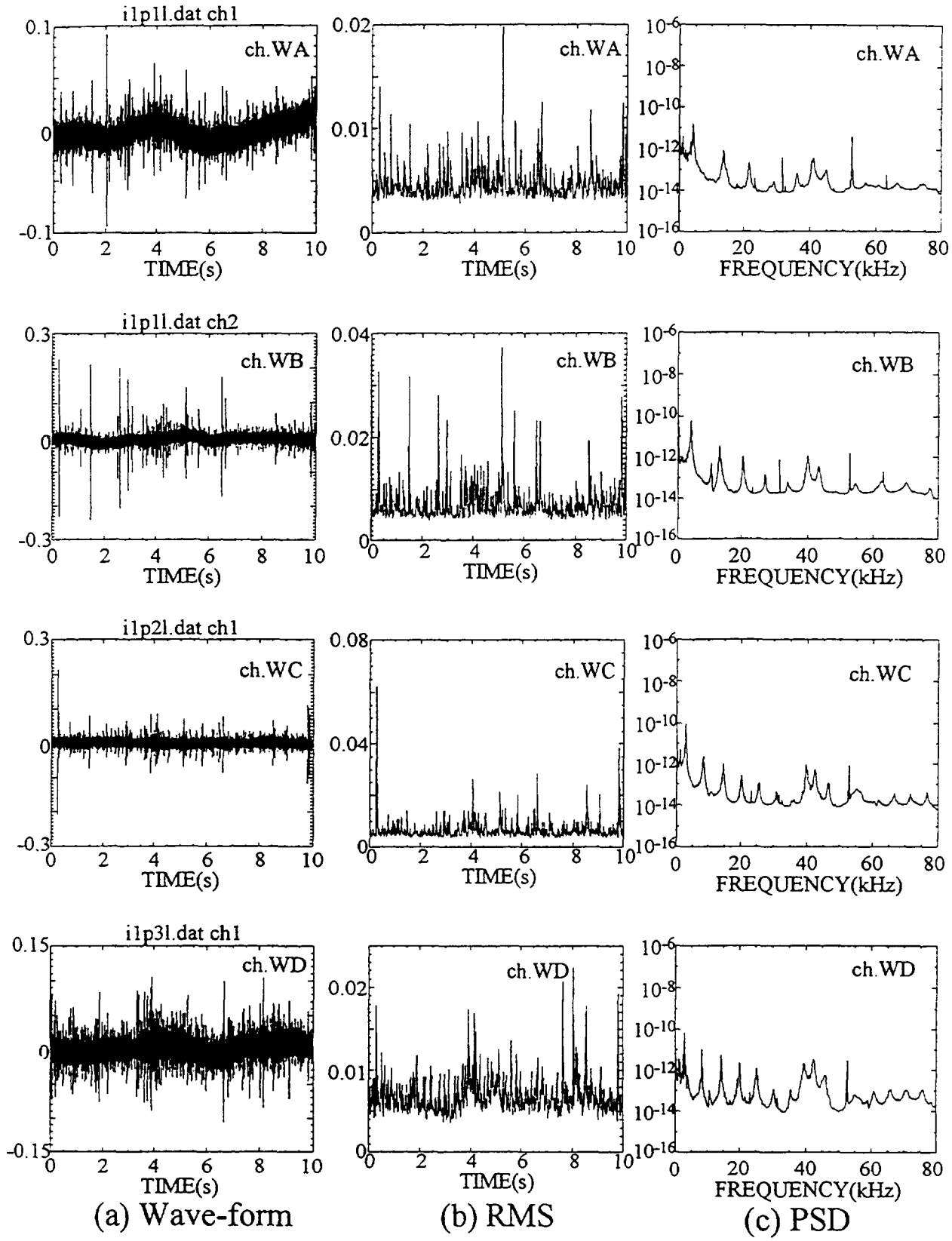

Fig. 3 Statistical features of data set Injection-1 (Hydrogen-1)

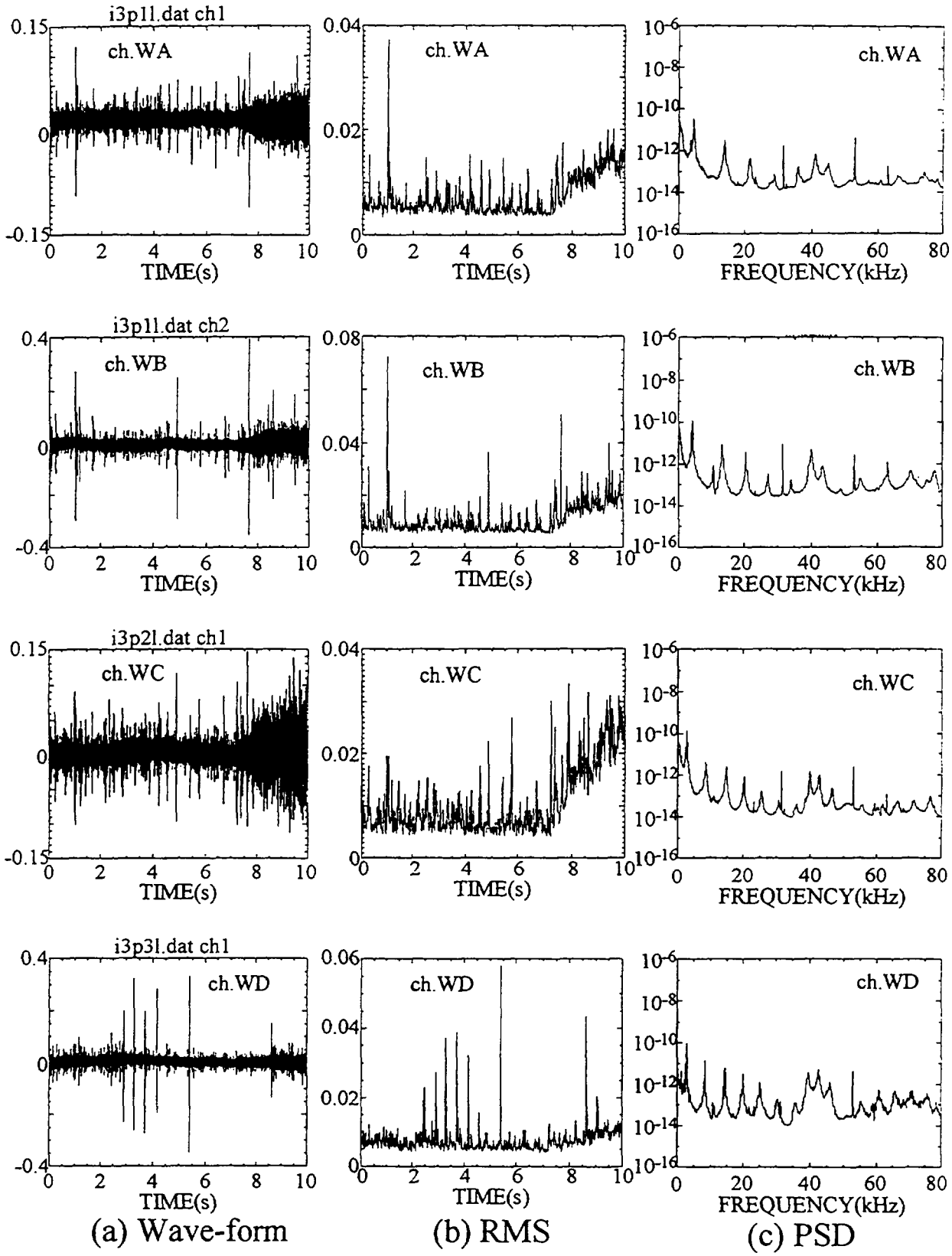

Fig. 4 Statistical features of data set Injection-3 (Argon-1)

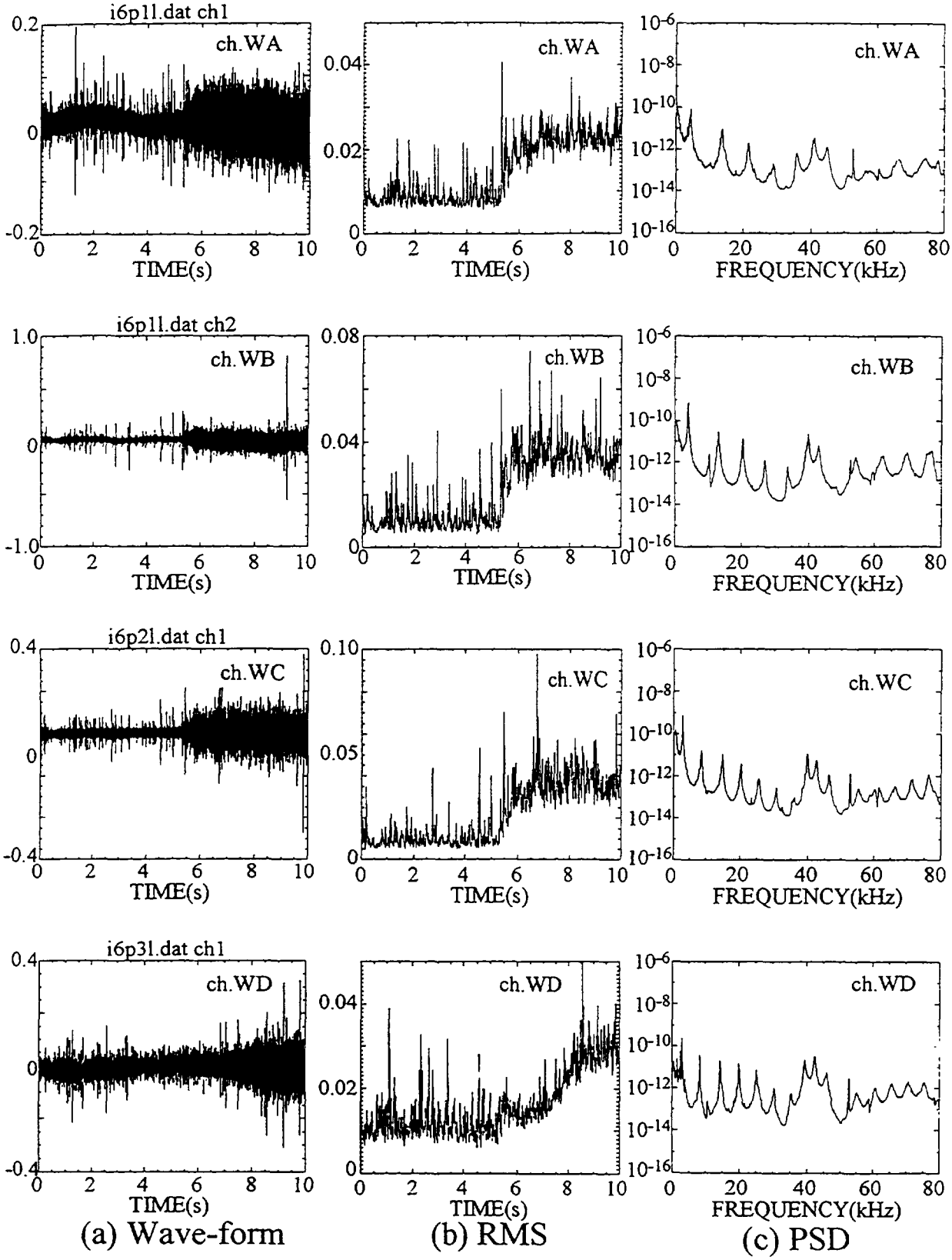

Fig. 5 Statistical features of data set Injection-6 (Water-1)

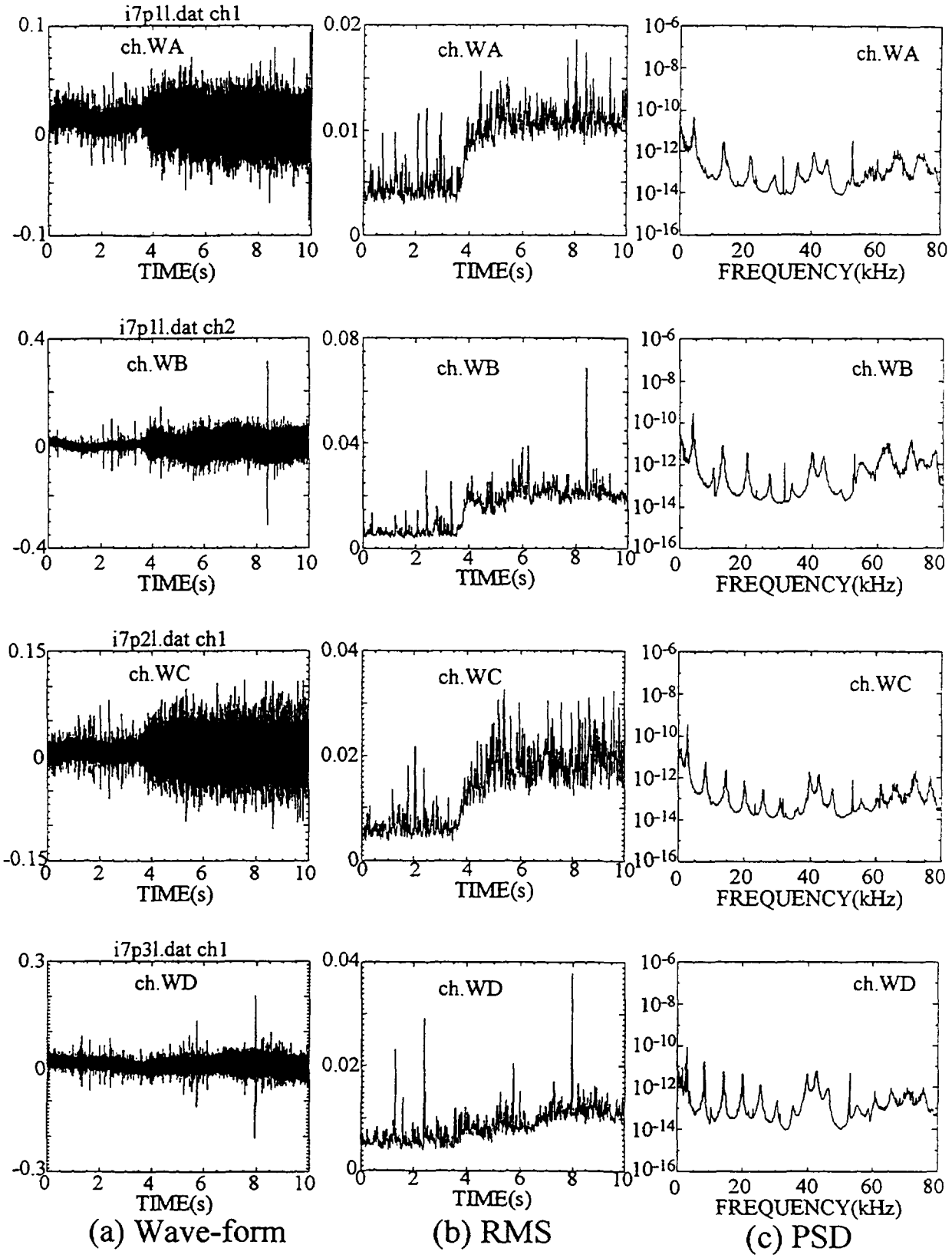

Fig. 6 Statistical features of data set Injection-7 (Water-2)

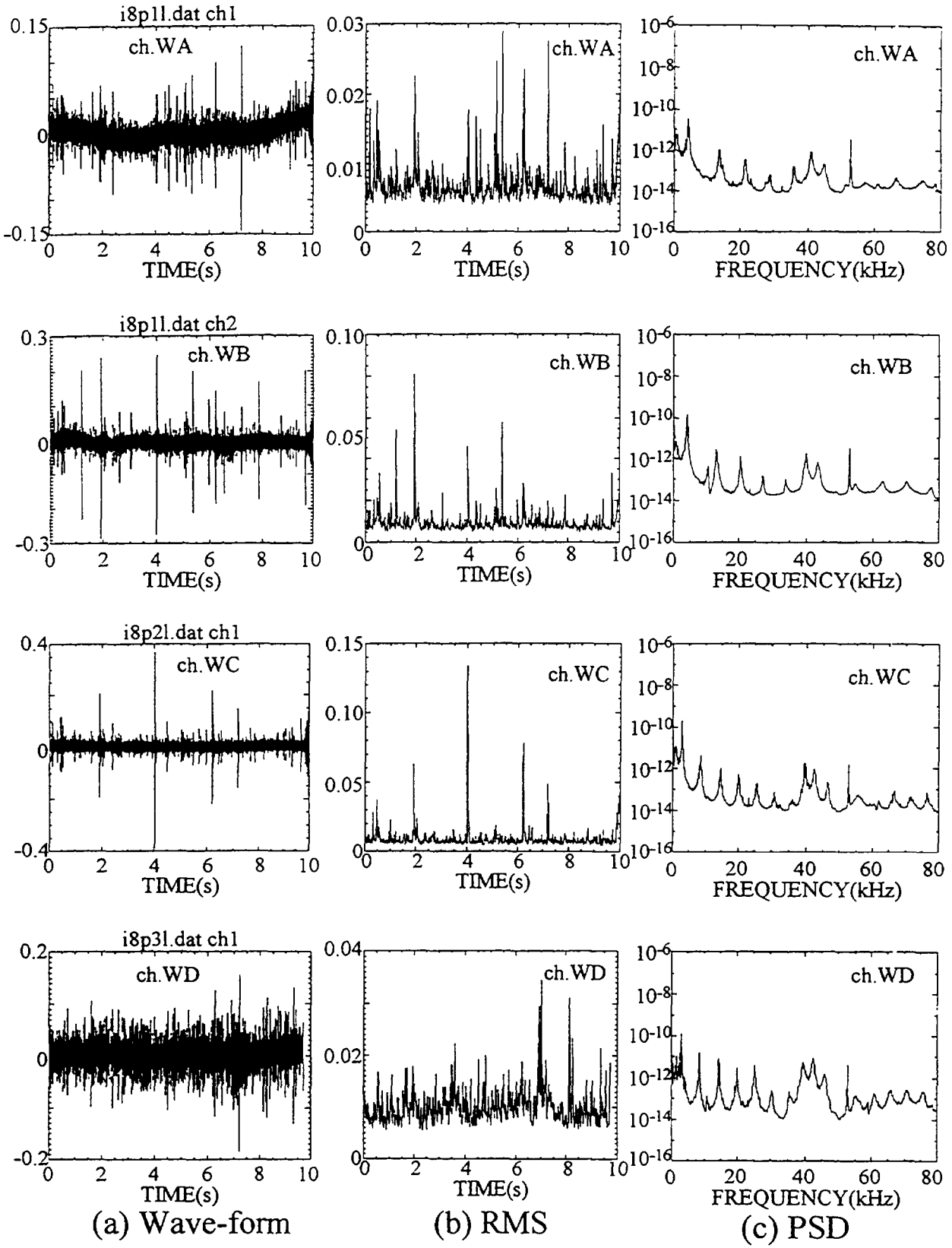

Fig. 7 Statistical features of data set Injection-8 (Water-3)

The spectral analysis was performed for whole data containing both stages before and during injection. It is found from the spectral analysis that the signals WA and WB have a similar pattern each other; they have multiple resonance peaks, the major peak appears at about 4 kHz and other peaks are located at the frequencies every 7 kHz. The signals WC and WD also have a similar pattern each other, the major peak appears at about 2.5 kHz and other peaks are located at the frequencies every 5.5 kHz.

(3) Injection-3: Argon-1

The wave-forms of acoustic signals WA, WB and WC show a high amplitude after 7 s. The RMS values also increase at the same time point. All signals contain many large pulses before and after high amplitude duration. The spectral pattern of each signal is very similar to the injection-1.

(4) Injection-6,7,8 : Water/Steam-1,2,3

The wave-forms and the RMS values of all signals show very clear changes in the cases of the injection-6 and 7 but the case of the injection-8. It is considered from the RMS values that the leak rate of each injection is set as follows;

Injection-6 > Injection-7 > Injection-8.

Other features of the signals are similar to the cases of the injection-1 and 3.

3. Background Signal Whitening Filter Using Autoregressive Model

In order to enhance the leak noises and to suppress the background noises in the sensor signals, we applied the autoregressive (AR) modeling techniques as same as the previous benchmark test.

3.1 Autoregressive Model

The AR model[7,8] is a well-known time series model defined as follows;

$$x_t = \sum_{m=1}^{M} a_m x_{t-m} + \varepsilon_t \qquad (1)$$

where $\{ x_t ; t=1,..,N \}$ is a time series data set, $\{a_m; m=1,..,M\}$ AR coefficients, M a model order and $\{\varepsilon_t; t=1,...,N \}$ a residual time series data set that is a Gaussian white noise with a mean $E[\varepsilon_t]=0$ and a variance $E[\varepsilon^2_t]=\sigma^2_M$. The AR coefficients and the model order can be obtained through a model fitting to a given time series data using a fitting procedure, e.g., the Yule-Walker method.

For the case of univariate autoregressive (UAR) model, the AR coefficient in Eq.(1) gives an impulse response function of a signal whitened process. In this model, the signal value x at current time t is expressed by linear combinations of past values $\{x_{t-1},..,x_{t-m}\}$ of signal x.

3.2 Background Signal Whitening Filter

When the AR coefficients are already obtained, the current signal value can be predicted from its past values as follows;

$$\hat{x}_t = \sum_{m=1}^{M} a_m x_{t-m}. \qquad (2)$$

The prediction error in Eq.(2) is calculated by

$$\varepsilon_t = x_t - \hat{x}_t = x_t - \sum_{m=1}^{M} a_m x_{t-m} \quad (3)$$

The prediction error is a Gaussian process when the signal x is a stationary process. However, if the signal deviates from the stationary process, the prediction error increases and it becomes a non-Gaussian process.

This property is very useful for detecting a leak noise masked by the background signal. The Eq.(3) can be used as a background signal whitening filter that suppresses only the background signal components in the test signal by using the AR model fitted to the background signal.

In practice, we fitted the UAR model to each background noise signal then built the background signal whitening filter. Since the background noise signals for each injection experiment were not supplied in the present benchmark test, initial 4096 samples in each data set of the injection experiments were used for the model fitting. The model order was set on about 60 for each case. **Figs.8(a)** through **8(d)** show power spectral density (PSD) functions of the background noise signals for the cases of Injection-1, 6, 7 and 8. They were calculated from the fitted UAR models.

3.3 Time-Frequency Spectrum

It should be noted that this filter can suppress only stationary background noise signal because the AR model expresses only a stationary process. The UAR whitening filter has an inverse pass-band characteristic (gain function) of PSD pattern of the background signal. Therefore, the prediction error (or filter output) increases when the input signal contains not only both stationary and nonstationary leak signal components but also nonstationary background signal components like a large amplitude pulsive noise. However, the non-leak or non-boiling large pulse component can be easy classified by use of spectral information as mentioned in the previous paper[5]. Especially, time-frequency spectrum estimated based on instantaneous UAR model is very useful for this purpose [5,6]. In the present benchmark test, we newly tried to use the time series of spectral components at a specified frequency as a feature signal.

4. Estimations of Start Time and Duration

4.1 Filtering Results

We processed four waveguide signals for three cases of the Injection-1, 6 and 8 using the UAR background signal whitening filter mentioned in the previous section.

(1) Injection-1: Hydrogen-1

The filtering results for the case of Injection-1 are shown in **Fig.9**; (a) is the waveforms of the filter output signals, (b) the RMS values calculated with a time interval 25.6 ms (4096 samples) and (c) Time-Frequency PSD values at a specified frequency point, calculated by UAR model with a time interval 12.8 ms (2048 samples).

It is found from the results that the large DC changes in original signals as seen in **Fig.3(a)** are suppressed but the high-amplitude pulsive noise still remains. Therefore, the RMS values show many pulses. It seems that the signal ground levels of the RMS step up at 2 s and at 3.5 s in the signal WC and at 3.5 s in the signal WD. However, we could not identify the signal state from this information because we have no reference data on the acoustic signals during an injection of hydrogen.

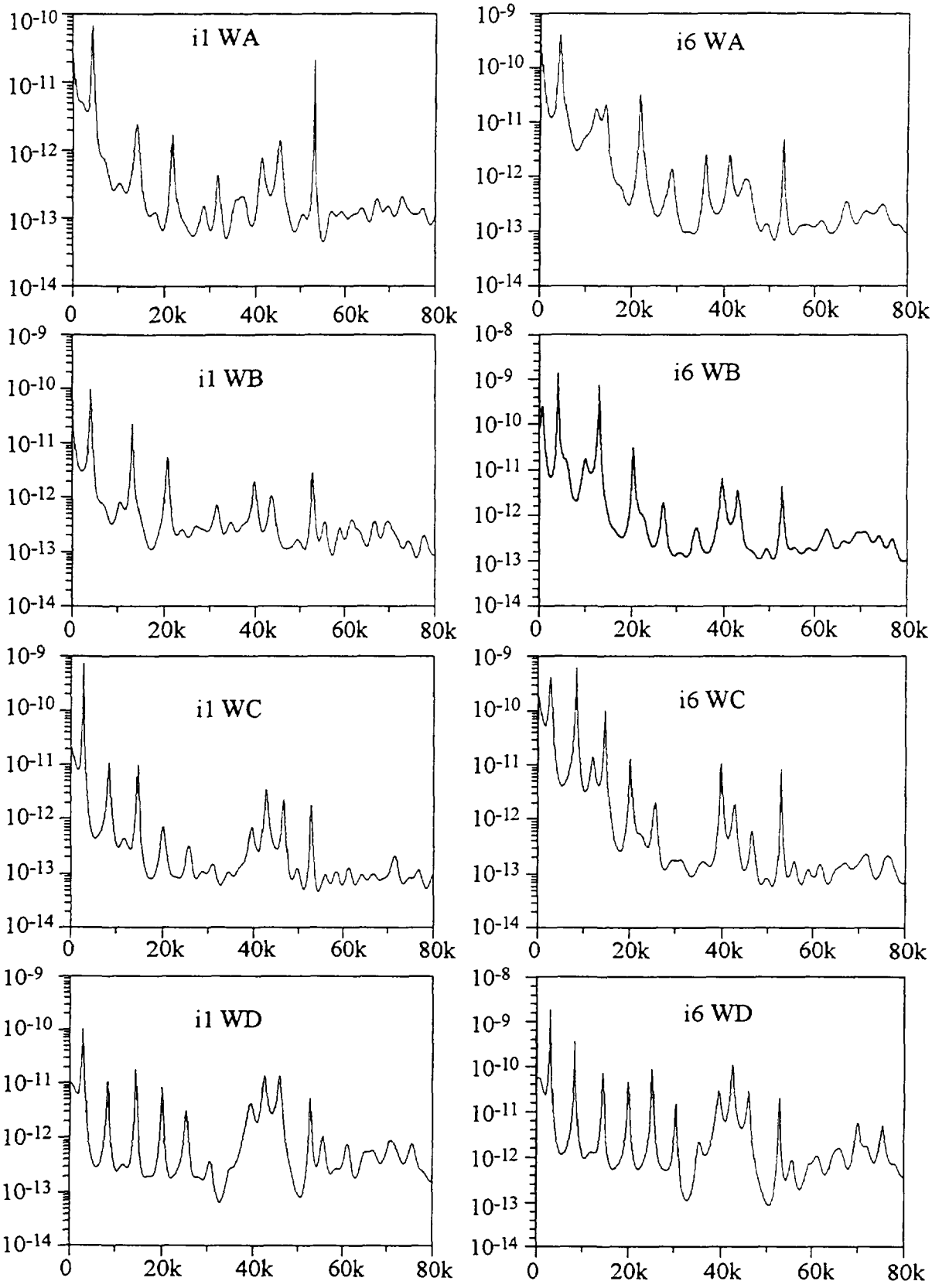

(a) Injection-1 (Hydrogen-1) (b) Injection-6 (Water-1)

Fig.8 APSDs of background noise signals (Initial parts of data set)

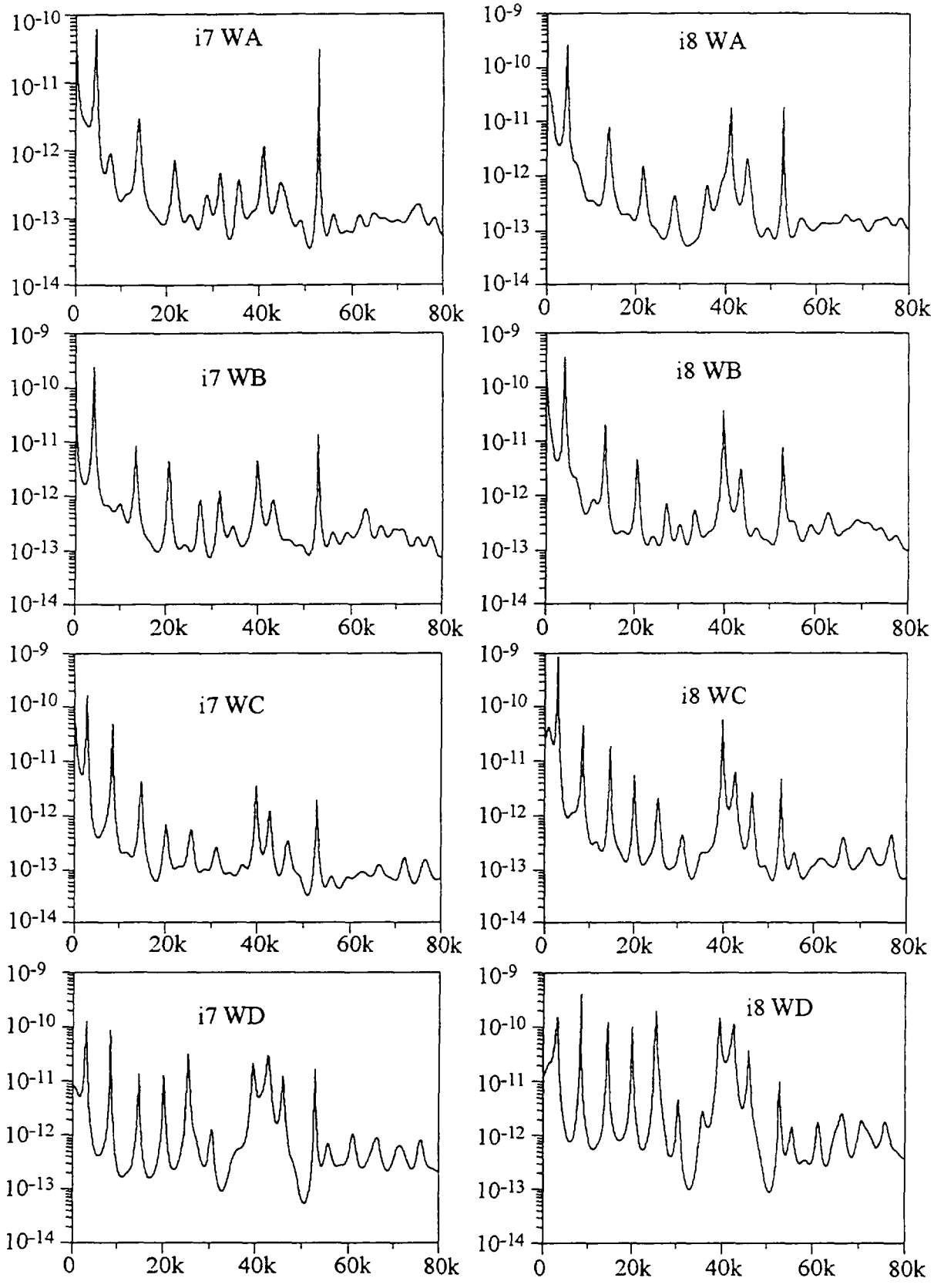

(c) Injection-7 (Water-2) (d) Injection-8 (Water-3)

Fig.8 APSDs of background noise signals (Initial parts of data set) (continued)

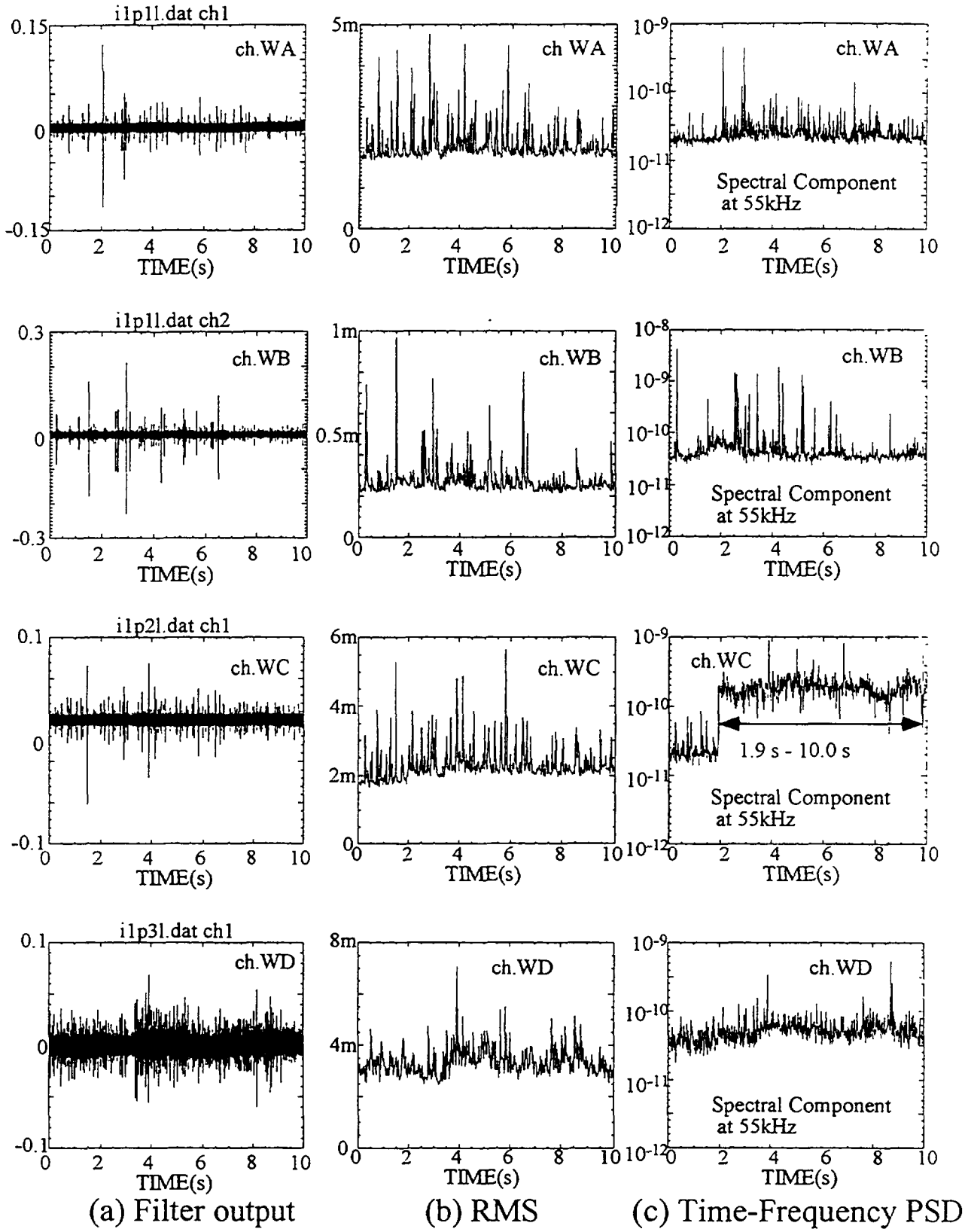

Fig. 9 Statistical features of whitening filtered signals
Injection-1 (Hydrogen-1)

Next, we tried to find a statistical feature that changes clearly between initial recording time and final recording time in the data set. **Fig.10** shows the time-frequency spectra of the waveguide-C for the cases of (a) the original signal and (b) the whitening filtered signal. We can find that the frequency component around at 55 kHz slightly changes at about 2 s in the graph (a). This frequency component can be extract clearly by use of the whitening filter as shown in the graph (b). **Fig.9(c)** shows the time-dependent property of this frequency component. The remarkable change of frequency component was observed only in the signal WC at 55 kHz.

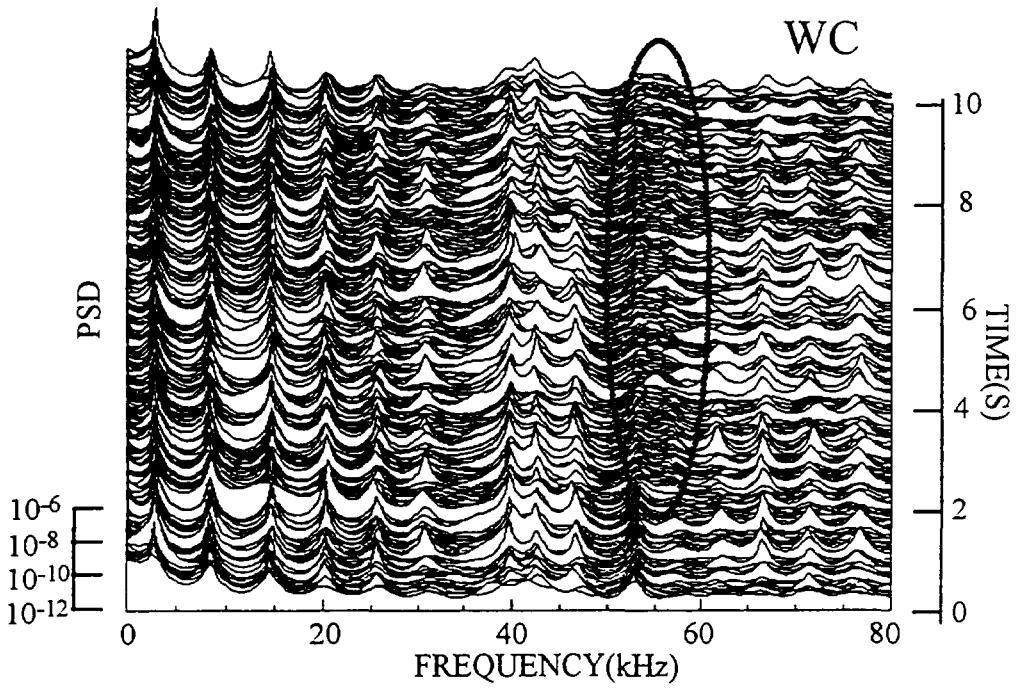

(a) Original signal

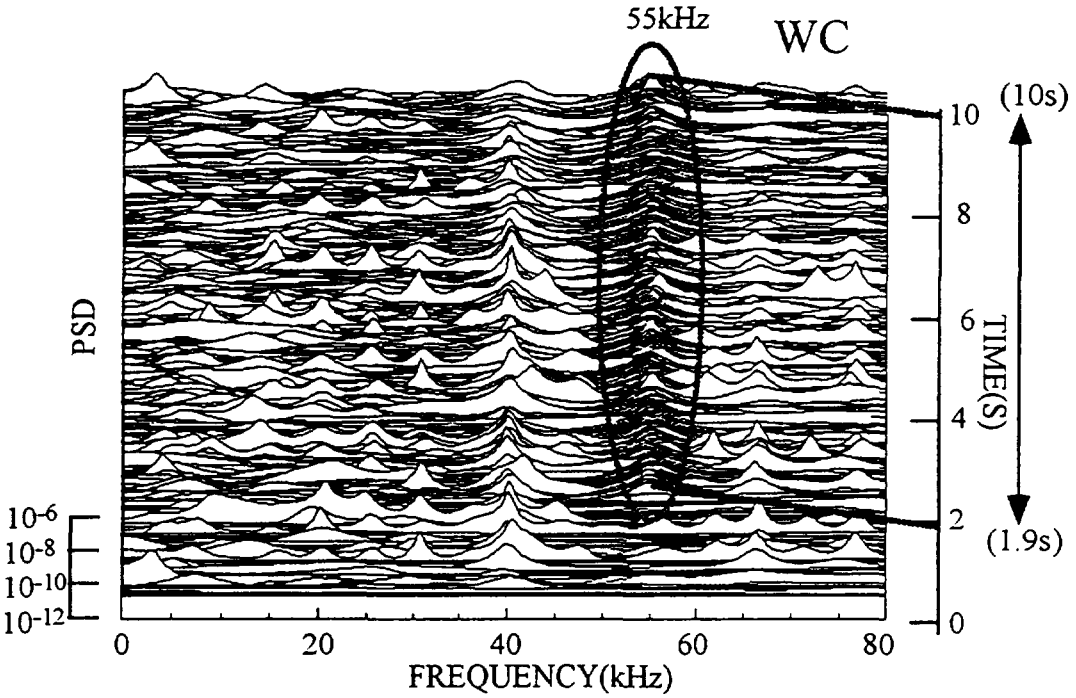

(b) Whitening filtered signal

Fig.10 Time-Frequency spectra of waveguide WC in data set Injection-1 (Hydrogen-1)

The frequency 55 kHz is out of range of the waveguide sensor response (45 kHz) but many weak frequency components still remain in the high frequency range over 45 kHz as seen in the PSD results Therefore, there is a possibility that the frequency component at 55 kHz has a physical meaning related to the hydrogen injection If this is true, we can determine from the result of the signal WC in **Fig.9(c)** that the injection started at 1 9 s and continued until 10 s

(4) Injection-6 : Water/Steam-1

The filtering results for the case of Injection-6 are shown in **Fig.11** The calculation conditions are the same as the case of Injection-1

It is found that the signal ground level of the RMS clearly steps up at 5 5 s in the signals WA, WB and WC and at 7 9 s in the signal WD The signal-to-noise ratio seems a sufficient for all case Only signal WD shows a different start time and the time delay is 2 4 s It is considered that only the waveguide WD was located at a far point from the injection point and that major acoustic components were attenuated strong in the signal propagating paths in sodium It is well known that attenuation of acoustic signal occurs strongly in high frequency range but small in low frequency range Therefore, it is considered that the signal WD still contains a wave component related to the start time 5 5 s

Fig.12 shows the time-frequency spectra of four waveguide signals after filtering For the cases of the signal WA, WB and WC, it is found that the frequency components in whole frequency range increase after 5 5 s On the other hand, the frequency component slightly increases in low frequency range less than 3 kHz after 5 5 s **Fig.11(c)** shows the time-dependent property of the frequency component at 1 kHz From this figure, we can find a signal level change at 5 5 s in the signal WD

(3) Injection-8 : Water/Steam-3

The filtering results for the case of Injection-6 are shown in **Fig.13** The calculation conditions are the same as the case of Injection-1 Major statistical features of four waveguide signals are the same as the case of the injection-1 Only the waveguide WC shows a weak change of the signal ground level in the RMS graph at about 4 s

Fig.14 shows the time-frequency spectra of four waveguide signals after filtering The signals WA, WB and WD show flat spectral patterns The signal WC shows continuous spectral peaks at around 57 kHz as same as the case of the injection-1 This is plotted in **Fig.13(c)** The time point of spectral change corresponds to that of the RMS

4.3 Start Time and Duration of the Leak State

Using the UAR background signal whitening filter, we analyzed several cases of the injection experiments The start time and duration of the leak state are summarized in **Table 4** Furthermore, the signal-to-noise ratio of each filtered signal, calculated from the signal ground levels in the RMS values, the detection margin of the method, the probabilities of missing Pm and spurious Ps are listed in **Table 5**

5. Estimation of Leak Location

In the present benchmark, we did not obtain complete results of the analysis on the estimation of leak location because of insufficient work time The following section is described on a preliminary analysis for the location estimation

5.1 Time Differences among Three Data Files

First, we evaluated the time differences existing among three data files in each data set of the injection experiment The results are listed in **Table 6**

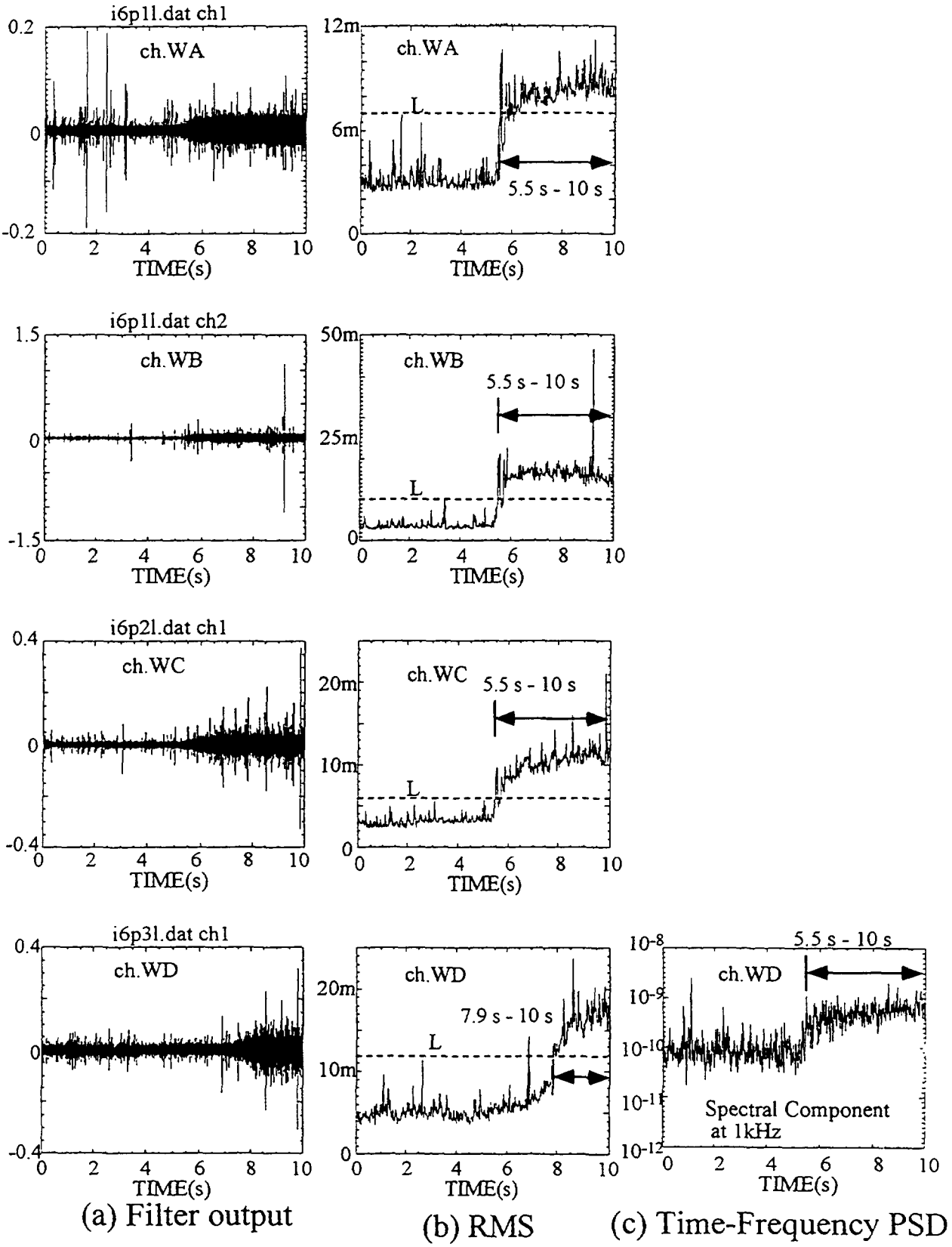

Fig. 11 Statistical features of whitening filtered signals
Injection-6 (Water-1)

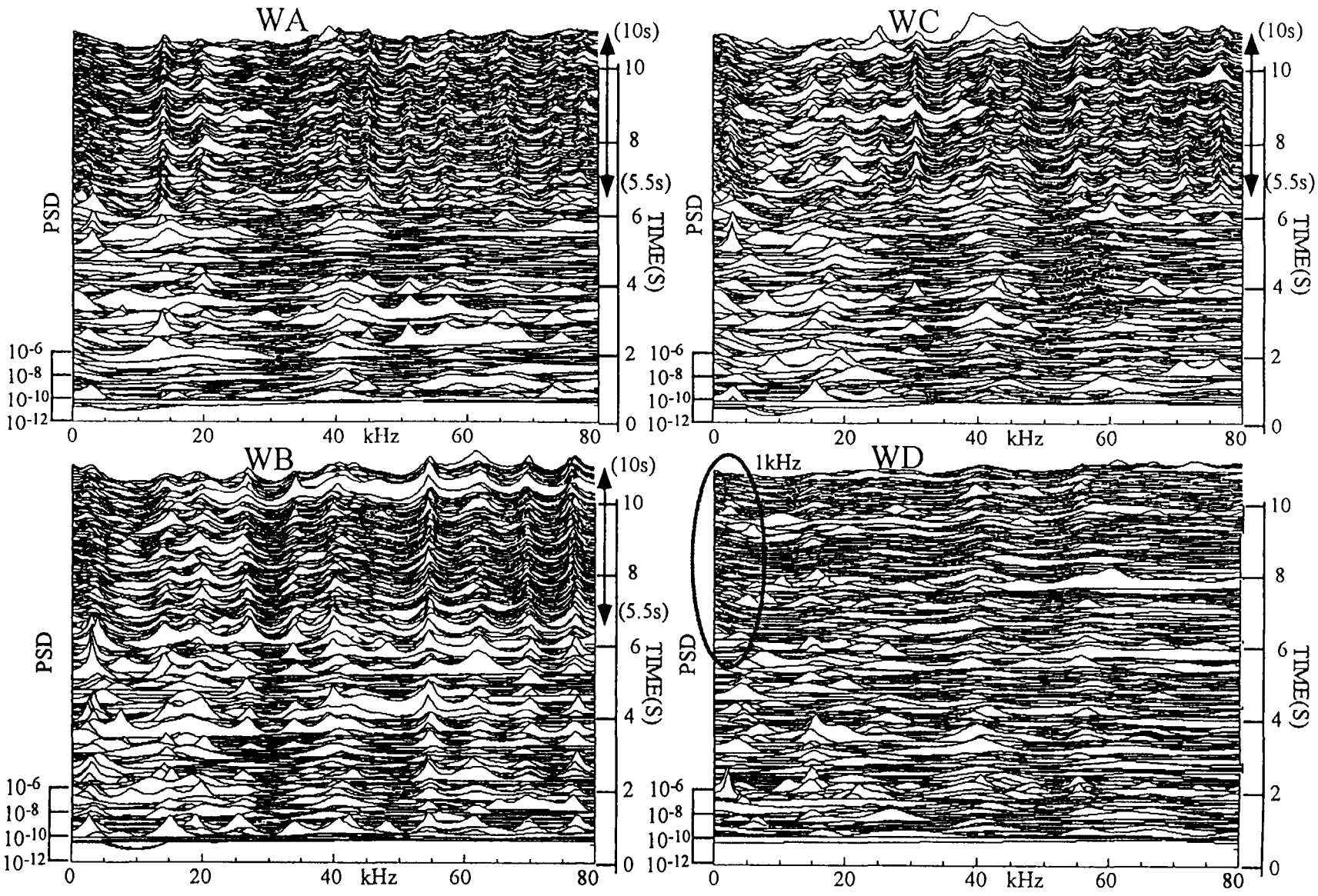

Fig.12 Time-Frequency spectra of data set Injection-6 (Water-1)

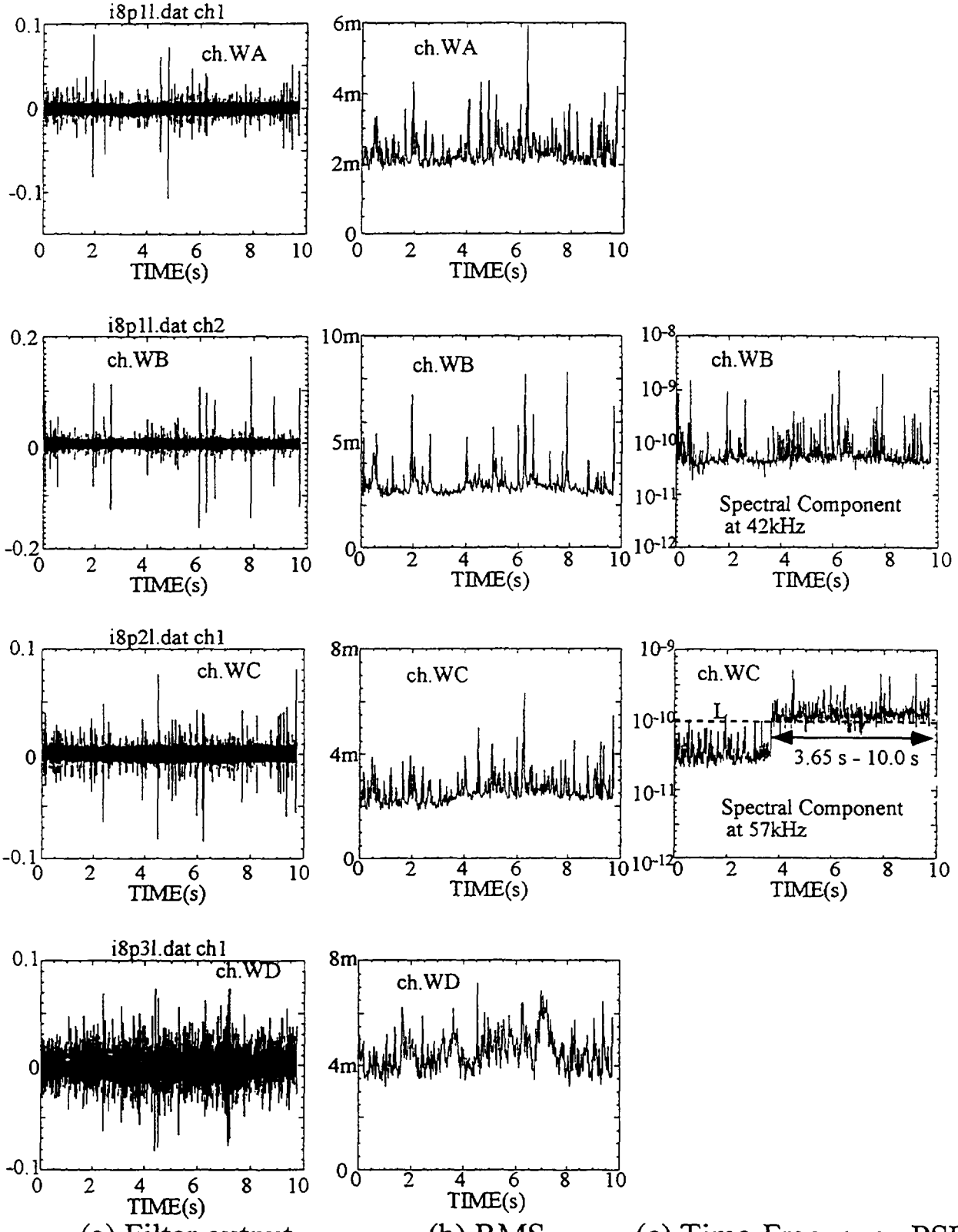

Fig. 13 Statistical features of whitening filtered signals
Injection-8 (Water-3)

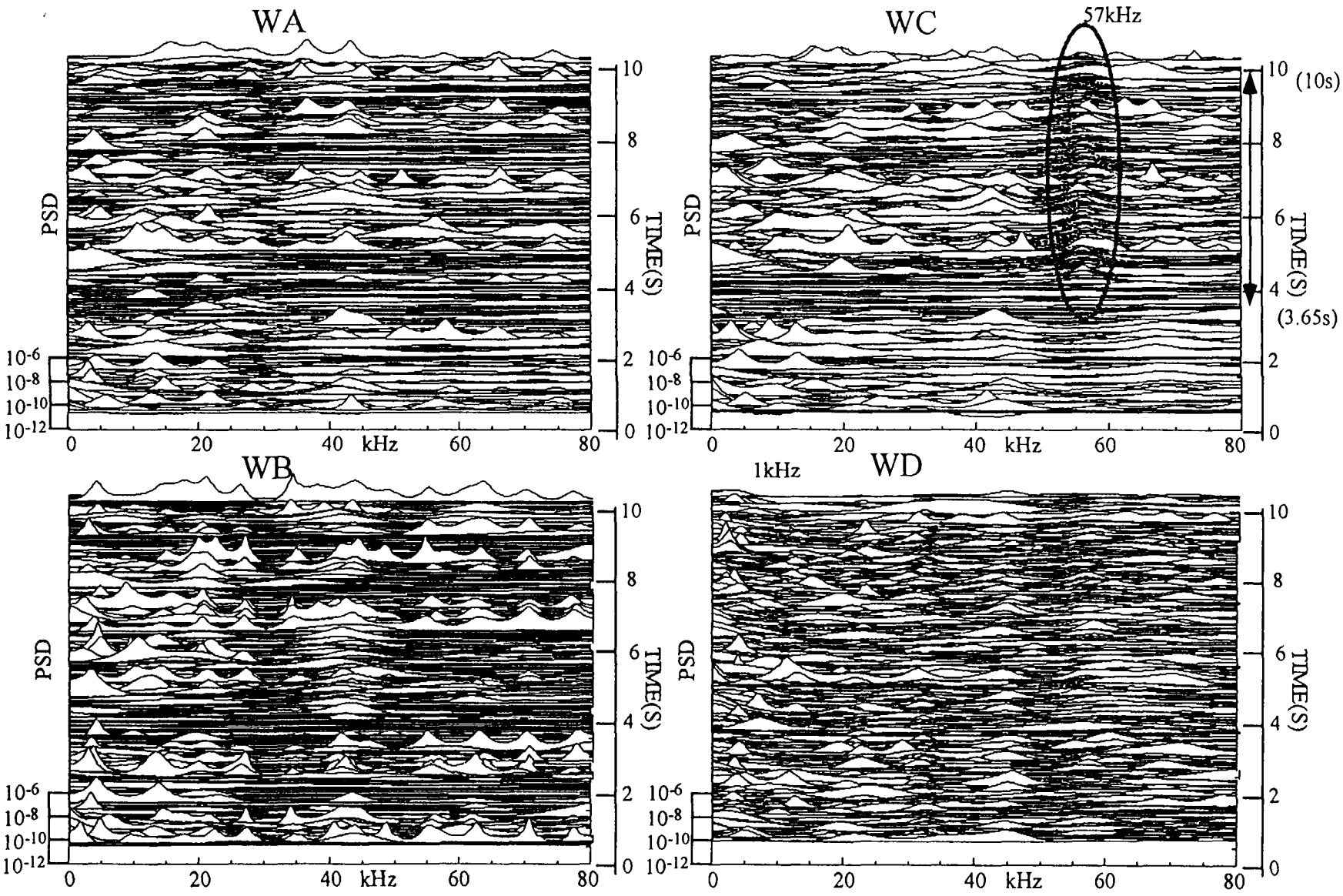

Fig.14 Time-Frequency spectra of data set Injection-8 (Water-3)

Table 4 The Start Time and Duration of the Leak

Data Set	Ch	Whitening Filter +RMS Start Time	Whitening Filter +RMS Duration Time	Whitening Filter +Time-Freq PSD Start Time	Whitening Filter +Time-Freq PSD Duration Time
Injection-1	WA	-	-	-	-
	WB	-	-	-	-
	WC	-	-	1 9s	8 1s
	WD	-	-	-	-
Injection-6	WA	5 5s	4 5s		
	WB	5 5s	4 5s		
	WC	5 5s	4 5s		
	WD	7 9s	2 1s	5 5s	4 5s
Injection-8	WA	-	-	-	-
	WB	-	-	-	-
	WC	-	-	3 65s	6 35s
	WD	-	-	-	-

Table 5 Signal-to-Noise Ratio of Filtered Signal, Detection Margin and Probabilities

		Whitening Filter + RMS							
		Signal Ground Level (BG)	(Leak)	S/N	Threshold Level L	Detection Margin (Mean)	(Peak)	Probability Miss Pm*	Spur Ps*
Injection-6	WA	0 003	0 0085	9 0 dB	0 007	1 7dB	3 9dB	0	0
	WB	0 004	0 016	12 0 dB	0 009	5 0dB	14 3dB	0	0
	WC	0 003	0 010	10 0 dB	0 006	8 0dB	11 3dB	0	0
	WD	0 005	0 015	9 5 dB	0 012	1 9dB	6 0dB	0	<0 003
		Whitening Filter + Time-Frequency PSD							
		Signal Ground Level (BG)	(Leak)	S/N	Threshold Level L	Detection Margin (Mean)	(Peak)	Probability Miss Pm*	Spur Ps*
Injection-1	WC	$10^{-10\,7}$	$10^{-9\,7}$	10 0dB	$10^{-10\,0}$	3 0dB	9 5dB	0	0
Injection-6	WD	$10^{-10\,1}$	$10^{-9\,3}$	8 0dB	$10^{-9\,5}$	2 0dB	8 0dB	0	<0 025
Injection-8	WC	$10^{-10\,5}$	$10^{-9\,9}$	6 0dB	$10^{-10\,0}$	1 0dB	7 0dB	0	<0 003

* (Until first leak pulse arrives)

Table 6 Time Differences

File	Point	Time(ms)	File	Point	Time(ms)
I1P1L	0	0	I7P1L	0	0
I1P2L	-3722	-23 2625	I7P2L	-8048	-50 3000
I1P3L	-447	-2 79375	I7P3L	-2194	-13 7125
I6P1L	0	0	I8P1L	0	0
I6P2L	+275	+1 71875	I8P2L	-893	-5 558125
I6P3L	+1748	+10 925	I8P3L	+2015	+12 59375

5.2 Multivariate Autoregressive model

In the estimation problem of the leak location, we tried to use an estimation method that uses the time constants of the acoustic signal propagating paths. The time constants of the sub-system in multivariate feedback system can be estimated using the multivariate AR modeling techniques [5,8].

For the case of multivariate autoregressive (MAR) model, $\{x_t\}$ and $\{e_t\}$ in Eq.(1) become vector time series and $\{a_m\}$ becomes matrix. The diagonal element in the MAR coefficient matrices gives impulse response function of a whitening process for each signal. The off-diagonal element gives an impulse response function, of sub-system between two signals, by convolution with an impulse response function of a whitening process.

From the equivalent expression of multivariate feedback system by the MAR model, we can understand that the MAR model gives not only the information for the feedback system consisting of sub-systems between the signals but also the information for the noise source signals. In the case of the present benchmark test, the feedback system corresponds to acoustic propagating path on the vessel surface of the evaporator-3, the noise source signals correspond to the arrived acoustic signal at the sensor location from vessel inside and the noise source process corresponds to acoustic propagating path in sodium.

The time constant of each sub-system is estimated by the MAR model using the acoustic signals during injection state. Only one case of the Injection-6 was calculated using the data sampled from the stationary injection stage around 6 s. Each time constant showed several μs. This value is very smaller than that in the case of ASB loop in the previous benchmark test. A difference between both cases of the PFR injection and the ASB loop is at cross correlation values among four sensor signals; the waveguide signals of the evaporator in PFR correlate very low with other signals.

7. Concluding Remarks

We applied the autoregressive modeling techniques to acoustic signal processing for detecting in-sodium water leak. In the present benchmark stage, we evaluated the performances of the method using the acoustic signals from the real injection experiments of hydrogen or water/steam.

Through the analysis of real experimental data, we concluded that the signal processing method using the UAR background signal whitening filter can detect reliably the leak signals with a sufficient signal-to-noise ratio. Even if the sensor signal contains non-boiling or non-leak high-amplitude pulses, they can be classified by spectral information. Especially, the feature signal made from the time-frequency spectrum of the filtered signal is very sensitive and useful.

In the estimation problem of the leak location, we have been developed the estimation method using the time constants of the acoustic signal propagating paths based on the multivariate AR modeling techniques. Unfortunately, this analysis for the injection data was stopped because of the time limit. However, we believe that this method has a possibility to give new and very useful information on the propagation paths.

References

[1] Y. Shinohara et al.: The Result of Sodium Boiling Noise Detection Benchmark Test, Report prepared for Research Coordination Meeting on Acoustic Signal Processing for the Detection of Sodium Boiling or Sodium/Water Reaction in LMFBR, Vienna, 20-22 November, 1990.

[2] Y. Shinohara et al.: The Result of Benchmark Test on Sodium Leak Noise Detection, Report prepared for Research Coordination Meeting on Acoustic Signal Processing for the Detection of Sodium Boiling or Sodium/Water Reaction in LMFBR, Chester, 25-27 September, 1991.

[3] Y. Shinohara et al.: The Result of Benchmark Test on Sodium Leak Noise Detection, Report prepared for Research Coordination Meeting on Acoustic Signal Processing for the Detection of Sodium Boiling or Sodium/Water Reaction in LMFBR, Vienna, 17-19 November, 1992.
[4] K. Hayashi et al.: The Result of Benchmark Test on Sodium Leak Noise Detection, Report prepared for Research Coordination Meeting on Acoustic Signal Processing for the Detection of Sodium Boiling or Sodium/Water Reaction in LMFBR, Vienna, 9-10 November, 1993.
[5] K. Hayashi, et al. : Autoregressive Techniques for Acoustic Detection of In-Sodium Water Leaks - The Results of 1994 Benchmark Test on Detection of Sodium/Water Reaction-, Report presented for Research Coordination Meeting on Acoustic Signal Processing for the Detection of Sodium Boiling or Sodium/Water Reaction in LMFBR, Kalpakkam, India, 1-3 November, 1994.
[6] R. Currie: Acoustic Leak Detection Experiments Performed in PFR, March 1993 to June 1994, Report presented for Research Coordination Meeting on Acoustic Signal Processing for the Detection of Sodium Boiling or Sodium/Water Reaction in LMFBR, Kalpakkam, India, 1-3 November, 1994.
[7] K. Hayashi et al.: A Method of Nonstationary Noise Analysis Using Instantaneous AR Spectrum and Its Application to Borssele Reactor Noise Analysis, Progress in Nuclear Energy, 1988, Vol.21, pp.707-716.
[8] K. Hayashi et al.: Study of the Goodness of System Identification Using Multivariate AR Modeling, Progress in Nuclear Energy, 1988, Vol.21, pp.697-706.

ADVANCED SIGNAL PROCESSING TECHNIQUES FOR ACOUSTIC DETECTION OF SODIUM/WATER REACTION

V.S. YUGHAY, A.V. GRIBOK, A.N. VOLOV
Institute of Physics and Power Engineering,
State Research Center,
Obninsk, Russian Federation

Abstract

In this paper results of development of a neural network technique for processing of acoustic background noise and injection noise of various media (argon, water steam, hydrogen) at test rigs and industrial steam generator are presented.

1. Introduction

In the report of the Russian participants of the Coordinated Research Program on Acoustic Signal Processing for the Detection of Boiling or Sodium / Water Reaction in LMFBR the results of development of a neural network technique for processing of acoustic background noise and injection noise of various media (argon, water steam, hydrogen) at test rigs and industrial steam generators are presented

Being a logic continuation of the investigation on sodium boiling noise processing in reactor core, the Coordinated Research Program on Acoustic Signal Processing for the Detection of Boiling or Sodium / Water Reaction in LMFBR was initiated in December 1989, when the Russian side transferred to the participants the data on acoustic leak simulation on IPPE test rig These data consisted of 8 records of noise of water injections with various flow rates (0 01-0 6 g / s) at sodium temperatures 300, 400 and 500 C °

During the research program the participants used various methods of signals processing and from fragmented knowledge on leak noise peculiarities came to the development of a prototype acoustic system

The largest contribution to recording of background noise of SGU and leak simulation noise in various conditions have been made by British experts which are the pioneers of acoustic leakage detection in LMFBR

The knowledge about background noise would not be comprehensive without participation of French experts, possessing large experience in the area. For leak detection French participants used root-mean-square value calculated in a narrow band of frequencies, determined by empirical way

The Japanese experts have demonstrated excellent technical opportunities, analyzing characteristic of pulses of background noise, and have proposed a method of twice squaring and integration for leak detection The method proposed for leak location is also interesting

Australian experts applied the newest techniques of signals processing such as Wavelet transform not leaving without attention theoretical aspects of leak noise generation

The Holland experts have joined the other participants of the program in 1994, however they proposed an interesting method for detection of abnormal signals The method is based on estimation of residual noise distribution

The Indian experts performed the careful analysis of power spectral densities of the signals and detect leak by changes in determinant and trace of covariance matrix

Results of researches on integration of an acoustic system into a distributed computer network, presented by German representative should be considered as perspective, as far as acoustic leakage detection system should be included in a system for complex diagnostics of the NPP equipment

The IPPE experts, having tried various statistical characteristics of signals as diagnostic features, came to a conclusion that statistical features do not exclude false alarms in real conditions, since 1992 develop adaptive filtering for background noise canceling and applied neural network for recognition of acoustic noise patterns

2. A status of the acoustic Surveillance Technology Development for SGU leak monitoring

As experiments have shown, a real water leak will escalate rapidly in a time with a fast increase of flow rate from microleak up to ~4 5 g /s within few seconds /1/, with subsequent stabilization of the flow rate At this time the steam jet, interacting with sodium, begins to destroy neighbour tubes, that results in a global accident The character of leak escalation depends on sodium temperature, tube materials and on the other conditions

To undertake proper action to prevent the accident it is necessary to detect a leak with the flow rate of 1-5 g /s within 1 sec and with false trip rate not more than 1 per 10 years /2/. Hydrogen monitoring system allows to detect a leak not faster than in 40 sec Leak generates noise due to the steam jet and due to hydrogen bubbles oscillations and collapses

Acoustic method of leak detection has a very fast response and provides required sensitivity. However, the problem of false trip rate minimization is the mostly challenging task for acoustic systems

The variety of physico-chemical processes under leak conditions, generates noise in a wide range of frequencies from hundreds of Hertz up to hundreds of kilohertz In a range of frequencies up to ~100 kHz a powerful masking noise take place consisting of background noise and abnormal impulsive noise which has a random nature and depends on a number of conditions Theoretically it is promising to use high frequency band meanwhile the area of frequencies 200-800 kHz is practically not investigated But in the area of ultra sound a masking noise can appear due to acoustic emission of constructional materials

Thus, to avoid false trips and to achieve maximum sensitivity in acoustic system it is necessary to differentiate between leak noise, normal background noise and abnormal background noise

3. Advanced signal processing techniques for acoustic detection of sodium-water reaction

The adaptive method of vibro-acoustical signals identification consists of adaptive filtering for extraction of weak signals from background noise, generation of compact time-frequency acoustic patterns and a neural network for their recognition.

Adaptive filtering being applied to acoustic leak detection is based on the fact that leak noise is less correlated than background noise Being learned on background noise adaptive filter is able to filter out powerful frequency components of the background noise meanwhile preserving uncorrelated components of leak noise If background noise and leak noise overlap in frequency range significantly it is purposewise to use nonlinear adaptive filtering The general layout of different adaptive filters are shown in Fig 1 If background noise changes(which is true) during plant operation adaptive filter changes its amplitude - frequency characteristics, thus adapting to new conditions The main problem in application of adaptive filtering is a

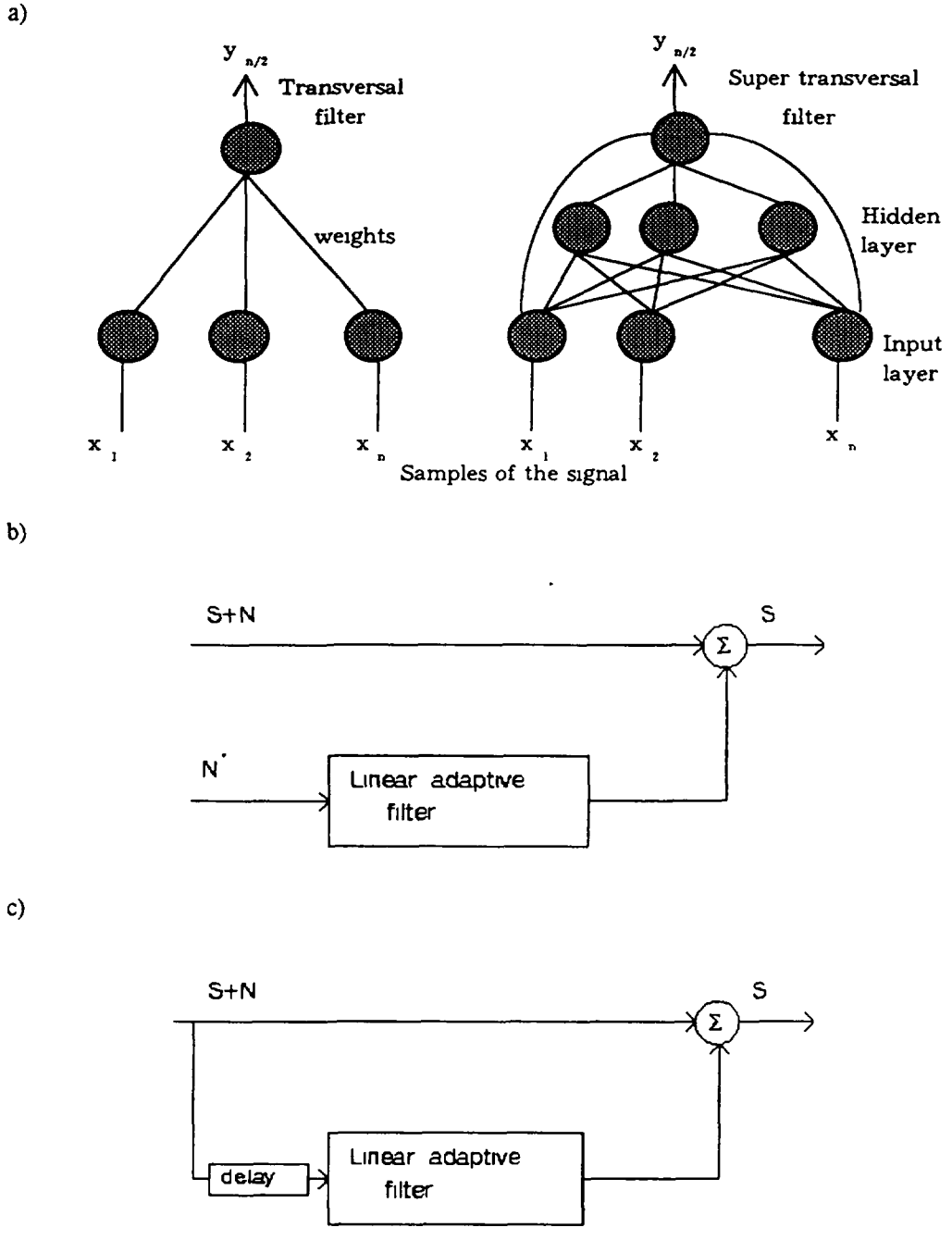

Fig 1 a) General layout of transversal and super transversal filters
b) Principle of noise canceling
c) Principle of noise canceling without external reference signal

proper reference signal which must be correlated with background noise and not correlated with leak noise For acoustic leakage detection system it is proposed to get such reference signal via delay in processing signal The digital adaptive filters, implemented in hardware , can work in a time scale, close to real However the highest frequency of working band is limited because of the large requirements to computing resources.

The pattern generation is necessary to extract useful information from the signal and to reduce the dimensionality of patterns which should be recognized by neural network. To determine the contribution of each frequency into total power of the signal, FFT is used which can be carried out using FFT processors. To achieve necessary frequency resolution FFT is calculating over 2048 samples thus resulting in 1024 of spectral points

The dimensionality of this array is too big to be fed into neural network and to ensure robust convergence That is why a feature extraction is necessary Different techniques are used to carry out this feature extraction and one of the most popular is principal component analysis Several spectra calculated at different time provide more complex pattern and describe the frequency components behaviour in time

The most known neural network which is used for recognition of complex patterns is multy-layer perseptron with backpropagation learning rule /3/ Each layer consists of nonlinear threshold elements neurons, thus if x - input value then the output will be as follows $y=(1+\exp(-x+\theta))^{-1}$ where θ - some threshold value Neurons of one layer are linked with neurons of the other layer by a principle each with each The strength of coupling between neurons is described by weights which are modified during training. A desired vector is presented to the output layer during training phase. An input pattern is presented into input layer The training consists in minimization of an error between desired and actual output of the network Then derivative for each weight of output layer is calculated using error value, the derivatives propagates through layers starting from the output to input that is why the name - backpropagation The weights are modified by gradient descent technique. For acceleration of training and avoiding local minima a variable learning step is used, which depends on the success of the previous iteration Process of training proceeds until then while the error on output layer of the network will not become less a beforehand given value The training will be correct, if training set really consists of two classes background noise and leak noise. If there are abnormal noises in background noise, which also take place during leak noise then the network will permanently relearn and unconvergence can take place. Therefore before training a careful preselecting of training patterns should be made and may be new classes must be added during learning procedure For this purpose self-organizing neural networks can be used to share the incoming signal into a preselected number of classes Being trained the network can generalize the new information Then the output layer provides the classification result During the processing of benchmark data the network did not relearned but in practice it is necessary to perform this procedure to adapt the weights to slow changes of background noise The time constrain during the recognition of complex acoustic patterns will require a hardware implementation of neural network

All the procedures of the data processing are written in Borland Pascal with graphic display of the information and run under operating system DOS 5 0 Algorithms of main procedures can be used for development of the software for leak detection

Process of training can take a time from several seconds up to several minutes depending on the computational power of the hardware and on the nature of patterns

in training set. The recognition is performed considerably faster, the time is comparable to time which is necessary for data reading from computer memory

At present time the investigations on application of adaptive techniques in vibro-acoustic monitoring systems are concentrated on the development of effective feature extraction algorithms and on recurrent networks for context-dependent recognition of incoming patterns

4. Summary of the work done during 93-95 and answers to standard questions

4.1 *Brief description of the benchmark data*

The benchmark data in 1993 contained background noise of Superheaters 2 and 3 of PFR mixed with noise of injections with flow rates 1 8 and 3 8 g / c, recorded on the ASB loop (Germany) The benchmark data have been prepared by Japanese experts and consisted from mixtures with signal to noise ratio from -24 up to -12 The benchmark signals were recorded on magnetic tapes in frequency band up to 40 kHz and consisted of 2 series with 4 records in each

For 1994 benchmark data background noise recorded at Superheater 2 of PFR, from 4 sensors has been mixed with leak simulation noise recorded on ASB loop also from 4 sensors The signal to noise ratio was from -6 dB down to -24 dB. The data have been prepared by French experts in digital form with sampling frequency of 131072 Hz Five test sets have been distributed among the participants

Closest to real situation are the benchmark data 1995, which differ from previous benchmarks and have been recorded without any artificial mixing The data were recorded by AEA Technology experts during the End - of - Life experiments on PFR. The benchmark data consist of the following records

- Background noise of Evaporator 3 loop at full power,
- Background noise of Superheater 3 loop at full power,
- Noise of two hydrogen injections,
- Noise of three argon injections,
- Noise of three water injections

The injections of hydrogen, argon and water were carried out into Evaporator 3, when the reactor was shut down, steam/water side was padded, and with the sodium pump was been operated at reduced speed. The noise of injections were recorded from 4 sensors (waveguides "a ", "b", "c" and "d"), and were chosen from numerous series of experiments so that the flow rates of injected media were different The records were enumerated from 1 to 8

The benchmark data were digitized (16 bit) with sampling frequency 160 kHz and 2 MHz with cut off filter of 72 kHz

The waveguides location on ASB loop and on PFR Superheater and Evaporator can be seen from Fig 2

4.2 Standard questions.

For all benchmark data it was required to determine start time of injection and its duration, as well as to evaluate reliability and probability of false alarms For benchmark data 93 it was desirable to determine signal to noise ratio, and for the data

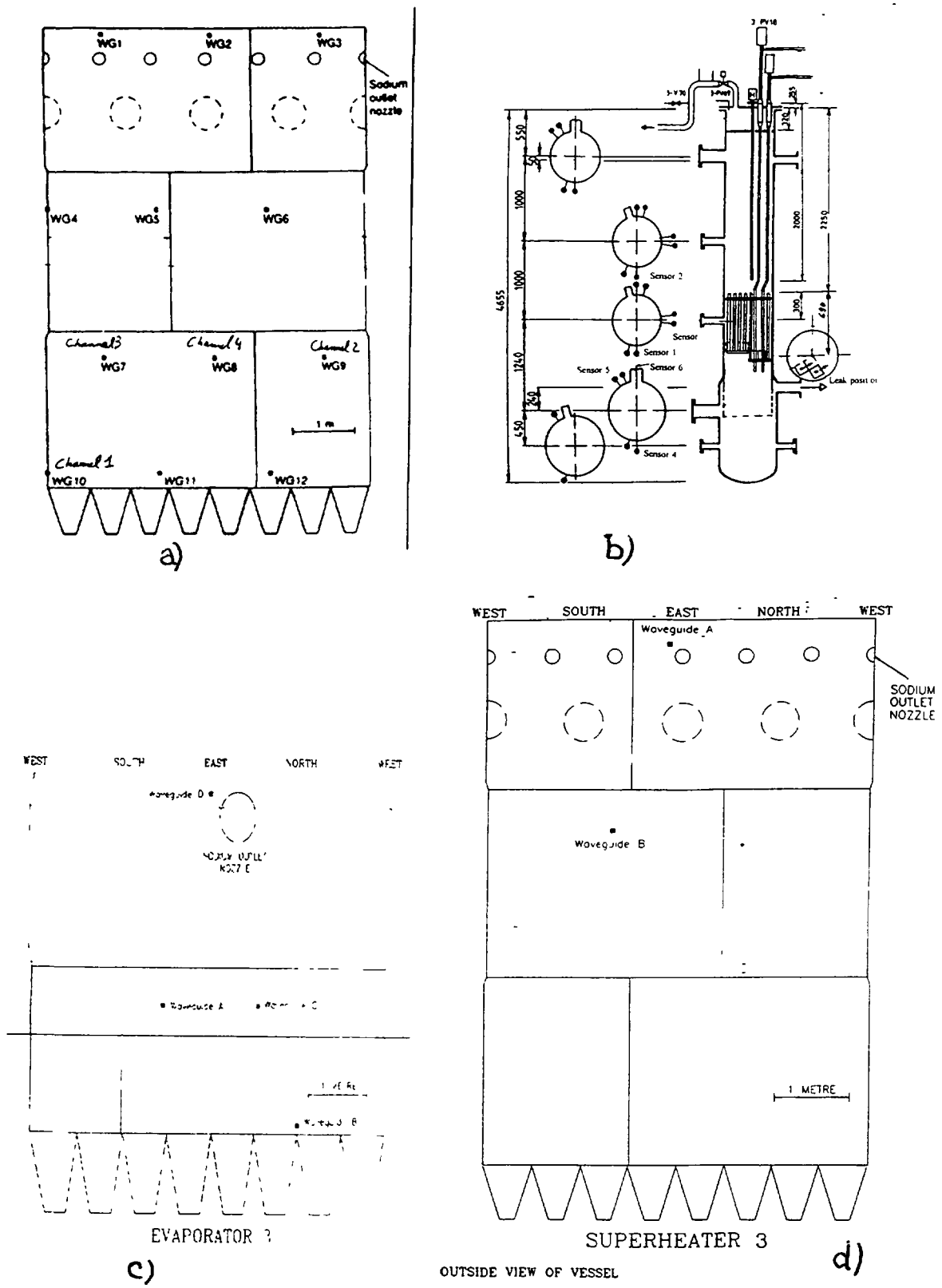

Fig 2 Location of the waveguides
a) PFR SuperHeater 2 b) ASB loop
c) PFR Evaporator 3 d) PFR SuperHeater 3

94 and 95 to perform leak location. The data 94 could serve for evaluation of advantages of multichannel processing in comparison with processing of signals from one channel. For benchmark data 95, in addition, is offered to determine type of injected media and give opinion about possibility of background noise recognition recorded at different units of SG at full power.

4.3. The results obtained by the moment.

Due to non coincidence of heads on recording and replaying tape recorders only part of 93 benchmark data has been processed, namely, 4 benchmark records with flow rate of 0.8 g/s with different signal to noise ratios. The benchmark data have been analyzed in frequency band up to 4 kHz because it was assumed that in this band the amplitude-frequency characteristics of the sensor is closest to linear. The results of detection of leak start time and duration are represented in Table 1. The applied method has allowed to detect leaks with signal to noise ratio, close to -24 but just for most powerful pulses local in time. Start time and duration were determined using the first and the last patterns identified as leak. The results for each records are represented in the Table 1 under the order, accordingly to deterioration of signal to noise ratio, that was estimated by comparison of patterns for each record. There were no false alarms for all benchmark data. The quantitative evaluations of probability of false alarm and leak missing were not carried out due to insufficient amount of data.

Table 1

	Leak Start, sec	Leak End, sec	Duration, sec
Record 2	15.05	18.43	3.38
Record 4	19.81	21.15	1.34
Record 1	12.54	13.11	0.57
Record 3	12.54	15.05	2.51

The processing of the benchmark data 94 has shown, that patterns from different sensors, recorded at the same moment can be recognized differently. That is if a pattern from one sensor is identified as leak, the pattern from the other sensor can be identified as background noise. Therefore the leak start and leak end were determined separately for each sensor. The reliability of method was determined by evaluation of quality of the recognition, for that it was necessary to identify the leak start and leak end , closest to real.A start of injection has been identified when the first pattern has been identified as leak . End of injection was fixed from the moment of absence of the messages about leak during recognition of several patterns on each sensor separately.

The quality of recognition of background noise was evaluated in a percentage on such parameters, as:

- Correctly recognized background noise;
- The background noise, recognized as leak (false alarm);
- Non recognized background noise (relearning is necessary).

The quality of leak recognition was evaluated similarly on such parameters as

- Leaks recognized as background noise,
- Correctly recognized leaks,
- Non recognized leaks.

The results of detection of leaks start and their duration along with quality of recognition are summarized in Table 2 The applied method allowed to detect a leak at signal to noise ratio down to 24 Judging by averaged patterns of background and leak noises the numbers of records can be ordered according to deterioration of signal to noise ratio in the following order 3, 0, 2, 1, 4

The absence of false alarms during background noise records is provided by impose this condition during training The obtained results testifies that it is possible to use insignificant volume of data, necessary for training, under condition of availability of the most characteristic examples of background noise It is necessary to note, that the more examples of different background noises is used during training the lower probability of false alarms

At the end of leak in the 2-nd record a short-term pulse takes place, which would be identified as leak However, this pulse should be classified as abnormal background noise, because it was recognized as non recognized In examples of pure background noise the similar powerful pulses were absent

The location of leak was not carried out in view of small time delay at registration of pulses in the readings of several sensors

For benchmark data 95 leak start and duration were determined as separately for each sensor, so for all sensors Adaptive filtering was not applied, patterns were formed by a new way, that will be in more detail considered further

In the first case the reliability of method was evaluated similarly to the previous benchmark data (see Table 3) To increase reliability of a leak detection algorithm of issue of the alarm message taking into account result of recognition of several patterns was in addition applied Times of issue of the alarm messages in the Table 3 are not presented It should be noted , that in spite of some false recognition of separate patterns , the false alarm messages were absent while processing as leak noise so background noise at full power

In records of 1-st and 2-nd injections leak noise was not recognized for all sensors One pattern from waveguide "d" was not recognized as background which means that further learning is necessary During injection 8 only some patterns from "c" and "d" waveguides were recognized as leak but without issue of the alarm messages about leak Obviously, the leak was not detected because of the small flow rate of injected media at low pressure Some patterns from sensors "c" and "d" were identified as requiring training probably due to insufficient training

Record 4 proved to be the most difficult for recognition During the 1-st second and further low frequency pulses took place, which are absent in background noise, on which training had been made Simultaneously with low-frequency effects there was no high-frequency noise, characteristic for injections However the contribution of low-frequency (up to 800 Hz) components has appeared to be enough, for the neural network to recognize some patterns as leak being not trained on such background noise If to assume, that the injection begins at 5-th second, when the patterns simultaneously on all the sensors were recognized as leak , the background noise before injection 4 is characterized by a smaller of level high-frequency components in comparison with background noise, on which the training had been

Table 2

N Injections	N sensors	Start of Injection, sec	Duration of injection, sec	% background noise recognized as leak	% rightly recognized background noise	% non recognized background noise	% leak noise recognized as background noise	% rightly recognized leak noise	% non recognized leak noise
	1	1 8906	5 4532	0	100	0	13 33	86 40	0 27
	2	1 8906	5 4532	0	100	0	9 33	89 87	0 8
	3	1 8906	5 4532	0	100	0	6 16	93 33	0 51
0	4	1 9063	5 4375	0	100	0	36 53	58 67	4 9
	1	2 0469	3 9219	0	100	0	97 60	2 16	0 24
	2	1 2344	4 7344	0	100	0	94 96	4 08	0 96
	3	1 2500	4 7188	0	100	0	80 58	15 11	4 31
1	4	2 1250	3 8438	0	100	0	98 32	1 68	0
	1	2 0313	5 375	0	99 6	0 4	40 98	54 64	4 38
	2	2 0313	5 375	0	99 6	0 4	25 41	71 31	3 28
	3	2 0313	5 375	0	99 6	0 4	8 47	90 71	0 82
2	4	2 0469	5 3437	0	99 6	0 4	68 85	27 05	4 1
	1	1 6250	5 4844	0	100	0	10 2	89 54	0 26
	2	1 6250	5 4844	0	100	0	10 2	89 8	0
	3	1 6250	5 4844	0	100	0	10 2	89 8	0
3	4	1 6250	5 4844	0	100	0	11 22	88 78	0
	1	4 6563	1 5781	0	100	0	98 14	1 15	0 71
	2	2 2969	3 5781	0	100	0	97 99	1 43	0 58
	3	2 6875	4 0625	0	100	0	87 97	8 31	3 72
4	4	2 6875	4 1094	0	100	0	98 57	1 15	0 38

Table 3

N injections	N sensors	Start of injections sec	Duration of injections, sec	% background noise recognized as leak	% rightly recognized background noise	% non recognized background noise	% leak noise recognized as background noise	% rightly recognized leak noise	% non recogni leak noise
1	a,b,c,d	-	-	-	-	-	-	-	-
2	a,b,c,d	-	-	-	-	-	-	-	-
3	a	7 89	2 09	0	100	0	5	85	10
	b	7 89	2 09	0	100	0	5	90	5
	c	7 58	2 40	1 57	93 15	5 48	0	100	0
	d	7 78	2 20	0	97 33	2 67	9 52	80 95	9 52
4	a	6 04	3 94	3 45	93 1	3 45	52 63	34 21	13 6
	b	6 04	3 94	0	91 38	8 62	71 05	21 05	7 89
	c	5 43	4 55	9 62	76 92	13 46	29 55	40 91	29 55
	d	5 84	4 14	55 36	26 79	17 86	22 5	60	17 5
5	a	2 87	7 11	0	96 3	3 7	2 9	88 41	8 7
	b	2 77	7 21	0	100	0	17 14	70	12 86
	c	2 77	7 21	0	100	0	0	100	0
	d	2 77	7 21	0	100	0	1 43	97 14	1 43
6	a	5 53	4 45	0	100	0	4 65	95 35	0
	b	5 53	4 45	0	100	0	0	100	0
	c	5 53	4 45	0	100	0	0	97 67	2 33
	d	5 53	4 45	0	100	0	4 65	88 37	6 98
7	a	4 61	5 37	0	100	0	13 46	59 62	26 92
	b	5 12	4 86	0	95 92	4 08	25 53	44 68	29 79
	c	4 40	5 58	0	95 24	4 76	5 56	64 81	29 63
	d	4 40	5 58	0	92 86	7 14	46 30	35 19	18 52
8	a,b	-	-	-	-	-	-	-	-
	c	6 35	3 63	0	98 36	1 64	94 29	5 71	0
	d	4 51	5 47	0	100	0	96 23	3 77	0

performed (see Fig 3) From comparison of averaged spectral densities of different background noises, shown in Fig 3 it is clear, that the noticed low-frequency effects consist of excess of a level of background noise at about 5 dB It should be pointed out , that the differences of background noise in the high-frequency area for the sensor on waveguide "d" are expressed in the least degree.

Nevertheless the heaviest quantity of false leak identification was received for this sensor, which proves the inferiority of training If the injection begins at 1-st second, then it is not clear why high-frequency components till 5-th seconds are more weak, than at background noise before 6-th injection. The situation would be more clear if analysis of flow rate changes during the injection would be carried out, because along with sound generation its attenuation takes place and these processes are the mostly difficult for hydrogen dissolving in sodium. The finding out of the reasons of background noise changes during a series of injections is important for acquisition of adequate understanding about distinctions between background noise and leak noise

The best results of recognition were obtained for 5-th and 6-th injections, when the prospective quantity of correct leak recognition reached up to 100 % at absence of false alarms Results of recognition of injections 3 and 7 give variation of correctly recognized leak from 50 up to 100 %

The researches made on location of noise while have given negative results Introduction of adaptive methods of localization complicated by the necessity very large computing resources Thus accuracy of localization and cost of a system can be far from desired

Approximate determination of position of a source of a sound based on attenuation of the amplitude at distance of a source is not acceptable for water leaks in SGU, as far as the effects of attenuation of noise in SGU can appear not unequivocal The leak noise will be attenuated by different manner passing through sodium, shell and hydrogen bubbles That is why closest sensor which is shadowed by hydrogen bubbles will register smaller noise than a sensor located at distance from injection place. Use of a principle, based on phase delays, arising at passage by sound of various distances, is complicated by the fact that the useful signal represents broadband noise with varied pulsing activity in accordance with leak escalation and, which is masked by broadband background noise, in which there can be present abnormal pulses because of local sources of a sound. The proliferation of sound waves in SGU has a complex nature because of shielding elements covers, lattices. tube bundle The waveguide registers a superposition of acoustic waves, passed through sodium and SGU shell The additional problems arise because of distribution of sources of noise under leak conditions in the space (oscillations and collapses of hydrogen bubbles) If to be guided only by noise of steam jet, its spectral maximum should be expected in the band , exceeding 80 kHz

Theoretically, the noise from argon , water and hydrogen injections can be differentiate by different spectra and by character of different components changes in time. In practice these distinctions can be less obvious because of dependence on pressure, size of injection nozzle , injected media and its flow rate It should be expected, that under equal listed conditions the noise of injection of hydrogen will differ from noise of argon injection, due to greater attenuation on gas bubbles, by lower amplitude of high-frequency components During water injections the formation of hydrogen bubbles will differ from hydrogen injections by higher intensity and bigger sizes of bubbles Some water particles can be circled by hydrogen bubbles and react with sodium at some distance from injection place

a)

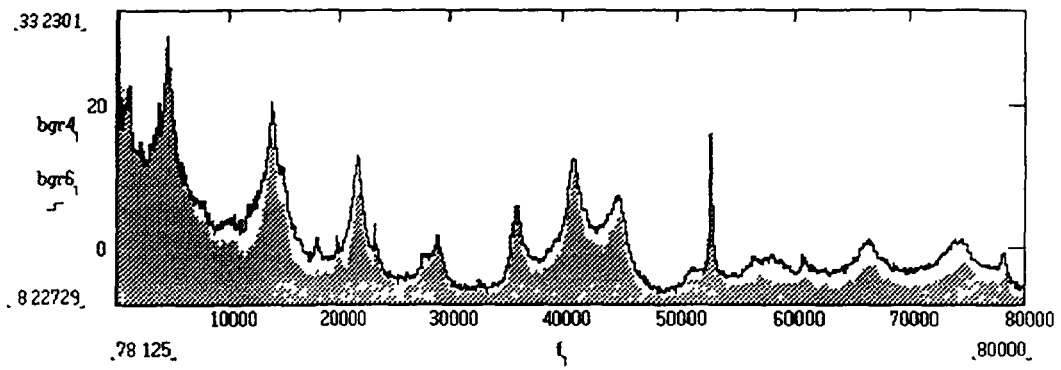

b)

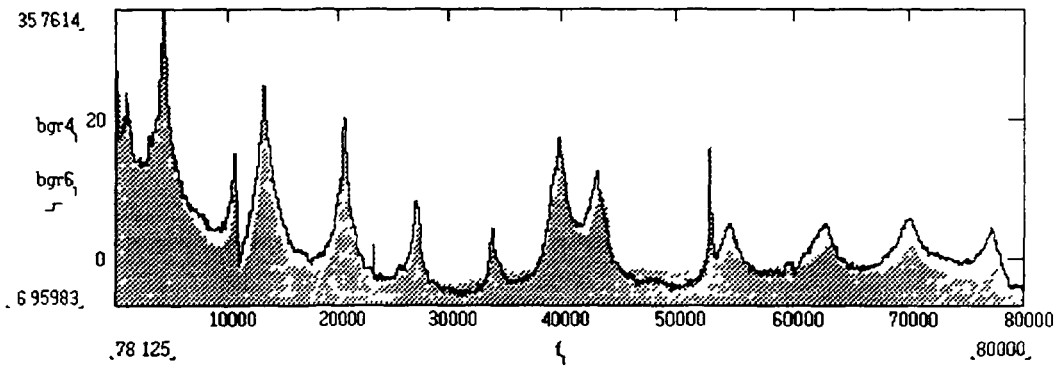

c)

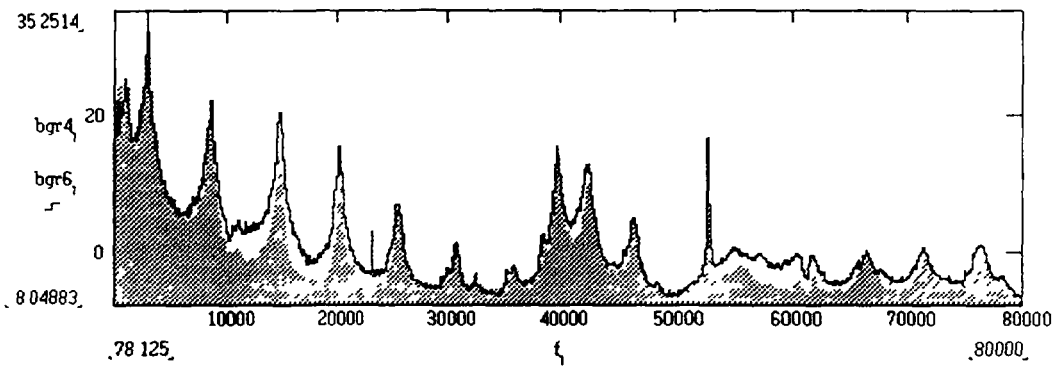

d)

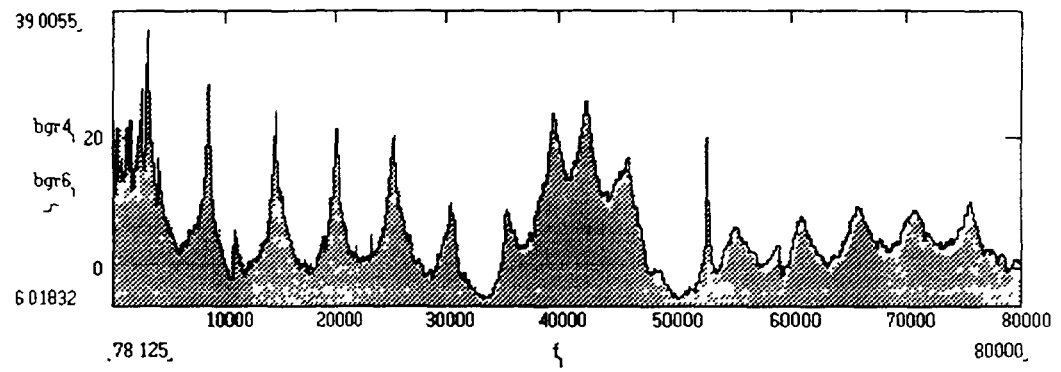

Fig 3 Averaged PSDs of the background noise before injections 4 and 6 for different waveguides - a, b, c, d

Thus, the noise of water injections can differ from the noise of injection of hydrogen by more intensive impulsing activity (which depends on flow rate) and by larger level as high frequency, so low-frequency components.

As far as the parameters of each injection are unknown for each detected injection, unequivocally to identify a type of injected media is problematic The analysis of noise changes in time has not allowed to allocate characteristic pulses, which could correspond to a particular type of injected media To simplify the identification power spectral densities (PSD) for various injections without background noise have been obtained by subtraction from an average spectrum during the injection an average spectrum of noise before the injection The PSDs are shown in dB relative to a basic level, equal to unity, in Fig. 4

PSDs of different injections, analyzed separately on each sensor, differ by value of frequency components in the whole frequency range It proves that even injections of identical media were carried out in different conditions From the comparison of PSDs of injections 5 and 7 follows, that for sensors mounted on waveguides "a" and "b" high frequency components (>50 kHz) during injection 7 have a greater level than during injection 5, but for sensors "c" and "d" vise versa

Obviously, these injections have been carried out by different media as far as less probably, that the noticed discrepancies are called by difference in flow rates or by difference in other parameters Judging by relationships of high and low frequencies water has been injected during injection 5 and argon during injection 7

As was expected, noise even from the same injection differs for different sensors, that it is possible to see from comparison of PSD's of any injection, the plots are represented in Fig. a,b, c and d Moreover leak noise from each sensors represents a nonlinear superposition of leak noise and background noise

5. Results of verification and improvements of the signal processing techniques using the experimental data

The leak noise in benchmark 93 is characterized by weak medium frequency components and by random occurrence of pulses, that can be invoked by specific character of water injection in conditions of the experimental rig Maximum of energy of high frequency pulses is concentrated around 30 kHz, that corresponds to sensor's resonant frequency . The low-frequency pulses have a spectral maximum (~2 5 kHz), which is very close to the most powerful spectral peak of background noise (~2 2 kHz) As far as the benchmark data were analyzed in frequencies band up to 4 kHz, the problem of leak detection consisted in recognition of signals, distinguished by occurrence of a weak spectral peak during leak noise overlapped with powerful spectral peak of background noise During training of adaptive filter a mixture of background noise, and white noise, are entered into input and leak noise was used as a desired signal. After training benchmark signals passed through the filter The patterns were generated over 4 spectra, calculated consistently

For one cycle of neural network training 4 patterns of pure background noise and 4 patterns of leak noise have been presented Criterion for completion of training was the absence of false alarms during background noise recognition

The benchmark data 94 had similar frequency spectra for signals from channels 1 and 3, whereas the signals from channel 2 differed by prevalence of low-frequency components (< 1 kHz) and the signals from channel 4 consisted predominary from frequency components up to 20 kHz The background noise had smaller differences

a)

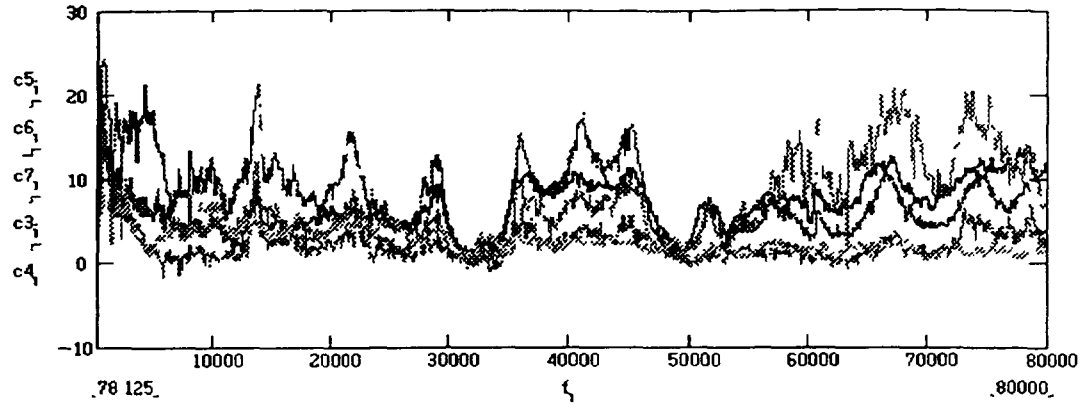

b)

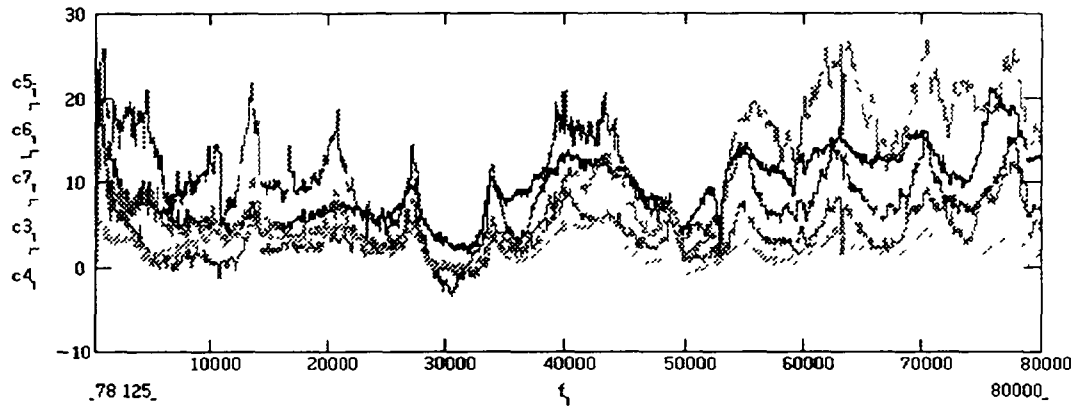

c)

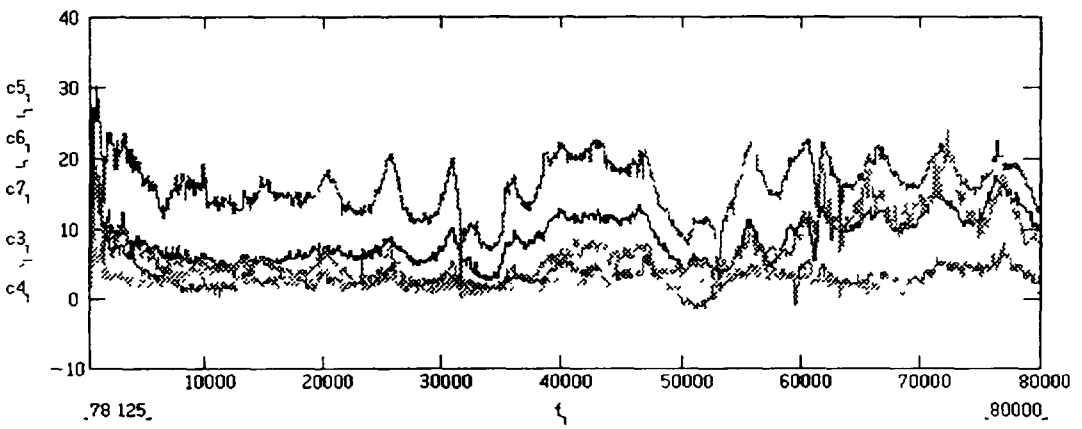

d)

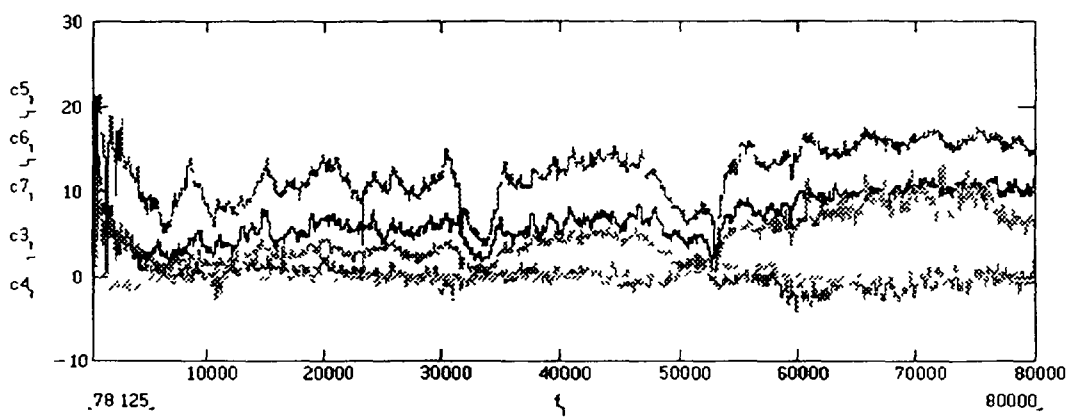

Fig 4 Averaged PSDs of "pure" injection noise for different injections (without background) for waveguides a b, c, d

between signals from different sensors, and in the spectrum it is possible to allocate about 10 peaks in the frequency band up to 40 kHz. Thus, the problem of leak detection was more difficult and consisted in recognition of broadband background noise and linear superposition of broadband background noise with broadband leak noise. In difference from the previous data, new version of an adaptive linear filter permanently learned new signals of background noise and benchmark data. This filter did not require reference leak signals, and a delay was used to get reference signal from the signal to be processed.

As far as the architecture and parameters of the filter were not optimized, the best results were received only for high frequency components of noise, whereas the useful information in the band of low frequencies after filtering has appeared insignificant and different for each sensor. Therefore, power of the useful signal on output of the filter was not proportional to real power of leak noise in the whole frequency band. Neural network was trained on patterns of background noise and patterns of background noise mixed with leak noise . For different sensors the same network was used but with different initial weights. It was assumed, that the decision on issue of an alarm will be accepted by operator based on the analysis of recognition results separately on each sensor.

In benchmark 95 there are no records of pure background noise before injection and pure leak noise but neural network training requires characteristic examples of background and leak noise. Therefore to get these reference signals a record with injection was taken, where the presence of injection can be identified by spectral analysis and by signal's RMS changes. Such injection was found with number 6.

The pattern generation is based on revealing frequency components , which the most informative from the point of view of leak detection. For correct realization of such a choice the analysis of the whole varieties of background and leak noise is necessary.

Before processing and recognition of benchmark data root-mean-square value of signals (RMS) over 2048 samples with subtraction of mean value of sample to exclude zero drift was calculated. Plots of RMS changes are shown in Figs. 5 and 6, from which it is obvious, that determination of a leak start time by RMS changes is quite difficult for the majority of injections because of background noise variation and abnormal pulses which present in it. After patterns generation their average values were calculated, which are shown in Figs. 7 - 8.

Comparing the plots of RMS changes and averaged patterns , it is possible to conclude that in some cases the pattern generation has allowed to exclude influence of abnormal pulses of background noise.

As far as the useful signal from remote sensors can be very small, that will deteriorate network's ability to recognize leak using the data from all sensors, the network was trained on patterns from each sensor separately. Thus one neural network was used , but with different weights depending on a particular sensor. Such approach permits to watch dynamics of recognition on each sensor, but complicates a decision making about leak occurrence if there is weak signal on some sensors. For issue of the alarm message an algorithm is used, which takes into account result of recognition and dynamics of patterns on all sensors.

With the purposes to bring system closer to practice it is purposewise to learn network on leak simulations with quickly growing leak rates and stable maximum flow rate, or on patterns from several simulations with the different flow rates. And it is highly desirable to train on patterns from injections with the minimum flow rates,

a)

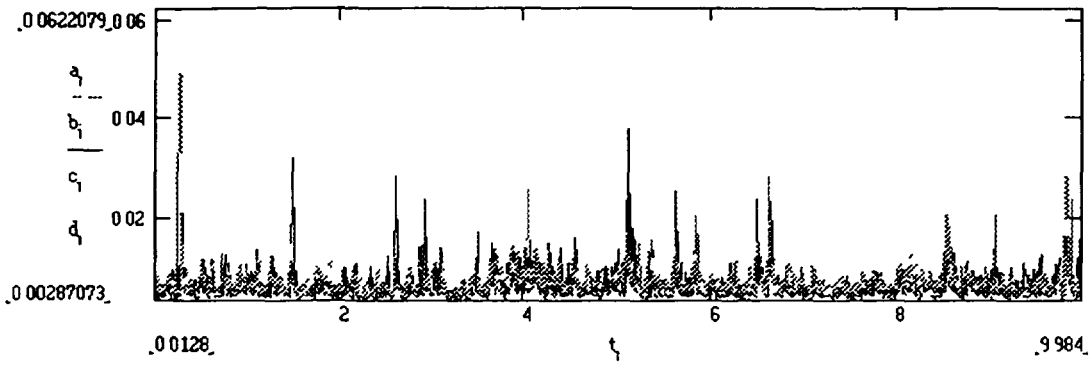

b)

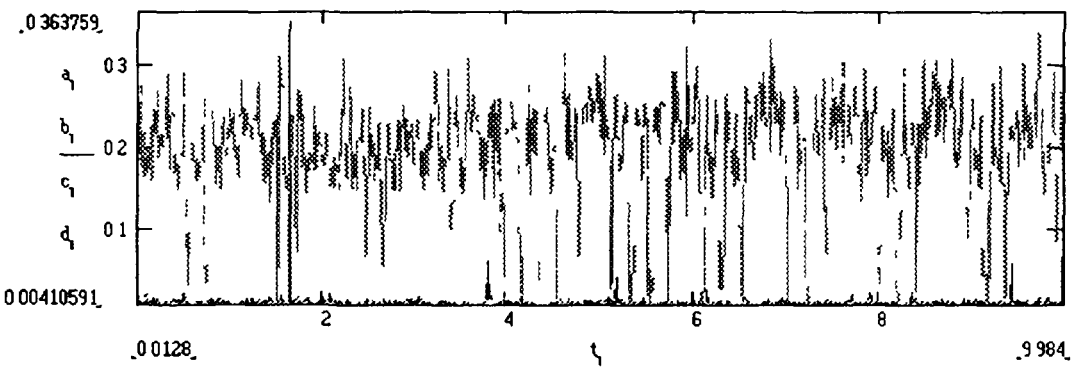

c)

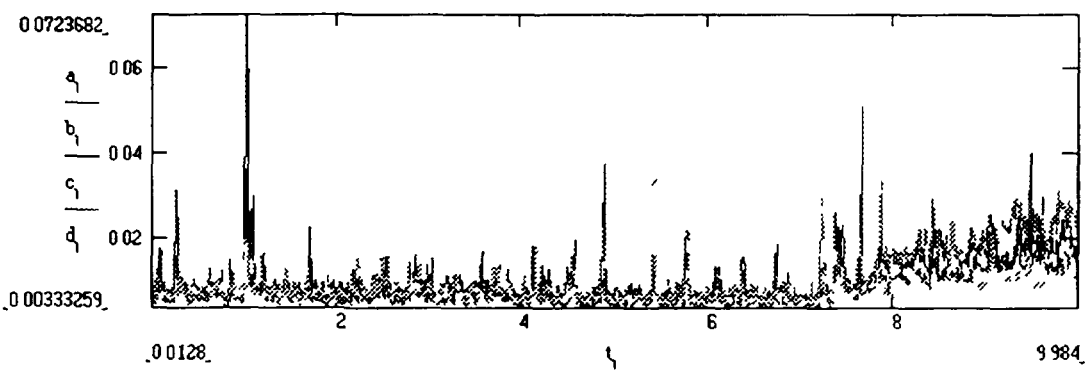

d)

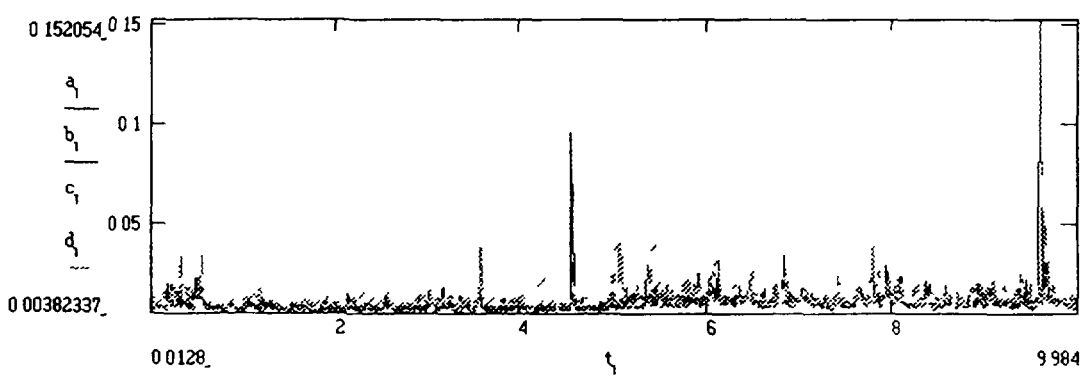

Fig 5 Behaviour of RMS (g) in time (sec) for injections 1-4
a) - 1, b) - 2, c) - 3, d) - 4

a)

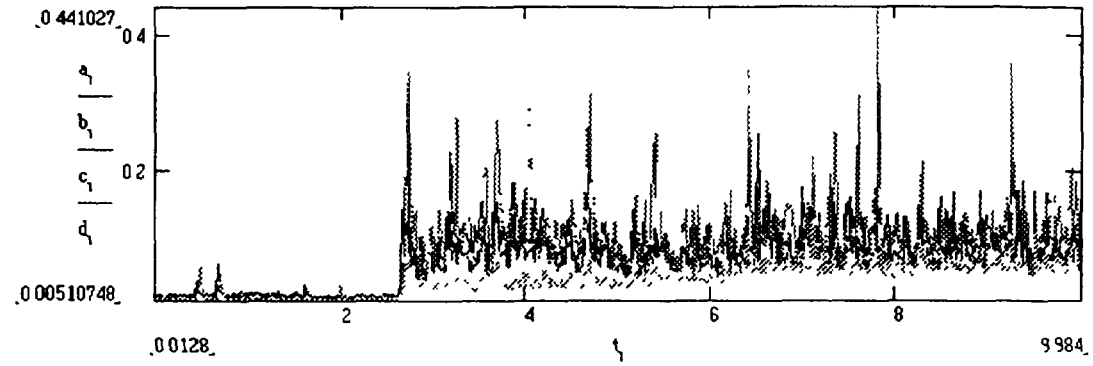

b)

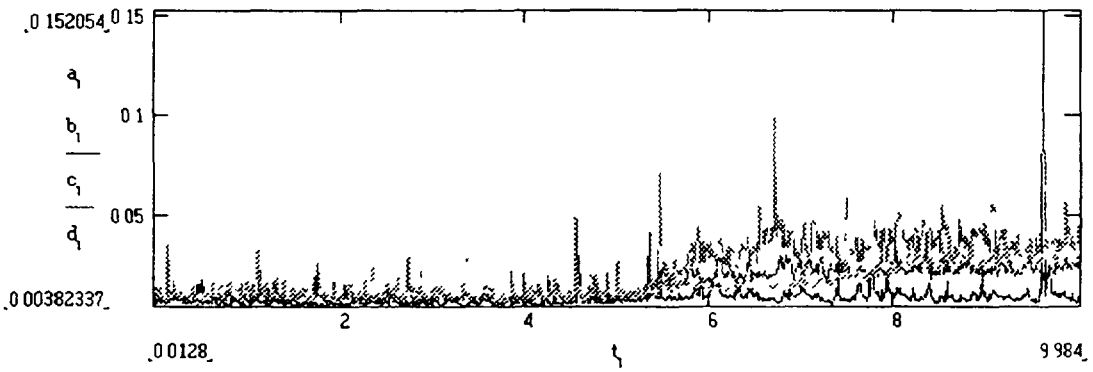

c)

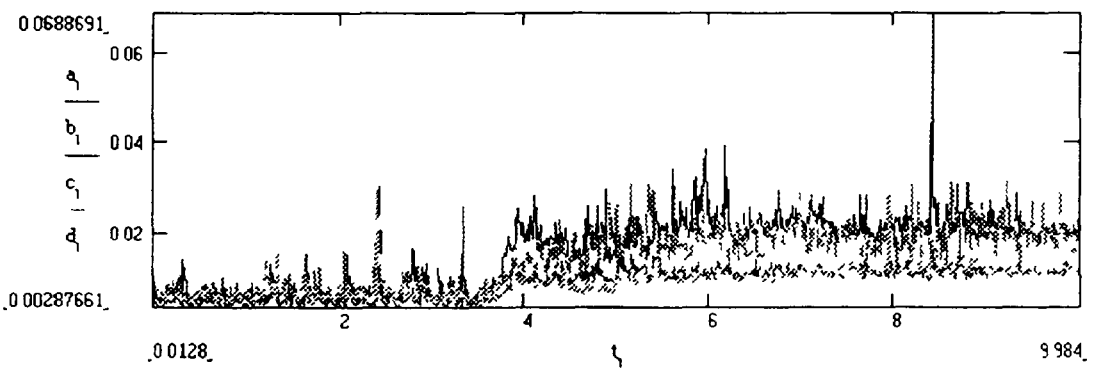

d)

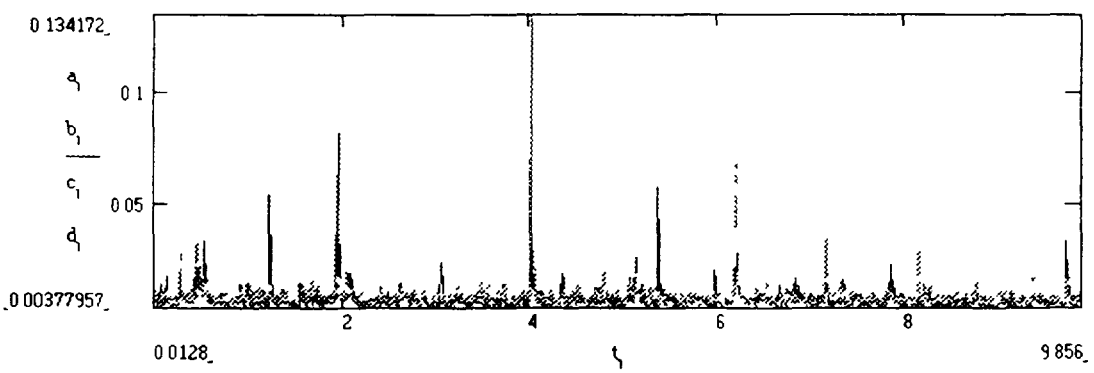

Fig 6 Behaviour of RMS (g) in time (sec) for injections 5-8
a) - 5, b) - 6, c) - 7 d) - 8

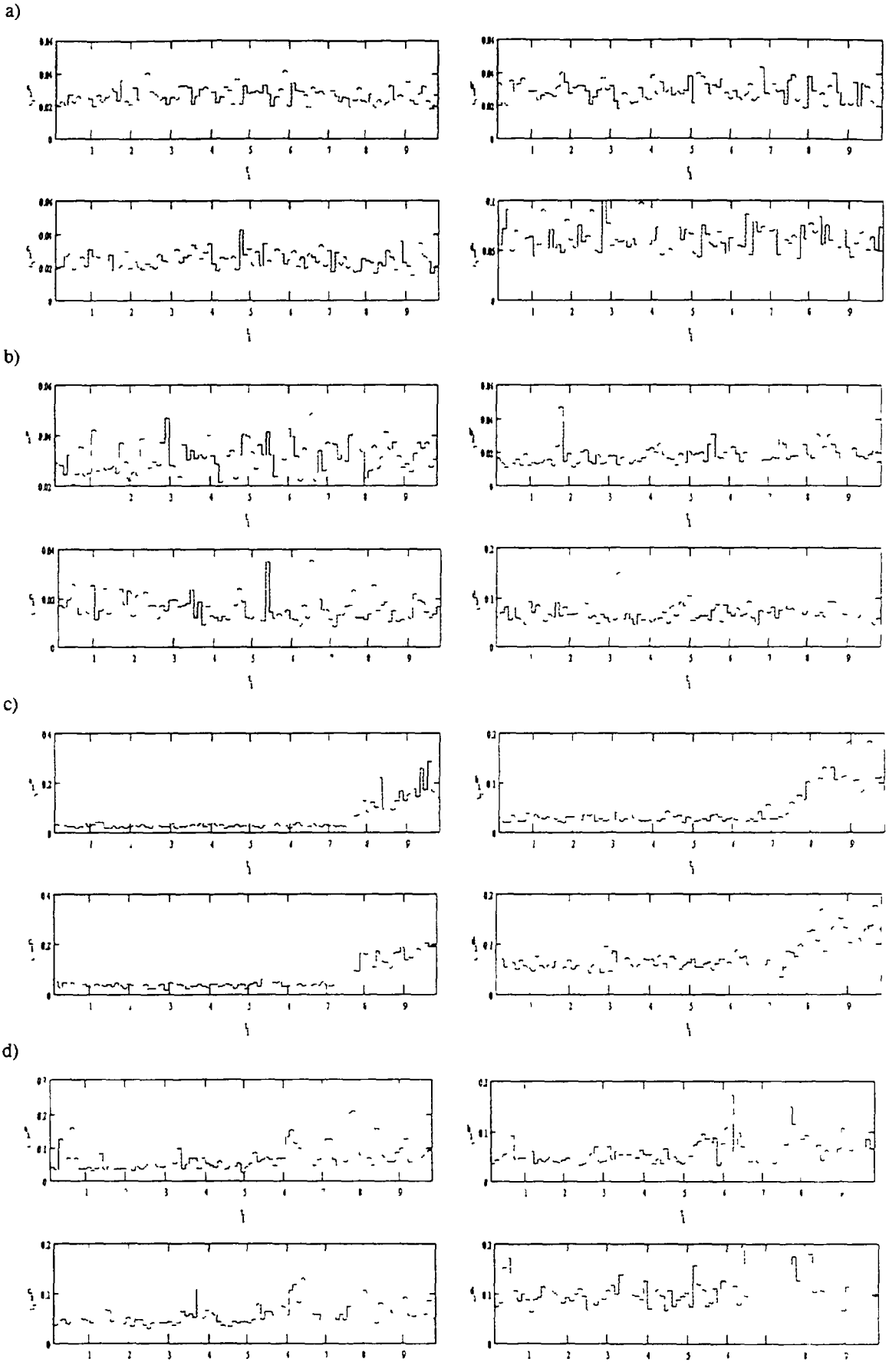

Fig 7 Behaviour of the averaged patterns in time for different waveguides a b c d
a) Injection 1 b) Injection 2 c) Injection 3 d) Injection 4

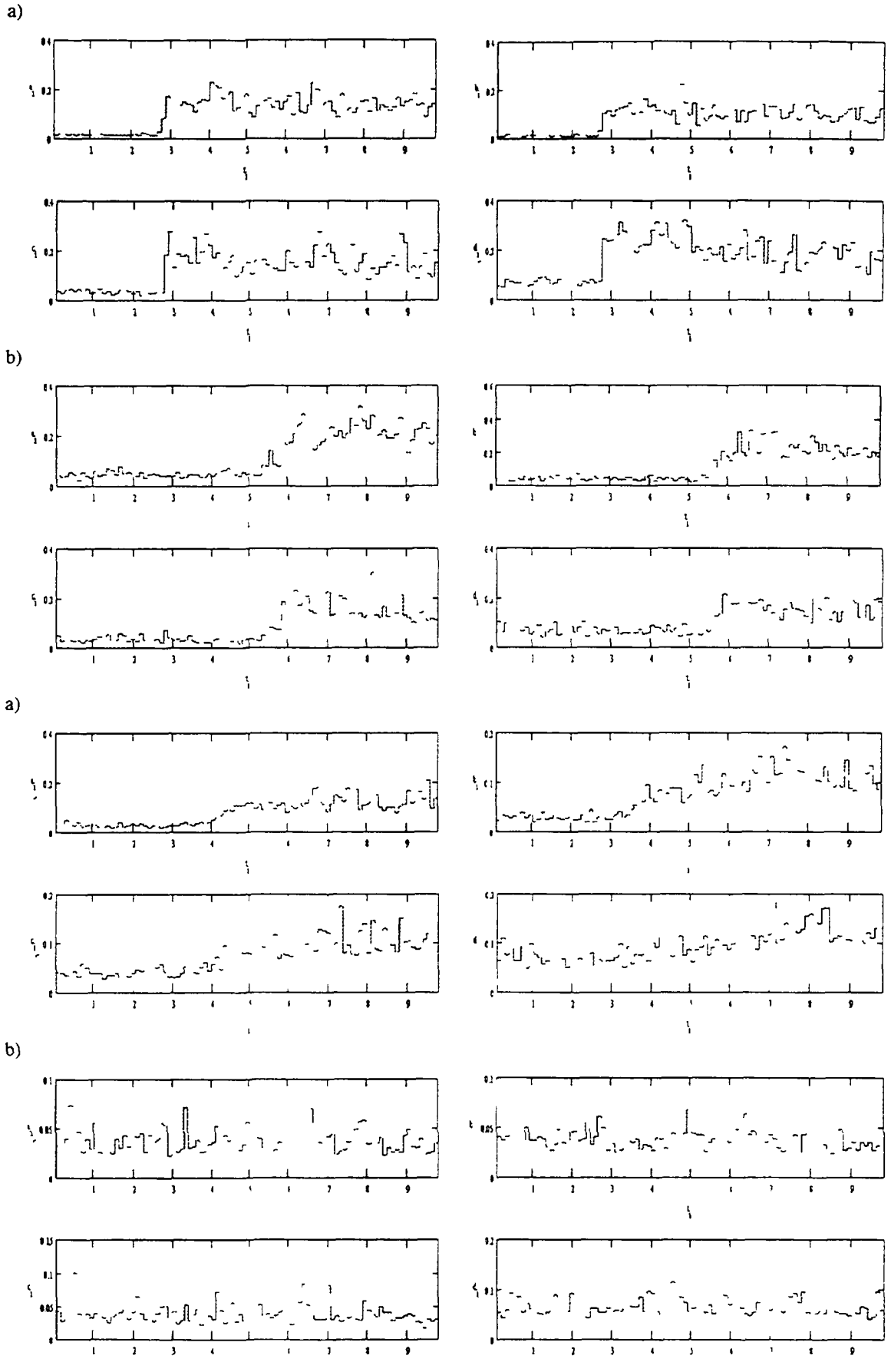

Fig 8 Behaviour of the averaged patterns in time for different waveguides a b c d
a) Injection 5 b) Injection 6 c) Injection 7 d) Injection 8

a)

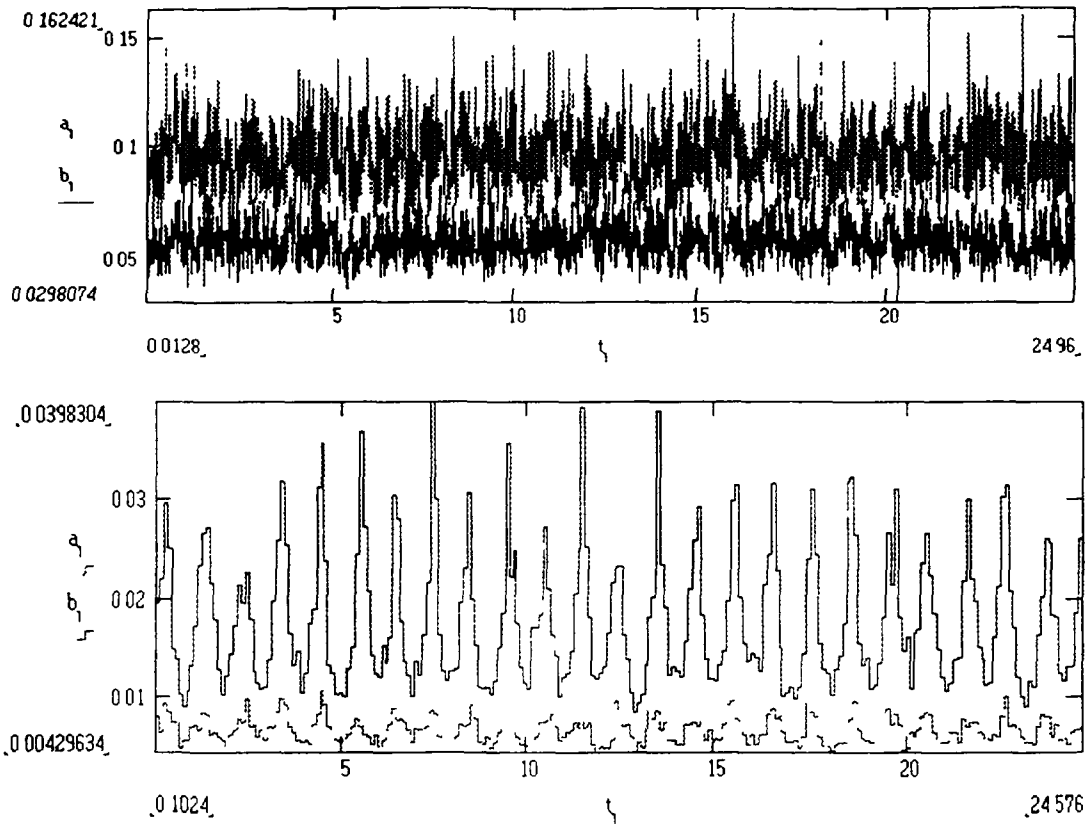

b)

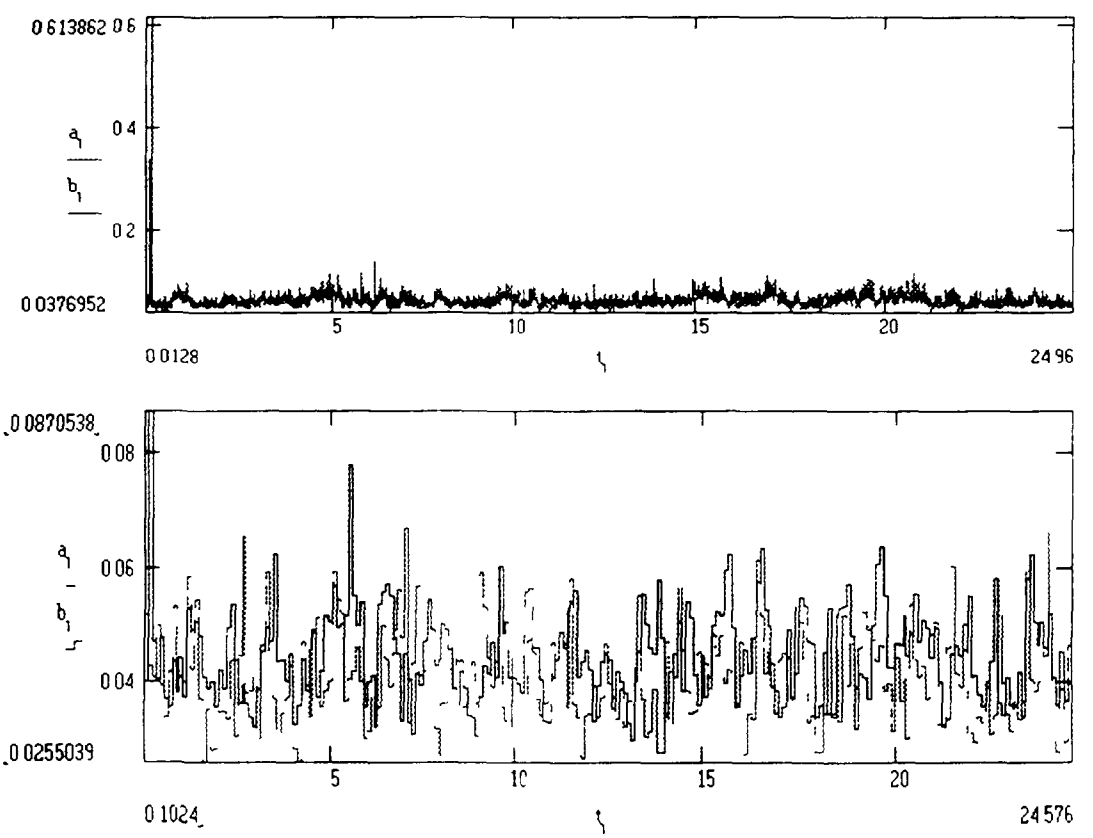

Fig. 9 Behaviour of RMS and averaged patterns in time for signals from waveguides A and B at full power a) SuperHeater b) Evaporator

which need to be detected by acoustic method The specific character of pattern generation and neural network performance is that being trained on an injection with particular flow rate the network will reliably recognize injections with larger flow rates, but reliable recognition of leaks with smaller flow rates will be problematic

Due to the fact that with removal from injection place the signal is attenuated some additional difficulties arrives for each separate sensor training A problem is complicated by variation of background noise recorded at different sensors For example, sensor mounted on waveguide "d" registers background noise, possessing more complex character, than other sensors, and more weak leak noise Being trained on patterns from this sensor, the network will recognize leaks with smaller flow rates in comparison with other sensors On the other hand, to exclude false alarm in connection with more complex character of background noise it is necessary to perform training on greater quantity of its patterns For ideal training from the point of view of achievement of maximum sensitivity it is desirable to have examples of injection noise , carried out in different SGU places It is related to possible nonlinear effects during sound propagation generated by leak and its superposition with background noise

The peculiarities of patterns generation allow recognition of leak noise and background noise in SGU , possessing other geometry than that in conditions of which training was performed However, amplitude - frequency characteristics of sensors along with waveguides, should be identical or as close as possible to that ones on which the training had been carried out At transition to new conditions it is purposewise to perform additional learning on background noise and on a linear combination of leak patterns without background noise with patterns of new background noise Additional learning is vital in case of specific noise, stipulated by design features of new SGU , because theses noises can be permanently present at background noise or appear for some regimes, and only for some sensors

It should consider separately the case, when the characteristic examples of background noise were recorded only at one power level but leak should be detected at different power levels

Probably, that at a higher power levels it is possible to detect leaks with larger flow rates on comparison with leaks at lower power levels irrespective of a way of signals processing It is necessary to specify, that the important role is played by not mean value of the background noise, but by its variation which can depend on power level Strictly speaking, correct recognition of background noise at different power levels not yet means successful leak recognition

The used way of patterns generation will be the most effective, if sensor's signal is directly proportional to noise power in all working band of frequencies or this dependence will be identical for all frequency components

In spite of the fact that the conditions listed above were not satisfied, recognition of background noise at full power was carried out without any false trips RMS changes and averaged patterns are shown in Fig 9 Preliminary estimations show, that without additional learning it would be possible to detect a leak at this power level with acoustic noise which two times exceeds the noise of injection on which the training has been performed (at minimum power level)

6. Recommendations for further activity in the subject area

To obtain a robust estimation of probability of false alarms for acoustic leakage detection an approbation on background noise, registered during transients from one

power level to another is necessary It is not less important to perform testing of methods on abnormal background noise, when additional souses of noise can be loose parts, vibration of various constructional elements check valves operations, etc For evaluation of probability of the leak missing the mostly unfavorable situation is the leak occurrence during fast decrease of power level

The leak detection in practice means issue by a system of a justified signal of alarm, for which a special algorithms of decision making are necessary which take into account the whole situation in SGU and not only acoustic noise

A general problem of vibro-acoustic diagnostics is registration of reference noise which characterizes abnormal situation Making use of linear model, discovered by experiments, does not allow to take into account the whole varieties of real situations For example , the noise of leak simulation recorded at minimum power, will differ from noise recorded at maximum power due to differences in background noises and nonlinear superposition of background noise and leak noise

Besides, the noise from the same injection, registered by waveguides of one type, will be problematic to predict using linear relations and other waveguides mounted in other places One more problem is getting pure leak noises and their utilization for adaptation of the system to SGU with other characteristics The leak simulations is not the best way due to economical and safety reasons

Thus, nonlinear mathematical models of leak noise should be developed, using real background noise to get simulated noise , closest to real one The experience of development of such models would be useful for getting reference noise signals, describing various abnormal situation in NPP

7. Conclusions

The problem of leak detection in SGU of LMFBR is a problem of acoustic noise recognition In fact acoustic leakage detection is not a problem even for quite small leaks (0 5-2 g/s) The problem is to discriminate between leak noise and other noises which are generated by SGU

With the purposes of improvement of signal to noise ratio, investigations on nonlinear filtering are purposewise Neural networks application for recognition of noisy acoustic signals has shown that it is a prominent approach for plant monitoring It was confirmed, that the additional advantage of neural network consists in ability to adapt to changing environment and to generalize the unknown earlier information

For fast and robust training optimal pattern generation and feature extraction is necessary The first positive results were obtained for power invariant pattern generation

The first experience of application of recurrent networks has been gained along with recognition of multichannel patterns

To obtain a robust estimation of probability of false alarm and leak missing it is necessary to carry out processing of the noises recorded during transients

Further research should be concentrated on recognition of other types of abnormal acoustic noises and on the development of nonlinear mathematical models of these noises

On the basis of experimental data, recorded during PFR End-of-Life Experiments it is purposewise to investigate different leak location techniques

References

1. D.C. Gabatz, E.L. Gluekler, F. Fletcher, T. Claytor On-line low and high frequency acoustic leak detection and location for an automated stem generator protection system // Report for IAEA Working Group on Fast Reactors Specialists' Meeting on "Acoustic Ultrasonic Detection of In-Sodium Water Leaks", Aix-en-Provence, France, October 1 - 3, 1990.
2. J.A.McKnight, R.Rowly, M.J.Beesly Acoustic surveillance techniques for SGU leak monitoring // IAEA IWGFR Specialists' Meeting on "Acoustic Ultrasonic Detection of In-Sodium Water Leaks", Aix-En-Province, France, October 1 - 3, 1990.
3. R.P.Lippmann An Introduction to Computing with Neural Nets // IEEE ASSP Magazine, April 1987, pp.4-22.

DETECTION OF ARGON, HYDROGEN AND WATER INJECTIONS IN A FBR STEAM GENERATOR

J.E. HOOGENBOOM
Interfaculty Reactor Institute,
Delft University of Technology,
Delft, Netherlands

Abstract

The analysis of the IAEA 1995 benchmark data on acoustic leak detection by IRI, The Netherlands, focussed on the timely detection of the onset of leak. The aim was to design a leak detection algorithm that can, in principle, be applied for on-line application and will give a fast and reliable detection of any anomalies in the signal with a pre-specified false alarm rate. To meet this goal, long and complicated computations which take long data series have to be avoided. Therefore, anomaly detection in the time domain seems most appropriate.
To eliminate all correlation from a measured signal, an autoregressive (AR) model was established based on the first 2048 signal values of the signal, which part is supposed not to contain any anomalous data. Applying the AR-model as a one-step prediction filter, a residual noise signal is obtained which should be uncorrelated (white noise) if the proper AR-model is applied. A fixed model order of 30 was chosen on basis of the reduction of the variance of the residual noise as a function of model order. The Burg algorithm was used to determine the AR-coefficient, while the Yule-Walker methods was not found suitable for this case.
The introduction of an anomaly in the original signal will influence the characteristics of the residual noise and can be detected by applying statistical tests to the residual noise. A X^2-test considering the variance of residual noise over N samples (N=1000 to 2000) was applied to the signals from waveguides WA and WB of all injecton experiments and to all four signals from injection experiment I5. For the injection experiments I3 to I7 the onset of the injection could clearly be detected, although for experiment I3 an appreciable alarm failure rate during the supposed injection was noted. All detected injections lasted to the end of the available data series.
All residual noise signals as well as the original signals exhibited many spurious pulses or spikes with magnitudes of many times the regular standard deviation. This introduced many false alarms during the period before the injection, which false alarms could only be eliminated on basis of their very short duration. During the injections the spikes prohibited proper calculation of limits on the X^2-value on basis of a theoretical (e.g. Gaussian) amplitude distribution of the residual noise. Now the limit of X^2 above which an anomaly is declared must be chosen from experience.
From the relative increase of variance of the residual noise before and during the injection of experiment I5 for all four waveguides a rough estimate of the position of the injection point was made.

1. Introduction

The IAEA supports a Co-ordinated Research Program on Acoustic Signal processing for the detection of sodium boiling or sodium/water reaction in LMFBRs. This program is already running for several years and includes different benchmark tests over the last years on acoustic signals from waveguides in a steam generator of a sodium cooled fast breeder reactor.

The general aim of these benchmark tests is to develop detection methods for boiling detection or water injection and to check whether unwanted water injection or leakage of water into the sodium can be detected sufficiently fast

and with sufficient sensitivity for routine application so that no danger can result to the steam generator of such nuclear power plants.

The 1995 edition of the benchmark test provided signals from four waveguides in a steam generator during injection of hydrogen, argon or water at different injection rates. The experiments were performed by AEA Technology at the Prototype Fast Reactor at Dounreay, United Kingdom.

Aim of the benchmark test is to

a) compare and characterize the background noise from the evaporator and superheater,
b) characterize and identify the type of leak noise (water/steam, argon or hydrogen),
c) estimate the onset of leak and duration in all leak files,
d) evaluate the transmission characteristics of the leak noise signals from leak location to transducers,
e) locate the leak

Although the department for Reactor physics of the Interfaculty Reactor Institute of the Delft University of Technology, the Netherlands, is not involved in a fast breeder research program, it has a research program in anomaly detection of signals from nuclear power plants or comparable systems and therefore has an interest in this IAEA research program. It is believed that the actual system producing the signals, nor its frequency range or type of signal sensor is of special relevance in testing the signal anomaly detection methods developed at IRI.

2. Signal preparation and preliminary tests

The signals for the benchmark test were obtained in digital form on 5 CD-ROM cassettes written in binary format. The CD-ROMs were provided by Mr. Ron Currie from AEA Technology. A short description of the recordings of the data and the resulting data files was included[1]. Besides a file with information the CD-ROMs altogether contained 8 sets of data files for different types of injections or injection rates and 2 sets of background noise. Each set of injection data consists of 3 files for different combinations of the signals of 4 wave guides. From each experiment data was recorded with a low sampling rate (160 kHz) and a high sampling rate (2 MHz). Altogether the signal data were 2.5 Gb.

Each file from a CD-ROM could be read from a CD-ROM drive at a PC and copied to a hard disk at the PC. Next the files could be copied onto a disk from a VAX or AXP workstation of the IRI computer system via a network transfer. A FORTRAN program was written to read the binary files with 2-

Table I. Overview of data files

file name[a]	file size (Mb)	signal combination	sampling rate (kHz)
InP1L	6.4	WA + WB	160
InP2L	6.4	WC + WB	160
InP3L	6.4	WD + WB	160
InP1H	80.0	WA + WB	2000
InP2H	80.0	WC + WB	2000
InP3H	80.0	WD + WB	2000
BEP1L	16.0	WA + WB	160
PEP1H	200.0	WA + WB	2000
BSP1L	16.0	WA + WB	160
BSP1H	200.0	WA + WB	2000

[a]n = 1 to 8 for the various injection experiments

byte integer data and to put the data in a file format defined for the IRI noise analysis system[2]. The IRI format for noise data files requires a conversion factor for each signal to relate the stored integer values to voltages as measured at the Analog to Digital Convertor. For all signals of all sets a conversion factor was chosen such that values in Volt must be multiplied by 4096 to get the integer value. Although this conversion influences the absolute magnitude of quantities like power spectral density or AR coefficients, it is irrelevant for the determination of time instances or duration of anomalies in the signals. It was verified that the first 20 integer values for both signals of file BEP1L correspond with the data shown in the data description.

The 200 Mb files with background noise at high sampling rate were too large to handle on our computer system. Although the 80 Mb high sampling rate injection files could be copied onto a disk of the computer system, there was not sufficient space to deal with these files in a convenient way. Therefore, the files with high sampling rate data are not considered in this report.

As emphasis is put on the anomaly detection, the background noise signals were not studied, as they were not the background noise measured by the waveguides during the experiments before the injections. Therefore, no attempt was made to characterize the background noise from the evaporator and superheater with PFR at full power.

3. Anomaly detection methods

Especially for high frequency signals like signals from acoustic sensors a very fast anomaly detection method is required, which needs only limited computational effort, if analysis is to be done on-line. We therefore chose for

detection in time domain instead of in the frequency domain. One could study statistical features of a signal like a short time average or standard deviation, but due to correlation within a signal, the signal itself is not very appropriate for that goal. To get higher sensitivity the correlation between successive sample values of a signal is eliminated by constructing an autoregressive model of the noise and subtracting the predicted signal values from the actual signal values. If a signal can be modelled properly in this way, the residual noise obtained will have a white frequency spectrum for stationary signals and is much more suited for detection of anomalies in a signal.
A univariate autoregressive (AR) model is given by

$$y_n = \sum_{i=1}^{p} A_i \, y_{n-i} + w_n \qquad (1)$$

with y_n the signal value at time instance n, A_i the AR coefficients for time lag *i* and w_n the white noise.
To determine the AR-parameters A_i for a certain model order p, different methods are available like solving the Yule-Walker equations if the correlation function is available, the least-squares method and Burg's method[3,4]. The last two methods use the original time series data directly. As it turned out in the previous benchmark test[5] that the Yule-Walker method did not provide a satisfactory AR-parameters for the type of signals under consideration, Burg's method as given by Marple[4] was implemented in a program in the IRI noise analysis system in a recursive way to obtain the AR-parameters for the next higher model order. This algorithm was used to obtain the AR-models for all signals considered.

From the AR model a signal prediction $\hat{y}_n$ can be calculated according to

$$\hat{y}_n = \sum_{i=1}^{p} A_i y_{n-i} \qquad (2)$$

and the residual noise from

$$\delta_n = y_n - \hat{y}_n \qquad (3)$$

During stationary operation of the system the residual noise is white with zero mean, hence successive sample values are independent. This makes the residual noise especially suitable for anomaly detection by monitoring specific statistical features.

For anomaly detection statistical tests can be applied to the residual noise signal δ. In this report two different methods are used for anomaly detection. The first method can be applied at each sample separately, but considering a number of samples together will increase the reliability of the detection.
Although it is possible to do a combined anomaly detection on both signals of a data file at the same time by considering a multivariate AR model, in this report the anomaly detection methods are applied to all signals individually.

The first method monitors a quantity proportional to the variance of the residual noise signal. It performs a χ^2-test as follows

$$D = \sum_{n=1}^{N} \left(\frac{\delta_n}{\sigma_0} \right)^2 \qquad (4)$$

with σ_0 the standard deviation of the stationary residual noise. When D lies outside certain limits, to be set by the user, an anomaly is declared. The limits on D together with the number N of samples considered determine the false alarm probability. If the white residual noise δ_n has a Gaussian distribution, D has a χ^2-distribution with N degrees of freedom. Applying a one-sided test D>U to declare an anomaly, the False Alarm Probability (FAP) is given by

$$FAP = \int_{U}^{\infty} p(\chi_N^2)\, d\chi^2 = Q(\frac{1}{2}N, \frac{1}{2}\chi^2) \qquad (5)$$

with Q(a,x) the complementary incomplete gamma-function. Inversely, for a given FAP the upper limit on D can be calculated.
The second method is the Sequential Probability Ratio Test[6], which is a variation on the first method but uses a variable number of samples N before a decision about the signal being normal or abnormal is made.
For testing a possible change in the standard deviation of a Gaussian white noise signal equal to or larger than σ_1, it calculates

$$\lambda_n = \lambda_{n-1} + \frac{\sigma_1^2 - \sigma_0^2}{2\sigma_0^2\sigma_1^2}\delta_n^2 - \ln\frac{\sigma_1}{\sigma_0} \qquad (6)$$

starting with $\lambda_0 = 0$. If λ_n crosses a negative lower bound A to be set by the user, the signal is declared to be normal. If λ_n crosses a positive upper bound B, the signal is declared to be abnormal. In both cases λ is reset to zero. Otherwise no decision is made and Eq.(6) is applied recursively to the next samples. The false alarm probability FAP and the alarm failure probability is given by

$$A = \ln\frac{AFP}{1-FAP} \qquad (7)$$

and

$$B = \ln\frac{1-AFP}{FAP} \qquad (8)$$

However, it has been shown[7] that the FAP and AFP from Eq.(7) and (8) are maximum values and that the actual probabilities can be much lower.
All methods can in principle be extended to multiple signals to be considered at the same time.

4. Results

As the AR-model of a signal must be constructed from a stationary part of that signal before any injection and the onset of injections were not known on beforehand, AR models were obtained for a single signal separately using the first 2048 samples a signal from each injection data file. To determine the model order p one normally accepts that model order that minimizes Akaike's Information Criterion (AIC). However, looking at the values of AIC for model orders up to 100, no clear minimum was seen. As the purpose of the AR-model in this study was not to model the dynamic response of a system accurately, but to eliminate most of the correlation from a signal, a compromise was made between accurate modelling and computational burden for the anomaly detection and a model order $p = 30$ was adopted in all cases. This value was chosen because for larger model orders there was no longer an appreciable reduction of the residual noise variance.

For visual inspection the residual noise for the signals WA and WB for all injection experiments were calculated and plotted. As an example, Fig. 1 shows the residual noise of waveguide WA from the data file I4P1L. From this figure a slight increase of the variance of the residual noise can be seen starting roughly at $t = 5.2$ s. It is also apparent that besides this long duration anomaly, there are many spikes with extremely large values compared with the standard deviation of the residual noise signal, both before and during the injection. This seems to be a characteristic of acoustic signals from a waveguide and appears in all residual noise signals. If these spikes are inherent to the residual noise signal its amplitude probability density is far from Gaussian. This complicates the application of the statistical tests discussed in section 3 as each spike, when sufficiently large, will cause an anomaly to be declared. Moreover, calculation of the false alarm probability is not possible as this is based on a Gaussian distribution of the residual noise signals.

The standard deviations of the original signals before injection were calculated from a short first part of each data. It turned out that the standard deviation of the signal of the same waveguide but in different experiments differed significantly. Some results are shown in table II, which also shows the standard deviation of the residual noise as obtained from the AR-model. Comparison of variances show the part of the variance in the original signal that is caused by correlation in the signal. This part of the variance is eliminated by the AR model. The application of the χ^2-test and the Sequential Probability Ratio Test (SPRT) requires the value of σ_0, the standard deviation of the (normal part of the) residual signal. This value is obtained from the AR-analysis, but refers only to 2048 samples of normal part of the signal.

The strongly non-Gaussian distribution of the residual noise also makes it difficult to choose proper limits for the anomaly detection. Therefore, for the χ^2 test the upper bound for the test was rather arbitrary set at 1200 if the number samples N for the anomaly detection was 1000 and at 2500 if

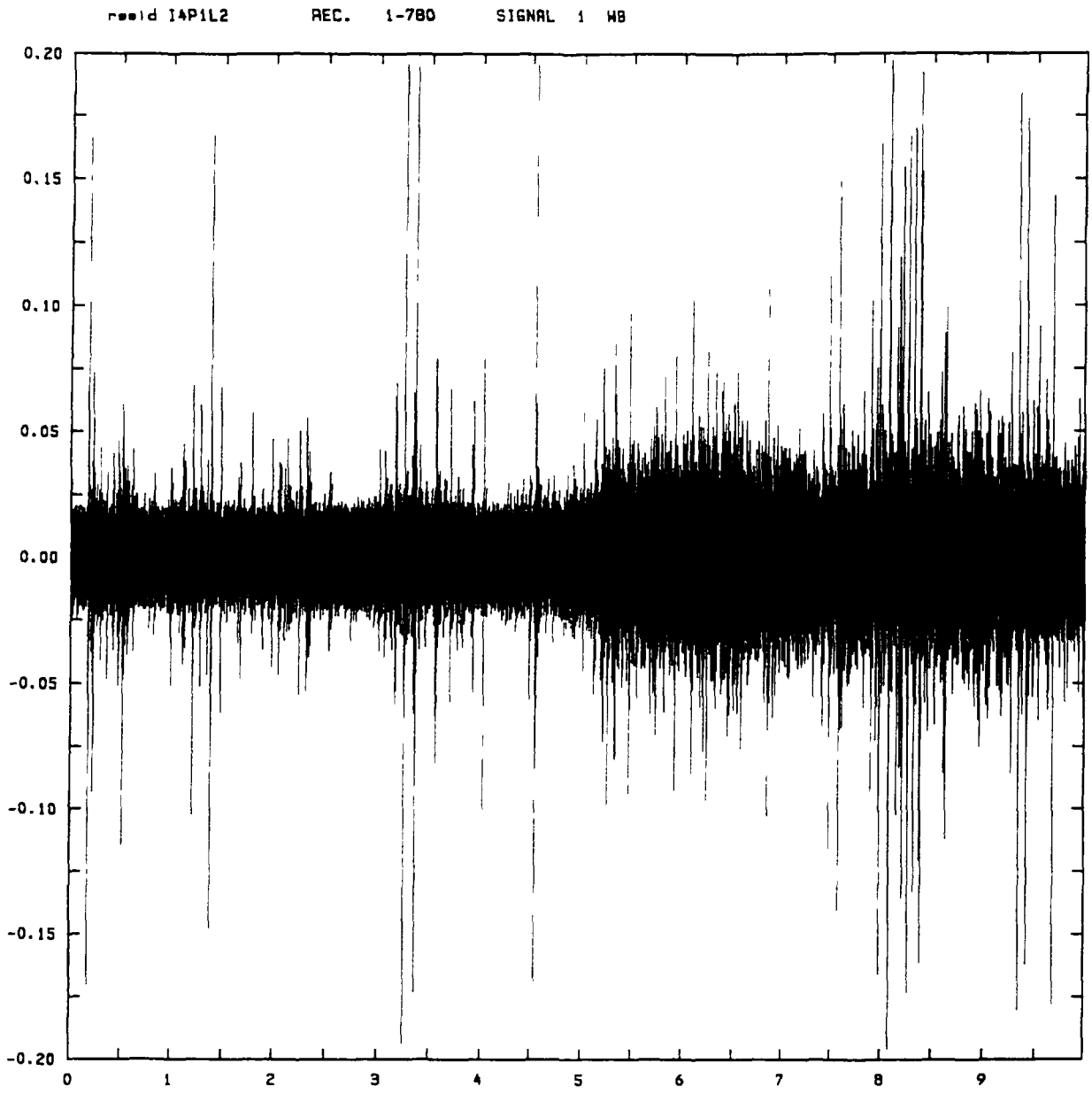

Fig.1. Residual noise of signal WB of file I4P1L

N = 2000. Even then many anomaly detections are obtained but of very short duration. On this basis they can be discriminated, resulting generally in only one long lasting anomaly, which is attributed to the injection of water, hydrogen or argon into the sodium of the steam generator.
To limit the analysis time and the number of files to be handled, for most injection experiments only the signal combination WA and WB (files InP1L) was considered. For both signals at each experiment the AR-model was determined and the anomaly detection method was applied separately to each signal.

For the experiment I5 all three signal combinations were investigated. It was found that the signals in different signal combinations during a certain

Table II. Standard deviation of noise signals

exp.	signal	σ original signal	σ_o residual noise
I1	WA	0.012	0.0067
I2	WA	0.018	0.011
I3	WA	0.018	0.010
I4	WA	0.019	0.0057
I5	WA	0.034	0.021
	WB	0.037	0.024
	WC	0.029	0.0092
	WD	0.025	0.014
I6	WA	0.025	0.0084
I7	WA	0.014	0.0056
I8	WA	0.022	0.0065

experiment were not sampled over exactly the same time span, nor the standard deviation of the signals of the same waveguide were the same, but the onset of the injection was for each data file at almost the same time. Therefore, for the other experiments only the signal combination P1 (waveguides WA and WB) were considered. Table III shows the time of onset of the injection as obtained by the χ^2-method for anomaly detection. In each case the anomaly lasted to the end of the sampled data.

Tabel III. Results of anomaly detection with the χ^2-method

set	signal	onset (s)	AFP (%)
I3	WA	7.3754	51.5
	WB	7.3702	5.8
I4	WA	5.2154	3.5
	WB	4.8314	0.0
I5	WA	2.6158	0.0
	WB	2.6067	0.0
I6	WA	5.4231	0.0
	WB	5.3175	0.0
I7	WA	3.5751	0.0
	WB	3.5750	0.0

For the experiments I5, I6 and I7 N=1000 was taken for the χ^2 anomaly detection method and N=2000 for the other experiments. For the experiments I1, I2 and I8 no clear, long lasting anomaly occurrence could be detected. For the experiments I3 and I4 not all samples after the onset of the injections always gave an anomaly detection. From the number of samples that did not gave the appropriate anomaly detection the alarm failure probability was calculated, which is also shown in Table III.
Table IV shows the time of onset found for all signals in experiment I5.

Table IV. Results of anomaly detection for all signals of experiment I5

set	signal	onset (s)
I5P1L	WA	2.6158
	WB	2.6067
I5P2L	WC	2.6397
	WB	2.6368
I5P3L	WD	2.6413
	WB	2.6269

Because of the non-Gaussian character of the residual noise signal it is even more difficult to choose proper detection limits A and B for the SPRT-method, as use of the false alarm and alarm failure probability and calculating A and B from Eqs.(7) and (8) is not applicable in this case. Therefore, no results of the SPRT-method are presented.

To determine the type of injection one needs reference material specific for different injection types and injection rates. As such reference signals are lacking it is not possible to determine for each experiment the type of injection.
However, from the residual noise signal (for waveguide WB, which seems to give the strongest change in signal during the injection), a certain pattern can be seen after the onset of the injection that is in common for some other experiments. For the experiments I5, I6 and I7 the residual noise show a sudden increase in amplitude for a short time which then again suddenly decreases and start increasing again but much slower. Hence, the experiments seems to represent the same type of injection, but at different injection rates. As these experiments show the largest relative change in standard deviation since the injection they may all concern water injection, as this probably gives the strongest impact on the system.

As the data files with high sampling rate were not considered no estimation was made of the differences in time delay between pairs of detector signals.

This could have been used to estimate the location of the injection point relative to the detectors. However, from the change in variance of the residual noise before and during the leak for the different detectors, some indication can be given. For injection experiment I5 the variance of the residual noise for the first 2.5 s and the last 6.8 s was calculated. The results in the relative increase of variance are shown in Table V.

Table V. Increase in variance of residual noise during injection at experiment I5

set	sig-nal	variance (V^2) before injection	varinance (V^2) during injection	rel. increase of var.
I5P1L	WA	$4.51\ 10^{-4}$	$6.48\ 10^{-3}$	13.4
	WB	$7.40\ 10^{-4}$	$2.28\ 10^{-2}$	29.9
I5P2L	WC	$7.31\ 10^{-5}$	$4.77\ 10^{-3}$	64.2
I5P3L	WD	$1.99\ 10^{-4}$	$4.55\ 10^{-3}$	21.8

Although there is no prove that a quantity like the relative increase of variance of the residual noise before and during the injection is a measure for the distance from the source of the increased noise to the detector, it seems a plausible assumption, although the functional dependence with the distance is not known. If we accept this hypothesis, we see from the relative large increase of the variance for detector C that the injection point must be close to C. Considering the positions of detector B and D (see Fig. 2 as supplied with the benchmark test description) the location of the injection must be roughly at the same height in the evaporator as detector C, as the distance to detector B is smaller and the increase in variance is larger for detector B than for Detector D. The relative small increase in variance for detector A does not fit completely in the picture. Anyway the location of the injection should be to the right of detector C (in Fig. 2), in the opposite direction of detector A.

5. Discussion and conclusions

The χ^2-method is able to detect the injections of water/hydrogen/argon from the signals of waveguides in a steam generator of a fast breeder reactor. From the 8 different injection experiment from which signals were available, for 5 experiments the injection and the time of onset could be detected.
The residual noise of all signals exhibited a large number of spikes which prohibited the exploitation of the full posibilities of the anomaly detection

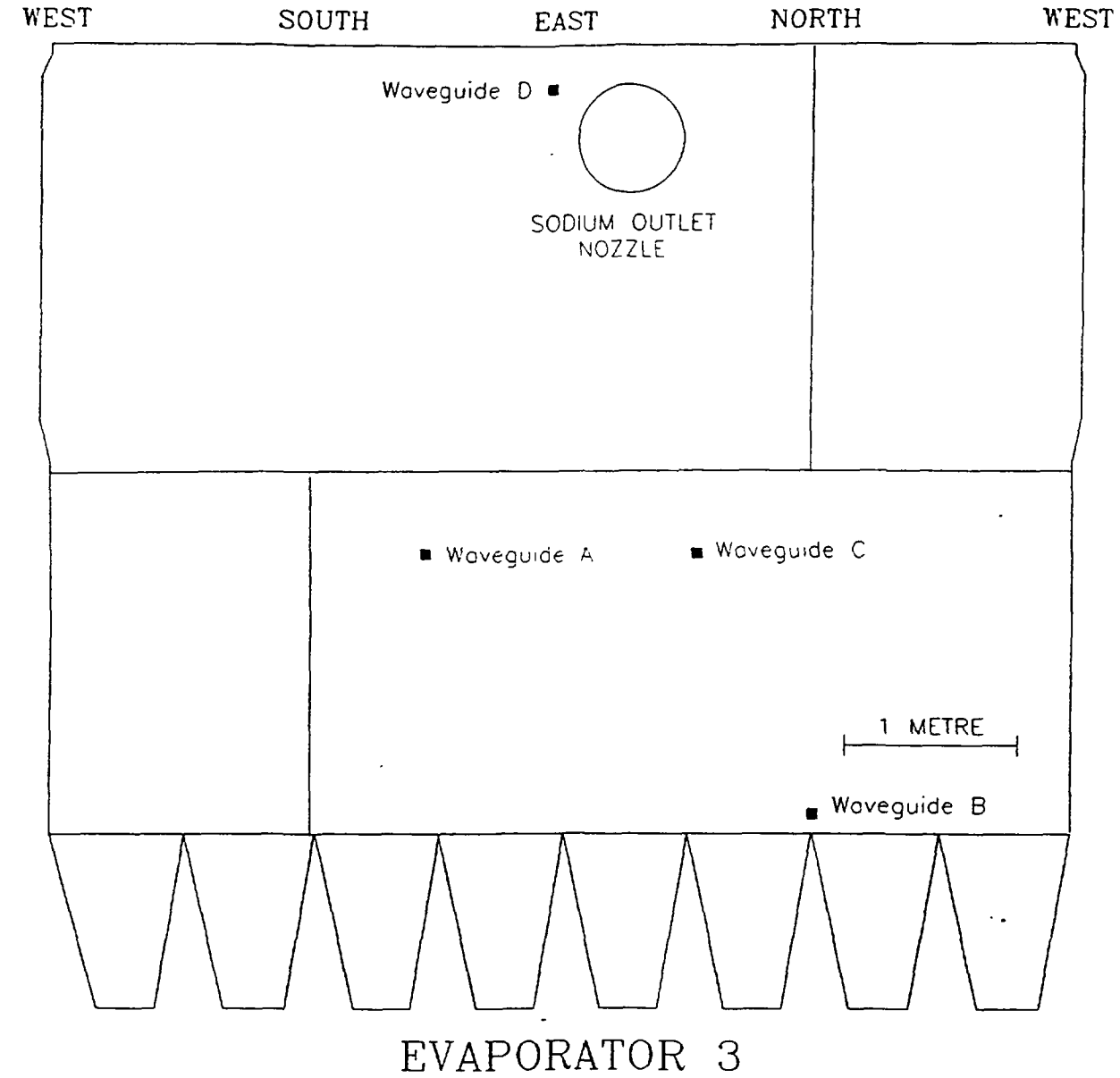

Fig.2. Location of waveguides in evaporator

method. Especially the setting of limit values to declare an anomaly cannot be derived from desired false alarm probabilities and values must be chosen not to get false alarms due to the spikes.
It seems therefore desirable to filter the original signals before processing or eliminating the spikes.
The times of onset of the injections are shown in Table III. The onset as found by the χ^2-method is sharply defined for most cases, within 1 ms. The method can basically applied on-line if a sufficiently fast sampling and data transfer system is available.

A rough estimation of the position of the injection relative to the detectors was made. To make this more precise the relation between the increase in variance of the residual noise during injection and the distance to the detector must be further studied.
To characterize the type of injection, reference signals are needed. It seems possible to analyse the residual noise further, for instance its frequency contents, to distinguish between different types of injections.

References

[1]AEA Technology, IAEA Benchmark-1995 (1995).
[2]J.E. Hoogenboom, Structure of data files for the IRI noise analysis system, report IRI 131-88-05 (1988).
[3]L. Ljung, *System Identification - Theory for the User*, Prentice-Hall, Englewood Cliffs, N.J., USA (1987).
[4]S.L. Marple, *Digital Spectral Analysis with Applications*, Prentice-Hall, Englewood Cliffs, N.J., USA (1987).
[5]J.E. Hoogenboom and H. Schoonewelle, IRI contribution to the 1994 benchmark test on leak detection in a fast breeder reactor, report IRI 131-94-020/1, Interfaculty Reactor Institute, Delft University of Technology, Delft, The Netherlands (1994).
[6]O. Glöckler, Fault detection via Sequential Probability Ratio Test of Multivariate Autoregressive Modelling-Based Residual Time Series, Sixth Symposium on Nuclear Reactor Surveillance and Diagnostics SMORN-6, Gatlinburg, USA,1991.
[7]H. Schoonewelle, T.H.J.J. van der Hagen and J.E. Hoogenboom, Theoretical Investigations into the SPRT method for anomaly detection, Annals of Nuclear Energy (1995).

FINAL RESULTS FROM THE DEVELOPMENT OF THE DIAGNOSTIC EXPERT SYSTEM DESYRE

K.P. SCHERER, H. EGGERT, K. SHELEISIEK,
P. STILLE, H. SCHÖLLER
Kernforschungszentrum Karlsruhe GmbH,
Karlsruhe, Germany

Abstract

In the *Kernforschungszentrum Karlsruhe (KfK)*, a distributed knowledge based diagnostic system is developed to supervise the primary system including the core of the *Kompakte Natriumgekühlte Kernreaktoranlage (KNK II)*, a 20 MWe experimental fast reactor. The problem is to detect anomalies and disturbances in the beginning state before fault propagation - *early diagnosis* - and provide the *scram analysis* to detect the causality when a system shutdown occurs.

1 Introduction

Fast reactors are very complex technical systems. Those systems are not operating undisturbed at every moment. A failure is always an intolerable irregularity of the normal operation of the reactor. Such irregularities are most undesirable effects because they are involving considerable economical loss and may even lead to endangerment of public health and life. Therefore, it is necessary to guarantee an almost faultless operation of a reactor. Technical system failures result from structural changes which occur at the beginning of a chain of operations. Based on this theory different classes of abstractions can be introduced by the occurrence of failures, which may be reflected from a diagnostic point of view. The Fig. 1 describes this classification.

The following essential goals of diagnosis can be concluded from this classification: A careful working method should identify system failures in a early stage, so that qualified (adequate) countermeasures could start in time. Many years of operating experience have shown that with an extending complexity of technical systems the variety of anomalies and failures during system operation increases. This is a result of the possible causes which affect the correct operation of the reactor and their subsequent effects due to the interaction of the reactor and the environment. As a result, for enhancement of reliability and economy precise construction as well as improved technology, production engineering and installation are necessary but not sufficient for prevention of failures or an early failure detection. Improving the reliability of fast reactors requires additionally the development of innovative diagnostic methods, for which computer techniques as well as methods of Artificial Intelligence may supply the classical tools.

In this context, a diagnostic system as a prototype for the KNK II is developed[1,2]. KNK II is a sodium-cooled 20 MWe experimental fast reactor at the Nuclear Research Center of Karlsruhe. The nuclear part of the plant consists of the primary system with the reactor core and two sodium circuits, two secondary sodium circuits, and the tertiary water/steam circuit. The core is composed of a test zone, a driver zone, breeder subassemblies, control rods and reflectors.

A general philosophy of the relationship between data processing and diagnosis is shown in Fig. 2. First, the signal environment of the fast reactor produces raw data and a preprocessor produces formated data. One part of this data stream (for example temperature noise signals) is the input for

Surveillance Class	Information	Goal
DAMAGE_PREVENTION	Structural description and model behaviour of the object according to the engineering documents.	Detection of possible failure concentrations, avoidance by taking preventive actions (i.e. robust construction) to guarantee correct operation despite of insignificant alterations in structure and behaviour.
LOCAL_DIAGNOSIS	Information about the current behaviour of the components during operation, i.e. reports about primary breakdowns (partial hypotheses).	Diagnostics of first indications of failure (early diagnosis), prevention of subsequent failures.
GLOBAL_DIAGNOSIS	Information about function and behaviour of the entire system.	Diagnostics of deviations in normal system operation, detection of causes and possible consequences (diagnosis of state conditions is followed by causal analysis).
POST_MORTEM_DIAGNOSIS	Recorded information about behaviour of the system during operation until a failure occurs.	Discovery of primary causes which lead to a system failure (diagnosis of state conditions and causal analysis).

Fig. 1: Abstract Classes of the Technical Diagnosis

an intelligent signal processor which produces partial hypotheses in the context of the surveillance class *local diagnosis*. The expert system correlates these partial hypotheses. Another part of the formated data (for example values of temperatures, speed of pumps, valve positions) is a direct input for the expert system. These inputs, the direct input and the partial hypotheses produce the dynamical facts as premises of the rules, given by the experience knowledge. So the inference engine of the expert system can produce hypotheses in the context of the *global diagnosis*.

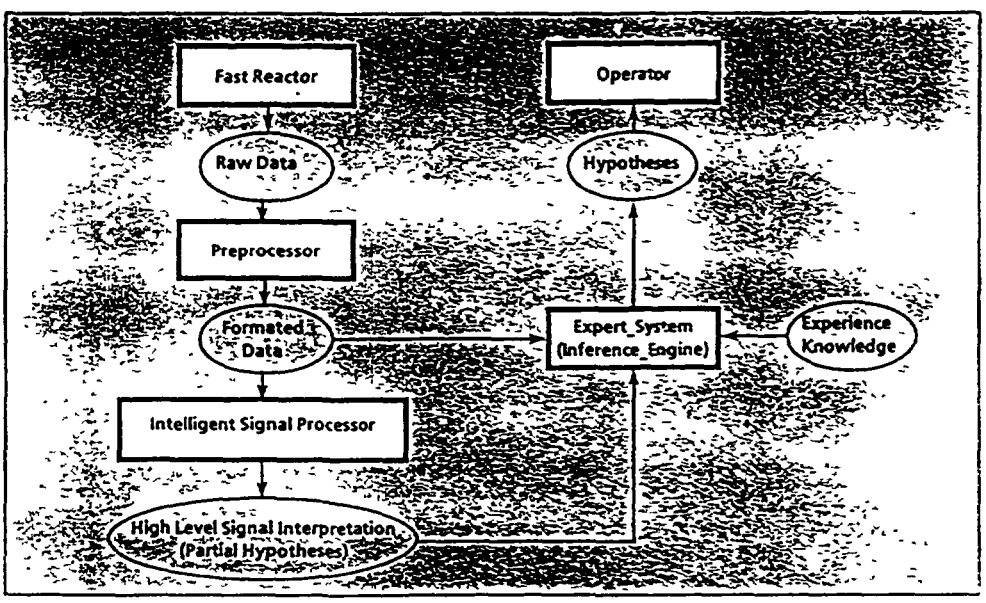

Fig. 2: Data Processing and Diagnosis

2 The Architecture of the whole System

We describe the architecture of the system in three steps of abstraction. For the first step of the system description we use the surveillance classes *local diagnosis*, *global diagnosis* and *post mortem diagnosis*. So it is possible to build a relation with the attributes *surveillance class*, *computer system* and *set of functions*. The following figure represents this relation:

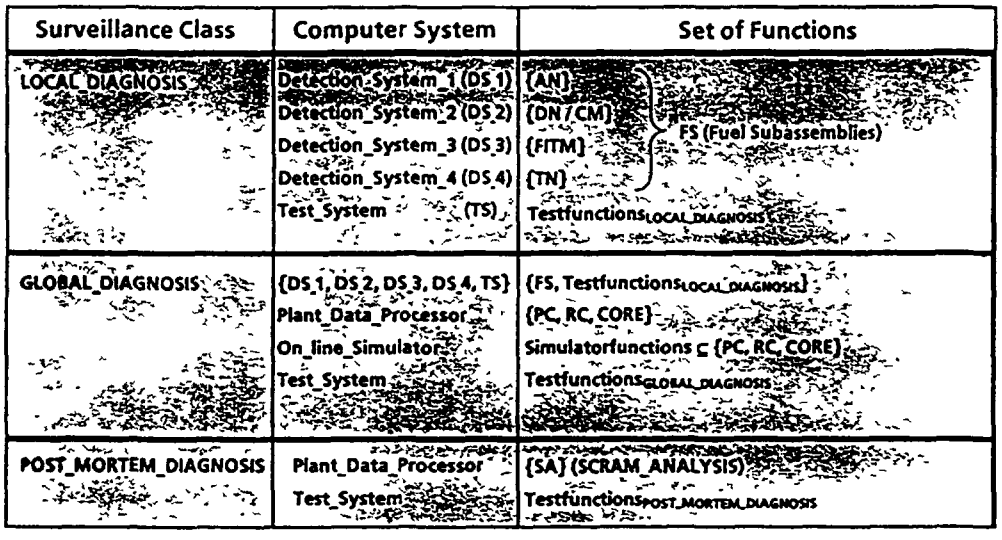

Fig. 3: Classes, Systems and Functions of the Diagnosis

The class *local diagnosis* includes collectively four detection systems in which five different functions are implemented. During operation of the experimental nuclear power plant KNK II, this functions are responsible to detect anomalies in the beginning state (*early diagnosis*), so that a propagation can be prohibited. The class *global diagnosis* includes all computer systems and functions of the class *local diagnosis* and additional the plant data processor and the on line simulator. The plant data processor includes furthermore three different functions for the detection of disturbances during the operation of the nuclear power plant. The on line simulator includes a partial set of the called functions for the simulation of disturbances. The simulation of plant disturbances is an effective method to demonstrate the behavior of the plant with respect to possible propagations of faults. Finally the class *post mortem diagnosis* includes also the process computer which provides the function scram analysis. More detailed information about all functions is given in the next chapter. For all classes a test system is available. The purpose of the testfunctions is to generate input informations for the test during the development of the knowledge base, which is a part of the expert system. For the second step of the system description a view of the system causality is appropriate. The figure 4 demonstrates this view.

The fast reactor process produces raw data as input for the computer systems which have been described already before. These computer systems produce preprocessed data for the dynamical storage in a further computer system, the so called data manager. The data handling in the data manager provides two strategies of the data support: First an event oriented strategy which is organized by a first in first out (FIFO) queue, and second a history oriented strategy which is organized by an index file.

On the top of this hierarchical organization an expert system can receive this preprocessed data from the data manager by its own requests and can store this received data as facts in its knowledge base for the dynamical work of the inference engine. The expert system is able to generate hypotheses, and in case of partial hypotheses (internal) it can send requests to the operator via the man machine interface. More detailed information about the expert system is given in chapter 4. All above mentioned systems (computers), without the data manager, are clients in a local area network (LAN). The data manager is the server for data handling in this network.
The last step of the system description is a representation of the real system in Fig. 5. The architecture of the diagnostic system is distributed. The detection systems, the plant data processor, the

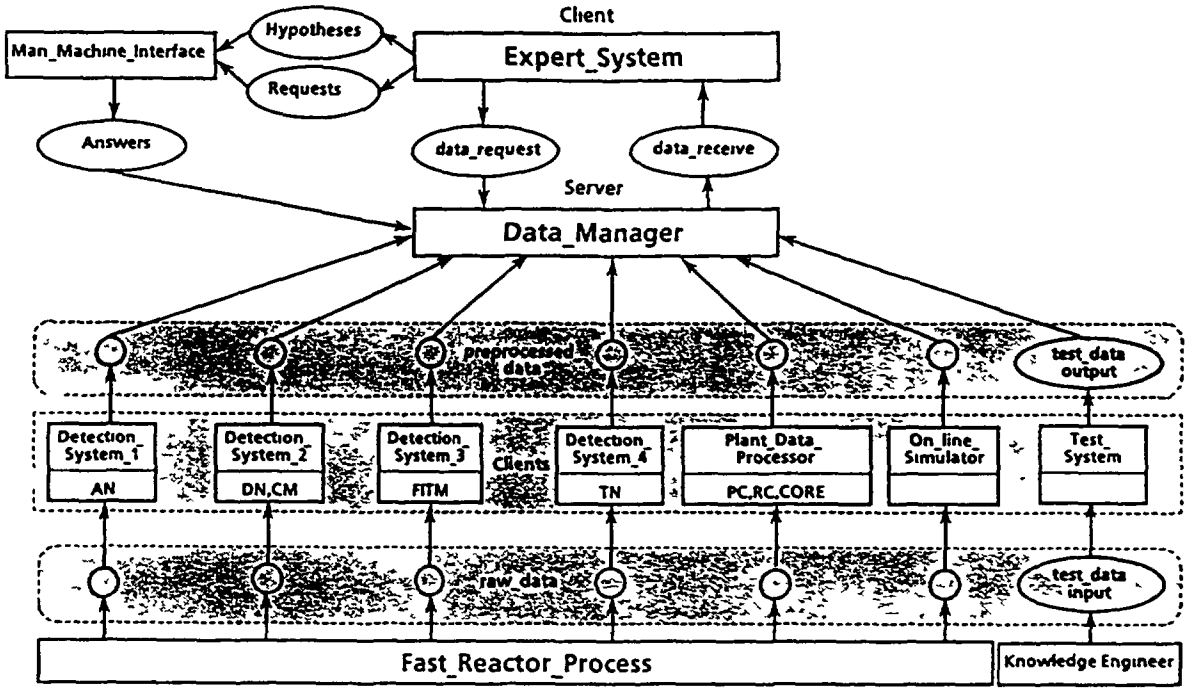

Fig. 4: DESYRE - Diagnostic Expert System for Reactor Surveillance (Causality)

test system, the data manager and the expert system are realized on different real computer systems with partially different operating systems. This computer systems are embedded in four LAN segments (Ethernet, IEEE 802.3) which are coupled via an active starcoupler. The internetworking (communication between the computer systems) is realized with special application software which is based on the TCP/IP protocol family.

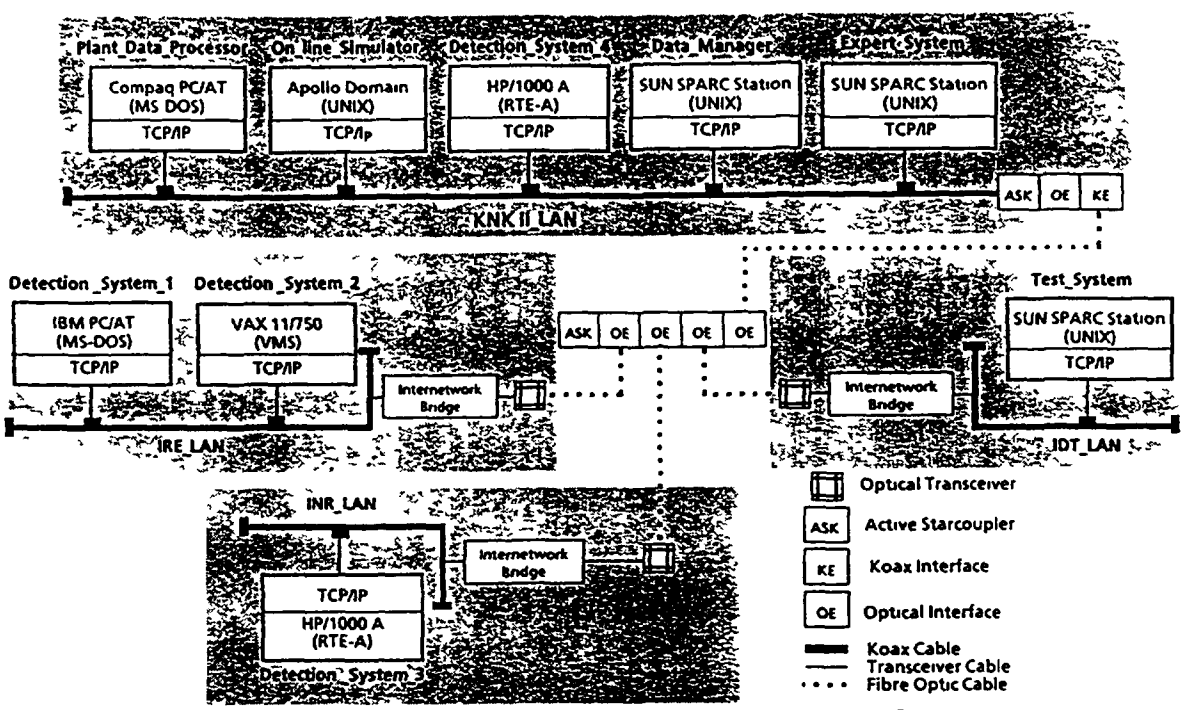

Fig. 5: DESYRE - Diagnostic Expert System for Reactor Surveillance (Network)

3 The process related knowledge domains of the expert system

Concerning figure 3, all three surveillance classes are realized, but in this paper, only the classes *local diagnosis* and *global diagnosis* are described in detail.

The main task of the KNK II diagnostic system is the surveillance of the core and the primary circuits. Data and information obtained from the sensors and the instrumentation systems are the main input to the diagnosis process. As already mentioned in chapters 1 and 2 several detection systems (AN, DN/CM, FITM and TN) are available at KNK II for the surveillance of the core (see figure 4 and figure 3). AN is the acoustic noise monitoring system to detect sodium boiling. For the preprocessing of the acoustic signals, method like spectrum analysis and pattern recognition are applied [3,4]. The main objective of the preprocessing step is the discrimination between the two process states boiling and no boiling.

DN and CM are the delayed neutron and covergas monitoring systems to detect failed fuel elements [5]. Preconditioning of the DN signals consists in substraction of the background, correction for the power dependency of the detector sensitivity, and the classification of the net signals. Additionally, in case of small DN signals a DN failure probability is calculated. Preprocessing of the CM signals consists in a simple yes/no classification using constant signal threshold.

FITM is a sensitive method to detect a power/flow mismatch in individual fuel subassemblies [6]. This is achieved by compensating the measured subassembly outlet temperatures for variations of the inlet temperature, the primary sodium flow and the reactor power. Under steady state conditions the method allows the detection of drifts as low as 0.1 K/day. The drifts are then classified using predefined thresholds. Furthermore, average drift values are calculated for the different zones of the core. This is an important information for the recognition of changes of the flow resistance in the whole core.

TN is the temperature noise measured by the thermocouples at the fuel subassembly outlets [7]. Preconditioning is carried out by calculating the RMS value of the noise and relating it to the temperature rise in the respective subassembly. The resulting k-factor is constant over a wide range of operational parameters, and sensitive to variations of the flow distribution in the respective subassembly, e.g. in the case of blockages.

The results of the local diagnosis functions described above (s.a. figure 3) are included in the following global diagnosis functions: PC (i.e. surveillance of the primary circuit), RC (i.e. reactor control system) and CORE (i.e. reactor core). For these functions, 57 additional process parameters are transmitted from the plant data processor to the diagnosis systems. A survey of the different domains of the global diagnosis function is given in figure 6. Each change of state of the reactor process - normal operational changes as well as disturbances - is connected with characteristic variations of the process parameters. The determination and formal description of these relations is the first step in establishing the knowledge base of the diagnostic system. The main source of knowledge is the experience of the KNK II designers, operators and experimenters. Additional information - in particular on the quantitative relations between changes of the plant state and the process parameters - is obtained from dynamic calculations using the KNK II simulator. This system which was developed by Interatom on the basis of the computer code DYANA represents the core, the primary and secondary circuits and the reactor control system of KNK II [8]. It allows the simulation of operational transients, e.g. power changes, and of disturbances like reactivity insertion, pump failures, increase of flow resistance etc.

Domain	Primary Circuits (PC)	Reactor Control (RC)	Reactor Core (CORE)	Fuel Subassemblies (FS)
Main process parameters	Primary sodium flow rate, Primary pump power	Mean core outlet temperature	Fuel subassembly outlet temperatures	AN, DN/CM, FITM, TN
No. of monitored process parameters	11	8	38	90
No. of possible hypotheses	25	13	26	25
Main recognizable plant states/ disturbances	Power changes, Failures of pump control, Pump seizure, Increase of flow resistance in the core and primary circuit	Power changes, Failures of reactor control, Failures of pump control, Reactivity disturbances, Cold shocks	Power changes, Increase of flow resistance in single SA's or core regions, Failures of thermocouples, Absorber rod runaway	Failure of detection systems, Changes of background, Fuel element failures, Local cooling disturbances, Power/flow mismatch in single SA's

Fig. 6 : Domains of the Global Diagnosis Functions

A typical result of a simulation is presented in Fig. 7, which shows the reaction of the main primary system parameters to the partial closure of a primary valve.

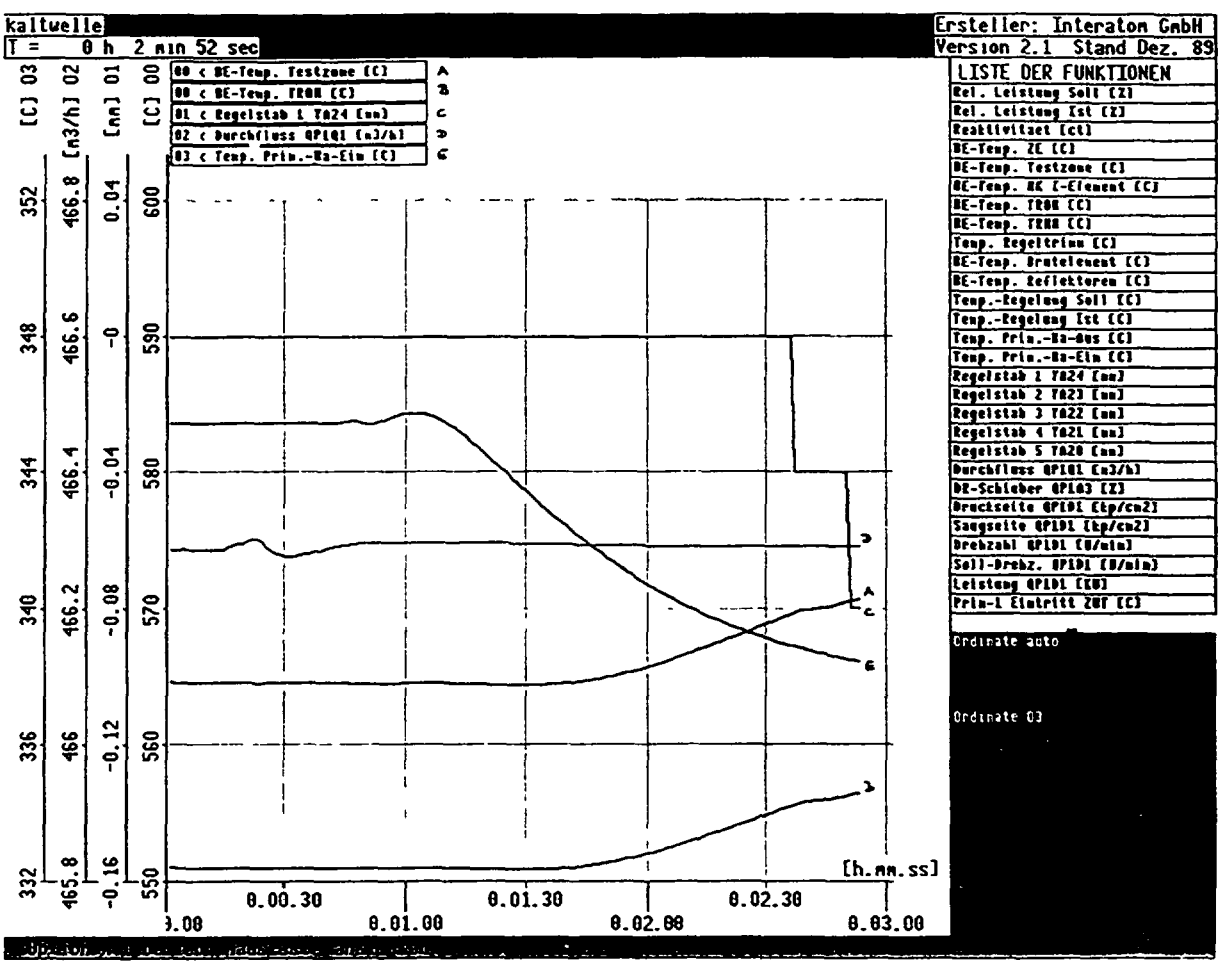

Fig. 7: Partial Closure of a Primary Valve

The diagnostic system recognizes variations of the process parameters by comparing actual values with reference values. The reference values are dynamically generated in the diagnostic system in

two different ways: either by algorithmic calculations using actual process parameters or by setting of previous values of the same parameter. An example for the first way is the calculation of an average outlet temperature from a group of fuel subassemblies as a reference to detect changes of the outlet temperature of individual subassemblies of this group. However, for most of the reference values the second way is used, e.g. the initial value of a parameter is taken as reference for all succeeding measurements. This implies that the initial state of the process is assumed as normal. The problem solution of the dynamical reference geberation is shown in figure 10.

A particular problem is the discrimination of disturbances against normal operational processes like power changes. From the part-load diagram of KNK II it follows that most of the process parameters of the primary and the secondary circuits depend on the reactor power in a distinct manner. This leads to characteristic patterns of the process parameter variations which can be used to identify a change in state as a power variation. In such a case the actual process parameters are set as new reference values.

The relations between the changes of the process state and the parameters are compiled as decision trees. Parameters with high sensitivity to changes of the process state are positioned at the top of the trees. Further parameters and other data are used at the subsequent decision points. The outputs of the trees are the hypotheses, i.e. the identified plant states. When possible, recommendations to the operator are added. Fig. 8 and 9 show as a representative examples a section of the decision tree *primary circuit surveillance*. Top parameters of this tree are the variations of the sodium flow rate in the primary circuits. Among the output states are the hypotheses *power change* and *partial closure of a primary valve*. The latter case corresponds to the event which has already been presented in Fig. 7 as a typical result of the KNK II simulator.

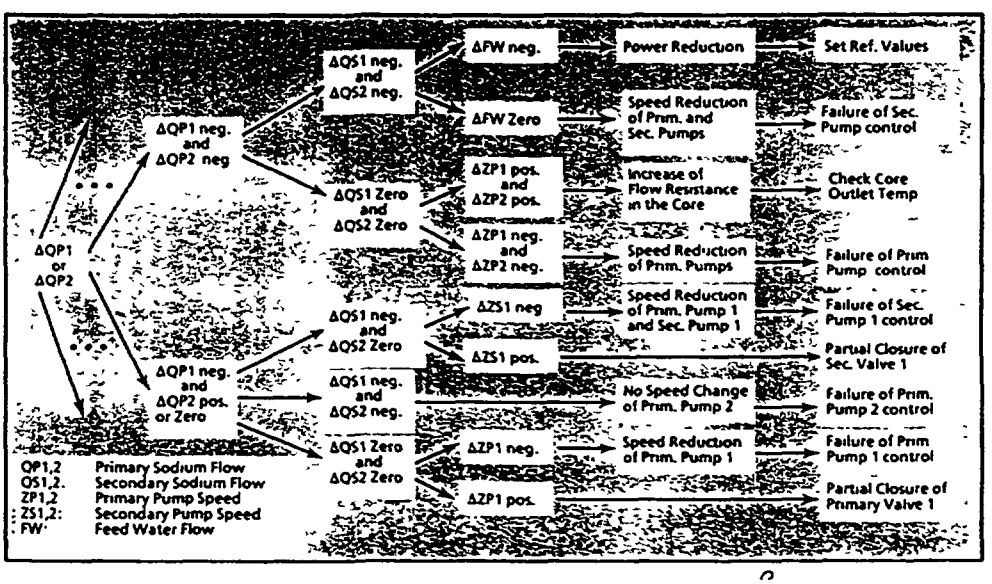

Fig. 8: Detail of the Decision Tree "Primary Circuit (PC) Surveillance"

A survey of the extent of knowledge implemented so far in the KNK II diagnostic system is given in figure 6 which shows for the different domains of surveillance the top parameter of the decision tree, the number of process parameters considered, the number of possible hypotheses and the main plant states and disturbances which can be recognized.

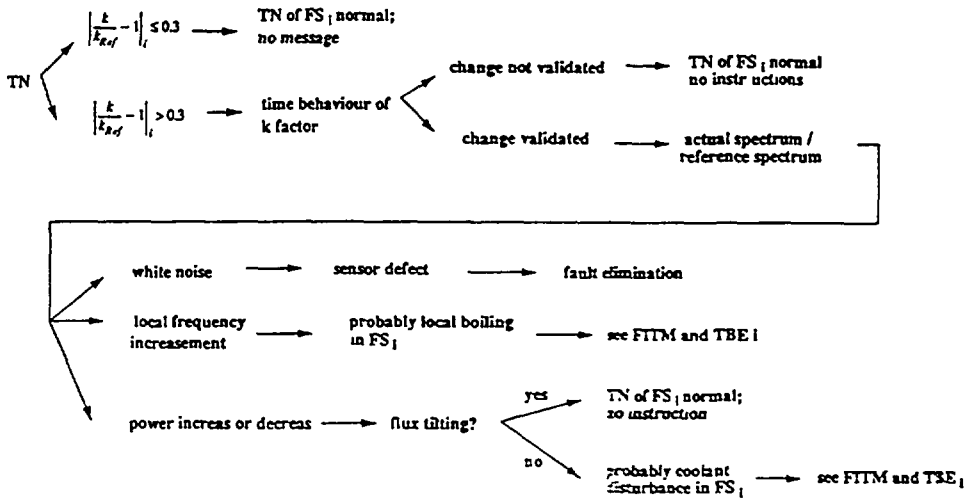

Fig. 9: Detail of the Decision Tree "Temperature Noise (TN) Surveillance"

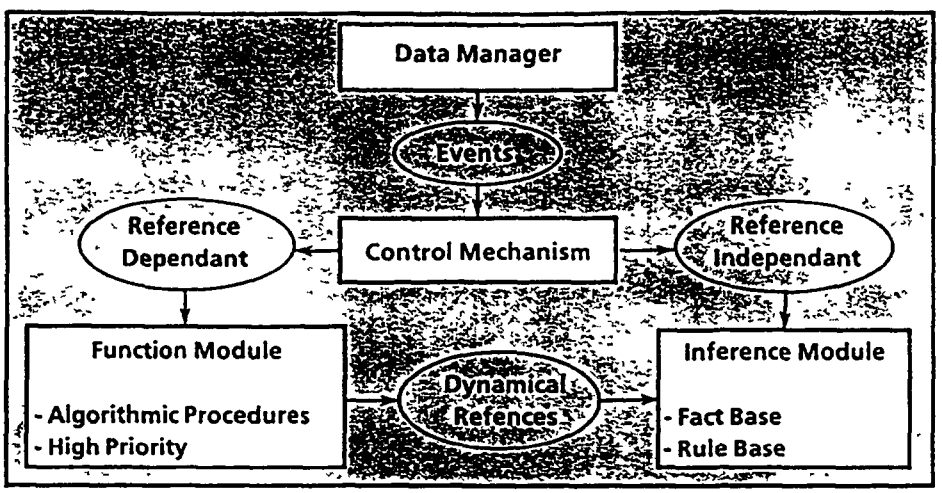

Fig. 10: Dynamical Reference Generation

4 Knowledge representation methods

To support the operator and the user, it is important to verify the typical knowledge of the human being and to model it into a computerized manner. There are typical knowledge modes, which are distinguished: technical knowledge, informal and formal knowledge.

Informal knowledge is based on regarding processes, imitations and so it is very difficult (sometimes impossible) to represent it in a computerized manner, also in AI techniques.

Technical knowledge is useful represented in conventional programming techniques like structured programs. It contains algorithmic solutions and programs. A characteristic feature is the separation of data and facts. So, data are stored in special files, where modifications can made easily. The facts in form of coded programes are very difficult to update. Such problems are solved

by the classic software techniques. In contradictory tho these both knowledge types the formal knowledge, represented by linguistic formalized expresssions, is a very powerful method to describe any real world components, based on characteristic features in a natural language. That means, both facts and data are included in one representation mode. So, special AI representations are used to favorite such statements. There is no separation between the data and the programs. The combined data and facts and logical programs are stored in a common knowledge base.

Concerning the support of the operator to recognize the instantaneous process, to evaluate it and to trigger new process activity, it seems powerful to give him a method for communication with the system in a linguistic manner with free formulated expressions. So, AI representation modes are employed for the diagnostic part (explanation component).

Because of early warning i.e. early diagnostic function, special algorithmic solutions are necessary and must be integrated into the AI reprentation mode. We have a combination of technical and formal knowledge types and regarding this fact, hybrid knowledge reprentations are used (see figure 11).

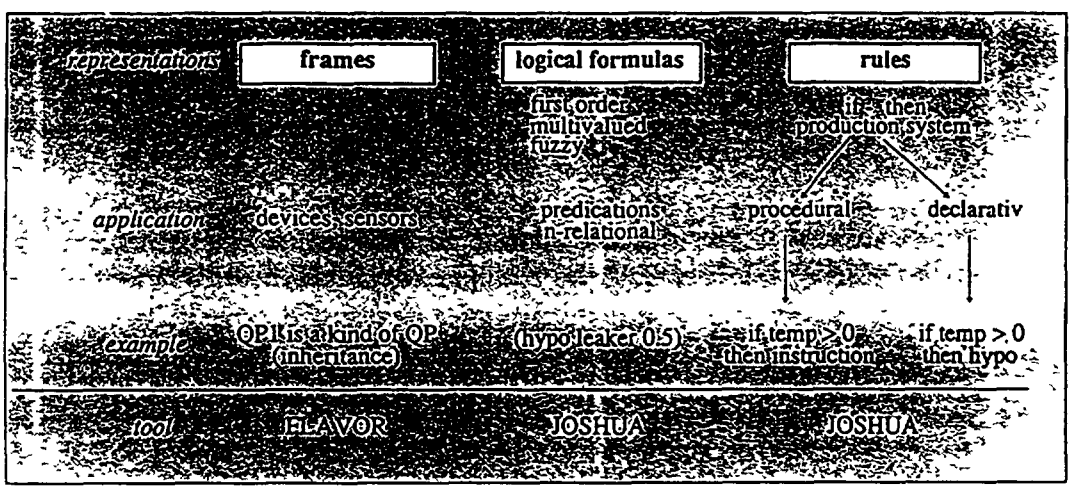

Fig. 11: Hybrid knowledge representations

The diagnostic part of the expert system is implemented in principal as a rule based production system. But the rule complexes are extended by logic expressions and frames. The representation mode depends on the contextual description of the situations and facts.

Hardware devices like pumpes, valves, measurement systems are described by frames. They are supplied with different attributes, specific for this object. The objects themselves are ordered in a hierarchical classe-subclasse structure with multi enheritance mechanisms of the features. The implementation is performed in a flavor system, the object oriented extension of Common Lisp. The kernel of the knowledge base is the form of IF THEN rule complexes (distributed on different domain experts), whereby we distinguish between the procedural and the declarative aspect of the rule.

The difference depends on the action part of the rule, which contains instructions (procedural) or hypotheses (declarative). Within the trigger and the action part of the rule complexes, the expressions, based on predicate calculus, are performed by n-relational predicates. This representation mode is supported by the AI tool JOSHUA.

A more detailled representation of the rule based production system by JOSHUA is shown in figure 12.

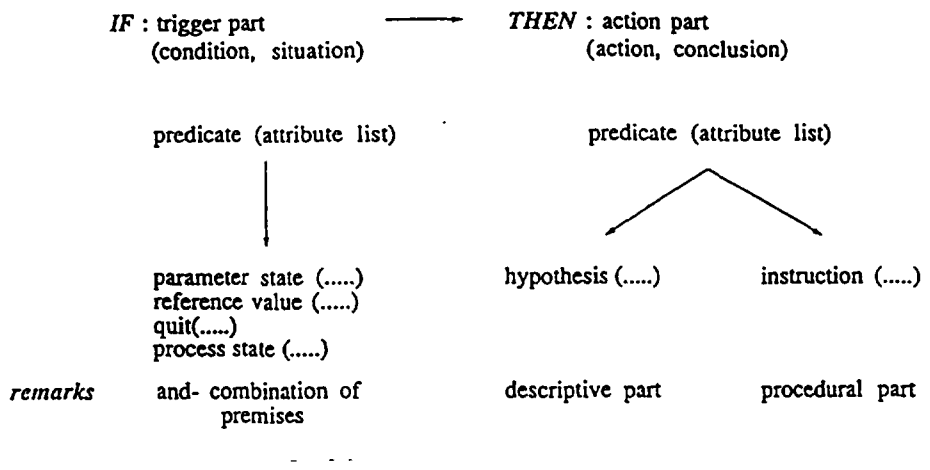

Fig. 12: A rule based production system

5 Knowledge Base and Inference Engine

The knowledge base of the expert system is divided into two structurally different parts. One is an object oriented knowledge base with a fix number of abstract objects (as representations of all core elements and all parameters, which must be considered during surveillance).

Starting point for the object oriented knowledge base is a domain specific approach. One result of the knowledge acquisition process is, that all knowledge statements and experiences are relations between any plant elements and any process parameters.

The plant consists of a lot of plant elements, which have specific features, represented as attributes. The objects can be classified into several classes, where inheritance strategies are used from class to subclass and typical features are represented by these attributes.

For example, the class of core elements consists of breeder subassemblies, fuel subassemblies, reflector elements and control rods. General class attributes like position number are subclass independent (inherited from the superclass) and other attributes like a noise spectrum are subclass specific. A typical tree for the hierarchical core and parameter modeling is shown in Fig. 13 and Fig. 14.

The second part is a rule base, which is furthermore distinguished in domain specific rule complexes. This is necessary for a modular structure of the knowledge base. DESYRE has many rule complexes, which can be activated domain specific and so separately. Such a specific rule base combines any object slots of the object knowledge base and produces hypotheses and gives instructions for the users and triggers special algorithmic procedures outside of the expert system[9]. A small extract of such a semantic rule network is shown in Fig. 8 and Fig. 9.

Before the inference engine can trigger the different rule complexes, the control mechanism activates a preprocessing algorithm to update the numerical slot values of the attributes, belonging to the objects involved in the rule sets. This is necessary for consistency of the semantic object contents. That is done by a high priority process, when data and event sets are transmitted from the data manager. One of the most important cases is the dynamical generation and setting of reference values, dependant on the current process state.

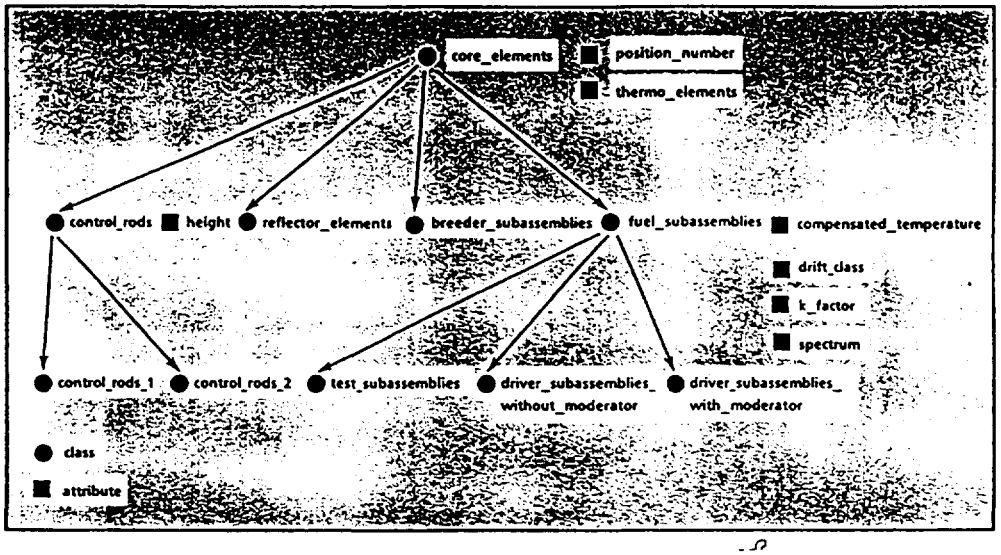

Fig. 13: Core Class Model

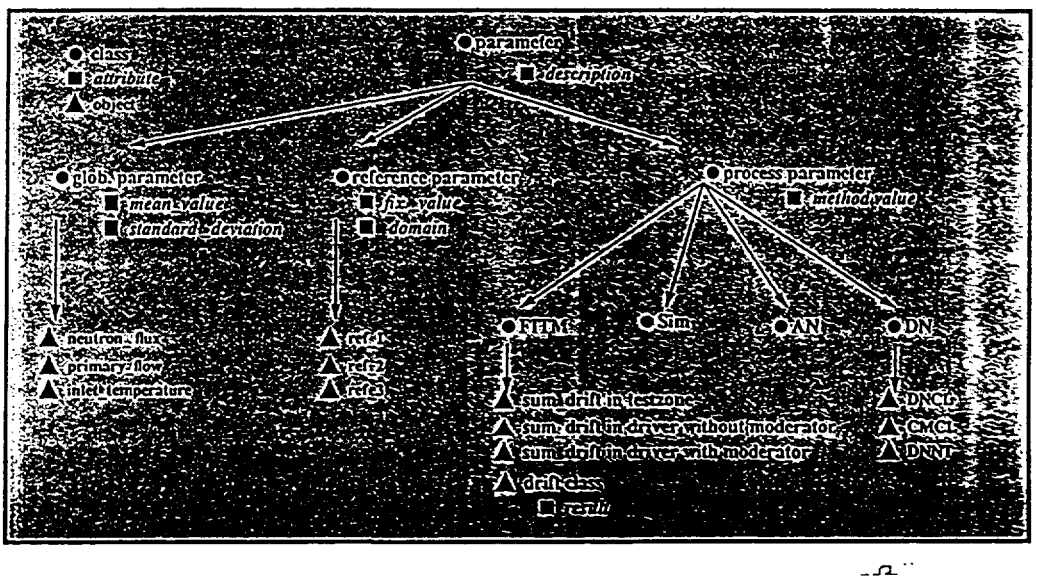

Fig. 14: Parameter Class Model

Principally, there is a rule based production system for evaluation of the process data and the pre-evaluated partial hypotheses of the different domain experts. It is a data driven but not strongly forward chaining mechanism, because a predeterminated set of hypotheses is placed on an agenda, which has to be suggested by the volunteered events in form of object slots.

A rule can be triggered in different manner: First, directly by the on line process and second in a mixed mode, partially on line combined with a needed interactive input from user (see Fig. 4 and Fig. 15, left side, upper part).

One of the very important features of the expert system is the explanation part, because the on line diagnostic system must be a support of the operator to recognize faults in the beginning state.

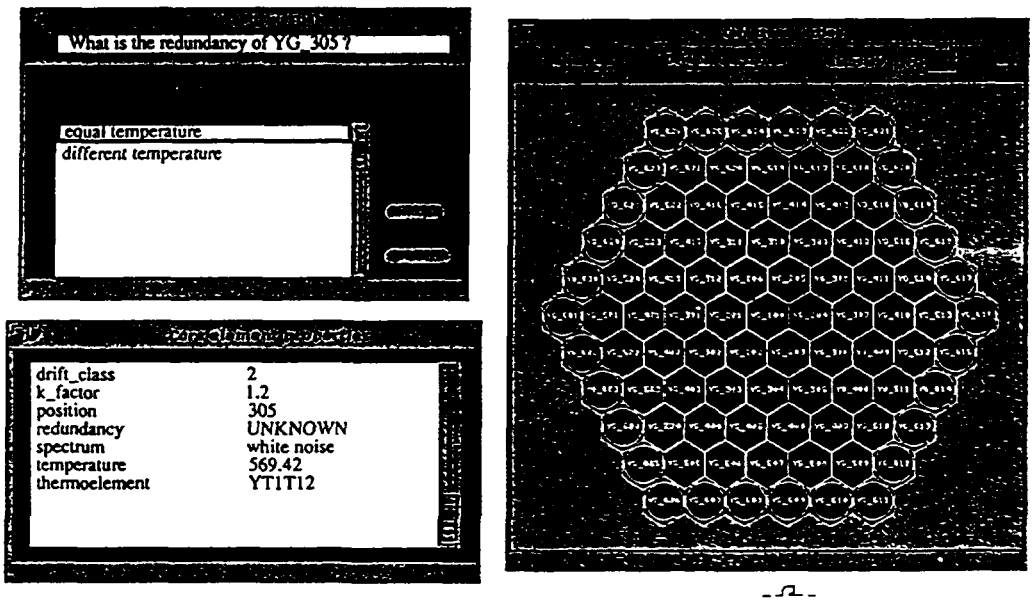

Fig. 15: Man Machine Interface

So, process changes and anomalies (for examples temperatures, position of the control rods) can be visualized directly as active values, for example by colors, representing core elements as objects. On line data from the data manager are transferred in the object knowledge base. The changed slot values of the object attributes are directly represented in the core graphics (see Fig. 15, right side).

Furthermore, every time special objects from the class of all core elements can be picked out, to get a frame based representation of the whole object information. That is independent of the instantaneous inference state (see Fig. 15, left side, lower part).

The hypotheses and the instructions are shown in a special window including all information about the premises or other details, necessary for plausible explanation. That is done in the on line mode. While modification and further development of the knowledge base and the inference engine, the complete powerful development tool of the expert system is given. In our case, a hybrid expert system shell is used.

6 Conclusion

Very large and extensive performance test series at the on line system were done since January 1989. Dependant of the rule number, the number of AND-conditions within one rule, the data packages as events concerning the process state and the different inference strategies, time behavior of the knowledge based system was analyzed.

Furthermore real-time tests of the complete diagnostic system have been performed since January 1991. As the KNK II was shut down during this test phase, the simulator was used to generate on line process data. However, the tests did not include the local core surveillance systems (AN, DN/CM, FITM, TN) because these functions are not implemented in the simulator. During the tests, several shortcomings and inconsistencies were recognized and eliminated and numerous extensions were realized. The development has now reached a stage that all plant situations which can be generated by the simulator, are recognized with high reliability and sensitivity.

Regarding the reactor components and the process behavior concerning the early fault diagnosis the knowledge processing step is no time critical aspect and so it seems to be useful to apply knowledge based systems.

Because of positive results of the syatem validation it is useful to transfer the conceptual design of a similar system for the European Fast Reactor (EFR).

References

1. H. EGGERT, K. P. SCHERER, H. W. KELBASSA, P. STILLER, C. DÜPMEIER, *A Framework of a Diagnostic Expert System for Real Time Application*, in: J. Zalewski and W. Ehrenberger (ed), Hardware and Software for Real Time Process Control, Proc. IFIP WG 5.4, Warsaw 1988, North-Holland 1989

2. H. EGGERT, K. P. SCHERER, P. STILLER, *A Knowledge Based on-line Diagnostic System for the Fast Breeder Reactor KNK II*, in: Advanced Controls for Fast Reactors, Proc. IAEA/ IWGFR Specialist's Meeting, Argonne/Illinois, USA 1989

3. J. ABERLE et al, *Acoustic Measurements for Boiling Detection at KNK II*, Experimental Thermal and Fluid Science 1991, 4: 152 - 165

4. K. P. SCHERER, *Pattern Recognition and Prediction Methods in Parametric Signal Models for Early Fault Detection*, KFK-Report 4197, Kernforschungszentrum Karlsruhe, Karlsruhe, FRG 1987

5. G. SCHMITZ, G. HOFFMANN, S. JACOBI, D. KLEIN, *Monitoring of Fuel Failure Development at KNK II by Measurement and Analysis Fission Products in the Sodium and Cover Gas*, Int. Fast Reactor Safety Meeting, Snowbird/Utah, USA, August 1990, Vol. IV p 243 - 252

6. M. EDELMANN, H. MASSIER, *Function and Structure of the Karlsruhe Subassembly Monitoring System KASUMOS*, Proc. SMORN III, Tokyo, Oct. 1981, in: Progr. Nucl. Eng., Vol 9, 1982

7. G. WEINKÖTZ, L. KREBS, H. MARTIN, *The Cooling Disturbances Indication and Analysis System CODINAS - An on-line Temperature Noise Surveillance of KNK II Subassemblies*, Fast Breeder Int. Conf, Pasco/Washington, USA, 1987

8. V. ERTEL et al, *Entwicklung eines Analyse-Simulators und exemplarische Erarbeitung der Wissensbasis für das Dignosesystem KNK II*, Interatom Report Nr.: 32.07592.0, Bergisch Gladbach, FRG 1989

9. K. P. SCHERER, P. STILLER, *Knowledge Representation Methods for Early Failure Detection*, in: P. Haapanen (ed), Artificial intelligence in nuclear power plants, Proc. IAEA/IWG NPPCI Specialist's Meeting, Helsinki, Finland 1989

LIST OF PARTICIPANTS

Black, J.L.	University of Southern Queensland, 2, Awoonga Court, Mooloolaba, Queensland 4557, Australia
Cornu, C.	Direction des Reacteurs Nucléaires, Centre d'Etudes Nucléaires de Cadarache, B.P. 21, F-13108 Saint-Paul-lez-Durance Cedex, France
Curry, R.	Fuel Performance Group, AEA Technology, Windscale B14/E312, United Kingdom
Gribok, A.V.	Institute of Physics and Power Engineering (IPPE), 249020 Bondarenko Square 1, Obninsk, Kaluga Region, Russian Federation
Hayashi, K.	Japan Atomic Energy Research Institute, Tokai-mura, Ibaraki-ken 319, Japan
Hoogenboom, J.E.	Delft University of Technology, Mekelweg 15, 2629JB TU Delft, Netherlands
Journeau, Ch.	Direction des Reacteurs Nucléaires, Centre d'Etudes Nucléaires de Cadarache, B.P. 21, F-13108 Saint-Paul-lez-Durance Cedex, France
Kozlov, F.A.	Institute of Physics and Power Engineering (IPPE), 249020 Bondarenko Square 1, Obninsk, Kaluga Region, Russian Federation
Ledwidge, T.J.	Faculty of Engineering and Surveying, University of Southern Queensland, 2, Awoonga Court, Mooloolaba, Queensland 4557, Australia
McKnight, J.	AEA Technology, Risely, United Kingdom
Muromura, T.	Japan Atomic Energy Research Institute, Tokai-mura, Ibaraki-ken 319-11, Japan
Nabeshima, K.	Japan Atomic Energy Research Institute, Tokai-mura, Ibaraki-ken 319-11, Japan

Om Pal Singh	Reactor Physics Division, Indira Gandhi Center for Atomic Research, Kalpakkam, Tamil Nadu 603 102, India
Oriol, L.	Centre d'Etudes Nucléaires de Cadarache, B.P. 21, F-13108 Saint-Paul-lez-Durance Cedex, France
Prabhakar, R.	Engineering Development Division, Indira Gandhi Center for Atomic Research, Kalpakkam, Tamil Nadu 603 102, India
Rinejski, A.	Division of Nuclear Power and the Fuel Cycle, International Atomic Energy Agency, Wagramerstrasse 5, P.O. Box 100, A-1400 Vienna, Austria
Rofe, S.E.F.	Airframes and Engines Division, Aeronautical and Maritime Research Laboratories, P.O. Box 4331, Melbourne, Victoria 3001, Australia
Rowley, R.	AEA Technology, Risely, United Kingdom
Scherer, P.	Kernforschungszentrum Karlsruhe GmbH, Postfach 3460, Karlsruhe, Germany
Stiller, P.	Kernforschungszentrum Karlsruhe GmbH, Postfach 3460, Karlsruhe, Germany
Srinivasan, G.S.	Reactor Physics Division, Indira Gandhi Center for Atomic Research, Kalpakkam, Tamil Nadu 603 102, India
Shinohara, Y.	Japan Atomic Energy Research Institute, Naritachyo 3607, Ohairai-machi 311-13, Japan
Volov, A.N.	Institute of Physics and Power Engineering (IPPE), 249020 Bondarenko Square 1, Obninsk, Kaluga Region, Russian Federation
Vyjayanthi, R.K.	Engineering Development Division, Indira Gandhi Center for Atomic Research, Kalpakkam, Tamil Nadu 603 102, India
Watanabe, K.	Japan Atomic Energy Research Institute, Naritachyo 3607, Ohairai-machi 311-13, Japan
Zheng, Z.	Japan Atomic Energy Research Institute, Naritachyo 3607, Ohairai-machi 311-13, Japan

Yamashita, K. Japan Atomic Energy Research Institute,
Naritachyo 3607, Ohairai-machi 311-13, Japan

Yughay, V.S. Institute of Physics and Power Engineering (IPPE),
249020 Bondarenko Square 1,
Obninsk, Kaluga Region, Russian Federation